

Univerzita Karlova

Přírodovědecká fakulta

Studijní program: Molekulární a buněčná biologie, genetika a virologie

Studijní obor: Molekulární a buněčná biologie, genetika a virologie



Mgr. Barbora Pokrývková

Fenotyp a funkce buněk infiltrujících spinocelulární karcinomy hlavy a krku různé etiologie
Phenotype and function of cells infiltrating head and neck squamous cell tumors of different
etiology

Typ závěrečné práce:

Disertační práce

Vedoucí práce: doc. RNDr. Ruth Tachezy, Ph.D.

Konzultant: prof. RNDr. Ivan Hirsch, CSc.

Praha, 2024

Prohlášení:

Prohlašuji, že jsem závěrečnou práci zpracovala samostatně a že jsem uvedla všechny použité informační zdroje a literaturu. Tato práce ani její podstatná část nebyla předložena k získání jiného nebo stejného akademického titulu.

V Praze, 21.06.2024

Podpis

Poděkování:

Děkuji své školitelce doc. RNDr. Ruth Tachezy, Ph.D. za předání cenných rad a zkušeností během celého mého studia a během přípravy této dizertační práce. Děkuji za vstřícný přístup, přátelskou pracovní atmosféru a možnost podílet se na mnoha zajímavých vědeckých projektech. Dále bych chtěla poděkovat konzultantovi práce, prof. RNDr. Ivanu Hirschovi, CSc. a celému kolektivu Laboratoře molekulární a nádorové virologie a Laboratoře imunoterapie za pomoc během studia, zejména RNDr. Ingrid Polákové, Ph.D., RNDr. Janě Šmahelové, RNDr. Martině Salákové, Ph.D. a RNDr. Michalu Šmahelovi, Ph.D.

Dále děkuji Mgr. Václavu Janovcovi, Ph.D. za komentáře k této dizertační práci a za podporu během studia. V neposlední řadě děkuji celé své rodině za podporu během studia.

Tato práce byla podpořena Grantovou agenturou Univerzity Karlovy (GAUK č. 1502118), Agenturou pro zdravotnický výzkum České republiky (AZV č. 17-28055A), Evropským fondem pro regionální rozvoj a Ministerstvem školství, mládeže a tělovýchovy (EFRR a MŠMT, č. CZ.1.05/2.1.00/19.0400 a CZ.02.1.01/0.0/0.0/16_019/0000785) a Národním institutem virologie a bakteriologie (Program EXCELES, Projekt č. LX22NPO5103) – financováno Evropskou unií – Next Generation EU.

Abstrakt

Nádory hlavy a krku (HNSCC) jsou heterogenní skupinou karcinomů, které jsou indukovány užíváním tabáku a alkoholu či perzistentní infekcí lidským papilomavirem (HPV). Incidence virově indukovaných HNSCC celosvětově narůstá. Virová etiologie pozitivně ovlivňuje přežívání pacientů a má výrazný vliv na účinnost protinádorové léčby, což může být vysvětleno přítomností specifické imunitní odpovědi cílené proti virovým antigenům HPV. Hlavním cílem této práce je detailní charakterizace nádorového mikroprostředí karcinomů virové a neviróvé etiologie s důrazem na *in situ* detekci a kvantifikaci imunitních buněk. Pro získání výsledků pro tuto práci byly zavedeny a optimalizovány pokročilé metody studia nádorového mikroprostředí, jako je multispektrální imunohistochemie či hmotnostní cytometrie. Četnost imunitních buněk, hladina exprese vybraných genů a vybraných proteinů v HNSCC byla hodnocena ve vztahu k etiologii nádoru a prognóze, ve snaze vytipovat potenciální terapeutické cíle. Naše výsledky ukazují, že mikroprostředí nádorů HPV-pozitivních vykazuje oproti imunosupresivnímu mikroprostředí karcinomů HPV-negativních vyšší hladinu prozánětlivých a protinádorových imunitních buněk a faktorů. Vyšší zastoupení PD-1⁺CD8⁺ (programmed cell death protein 1, cluster of differentiation 8) T lymfocytů a buněk produkujících GLUT1 (glucose transporter 1) a Hif-1 α (hypoxia-inducible factor 1 α) je spojeno s lepším přežíváním pacientů s HNSCC, naopak vyšší hladina mRNA arginázy 1 predikuje horší přežívání těchto pacientů.

Klíčová slova

Orofarynx, dutina ústní, nádor, lidské papilomaviry, imunita, nádorové mikroprostředí

Abstract

Head and neck cancers (HNSCC) are a heterogeneous group of tumors that are induced by tobacco and alcohol use or persistent human papillomavirus (HPV) infection. The incidence of virally induced HNSCC is increasing worldwide. The viral etiology positively influences patient survival and effectiveness of antitumor treatment, which may be explained by the presence of a specific immune response directed against HPV viral antigens. The main objective of this study is to characterize in detail the microenvironment of cancers of viral and non-viral etiology with a focus on *in situ* detection and quantification of immune cells. For this purpose, advanced methods for studying the tumor microenvironment were introduced and optimized, such as multispectral immunohistochemistry or mass cytometry. The frequency of immune cells, expression levels of selected genes and selected proteins in HNSCC were evaluated in relation to tumor etiology and prognosis with the aim to identify potential therapeutic targets. Our results indicate that the microenvironment of HPV-positive tumors shows higher levels of pro-inflammatory and anti-tumor immune cells and factors, compared to the immunosuppressive microenvironment of HPV-negative tumors. Higher levels of PD-1⁺CD8⁺ (programmed cell death protein 1, cluster of differentiation 8) T lymphocytes, GLUT1 (glucose transporter 1) and Hif-1 α (hypoxia-inducible factor 1 α) producing cells are associated with better survival, whereas higher level of arginase 1 mRNA predicts poorer survival of HNSCC patients.

Key words

Oropharynx, oral cavity, tumors, human papillomaviruses, immunity, tumor microenvironment

Obsah

1.	Úvod.....	10
2.	Přehled literatury.....	12
2.1.	Nádory hlavy a krku.....	12
	Obecná charakteristika, klasifikace a epidemiologie.....	12
	Nádory nevirové etiologie	13
	Nádory virové etiologie	15
2.2.	Lidský papilomavirus.....	16
	Obecná charakteristika a klasifikace.....	16
	Životní cyklus	16
	Onemocnění asociovaná s HPV.....	18
	Mechanismy kancerogeneze	19
2.3.	Nádorové mikroprostředí HNSCC.....	21
	Obecná charakteristika TME	22
	Imunitní buňky TME	23
	Neimunitní buňky TME.....	31
	Hypoxie a její vliv na TME	32
	Metody studia nádorového mikroprostředí.....	33
3.	Cíle práce	37
4.	Přehled využitého materiálu a metod.....	38
5.	Výsledky	41
	Publikace vztahující se k tématu dizertační práce	41
	Publikace nevztahující se k tématu dizertační práce.....	43
	Nepublikované výsledky vztahující se k dizertační práci.....	43
6.	Diskuze	45
7.	Souhrn.....	53
8.	Seznam použité literatury	55
9.	Přílohy.....	72
9.1.	Příloha č. 1	72
9.2.	Příloha č. 2	82
9.3.	Příloha č. 3	100
9.4.	Příloha č. 4	117

Seznam zkratek

ARG1	arginase 1	argináza 1
Breg	regulatory B cells	regulační B buňky
BTLA	B- and T-lymphocyte atenuator	atenuátor B a T lymfocytů
CAF	cancer associated fibroblasts	fibroblasty asociované s nádory
CD	cluster of differentiation	diferenciační skupina
cDC	classical DC	klasické DC
CDKN2A	cyclin dependent kinase inhibitor 2A	inhibitor 2A cyklin dependentní kinázy
CIB1	calcium- and integrin-binding protein 1	protein 1 vázající vápník a integrin
COX-2	cyclooxygenase-2	cyklooxygenáza-2
CTLA4	cytotoxic T-lymphocyte associated protein 4	protein 4 asociovaný s cytotoxickým T lymfocylem
CytoF	cytometry time of flight	cytometrie „čas letu“
DAMPs	danger-associated molecular patterns	molekulární vzory asociované s nebezpečím
DAPI	4',6-diamidino-2phenylindole	4',6-diamidino-2fenylindol
DC	dendritic cells	dendritické buňky
E	early	časný
E2BS	E2 binding sites	vazebná místa proteinu E2
E2F	E2 factor	faktor E2
E6-AP	E6 adaptor protein	adaptorový protein E6
ECM	extracellular matrix	extracelulární matrix
EGF	epidermal growth factor	epidermální růstový faktor
EGFR	epidermal growth factor receptor	receptor epidermálního růstového faktoru
EV	epidermodysplasia verruciformis	
FACS	fluorescent activated cell sorter	třídič buněk aktivovaný fluorescencí
FAP	fibroblast activation protein	aktivační protein fibroblastů
FFPE	formalin-fixed paraffin embedded	fixovaný formalinem zalitý parafinem
FGFR	fibroblast growth factor receptor	receptor růstového faktoru fibroblastů
FOXP3	forkhead box P3	vidlicový box P3
FSP-1	fibroblast specific protein 1	specifický protein fibroblastů 1
GITR	glucocorticoid-induced TNFR-related protein	protein spojený s TNFR indukovaný glukokortikoidy
GLUT1	glucose transporter 1	glukózový transportér 1
GPNMB	glycoprotein non-metastatic melanoma protein B	glykoprotein nemetastazujícího melanomového proteinu B
HSPG	heparan sulphate proteoglycans	heparan sulfát proteoglykany

HGF	hepatocyte growth factor	hepatocytární růstový faktor
Hif-1 α /2 α	hypoxia-inducible factor 1- α /2- α	faktor 1- α /2- α indukovaný hypoxií
HLA-DR	human leukocyte antigen – DR isotype	lidský leukocytární antigen – izotyp DR
HNSCC	head and neck squamous cell carcinoma	spinocelulární karcinom hlavy a krku
HPV	human papillomavirus	lidský papilomavirus
HPV ⁻		HPV-negativní
HPV ⁺		HPV-pozitivní
HR	high risk	vysoce rizikový
HRAS	HRas protooncogene	protoonkogen HRas
HRP	horseradish peroxidase	křenová peroxidáza
ICD-11	International classification of diseases	Mezinárodní klasifikace onemocnění
ICOS	inducible T cell costimulator	inducibilní kostimulátor T buněk
IDO-1	indoleamine 2,3dioxygenase 1	indoleamin 2,3dioxygenáza 1
IFN	interferon	interferon
IL	interleukine	interleukin
IRF4	interferon regulatory factor 4	regulační faktor interferonu 4
KLF5	intestinal-enriched Krueppel-like factor 5	střevně obohacený faktor podobný Krueppelovi 5
L	late	pozdní
LAG3	lymphocyte-activation gene 3	lymfocytární aktivační gen 3
LC	Langerhans cells	Langerhansovy buňky
LR	low risk	nízce rizikový
MDSC	myeloid-derived suppressor cells	supresorové buňky odvozené z myeloidní řady
MHC	major histocompatibility complex	hlavní histokompatibilní komplex
mIHC	multispectral immunohistochemistry	multispektrální imunohistochemie
MIP-3 α	macrophage inflammatory protein 3 α	makrofágový zánětlivý protein 3 α
MMP	matrix metaloproteinases	matrixové metaloproteinázy
MoDC	monocyte DC	monocytární DC
Myc	myelocytomatosis	myelocytomatoza
NE	neutrophil elastase	neutrofilová elastáza
NK	natural killer cells	buňky přirozeně zabíjející
NOS2	NO synthase 2	syntáza NO 2
NOTCH1	neurogenic locus notch homolog protein 1	homologní protein 1 neurogenního lokusu notch
ORF	open reading frame	otevřený čtecí rámec

PAMPs	pathogen-associated molecular patterns	molekulární vzory asociované s patogeny
p53	protein 53	protein 53
PBMC	peripheral blood mononuclear cells	mononukleární buňky periferní krve
PCR	polymerase chain reaction	polymerázová řetězová reakce
PD-1	programmed cell death protein 1	protein programované buněčné smrti 1
pDC	plasmacytoid DC	plasmacytoidní DC
PD-L	programmed death ligand	ligand receptoru programované smrti
PIK3CA	phosphatidylinositol-4,5-bisphosphate 3-kinase catalytic subunit alpha	katalytická podjednotka alfa fosfatidylinositol-4,5-bisfosfát 3-kinázy
pRB	retinoblastoma protein	retinoblastomový protein
PTEN	phosphatase and tensin homolog	homolog fosfatázy a tenzinu
PTGS2	prostaglandin-endoperoxide synthase 2	prostaglandin-endoperoxid syntáza 2
ROS	reactive oxygen species	reaktivní kyslíkové formy
SOX2	sex determining region Y-box 2	region určující pohlaví box Y 2
TAM	tumor associated macrophages	makrofágy asociované s nádory
TAN	tumor associated neutrophils	neutrofilly asociované s nádory
TCR	T cell receptor	receptor T buněk
TGF- β	tumor growth factor β	nádorový růstový faktor β
Th	helper T cell	pomocná T buňka
TIL	tumor infiltrating lymphocytes	tumor infiltrující lymfocyty
Tim-3	T-cell immunoglobulin and mucin- domain containing-3	protein 3 obsahující imunoglobulin T buněk a mucinovou doménu
TLR	toll-like receptor	receptor podobný toll
TME	tumor microenvironment	nádorové mikroprostředí
TNF- α	tumor necrosis factor α	faktor nádorové nekrózy α
TNM	tumor, node, metastasis	stadium nádoru, zasažení uzlin, metastaze
TP53	tumor protein 53	nádorový protein 53
Treg	regulatory T cell	regulační T buňka
TSA	tyramide signal amplification	amplifikace tyramidového signálu
URR	upstream regulatory region	předcházející regulační oblast
VEGF	vascular endothelial growth factor	vaskulární endoteliální růstový faktor
ZAP70	zeta-chain-associated protein kinase 70	proteinkináza 70 asociovaná se zeta řetězcem
ZN		zhoubný novotvar
α -SMA	α -smooth muscle actin	α aktin hladké svaloviny

1. Úvod

V roce 2022 bylo celosvětově diagnostikováno 19 964 811 případů rakoviny všech typů, přičemž na následky rakoviny zemřelo 9 736 779 osob (Bray et al. 2024). Tato obrovská čísla zdůvodňují obrovské úsilí lékařské a vědecké obce najít odpovědi na otázky: Jak rakovinovým onemocněním předcházet, jak rakovinu včas odhalit a diagnostikovat, jak ji léčit a jak zabránit její rekurenci a metastazování. Pro zodpovězení těchto otázek je nezbytné porozumět biologii nádorů, jejich složení a vztahům mezi jednotlivými složkami nádorů a funkcí imunitních buněk v prostředí nádoru. Nádorové mikroprostředí (TME, tumor microenvironment) je složitý systém, který vzniká interakcemi buněk nádorového parenchymu, stroma a nebuněčných složek, jako jsou cytokiny, růstové faktory či hormony. Ke studiu TME je využívána řada přístupů, přičemž v posledních desíti letech došlo k intenzivnímu rozvoji pokročilých metod jako je multispektrální imunohistochemie či hmotnostní cytometrie, které umožňují komplexní analýzy mikroprostředí nádoru.

Tato práce se zabývá studiem TME spinocelulárních karcinomů hlavy a krku (HNSCC, head and neck squamous cell carcinoma), jejichž incidence přes 600 000 případů ročně je řadí na 8. místo v incidenci nádorových onemocnění (Bray et al. 2024). HNSCC jsou heterogenní skupinou karcinomů lokalizovanou v různých anatomických oblastech hlavy a krku, přičemž narůstající prevalence zejména karcinomů orofaryngu je spojena s infekcí lidským papilomavirem (HPV, human papillomavirus) (Windon et al. 2018). Mezi HNSCC indukovanými činnostmi virových onkoproteinů a karcinomy indukovanými fyzikálními či chemickými agens jsou značné biologické rozdíly, s čímž souvisí i rozdílná odpověď pacientů na protinádorovou léčbu a celkově lepší prognóza pacientů s HPV-asociovanými karcinomy (Gillison et al. 2000). Nehledě na etiologii nádoru, mezi standardní postupy léčby HNSCC patří chirurgické odstranění karcinomu následované chemoterapií cisplatinou či karboplatinou a/nebo radioterapií. Léčba bývá úspěšnější u pacientů s karcinomy virové etiologie, u nichž je prokázána vyšší citlivost těchto karcinomů k radioterapii (Spanos et al. 2009). Důsledkem chemoterapie a radioterapie není pouze cytotoxické poškození buněčné DNA, ale také zvýšení imunitní odpovědi, kterou u HPV-positivních (HPV⁺) karcinomů současně indukují i virové onkoproteiny. Usuzuje se, že skladba nádorů a profil imunitních buněk infiltrujících nádor může být u karcinomů virové a neviróvé etiologie rozdílný, což může alespoň částečně vysvětlit odlišnou prognózu obou skupin pacientů.

Od roku 2016 je schválená imunoterapie protilátkami proti receptoru programované buněčné smrti PD-1 (programmed cell death protein 1) pro léčbu pacientů s metastatickými či neresektovatelnými rekurentními HNSCC (protilátky pembrolizumab a nivolumab), bohužel až 80 % pacientů s metastazujícími HNSCC na tuto terapii neodpovídá (Bauml, Aggarwal, and Cohen 2019). Detailní charakterizace nádorového mikroprostředí je předpokladem pro identifikaci nových imunoterapeutických cílů, které by umožnily individualizovat a zefektivnit protinádorovou léčbu a snížit nutnost kombinovaných terapií, v jejichž důsledku trpí pacienti řadou vedlejších účinků.

Na následujících stranách literárního úvodu jsou popsány nádory hlavy a krku z hlediska epidemiologie a uvedeny rozdíly mezi nádory indukovanými jak virově, tak neviróvými faktory. Dále je podrobněji popsán lidský papilomavirus a s ním spojené mechanismy kancerogeneze. Nejrozsáhlejší částí je popis nádorového mikroprostředí HNSCC a stručné představení metody multispektrální imunohistochemie a hmotnostní cytometrie, jež byly, jako hlavní, použity pro získání výsledků této dizertační práce.

2. Přehled literatury

2.1. Nádory hlavy a krku

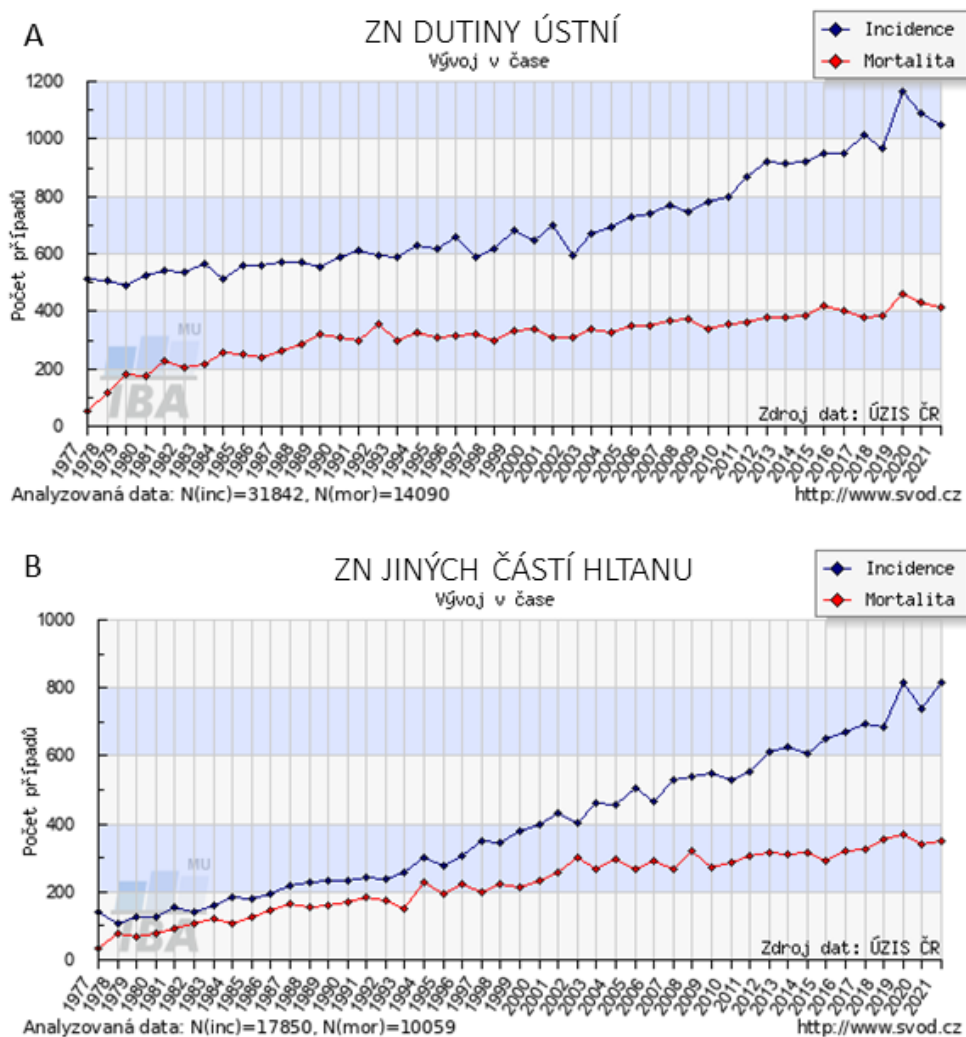
Obecná charakteristika, klasifikace a epidemiologie

Karcinomy hlavy a krku jsou velmi heterogenní skupinou nádorů, jsou detekovány v různých anatomických oblastech orofaryngu, dutiny ústní, hypofaryngu, nazofaryngu a laryngu a zároveň jsou indukovány různými mechanismy. Tabulka 1 uvádí klasifikaci zhoubných novotvarů v oblasti hlavy a krku dle Mezinárodní klasifikace onemocnění ICD-11 (International classification of diseases, 11. vydání; dostupné online: <https://icd.who.int/en>).

Tabulka 1. Anatomické lokality zhoubných novotvarů (ZN) v oblasti hlavy a krku a jejich klasifikace dle Mezinárodní klasifikace onemocnění (ICD-11).

ICD-11 kód	lokalizace	ICD-11 kód	lokalizace
2B60	ZN rtu	2B6B	ZN nazofaryngu
2B61	ZN kořene jazyka	2B6C	ZN pyriformního sinu
2B62	ZN jiných a neurčených částí jazyka	2B6D	ZN hypofaryngu
2B63	ZN dásně	2B6E	ZN jiných a nepřesně určených lokalizací rtu, ústní dutiny a faryngu
2B64	ZN ústní spodiny	2B6Y	Jiné specifikované ZN rtu, dutiny ústní nebo hltanu
2B65	ZN patra	2B6Z	ZN rtu, dutiny ústní nebo hltanu, blíže neurčené
2B66	ZN jiných a neurčených částí úst	2C20	ZN dutiny nosní
2B67	ZN příušní žlázy	2C21	ZN středního ucha
2B68	ZN podčelistních nebo podjazykových žláz	2C22	ZN vedlejších dutin
2B69	ZN tonzily	2C23	ZN laryngu
2B6A	ZN orofaryngu	2D10	ZN štítné žlázy

Počet nových případů HNSCC každoročně narůstá. Celosvětově bylo v roce 2020 detekováno více než 600 000 nových případů onemocnění (Bray et al. 2024). V České republice bylo v roce 2021 detekováno 1 050 karcinomů v oblasti dutiny ústní (2B60-2B68, obrázek 1A) a 815 karcinomů jiných částí hltanu (2B69, 2B6A, 2B6C-2B6E, obrázek 1B) (Dušek et al. 2005).



Obrázek 1. Incidence a mortalita v České republice mezi lety 1977–2021 A) pro zhoubné novotvary (ZN) dutiny ústní (diagnózy 2B60–2B68), B) pro ZN jiných částí hltanu (diagnózy 2B69, 2B6A, 2B6C–2B6E). Převzato a upraveno dle Systému pro vizualizaci onkologických dat; dostupné online: <http://www.svod.cz> (Dušek et al. 2005).

Mezi rizikové faktory indukce onemocnění patří zejména kouření, konzumace alkoholu a perzistentní infekce vysoce rizikovými (HR, high risk) typy HPV (Gillison et al. 2008). HNSCC indukované virově a indukované chemickými agens jsou odlišné nejen mechanismem kancerogeneze, ale i klinickými a epidemiologickými charakteristikami, či odpovědí na protinádorovou léčbu. Tyto rozdílnosti jsou podrobněji vysvětleny v následujících dvou podkapitolách.

Nádory nevirové etiologie

Hlavním rizikovým faktorem HNSCC nevirové etiologie je kouření a konzumace alkoholu, přičemž tyto faktory jsou zodpovědné až za 75 % celosvětově

diagnostikovaných HNSCC (Hashibe et al. 2007). Tabákový kouř obsahuje 72 prokázaných karcinogenních složek, mezi něž patří nitrosaminy, polycyklické aromatické uhlovodíky, acetaldehyd či formaldehyd (Khariwala, Hatsukami, and Hecht 2012). Tyto sloučeniny, podobně jako acetaldehyd vznikající metabolismem alkoholu, fungují jako mutageny (IARC 2012). Chemické sloučeniny tabákového kouře způsobují vznik DNA aduktů, G→T transverze a mutace DNA, které jsou nejčastěji detekované v karcinomech laryngu (South et al. 2019; Stransky et al. 2011). Velmi častou mutací indukovanou tabákovým kouřem (přibližně 30 % HNSCC) je mutace v genu *TP53* (tumor protein 53), jehož produkt působí jako nádorový supresor. Alterací funkce p53 (protein 53) dochází k hromadění změn ve struktuře DNA a ke genomové nestabilitě. Mutace v genu *TP53* jsou v nádorech indukovaných tabákovým kouřem dvakrát četnější oproti nádorům virové etiologie (Gaykalova et al. 2014). Dále jsou popsány mutace v genech pro regulační proteiny buněčného cyklu a nádorové supresory, jako jsou *NOTCH1* (neurogenic locus notch homolog protein 1), *CDKN2A* (cyclin dependent kinase Inhibitor 2A), *pRB* (retinoblastoma protein) *HRAS* (HRas protooncogene), *PTEN* (phosphatase and tensin homolog) či *PIK3CA* (phosphatidylinositol-4,5-bisphosphate 3-kinase catalytic subunit alpha) (Gaykalova et al. 2014; C.Y. Fan 2001; Stransky et al. 2011). Dlouhodobé vystavení karcinogenům obsaženým v tabáku a alkoholu, ztráta opravných mechanismů DNA a inaktivace nádorových supresorů vedou k hromadění genetických změn a karcinogenezi (C.Y. Fan 2001). Vzhledem k zvýšenému kontaktu epitelu, zejména dutiny ústní, s možnými karcinogeny, vykazuje tato oblast zvýšené riziko tvorby maligních lézí a rekurence onemocnění. V důsledku dlouhodobého působení karcinogenu dochází k (místně i časově) náhodnému vzniku mutací u většího množství epiteliálních buněk, které se posléze díky klonální expanzi nezávisle podílejí na vzniku rakoviny v oblasti (tzv. efekt nádorového pole) (Mohan and Jagannathan 2014).

Oproti nekuřákům je u kuřáků vyšší riziko karcinomu laryngu (6,8×), orofaryngu (2×) i karcinomu dutiny ústní (1,4×). Riziko rozvoje HNSCC se zvyšuje s mírou kouření (Hashibe et al. 2007). Pokud pacient po diagnóze či léčbě HNSCC přestane kouřit, jeho délka celkového 5 letého přežití je delší a četnost rekurencí nižší oproti pacientům, kteří v kouření pokračují (van Imhoff et al. 2016).

Konzumace alkoholu je dalším nezávislým rizikovým faktorem pro rozvoj HNSCC (Hashibe et al. 2007). Pro rozvoj nádorů dutiny ústní, hypofaryngu a laryngu je rozhodující intenzita užívání alkoholu, kdežto pro rozvoj nádorů v oblasti orofaryngu je podstatná vyšší intenzita společně s délkou užívání alkoholu (Di Credico et al. 2020).

Kouření a konzumace alkoholu jsou nezávislé rizikové faktory rozvoje HNSCC (Hashibe et al. 2007), avšak současné kouření a užívání alkoholu signifikantně zvyšuje riziko rozvoje nádorového onemocnění. Studie Dal Masa a kol. ukazuje kombinovaný efekt užívání alkoholu a kouření, osoby užívající 89 g ethanolu a zároveň kouřící 10 cigaret denně mají 35× zvýšenou pravděpodobnost rozvoje HNSCC oproti abstinentům a zároveň nekuřákům (Dal Maso et al. 2016).

Nádory virové etiologie

Prevalence HNSCC virové etiologie v čase celosvětově narůstá, z hlediska anatomické lokalizace je virus HPV nejčastěji detekován v nádorech orofaryngu (Stein et al. 2015; Windon et al. 2018). Procento karcinomů orofaryngu indukovaných HR typy HPV je odlišné v různých oblastech světa (téměř 60 % karcinomů v USA, 30 % v Evropě a 4 % v Brazílii), přičemž podobné procento HPV-pozitivních karcinomů je detekováno v oblasti dutiny ústní (11 % v USA, 6 % v Evropě) a laryngu (3 % v USA a 5 % v Evropě) (Castellsague et al. 2016; Anantharaman et al. 2017). V České republice byl ve studii prováděné v letech 2001–2007 HPV detekován u 68 % karcinomů orofaryngu a 17 % karcinomů dutiny ústní (Koslabova et al. 2013). Celosvětový nárůst HPV⁺ HNSCC způsobuje zejména změna sexuálního chování populace, zvýšený počet sexuálních partnerů a zvýšená četnost pohlavního styku jsou rizikovými faktory nákazy HPV (Gillison et al. 2008).

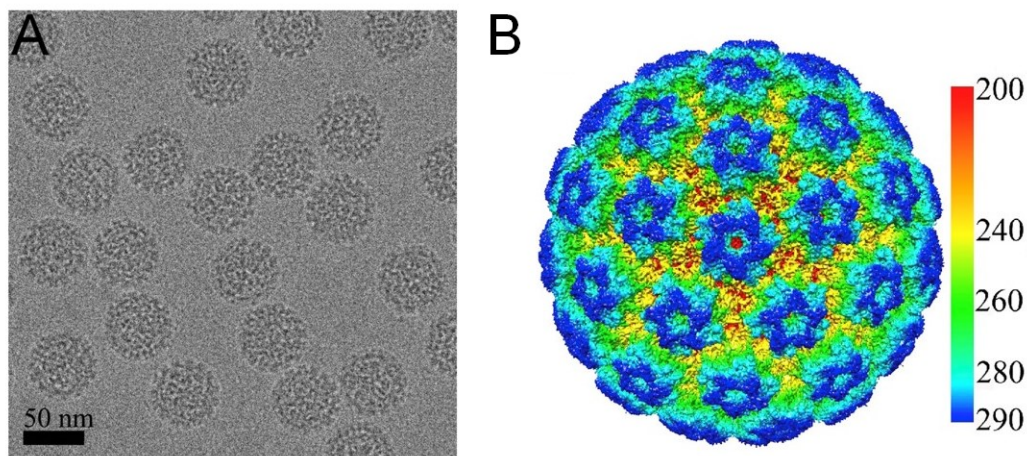
Nejčastěji zastoupeným typem papilomaviru je HPV16, v menší míře jsou detekovány typy HPV18, HPV33, HPV35, HPV45 a další HR typy HPV (Castellsague et al. 2016), přičemž přibližně 95 % nádorů je pozitivních pouze na 1 typ (Anantharaman et al. 2017). Pacienti s HPV⁺ nádory jsou převážně muži a onemocnění bývá častější u pacientů mladšího věku oproti pacientům s nádory HPV-negativními (HPV⁻) (Gillison et al. 2008). Také je pozorována lepší prognóza HPV⁺ pacientů a méně častá rekurence onemocnění, a to bez ohledu na léčebnou modalitu (Koslabova et al. 2013; Ang et al. 2010). Pacienti s HPV⁺ nádory lépe odpovídají na chemoterapii, radioterapii, chemoradioterapii a imunoterapii oproti pacientům s nádory HPV⁻ (J. Wang et al. 2019; Vu et al. 2010). Pro léčbu HNSCC je v současné době dostupná terapie založená na blokádě receptoru PD-1 monoklonálními protilátkami (pembrolizumab, nivolumab) či blokádě EGFR (epidermal growth factor receptor) monoklonální protilátkou cetuximab (Y. Sun et al. 2021).

2.2. Lidský papilomavirus

Obecná charakteristika a klasifikace

Papilomaviry se řadí mezi malé, neobalené, tumorogenní viry s genomem ve formě cirkulární dvouřetězcové DNA. Papilomaviry jsou tkáňově specifické, napadají buňky kůže nebo sliznic. Rodina *Papillomaviridae* zahrnuje 53 rodů (podle databáze International Committee on Taxonomy of Viruses; dostupné online: <https://talk.ictvonline.org/taxonomy/>), přičemž nejvýznamnějšími jsou rody α -, β -, γ -, μ - a ν -papilomavirus, kam patří lidské papilomaviry (de Villiers 2013).

Virion HPV tvoří ikosahedrální kapsida o průměru přibližně 55 nm (obrázek 2). Uvnitř kapsidy se nachází virová DNA, která má velikost přibližně 8 000 párů bází a je asociována s buněčnými histony. Genom HPV se dělí na oblasti časných genů (E, early), pozdních genů (L, late) a regulační oblasti (URR, upstream regulatory region). Časně geny (*E1*, *E2*, *E4*, *E5*, *E6* a *E7*) se exprimují ihned po infekci keratinocytů a umožňují replikaci viru. Pozdní geny (*L1* a *L2*) se exprimují v pozdějších fázích cyklu, proteiny L1 a L2 jsou strukturálními podjednotkami kapsidových pentamer (Zheng and Baker 2006).



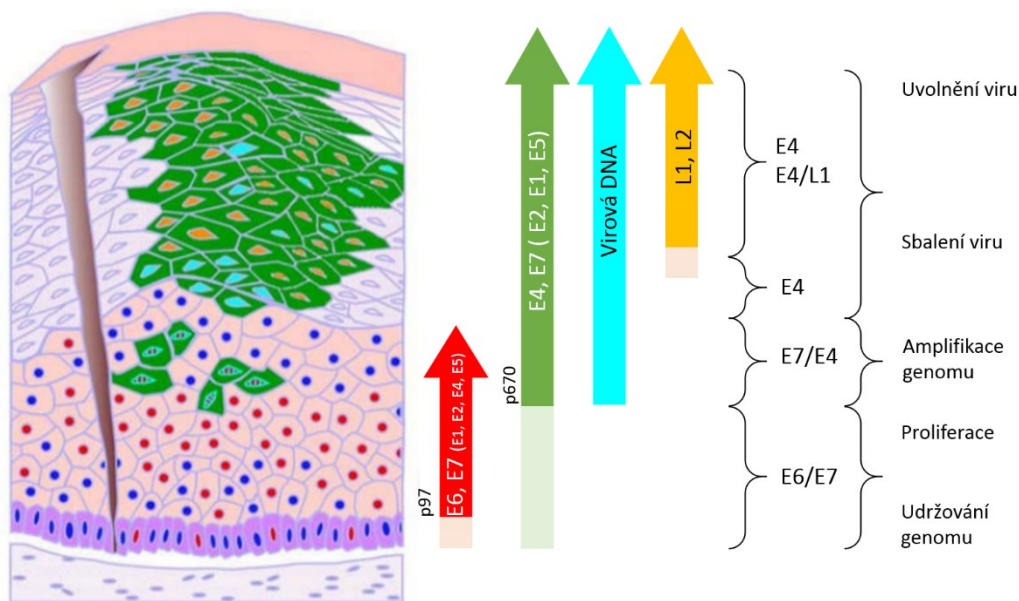
Obrázek 2. Kapsida HPV16. A) Kapsidy HPV16 vizualizované metodou kryo-elektronové mikroskopie. B) Rekonstrukce kapsidy s mapou znázorňující vzdálenost od středu kapsidy (Å). Převzato a upraveno dle Guana a kol. (2017).

Životní cyklus

Životní cyklus viru je úzce spojený s diferenciací bazálních epiteliálních buněk. K infekci HPV dochází v místě mikroporanění kůže nebo sliznice, které umožňuje kontakt virionu s receptory, kterými jsou heparan sulfát proteoglykany (HSPG, heparan sulphate proteoglycans) na povrchu bazální membrány (Shafti-Keramat et al. 2003).

Vazbou kapsidových proteinů L1 na HSPG dochází ke změně konformace kapsidových proteinů a odštěpení N-koncové oblasti L2 furiny, které jsou přítomné na povrchu hostitelské buňky (Day, Lowy, and Schiller 2008). Tím dochází ke změně konformace L2 a odkrytí vazebných míst pro sekundární receptor či receptory, které však v současné době nejsou potvrzeny. Jako jeden z možných sekundárních receptorů byl navrhnout annexin A2 heterotetramer, na který se váže N-koncový úsek L2 (Woodham et al. 2012), avšak novější studie ukazuje úlohu annexin A2 heterotetrameru v post-internalizačním buněčném transportu virionu (Taylor et al. 2018). Po transportu virionů do jádra nediferencovaných, mitoticky aktivních keratinocytů dochází k expresi genů *E1* a *E2*. Monomery proteinu E1 se v komplexu s proteinem E2 váží do místa počátku replikace DNA (ori) a dochází k tvorbě hexamerů, které rozvolňují DNA dvoušroubovici (Bergvall, Melendy, and Archambault 2013). Protein E2 se také váže do oblasti promotoru p97 genů *E6* a *E7* a působí zde jako transkripční faktor (Romanczuk, Thierry, and Howley 1990). Zvyšující se hladina proteinů E5, E6 a E7 umožňuje efektivní replikaci viru. Protein E5 ovlivňuje řadu buněčných procesů, které pomáhají navodit vhodné prostředí pro virovou replikaci (Moody and Laimins 2010). Protein E6 váže p53 a skrze ubiquitin ligázu E6-AP (E6 adaptor protein) jej navádí k degradaci proteasomem (Huibregtse, Scheffner, and Howley 1993). Protein E7 vyvazuje pRb z komplexu s transkripčním faktorem E2F (E2 factor), čímž dochází k navození S-fáze buněčného cyklu. Součinnost těchto tří proteinů umožňuje replikaci viru i v pozdější fázi diferenciaci keratinocytů. V další fázi dochází v terminálně diferencovaných keratinocytech k expresi pozdních genů, jejichž produkty umožňují vznik nových virionů (Moody and Laimins 2010). V pozdní fázi infekce se exprimuje časný protein E4, který se váže na vlákna cytoskeletu, čímž dochází k ruptuře keratinocytu a uvolnění infekčních virionů do okolí (Doorbar et al. 1991) (obrázek 3). Produktivní životní cyklus viru je charakteristický pro infikované buňky, v nichž se virový genom nachází v extrachromozomální formě.

Podle recentních studií však u 88 % cervikálních karcinomů (Kamal et al. 2021) a u 77 % nádorů orofaryngu (Symer et al. 2022) dochází k integraci virového genomu do genomu hostitelské buňky. Důsledkem je přerušení části genetické informace viru, nemožnost tvorby nových virionů a v neposlední řadě zvýšené riziko buněčné transformace (Romanczuk and Howley 1992; Symer et al. 2022).



Obrázek 3. Schéma produktivního životního cyklu HPV 16. V důsledku virové infekce bazálního keratinocyty dochází k postupné expresi časných genů z promotorů p97 a p670 a pozdních genů, sestavení nových virionů a jejich uvolnění do prostředí. Převzato a upraveno podle Zhenga a Bakera (2006).

Onemocnění asociovaná s HPV

Infekce HPV je v lidské populaci běžná a v převážném počtu případů bezpříznaková. Papilomaviry však mohou vyvolávat různě závažná onemocnění, HR typy HPV jsou asociovány s nádorovými onemocněními. Nízce rizikové (LR) typy HPV, mezi které patří HPV6, 11, 40, 42, 43, 44, 54 či 61, způsobují benigní onemocnění, jako jsou kožní a genitální bradavice, či léze v oblasti dutiny ústní. V současné době je popsáno 14 HR HPV typů, a to HPV 16, 18, 31, 33, 35, 39, 45, 51, 52, 56, 58, 59, 66 a 68, které mohou způsobovat maligní onemocnění, jako jsou karcinomy hrdla děložního, penisu, vagíny, vulvy, anu a karcinomy v oblasti hlavy a krku (Arbyn et al. 2021; Kreimer et al. 2005). Prevalence jednotlivých typů HPV je geograficky odlišná, avšak dominantním typem v oblasti hlavy a krku i hrdla děložního je HPV16 (Castellsague et al. 2016; Li et al. 2011; Kreimer et al. 2005).

Nejčastějším karcinomem anogenitální oblasti je karcinom hrdla děložního. Až u 100 % cervikálních karcinomů je přítomna infekce HPV, přičemž nejčastějšími typy jsou HPV16 a HPV18 (Li et al. 2011). Tyto dva typy HPV jsou nejčastěji detekovány i u ostatních karcinomů anogenitální oblasti (de Martel et al. 2017). V České republice jsou typy HPV16/18 přítomny u 76 % cervikálních karcinomů, 25 % vulválních a 82 % análních karcinomů (Tachezy et al. 2011).

Dále je HPV kofaktorem onemocnění Epidermodysplasia verruciformis (EV). Toto dědičné onemocnění je charakteristické mutacemi v genech *EVER1*, *EVER2* a *CIB1* (calcium- and integrin-binding protein 1), které usnadňují infekci HPV z rodu β (zejména HPV3, 5, 8 a 10) (de Jong, Créquer, et al. 2018). Onemocnění se projevuje četnými kožními lézemi a vysokou pravděpodobností rozvoje nemelanomového karcinomu kůže (de Jong, Imahorn, et al. 2018).

Mechanismy kancerogeneze

Virem indukovaná kancerogeneze je náhodný proces, který může být navozen několika mechanismy. HPV kódují onkogeny *E6* a *E7*, jejichž produkty, onkoproteiny E6 a E7, mají transformační potenciál *in vitro* i *in vivo*. Protein E6 skrze vazbu s ubiquitin ligázou E6-AP váže p53, což vede k jeho proteasomální degradaci (Huibregtse, Scheffner, and Howley 1993). Degradace p53 má za následek snížení účinnosti oprav DNA a umožňuje replikaci poškozených buněk, u nichž by za normální situace byla indukována apoptóza (Ozaki and Nakagawara 2011). Protein E6 dále aktivuje transkripci telomerázové reverzní transkriptázy, a to indukcí c-Myc (myelocytomatosis), který uvolňuje represivní faktory z promotoru transkriptázy. Aktivovaná telomeráza je jedním z faktorů, které se podílí na imortalizaci buněk (McMurray and McCance 2003). Protein E7 se podílí na degradaci pRb, p107 a p130, jež patří do rodiny proteinů inaktivujících transkripční faktor E2F (Gonzalez et al. 2001). Protein E7 vyvazuje pRb z komplexu s transkripčním faktorem E2F, volný E2F se podílí na navození a udržení S-fáze buněčného cyklu (Chellappan et al. 1992).

Hladinu virových onkoproteinů E6 a E7 za normálních okolností reguluje protein E2, a to na úrovni iniciace transkripce onkogenů (Romanczuk, Thierry, and Howley 1990). V časně fázi infekce, kdy je hladina proteinu E2 nízká, se E2 váže do vysokoafinitních vazebných míst (E2BS, E2 binding sites) promotoru a funguje jako transkripční aktivátor *E6* a *E7* genů. Tím dochází k nárůstu hladiny virových onkoproteinů a zároveň nárůstu hladiny E2. V pozdější fázi, kdy je množství E2 vysoké, dochází k vazbě do nízkoafinitních E2BS, což má za následek represí transkripce *E6* a *E7* a zajištění regulované hladiny virových onkoproteinů (Romanczuk, Thierry, and Howley 1990). Funkce proteinu E2 je tedy stěžejní pro zajištění produktivního životního cyklu a narušení tohoto kontrolního mechanismu může vést ke kancerogenezi, neboť kontinuální exprese virových onkogenů je nezbytná pro navození a udržení

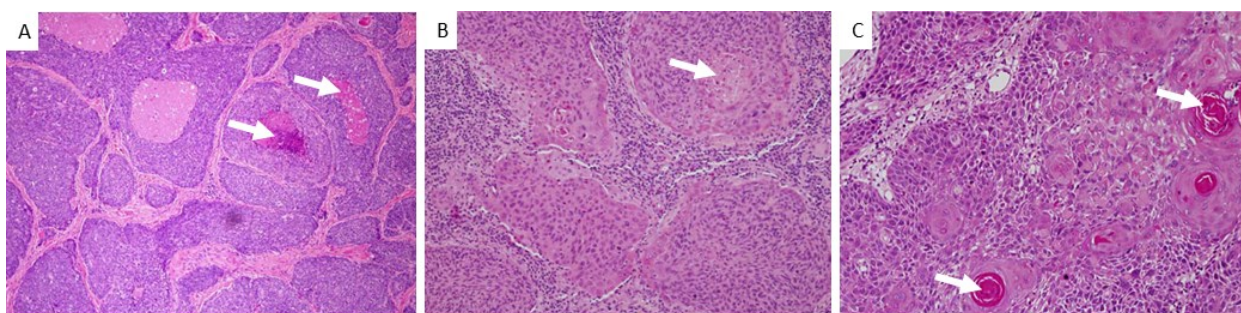
transformovaného fenotypu (J.T. Chang et al. 2010; Romanczuk and Howley 1992). Jedním z mechanismů vedoucím ke ztrátě proteinu E2 je virová integrace, při níž může dojít k narušení otevřeného čtecího rámce *E2* (ORF, open reading frame) (Choo, Pan, and Han 1987; Pinatti et al. 2021). K přerušení virového genomu integrací ale dochází rovnoměrně v rámci celé virové DNA (Symer et al. 2022). Místa integrace do hostitelské DNA jsou také náhodná, jsou však popsána s větší četností ve fragilních místech chromozomů a místech rozvolněného chromatinu (Akagi et al. 2014; Symer et al. 2022). V karcinomech orofaryngu jsou pozorovány časté integrace v blízkosti genů *TP63*, *SOX2* (sex determining region Y-box 2), *FGFR* (fibroblast growth factor receptor), *Myc* a *KLF5* (intestinal-enriched Krueppel-like factor 5), jejichž produkty se podílí na udržení fenotypu kmenových buněk, a v blízkosti genu pro PD-L1 (programmed death ligand 1), který se uplatňuje v protinádorové imunitě. Integrace v blízkosti zmíněných genů vede k jejich masivní amplifikaci, růstové výhodě buněk a podpoře kancerogeneze (Symer et al. 2022).

V části cervikálních karcinomů a karcinomů hlavy a krku se však virový genom nachází v extrachromozomální formě, tudíž s intaktním virovou DNA (Pokrývková et al. 2019; D. Hong et al. 2017). Ukazuje se, že karcinomy s extrachromozomální formou viru mají podobný vzor transkripce (včetně transkripce *E6/E7*) jako karcinomy s integrovanou formou genomu, v některých epizomech dochází k přerušení a přeskupení genomu, převážně v oblasti ORF *E1/E2* (Rossi et al. 2023). Již v prvopočátcích studia funkce proteinů E2 byl popsán vliv mutací v ORF *E2* na zvýšený transformační potenciál *in vitro* (Romanczuk and Howley 1992). Dalším popsáním mechanismem kancerogeneze je metylace E2BS, která zabraňuje vazbě E2 do E2BS, čímž nedochází k represí transkripce *E6* a *E7* (Chaiwongkot et al. 2013). Na stabilní hladinu onkoproteinů má také vliv zvýšená nálož viru v buňkách s extrachromozomální formou genomu (D. Hong et al. 2017; Mir et al. 2023; Anayannis et al. 2018).

2.3. Nádorové mikroprostředí HNSCC

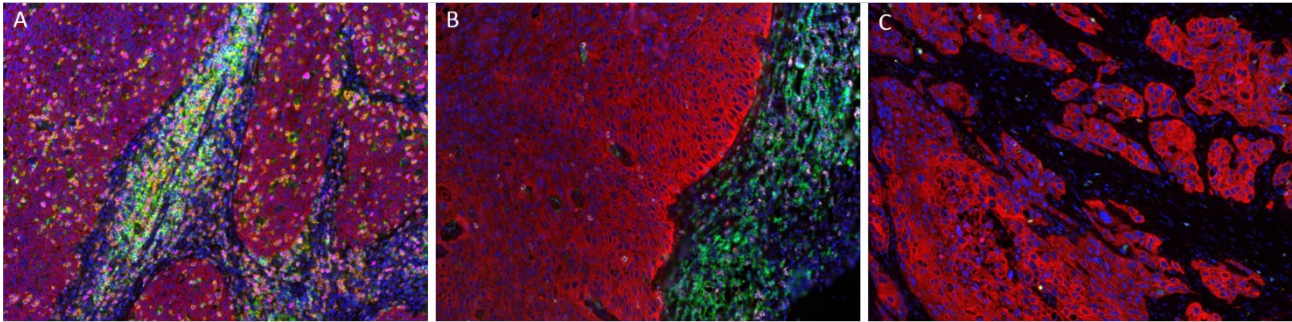
Vzhledem k rozdílným charakteristikám HNSCC virové a nevirové etiologie předpokládáme i různé buněčné složení nádorů, zejména rozdílné zastoupení imunitních buněk a tím pádem rozdílnou protinádorovou imunitní odpověď.

Z histologického hlediska u HPV⁺ pacientů detekujeme nekeratinizující typ karcinomu s četnými nekrotickými oblastmi (obrázek 4A) nebo hybridní variantu s částečnou keratinizací (fokální oblasti keratinocytické maturace, obrázek 4B). Na histologickém snímku HNSCC nevirové etiologie (obrázek 4C) lze detekovat oblasti s vysokou produkcí keratinu, tzv. keratinové perly („keratin pearls“), keratinizace v oblastech nádorového parenchymu je typická právě pro HPV⁻ HNSCC (El-Mofty, Zhang, and Davila 2008).



Obrázek 4. Histologické snímky HPV⁺ a HPV⁻ HNSCC A) Nekeratinizující HPV⁺ karcinom s nekrotickými oblastmi (označeno šipkou), B) částečně keratinizující (označeno šipkou) HPV⁺ karcinom, C) keratinizující HPV⁻ karcinom. Oblasti keratinizace jsou označeny bílou šipkou. Převzato a upraveno dle El-Mofty, Zhanga a Davily (2008).

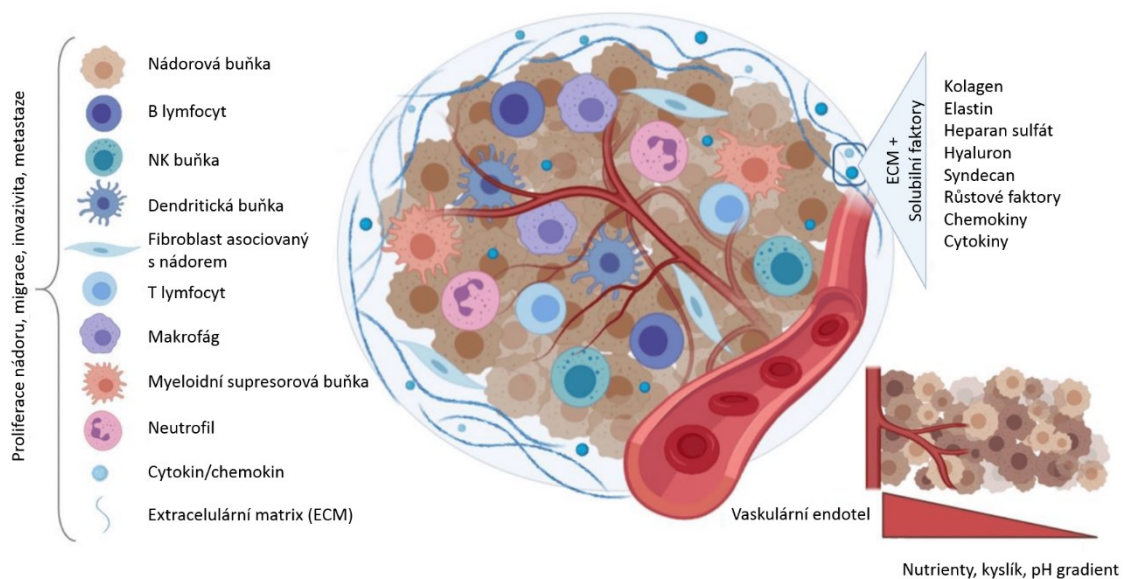
Z hlediska zastoupení imunitních buněk v nádorovém parenchymu a stroma se nádory rozdělují na několik skupin, a to na zánětlivé, imunitně vyloučené a imunitně pusté (obrázek 5). Karcinomy s vysokou hladinou parenchymálních a stromálních lymfocytů se označují jako zánětlivé. Jako imunitně vyloučené se značí karcinomy s vyšší hladinou stromálních lymfocytů a zároveň nízkou parenchymální hladinou lymfocytů a jako imunitně pusté se značí karcinomy se zanedbatelnou parenchymální i stromální hladinou lymfocytů (D.S. Chen and Mellman 2017). Dle této metodiky mohou být HNSCC rozděleny podle hladiny CD3⁺ (cluster of differentiation 3) T lymfocytů (Brooks et al. 2019) či CD8⁺ T lymfocytů (Echarti et al. 2019). Podobně dle studie Zenga a kol. mohou být karcinomy orofaryngu rozřazeny dle hladiny mRNA CD3, IRF4 (interferon regulatory factor 4) a ZAP70 (zeta-chain-associated protein kinase 70) na imunitně bohaté, imunitně pusté a smíšeného typu (P.Y.F. Zeng et al. 2022).



Obrázek 5. Skupiny karcinomů hlavy a krku dle imunitní infiltrace. A) Typ zánětlivého karcinomu s výraznou parenchymální (červeně) a stromální infiltrací CD4⁺ (zeleně) a CD8⁺ (oranžově) T lymfocytů. B) Typ imunitně vyloučeného karcinomu s vysokou hladinou stromálních CD4⁺ (zeleně) a CD8⁺ (růžově) T lymfocytů, v oblasti nádorového parenchymu (červeně) je hladina lymfocytů nízká. C) Typ imunitně pustého karcinomu s minimálním zastoupením lymfocytů ve stroma i parenchymu (červeně). Jádra buněk označena modře (DAPI, 4',6-diamidino-2fenyindol). Autor fotografií: Mgr. Barbora Pokrývková.

Obecná charakteristika TME

Nádorové mikroprostředí je složitý systém, který vzniká interakcemi buněk nádorového parenchymu a stroma. Stroma tvoří imunitní buňky a buňky, které jsou důležité pro výživu nádoru nebo mají podpůrnou funkci, jako jsou fibroblasty asociované s nádory (CAF, cancer associated fibroblasts), endoteliální buňky a extracelulární matrix (obrázek 6). Tyto buňky nebývají nijak geneticky alterované, do oblasti nádoru jsou atrahovány produkcí cytokinů a chemokinů transformovanými buňkami a buňkami TME. Nežádka zde plní svou fyziologickou funkci, čímž však přispívají k progresi nádoru. Oproti tomu, buňky nádorového parenchymu nekontrolovatelně proliferují, což je umožněno neschopností imunitního systému rozeznat tyto buňky jako poškozené a nebezpečné a spustit adekvátní imunitní reakci (Hanahan and Weinberg 2011).



Obrázek 6. Buněčná struktura nádorového mikroprostředí. V nádorovém mikroprostředí se nachází řada typů imunitních buněk, buňky nádorového parenchymu, fibroblasty, endotelové buňky, extracelulární matrix a řada cytokinů a chemokinů. Převzato a upraveno dle Pinta a kol. (2020).

Imunitní buňky TME

Makrofágy asociované s nádory

Nejpočetnější skupinu imunitních buněk představují makrofágy asociované s nádory (TAM, tumor associated macrophages). Makrofágy jsou buňky zajišťující homeostázu prostředí, mají schopnost fagocytózy apoptotických buněk a zároveň jsou to buňky prezentující antigeny (Gordon 2007). TAM je velmi heterogenní skupinou buněk, a i přes velmi rozsáhlý výzkum jsou některé jejich charakteristiky stále předmětem vědeckých diskuzí.

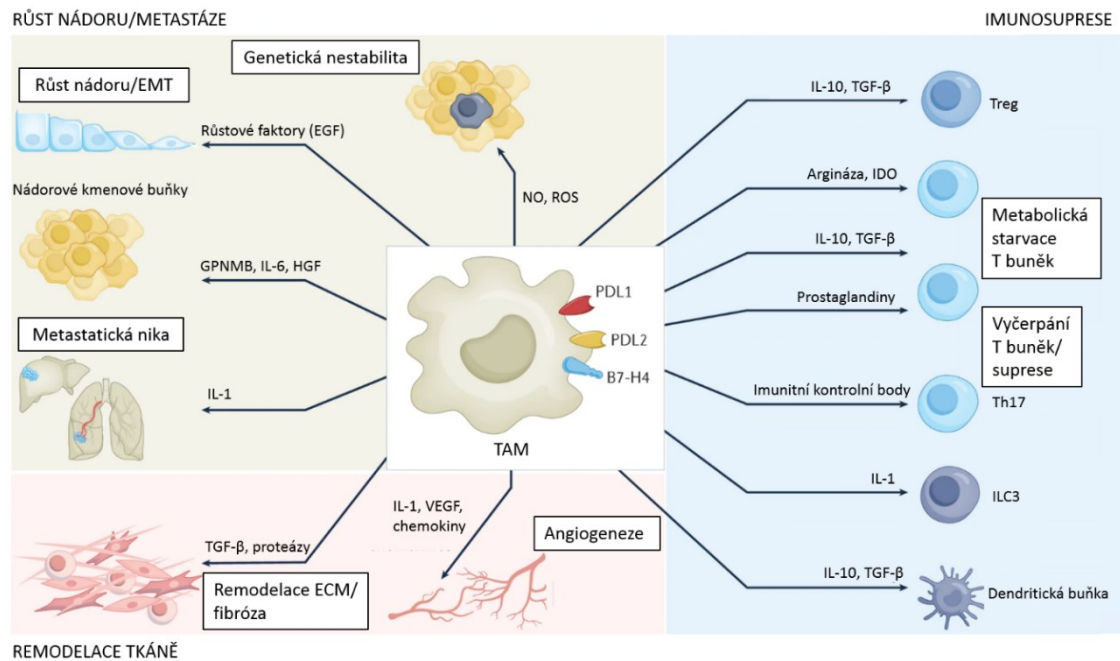
TAM majoritně diferencují z cirkulujících monocytárních prekurzorů vznikajících v kostní dřeni, pouze malá část TAM vzniká diferenciací tkáňově rezidentních makrofágů (Mantovani et al. 2022). Prekurzory TAM jsou cíleny do TME pomocí chemoatraktantů, které produkují buňky stroma či samotné nádorové buňky, a v závislosti na cytokinovém prostředí dochází k jejich diferenciaci a polarizaci. Je však nutné podotknout, že podobně jako u aktivovaných makrofágů v normálních tkáních, polarizace TAM v nádorech není striktní a jejich fenotyp je velmi plastický. Přechody mezi jednotlivými fenotypy makrofágů jsou výsledkem dynamiky okolního mikroprostředí, především změn v produkci cytokinů. Přesto se pro zjednodušení

makrofágy rozdělují na fenotypy M1 a M2, přičemž většina TAM má fenotyp podobný M2 (Aras and Zaidi 2017; Sica and Mantovani 2012). S vysokou heterogenitou a plasticitou TAM souvisí i jejich obtížná detekce a kvantifikace v biologických vzorcích. Nejčastěji se makrofágy detekují pomocí pan-makrofágového znaku CD68 společně se znaky rozlišující mezi typy M1 (zejména HLA-DR (human leukocyte antigen-DR isotype), NOS2 (NO synthase 2)) a M2 (CD163, CD204, CD206) (Jayasingam et al. 2019).

Makrofágy typu M1 mají v TME prozánětlivou a protinádorovou funkci. K polarizaci na fenotyp M1 dochází v přítomnosti IFN- γ (interferon- γ), TNF- α (tumor necrosis factor- α) či ligandů TLR (toll-like receptor). Naproti tomu, makrofágy M2 se vyznačují protizánětlivými a protumorogenními vlastnostmi. Fenotyp M2 je získáván v přítomnosti TGF- β (tumor growth factor β), IL-4 (interleukin), IL-10, IL-13, jež produkují nádorové a stromální buňky, či samotné makrofágy (Mantovani et al. 2004). Jak už z výše uvedeného vyplývá, role makrofágů v TME je duální (obrázek 7). V časných stádiích převažuje prozánětlivá a cytotoxická role makrofágů (odpovídá fenotypu M1), která je spojená s produkcí prozánětlivých cytokinů (IL-1, IL-6, IL-12, TNF- α) a silnou produkcí reaktivních kyslíkových radikálů (ROS, reactive oxygen species) či NO. S narůstající progresí nádorů převažuje fenotyp M2 a s tím spojená imunosupresivní a tumor podporující role makrofágů (Sica and Mantovani 2012; J. Liu et al. 2021). TAM podporují proliferaci a invazivitu nádorů na mnoha úrovních: podporou angiogeneze produkcí VEGF (vascular endothelial growth factor) či remodelací tkáně, na které se podílejí matrixové metaloproteinázy (MMP, matrix metalloproteinases), jako jsou např. MMP-2, MMP-9 či MMP-13 (Rosenthal and Matrisian 2006; Du et al. 2006). Cytokiny produkované TAM (např. TGF- β , IL-10) regulují imunitní odpověď a nastolují protizánětlivé prostředí (Aras and Zaidi 2017). Dalšími imunosupresivními molekulami TAM jsou IDO1 (indoleamine 2,3-dioxygenase 1), COX-2/PTGS2 (cyclooxygenase-2/prostaglandin-endoperoxide synthase 2) nebo ARG1 (arginase 1) (Struckmeier et al. 2023; Che et al. 2017; C.I. Chang, Liao, and Kuo 1998).

V oblasti hlavy a krku jsou výsledky detekce TAM nekonzistentní, dle výsledků některých studií se makrofágy M2 nachází ve zvýšené míře ve stroma nádorů HPV⁻ oproti stroma nádorů HPV⁺ (Ou et al. 2019; Pokrývková et al. 2021), naopak více parenchymálních M2 a PD-L1⁺ M2 popisuje Tosi a kol. u karcinomů HPV⁺ ve srovnání s karcinomy HPV⁻ (Tosi et al. 2022), ale zároveň ukazuje silnější infiltraci TAM

ve stroma ve srovnání s nádorovým parenchymem bez ohledu na etiologii nádoru (Tosi et al. 2022; Pokrývková et al. 2021).



Obrázek 7. Přehled vlivu TAM na rozvoj nádoru. TAM způsobují genetickou nestabilitu působením NO a ROS na DNA buněk. Produkci růstových faktorů jako je EGF (epidermal growth factor) podporují proliferaci nádoru a produkci IL-6, HGF (hepatocyte growth factor) a GPNMB (glycoprotein non-metastatic melanoma protein B) podporují expanzi nádorových kmenových buněk. TAM dále přispívají k metastatickému šíření (IL-1 a TGF-β), k remodelaci extracelulární matrix (ECM) a k patologické fibróze (TGF-β a MMP) a významně podporují angiogenezi (produkce VEGF a proangiogenních chemokinů). TAM také podporují vznik imunosupresivního prostředí sekrecí IL-10, TGF-β, prostaglandinů, ARG1 a IDO-1, což vede k expanzi regulačních T lymfocytů (Treg), navození tolerogenního stavu dendritických buněk a metabolickému hladovění T lymfocytů. Vysoká exprese molekul imunitního kontrolního bodu (PD-L1, PD-L2, B7-H4) vede k vyčerpání T lymfocytů. Převzato a upraveno podle Mantovani a kol. (2022).

Neutrofilny asociované s nádory

Podobně jako TAM, i neutrofilny asociované s nádory (TAN, tumor associated neutrophils) představují buněčnou populaci, která má v TME duální funkci. Tyto buňky vznikají z myeloidního prekursoru. Působením cytokinů a chemokinů, či v důsledku genetické nestability TME, migrují cirkulující neutrofilny do oblastí nádorů, kde mění svůj fenotyp na TAN. Další společnou vlastností TAM a TAN je jejich obrovská plasticita a schopnost polarizace v závislosti zejména na hladině IFN- γ a TGF- β (Fridlender et al. 2009; Andzinski et al. 2016). Protnádorová funkce TAN se pojí s produkcí ROS a neutrofilové elastázy (NE, neutrophil elastase), které působí cytotoxicky na nádorové

buňky, zejména v časných stádiích onemocnění (Jaganjac et al. 2012; Fridlender et al. 2009). Na druhou stranu, v prostředí s vysokou hladinou TGF- β , se NE společně s MMP-9 podílí na degradaci okolní tkáně a extracelulární matrix, angiogenezi a nádorové progresi (Dumitru et al. 2012).

Orofaryngeální karcinomy pacientů s HPV⁻ karcinomy obsahují větší množství neutrofilů oproti HPV⁺ karcinomům (X. Liu et al. 2022; Tosi et al. 2022), avšak studie Qureshiho a kol. (2022), analyzující karcinomy dutiny ústní a orofaryngu, neukazuje rozdíly v počtu neutrofilů mezi karcinomy HPV⁺ a HPV⁻. Na úrovni genové exprese nádory HPV⁺ vykazují sníženou expresi genů souvisejících s chemotaxí neutrofilů (Tosi et al. 2022). Vliv TAN na prognózu pacientů závisí na typu nádoru. Zvýšená četnost intratumorálních TAN se pojí s horším přežíváním pacientů s hepatocelulárním karcinomem, hepatálním cholangiokarcinomem, nemalobuněčným karcinomem plic, renálním karcinomem i s karcinomem hlavy a krku v oblastech orofaryngu, hypofaryngu, laryngu i dutiny ústní (Shen et al. 2014; Lonardi et al. 2021). Na druhou stranu, zvýšená hladina TAN se pojí s lepším přežíváním pacientů s nediferencovaným pleomorfním sarkomem či pacientů s kolorektálním karcinomem, pravděpodobně vzhledem k silné expresi IFN- γ v těchto nádorech (Ponzetta et al. 2019).

Myeloidní supresorové buňky

Myeloidní supresorové buňky (MDSC, myeloid-derived suppressor cells) jsou buňky vznikající z myeloidního prekurzoru, pro něž je typická silná produkce ROS, NO, ARG1 a inhibičních cytokinů (W. Ren et al. 2020; Corzo et al. 2010). Působením chemokinů TME infiltrují nádor, kde tlumí protinádorovou imunitní odpověď (Kumar et al. 2016). Oproti MDSC v periférii v TME narůstá jejich supresivní aktivita, a to zejména zvýšenou expresí supresivních genů, např. *ARG1* a *NOS2* (Corzo et al. 2010). V posledních letech bylo prokázáno, že se část MDSC (monocytické MDSC) po infiltraci do TME diferencuje v TAM (Kwak et al. 2020). Další část MDSC (polymorfonukleární MDSC) má v TME totožné vlastnosti jako TAN a v současnosti neznáme znaky, kterými by bylo možné je odlišit (Bronte et al. 2016). Zároveň je předmětem diskuze, jak a zda od sebe polymorfonukleární MDSC a TAN rozlišit (Quail et al. 2022; Antuamwine et al. 2023).

V mikroprostředí nádorů MDSC inhibují funkci CD8⁺ lymfocytů T a přitahují Treg do TME, což vede k potlačení protinádorové imunitní odpovědi (Jiang et al. 2023;

Schlecker et al. 2012). Vysoká infiltrace MDSC je spojená s horším celkovým přežíváním pacientů s HNSCC (Jiang et al. 2023).

Dendritické buňky

Dendritické buňky (DC, dendritic cells) jsou heterogenní populací buněk prezentujících antigen. Vznikají z myeloidního prekursoru v kostní dřeni. Po stimulaci jejich receptorů pomocí molekul asociovaných s patogeny (PAMPs, pathogen-associated molecular patterns), jako jsou virové nukleové kyseliny, proteiny buněčné stěny a lipopolysacharidy, nebo poškozením tkáně (DAMPs, danger-associated molecular patterns) dochází k maturaci DC, které migrují do lymfatických uzlin. Zde posléze iniciují $CD4^+$ a $CD8^+$ T-buněčnou odpověď skrze vystavení pohlceného antigenu na svých glykoproteinech MHC I a II (major histocompatibility complex I, II) a prezentací kostimulačních molekul T lymfocytům (Savina and Amigorena 2007).

Lidské DC se dělí na několik skupin, které se liší svými funkcemi, a to klasické DC (podskupiny cDC1, cDC2), MoDC (DC odvozené z monocytů), plasmacytoidní DC (pDC) či epiteliální Langerhansovy buňky (LC, Langerhans cells). Aktivované cDC1 a cDC2 jsou buňky s výraznou schopností prezentace antigenu, zatímco aktivované pDC jsou silnými producenty IFN-I, účinného protinádorového cytokinu (Collin and Bigley 2018).

DC migrují i do oblasti TME, kde procesují tumor specifické antigeny a pomocí křížové prezentace skrze MHC I indukují protinádorovou $CD8^+$ T-buněčnou imunitu (Tel et al. 2013). Na druhou stranu, mnohé studie ukazují alterovanou funkci DC v TME a jejich sníženou schopnost indukce imunitní odpovědi. V případě HNSCC indukovaných HPV alterací funkce DC způsobuje činnost onkoproteinů E6 a E7. Virové onkoproteiny inhibují transkripci MIP-3 α (macrophage inflammatory protein 3 α), který funguje jako chemoatraktant prekursorů LC (Guess and McCance 2005) a v nádorovém parenchymu HPV⁺ HNSCC je nižší infiltrace LC, oproti parenchymu nádorů HPV⁻. Vyšší počet LC ve stroma se pojí s lepším celkovým přežíváním pacientů a je charakterizován jako silný nezávislý prognostický faktor pacientů s HNSCC (Kindt et al. 2016).

Rozdílné cytokinové prostředí pacientů HPV⁺ a HPV⁻ ovlivňuje funkci pDC, jakožto silných producentů IFN-I (Kalb et al. 2012). Ukazuje se, že pDC HPV⁺ pacientů mají srovnatelnou schopnost produkce IFN-I jako pDC izolované z nenádorové tonsilární

tkáně, kdežto pDC HPV⁻ pacientů vykazují sníženou produkci IFN-I, což je důsledkem vyšší produkce imunopresivních cytokinů (IL-10, TNF- α) u těchto pacientů (Koucký et al. 2021). Protinádorovou funkci pDC dále negativně ovlivňuje hypoxie, neboť za hypoxických podmínek dochází ke snížení hladiny pDC, a to inhibicí transkripčního faktoru E2-2, který se podílí na diferenciaci pDC z prekurzorů (Weigert et al. 2012). Hypoxické prostředí dále vede ke snížení produkce IFN-I pDC a zároveň pDC podporují aktivaci Treg (Weigert et al. 2012; Pang et al. 2021). Role pDC v karcinogenezi je tedy duální a jak bylo zmíněno výše, je též ovlivněna přítomností virových onkoproteinů.

Tumor infiltrující lymfocyty

Mezi tumor infiltrující lymfocyty (TIL) se řadí skupina CD4⁺ T lymfocytů, CD8⁺ T lymfocytů, $\gamma\delta$ T lymfocytů, B lymfocytů a NK (natural killer) buněk, které se nacházejí v oblasti TME.

CD4⁺ T lymfocyty rozdělujeme na pomocné (Th, helper T cell), Treg a minoritní populace, jako jsou folikulární pomocné lymfocyty, Th17, Th22 a CD4⁺ cytotoxické T lymfocyty. Aktivované Th lymfocyty v závislosti na cytokinovém prostředí diferencují na lymfocyty Th1 či Th2. Lymfocyty Th1 diferencují za přítomnosti IFN- γ a IL-12, produkují IFN- γ , TNF- α a IL-2 a napomáhají aktivaci makrofágů a CD8⁺ T lymfocytů, což představuje účinnou obranu proti intracelulárním patogenům. Naproti tomu lymfocyty Th2 diferencují za přítomnosti IL-2 a IL-4, produkují cytokiny IL-2, IL-4 či IL-10 a podporují humorální imunitu aktivací B lymfocytů, aktivují eozinofily či NK buňky (L. Sun et al. 2023). Zvýšená hladina CD4⁺ T lymfocytů se v mnoha studiích popisuje u HNSCC HPV⁺ ve srovnání s pacienty s HPV⁻ HNSCC (Oguejiofor et al. 2017; Nordfors et al. 2013; Wood et al. 2016; Tosi et al. 2022). Zároveň T lymfocyty nádorů HPV⁺ vykazují větší diverzitu v TCR (T cell receptor) oproti nádorům HPV⁻ (J. Wang et al. 2019).

Populace Treg se podílí na regulaci imunitní odpovědi, brání autoimunitním reakcím, a to utlumením proliferace efektorových T lymfocytů. Tento typ lymfocytů charakterizuje zejména exprese znaků CD25 a intracelulárního FOXP3 (forkhead box P3) (Fontenot, Gavin, and Rudensky 2003). Regulační funkci Treg umožňuje exprese supresivních cytokinů IL-10 a TGF- β a molekul CTLA4 (cytotoxic T-lymphocyte associated protein 4) a Tim-3 (T-cell immunoglobulin and mucin-domain containing-3), kterými snižují aktivaci T lymfocytů (L. Sun et al. 2023). Další významnou molekulou

Treg je ICOS (inducible T cell costimulator), který podporuje transkripci FOXP3, a tím i supresivní aktivitu Treg (Q. Chen et al. 2018). Ukazuje se, že hladina Treg je v HNSCC HPV⁺ a HPV⁻ srovnatelná (Poropatich et al. 2017; Tosi et al. 2022). V karcinomech orofaryngu je vzdálenost Treg vůči CD8⁺ T lymfocytům v nádorovém parenchymu a stroma nižší v nádorech HPV⁺ oproti HPV⁻ (Tosi et al. 2022).

Mezi CD8⁺ T lymfocyty se řadí efektorové lymfocyty, vyčerpané („exhausted“) lymfocyty, paměťové lymfocyty, či tkáňově rezidentní paměťové lymfocyty. Vazbou antigenu navázaném na MHCI antigen prezentující buňky a dalšími kostimulačními mechanismy dochází k aktivaci CD8⁺ T lymfocytů. Jejich efektorové funkce jsou cytotoxické, produkují IFN- γ , TNF- α a sekretují granzymy a perforiny, což vede k apoptóze cílové buňky, a dělá z nich účinnou protinádorovou zbraň (L. Sun et al. 2023). Vyšší parenchymální i stromální infiltrace CD8⁺ T lymfocytů je mnohými studii pozorována u pacientů HPV⁺ oproti pacientům HPV⁻ (Qureshi et al. 2022; Oguejiofor et al. 2017; Partlova et al. 2015; J. Wang et al. 2019; Pokrývková et al. 2022). V nádorech HPV⁺ se vyskytuje více CD8⁺ T lymfocytů lokalizovaných v blízkosti makrofágů M1 a M2, dále CD8⁺ T lymfocyty lokalizované ve stroma čteněji interagují s nádorovými buňkami oproti nádorům HPV⁻ (Qureshi et al. 2022; Xu et al. 2020; Tosi et al. 2022). Podobně v nádorovém parenchymu i stroma HPV⁺ HNSCC se ve zvýšené míře (oproti HPV⁻ HNSCC) nacházejí CD8⁺ T lymfocyty v blízkosti B lymfocytů, vyšší hladina takto lokalizovaných lymfocytů koreluje s vyšší hladinou HPV16 E6/E7-specifických CD8⁺ T lymfocytů u těchto pacientů (Hladíková et al. 2019). Xu a kol. v kohortě HPV⁻ HNSCC popisuje několik vzorů, jakými lze charakterizovat infiltraci nádorů CD8⁺ lymfocyty, zatímco u většiny nádorů parenchym vykazuje silnou infiltraci CD8⁺ T lymfocyty, v oblasti stroma pozoruje velmi variabilní hladinu infiltrace (Xu et al. 2020).

Minoritní skupinou TIL jsou $\gamma\delta$ T lymfocyty, které rozpoznávají antigen mechanismem nezávislým na MHCI, díky čemuž rozeznávají širší škálu antigenů (cizorodých i tělu vlastních). Vzhledem k těmto vlastnostem se v současné době hojně studuje jejich protinádorový potenciál (Hu et al. 2023). Vysoká hladina $\gamma\delta$ T lymfocytů se v HNSCC pojí se silnější infiltrací CD4⁺, CD8⁺ T lymfocyty a B lymfocyty. Zároveň se vyšší hladina $\gamma\delta$ T lymfocytů pojí s lepším přežíváním pacientů s HNSCC (Lu et al. 2020).

Podobné cytotoxické efektorové funkce jako CD8⁺ T lymfocyty mají NK buňky. NK buňky jsou efektorové lymfocyty vrozeného imunitního systému, jejich imunitní odpověď je nespecifická. Jsou to producenti IFN- γ a TNF- α , a produkce těchto faktorů

aktivuje makrofágy, DC i T lymfocyty (Paul and Lal 2017). Na úrovni genové exprese HPV⁺ nádory vykazují zvýšenou exprese genů asociovaných s NK buňkami, oproti nádorům HPV⁻ (Tosi et al. 2022).

B lymfocyty zahrnují antigen prezentující B lymfocyty, plazmatické buňky a regulační B buňky (Breg) (Wei et al. 2021). B lymfocyty jsou zodpovědné za humorální imunitní odpověď, plazmatické buňky jsou producenty specifických protilátek. Aktivaci a přeměně B lymfocytu na plazmatickou buňku napomáhají pomocné folikulární T lymfocyty (L. Sun et al. 2023). B lymfocyty mohou také v menší míře prezentovat antigeny CD4⁺ T lymfocytům (Rodríguez-Pinto 2005). Populace Breg se podílí na imunitní regulaci, a to produkcí IL-10 (Wei et al. 2021). V HNSCC se vyšší infiltrace B lymfocytů v oblasti parenchymu a stroma nachází u nádorů HPV⁺ ve srovnání s nádory HPV⁻ (Qureshi et al. 2022; Hladíková et al. 2019). Na úrovni genové exprese se u HPV⁺ nádorů silněji exprimují geny podílející se na aktivaci B lymfocytů oproti nádorům HPV⁻ (Wood et al. 2016; J. Wang et al. 2019; Hladíková et al. 2019). Naproti tomu se ukazuje, že hladina Breg je v nádorech HPV⁺ a HPV⁻ podobná (S. Zhang, Wang, Ma, et al. 2021).

Na povrchu TIL se vyskytují receptory pro kontrolní inhibitory, jako je PD-1, CTLA4, Tim-3, LAG3 (lymphocyte-activation gene 3), OX40, GITR (glucocorticoid-induced TNFR-related protein) nebo BTLA (B- and T-lymphocyte attenuator) (He and Xu 2020). Nádorová tkáň HNSCC obsahuje vyšší hladinu lymfocytů s PD-1, CTLA4, GITR nebo OX40 znaky ve srovnání s lymfocyty s těmito znaky v periferní krvi těchto pacientů (Puntigam et al. 2020; Poropatich et al. 2017). Imunoterapie založená na blokadě PD-1/PD-L1 je slibnou terapií pro léčbu HNSCC, přičemž pacienti HPV⁺ lépe odpovídají na tuto léčbu oproti pacientům HPV⁻ (J. Wang et al. 2019). Obecně se na základě analýzy transkriptomu HNSCC různé etiologie ukazuje, že v nádorech HPV⁺ je v důsledku přítomnosti viru podporováno zánětlivé prostředí manifestované zvýšenou infiltrací T lymfocytů, a zvýšenou diverzitou TCR, což zlepšuje imunitní rozeznávání a zvyšuje citlivost vůči imunoterapii anti-PD-1/PD-L1 (J. Wang et al. 2019). Ve srovnání s nádory HPV⁻, nádory HPV⁺ obsahují vyšší hladinu PD-1⁺CD8⁺ T lymfocytů a vyšší hladinu všech PD-1⁺ T lymfocytů v blízkém kontaktu s PD-L1⁺ nádorovými buňkami a PD-L1⁺ makrofágy. Naproti tomu, v nádorech HPV⁻ se vyskytují ve zvýšené míře CD8⁺PD-1⁺ lymfocyty se sníženou schopností produkce IFN- γ (Kansy et al. 2017; Xu et al. 2020; Tosi et al. 2022). Vyšší infiltrace CTLA4⁺ T lymfocytů se nachází v HPV⁺ karcinomech orofaryngu oproti karcinomům HPV⁻ (Tosi et al. 2022).

Neimunitní buňky TME

Fibroblasty asociované s nádory

Nejčtenějšími buňkami nádorového stroma jsou CAF, které podporují progresi řady nádorů, včetně HNSCC. Jedná se o heterogenní populaci, která vzniká z různých prekurzorů, např. aktivovaných fibroblastů, endoteliálních, epiteliálních, či nádorových buněk (Kanzaki and Pietras 2020). CAF jsou velmi heterogenní i v rámci jednoho typu nádoru. Analýza transkriptomu metodou sekvenace RNA z jednotlivých buněk („single-cell RNA-seq“) odhalila 8 různých skupin CAF v TME HNSCC vykazující odlišné biologické funkce (Q. Zhang, Wang, Xia, et al. 2021). CAF neexprimují specifické znaky, společnými znaky pro CAF jsou např. vimentin, α -SMA (α -smooth muscle actin), FSP-1 (fibroblast specific protein 1), či FAP (fibroblast activation protein) a zároveň absence epiteliálních, endoteliálních a leukocytických znaků (Kanzaki and Pietras 2020; Xie et al. 2021). CAF produkují řadu růstových faktorů, cytokinů, chemokinů a proteinů ECM, které podporují růst nádoru. Silnou sekrecí faktoru TGF- β navozují imunosupresivní prostředí a podílí se na polarizaci TAM a migraci MDSC či neutrofilů do TME (Biffi and Tuveson 2021).

Ukazuje se, že HPV⁺ HNSCC jsou méně infiltrované CAF oproti HPV⁻ HNSCC a nízká hladina CAF v TME se pojí s lepším přežíváním HPV⁺ pacientů (X. Liu et al. 2022; B. Wang et al. 2022). V extrabuněčných vezikulech HPV⁺ HNSCC se nachází zvýšená hladina miR-9-5p, která blokuje signalizaci TGF- β vedoucí k přeměně fibroblastů na CAF (B. Wang et al. 2022).

Endoteliální buňky

Endoteliální buňky hrají v TME velmi významnou roli, neboť se podílejí na angiogenezi, která je předpokladem pro další růst nádoru. Jak již bylo popsáno výše, řada buněk TME produkuje proangiogenní faktory, z nich nejvýznamnější roli hraje VEGF-A, který se váže na receptory endoteliálních buněk a podporuje jejich proliferaci (Ghalehandi et al. 2023). V souvislosti s rychlým růstem nádoru, nádorové buňky exprimují také lymfangiogenní faktory (např. VEGF-C), které se váží na receptory lymfatických endoteliálních buněk, čímž podporují vznik nových lymfatických cév v nádoru (Sedivy et al. 2003). V HNSCC je lymfangiogeneze velmi častým jevem, což souvisí i s častým vznikem metastáz právě v lymfatických uzlinách u pacientů s HNSCC (Z. Zhang, Helman, and Li 2010).

Nádorové kmenové buňky

Nádorové kmenové buňky jsou skupinou buněk, která má schopnost sebe obnovy. Zatím není zcela jasné, které znaky definují tuto buněčnou populaci. Mezi kandidátní znaky patří CD44, CD133 a aldehyd dehydrogenáza (Singh et al. 2021). Tyto buňky jsou pravděpodobně zodpovědné za iniciaci či progresi nádorů a tvorbu metastází (Han et al. 2014).

Hypoxie a její vliv na TME

TME mnoha karcinomů včetně HNSCC je silně hypoxické, což pozitivně ovlivňuje progresi nádoru. Hypoxie vzniká v důsledku rychlého růstu nádoru, který tak není dostatečně zásobován kyslíkem. Hlavním regulátorem odpovědi na hypoxii je transkripční faktor Hif-1 α (hypoxia-inducible factor 1- α), který se za hypoxických podmínek exprimuje ve zvýšené míře a stabilizuje se, a který ovlivňuje řadu procesů v TME (Wicks and Semenza 2022). Hladina exprese Hif-1 α je v HNSCC studována na úrovni mRNA i proteinu, avšak výsledky jsou nekonzistentní. Vyšší hladina proteinu Hif-1 α se nachází v karcinomech dutiny ústní oproti karcinomům orofaryngu (Swartz et al. 2021). Karcinomy orofaryngu HPV⁺ vykazují nižší expresi *Hif-1 α* a dalších genů asociovaných s hypoxií (např. *GLUT1*, glucose transporter 1) ve srovnání s karcinomy HPV⁻ (Hanns et al. 2015). Některé studie u karcinomů dutiny ústní a orofaryngu popisují vyšší hladinu Hif-1 α na úrovni proteinu u karcinomů HPV⁺ ve srovnání s karcinomy HPV⁻ (Rodolico et al. 2011; Smahelova et al. 2024), zatímco jiná studie nepozoruje rozdíly v hladině proteinu Hif-1 α mezi skupinami karcinomů orofaryngu s různou etiologií (A. Hong et al. 2013). Fan a kol. zjistili, že činnost onkoproteinů E6 a E7 HPV ovlivňuje hladina Hif-1 α a GLUT1 proteinů (R. Fan et al. 2016).

V HNSCC Hif-1 α reguluje expresi miR-21 či miR-5100, což podporuje vznik CAF, které produkcí řady faktorů podporují proliferaci a invazivitu nádoru a tvorbu metastáz v lymfatických uzlinách (Ye et al. 2023; Xie et al. 2021; Duan et al. 2024). Za hypoxických podmínek CAF též produkují zvýšenou hladinu serglycinu, který zvyšuje expresi znaku CD44, což je znak nádorových kmenových buněk (Xie et al. 2021).

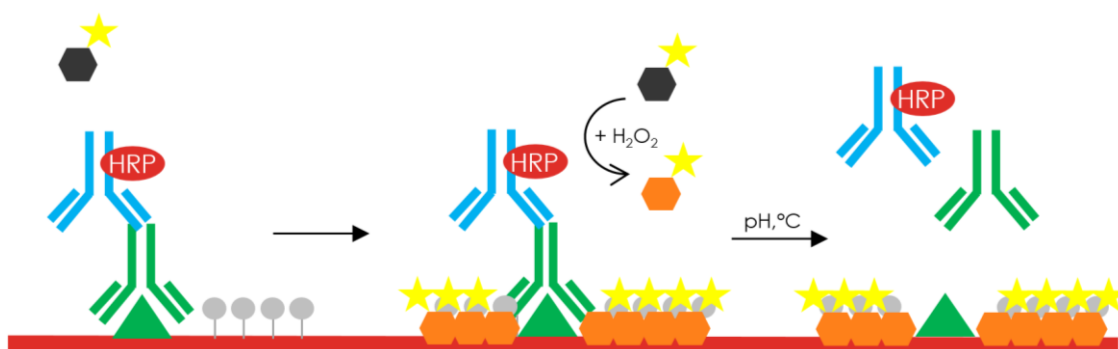
Hypoxie také ovlivňuje množství a funkci imunitních buněk v TME. Vyšší míra hypoxie v HNSCC je spojená s nižší infiltrací CD8⁺ T lymfocyty a horší odpovědí vůči imunoterapii anti-PD-1/PD-L1 (Zandberg et al. 2021). Pacienti s nižší hladinou hypoxie a zároveň vysokou hladinou imunitních buněk vykazují lepší odpověď na terapii

(chemoterapii a imunoterapii) a lépe přežívají, než pacienti s vysokou hladinou hypoxie a zároveň nízkou hladinou imunitních buněk (H. Wang and Zheng 2022).

V návaznosti na vysokou hladinu hypoxie dochází k novotvorbě cév, kterou zprostředkovávají proangiogenní (Hif-1 α závislé) faktory, jako je VEGF. V HNSCC se nachází zvýšená hladina tohoto faktoru oproti kontrolní tkáni (Eisma, Spiro, and Kreutzer 1997). Vyšší hladinu VEGF popisují některé studie v HPV⁻ karcinomech dutiny ústní a orofaryngu oproti karcinomům HPV⁺ (Baruah et al. 2015; Smahelova et al. 2024), avšak jiné studie nepozorují rozdíly v hladině VEGF v závislosti na přítomnosti HPV (Fei et al. 2009; Troy et al. 2013).

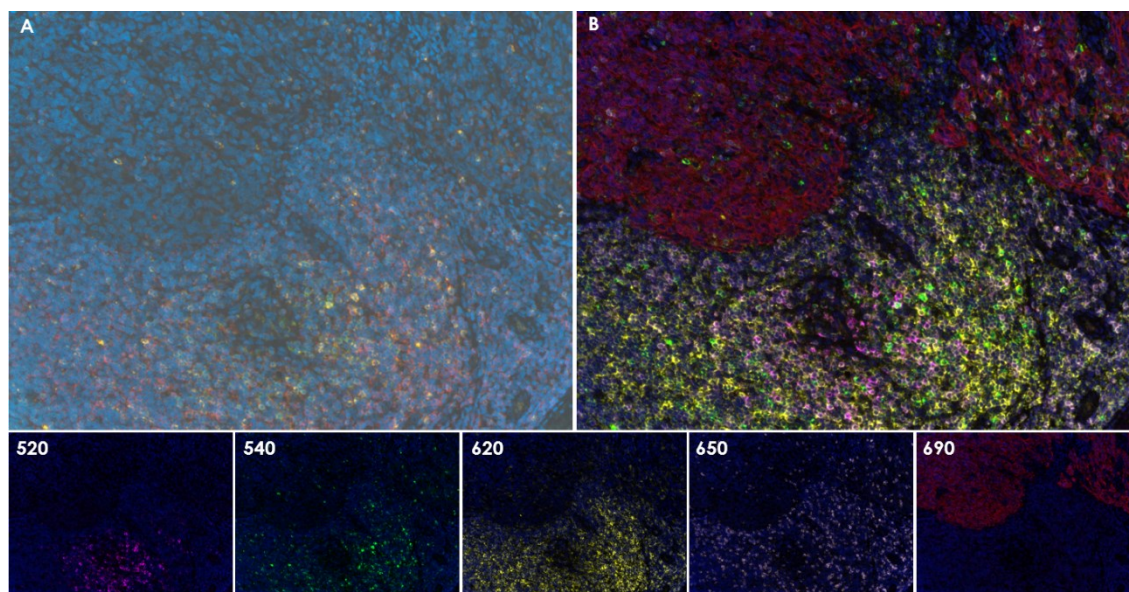
Metody studia nádorového mikroprostředí

Nádorové mikroprostředí lze studovat mnoha metodami, přičemž zejména v posledních letech byly vyvinuty pokročilé metody detekce a kvantifikace různých buněčných typů a jejich povrchových či intracelulárních molekul. Jednou z metod, která umožňuje detekovat buňky v TME *in situ*, je multispektrální imunohistochemie (mIHC, multispectral immunohistochemistry). Pomocí této metody lze zároveň detekovat v histologických vzorcích fixované tkáně více buněčných typů, přičemž architektura tkáně zůstává neporušena, čímž lze určit přesnou lokalizaci detekovaných buněk či jejich shluků. Nejvíce užívanou technikou je metoda založená na amplifikaci tyramidového signálu (TSA, tyramide signal amplification), kterou znázorňuje obrázek 8. Při této metodě se fluorofor kovalentně váže do těsné blízkosti epitopu, přičemž komplex primární a sekundární protilátky je odmyt v pufru za vysoké teploty. Následovat může značení dalšího epitopu a barvení fluoroforem o jiné vlnové délce (Mansfield 2014; Toth and Mezey 2007). V současné době je tímto chemismem možno označit až 9 různých epitopů na jedné tkáni.



Obrázek 8. Princip značení antigenů metodou TSA. Epitop (zeleně) je označen primární protilátkou (zeleně), poté sekundární protilátkou (modře) s navázanými polymery HRP (horseradish peroxidase), a nakonec fluoroforem (žlutě) obsahujícím tyramidový substrát (černě) pro HRP. Peroxidázou aktivovaná forma tyramidu (oranžově) poté kovalentně reaguje s tyrosinovými residuy na nebo v těsném okolí detekovaného epitopu (šedě). Komplex primární a sekundární protilátky je následně odmyt, ale kovalentně navázaný fluorofor zůstává navázan v místě epitopu.

Se vzrůstajícím počtem použitých fluoroforů narůstá také pravděpodobnost překryvu spekter jednotlivých fluoroforů. Jejich softwarové rozlišení vyžaduje vytvoření tzv. spektrálních knihoven, čímž získáme informaci o emisních spektrech každého z použitých fluoroforů. Procesem tzv. lineárního rozlišení („linear unmixing“) se z nezpracovaného obrazu vyfocené fluorescenčním mikroskopem získá upravený obraz, ve kterém jsme schopni izolovat jednotlivé fluorofory, a tudíž detekovat jednotlivé epitopy a zároveň odstínit autofluorescenci (obrázek 9).



Obrázek 9. Lineární rozlišení fluoroforů v programu InForm 2.4.6. (Akoya Biosciences). A) Nezpracovaný obraz získaný po vyfocení spektrálním fluorescenčním mikroskopem. B) Upravený obraz po použití spektrálních knihoven, jednotlivé fluorofory (Opal 520, Opal 540, Opal 620, Opal 650, Opal 690, DAPI (modře) jsou zřetelně rozlišené. Autor fotografií: Mgr. Barbora Pokrývková.

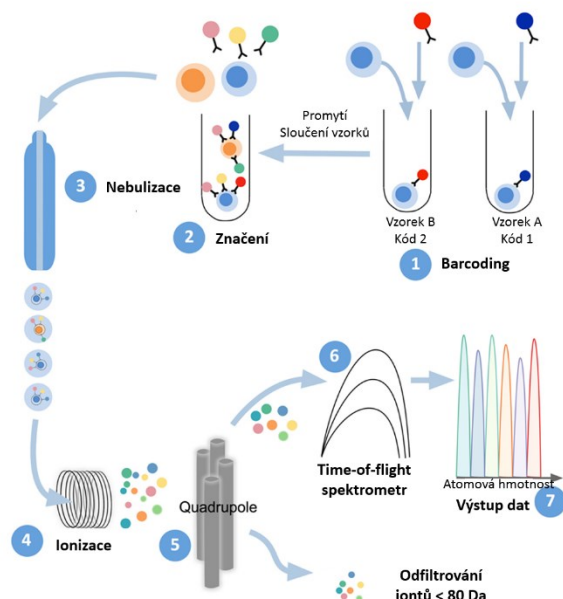
Moderní programy pro digitální patologii jsou schopny nejen detekovat jednotlivé fluorofory, ale také tkáň segmentovat na určité oblasti (např. nádorový parenchym, stroma), segmentovat jednotlivé buňky a odlišit jejich jádra, cytoplazmu a membránu, a nakonec určit fenotyp buněk.

Mimo systémy TSA existuje další přístup, který využívá koktejl oligonukleotidových „značek“ (barcodes) s navázanými protilátkami, které se specificky váží na dané antigeny (metoda Ultivue). Následně dochází k *in situ* amplifikaci barcodes a komplementární vazbě fluorescenčních sond, čímž je umožněna detekce až 16 antigenů (Wharton et al. 2021). Na podobném principu funguje nová metoda firmy Akoya Biosciences (metoda CODEX), která umožňuje najednou detekovat až 101 protilátek (Jhaveri et al. 2023).

Na principu značení pomocí koktejlu protilátek je postavena i zobrazovací hmotnostní cytometrie „time of flight“ (Imaging CyTOF[®]). V tomto případě jsou protilátky označeny vzácnými kovy. Pomocí laseru se 1 μm kousky tkáně odpařují a přenáší se do hmotnostního detektoru měřícího „čas letu“ (time of flight), který je specifický pro každý vzácný kov. Každá buňka má navíc informaci o svých souřadnicích, což umožňuje digitální rekonstrukci tkáně (Cereceda, Jorquera, and Villarroel-Espíndola 2022). Metodou Imaging CyTOF[®] lze v současné době detekovat až 40 znaků na FFPE (formalin-fixed paraffin embedded, fixované formalinem zalité parafinem) tkáni (Ijsselsteijn et al. 2019).

Pro studium nádorů se hojně využívají metody průtokové cytometrie, a to pro jejich rychlost a mnohdy i nižší cenu. Pro průtokovou cytometrii je nezbytná homogenizace nádorů a vytvoření buněčné suspenze, čímž se ztrácí informace o lokalitě studovaných buněk. Na druhou stranu, přístroje FACS (fluorescent activated cell sorter, třídíč buněk aktivovaný fluorescencí) umožňují selektovat živé buněčné populace, které mohou být dále použity například pro kultivace či funkční testy.

Jednou z pokročilých metod cytometrie je hmotnostní cytometrie CyTOF[®], která je schopna zároveň detekovat až 60 antigenů, čímž umožňuje kvantifikovat širokou škálu imunitních i neimunitních buněk v TME a detailně je charakterizovat. Oproti klasické fluorescenční cytometrii, CyTOF[®] využívá protilátek s konjugovanými izotopy kovů, čímž odpadá problém s překryvem emisních spekter, neboť každý z kovových izotopů má své jasně definované parametry hmotnostní spektrometrie (Iyer, Hamers, and Pillai 2022). Stručný princip metody je uveden na obrázku 10.



Obrázek 10. Princip hmotností cytometrie CyTOF®. Buněčná suspenze se značí protilátkami pro barcoding (1), což umožňuje analýzu více vzorků najednou. Vzorky označené kódy se poté sloučí a značí protilátkami s konjugovanými kovovými izotypy (2). Buněčná suspenze poté prochází nebulizérem, přičemž vznikají drobné kapky obsahující právě 1 buňku (3). Působením proudu argonové plasmy dochází k zahřátí na teploty přibližně 7000 K odpaření a ionizaci jednotlivých buněk na oblačí iontů (4), které se poté filtrují skrze řadu kvadrupólů (5). Ionty o atomové hmotnosti <80 Da se odstraní, zatímco ionty o vyšší atomové hmotnosti se analyzují hmotnostním spektrometrem TOF (6). Každý izotop kovu se separuje podle jeho poměru atomové hmotnosti vůči náboji, množství iontů pak odpovídá množství protilátky v dané buňce. Převzato a upraveno podle Sterna a kol. (2018).

V posledních letech došlo k výraznému pokroku fluorescenční cytometrie z hlediska množství použitých protilátek. V roce 2020 byla publikována studie, ve které panelem 40 protilátek vyšetřili lidskou periferní krev (Park, Lannigan, and Jaimes 2020), v roce 2023 myší lymfoidní tkáň (Kare et al. 2023) a nakonec v roce 2024 byl optimalizován panel 50 protilátek pro detekci imunitních buněk v lidské krvi a tkáni průtokovou cytometrií (Konecny et al. 2024).

V současné době je tedy možné pro studium TME využít pokročilých metod, které v jednom vzorku detekují a kvantifikují různé buněčné populace a jejich důležité molekuly. Imunohistochemické metody dovolují detekovat buňky *in situ* ve fixované tkáni, naproti tomu metody cytometrické dovolují pracovat s nefixovanou tkání umožňující izolaci určité buněčné viabilní populace. Kombinací obou přístupů jsme schopni velmi detailně popsat TME, což umožňuje nalezení nových terapeutických cílů či ranných ukazatelů nádorového onemocnění.

3. Cíle práce

Hlavním cílem této práce byla charakterizace nádorového mikroprostředí karcinomů hlavy a krku virové i neviróvé etiologie. Důraz byl kladen na studium fenotypu, funkce a počtu imunitních buněk TME. Za tímto účelem byly charakterizovány vzorky tkáně nádorů hlavy a krku a periferní krve pacientů metodami mIHC, CyTOF[®], průtokové cytometrie a dalšími molekulárně biologickými metodami.

Detailní charakteristika fenotypu a četnosti imunitních buněk v nádoru pacientů byla hodnocena ve vztahu ke klasifikaci nádoru a prognóze ve snaze vytipovat potenciální terapeutické a prognostické cíle.

Dílčí cíle práce:

1. Zavedení a optimalizace metody mIHC pro současné značení až 7 protilátkami na FFPE vzorcích tkáně. Navrhnutí panelů protilátek schopných detekovat vybrané populace imunitních buněk.
2. Vyšetření retrospektivních vzorků pacientů metodou mIHC, jež byli sledováni po dobu až 20 let. Optimalizace algoritmu pro detekci a kvantifikaci imunitních buněk v jednotlivých oblastech nádorového mikroprostředí. Identifikace potenciálních prognostických znaků ovlivňujících přežívání pacientů.
3. Vyšetření prospektivních vzorků metodou mIHC – optimalizace panelů, vyšetření prospektivních vzorků, optimalizace algoritmů a vyhodnocení prospektivní studie.
4. Vyšetření prospektivních vzorků nádorů metodou CyTOF[®], kdy jednobuněčná suspenze získaná z čerstvé nádorové tkáně je značena 31 protilátkami. Identifikace potenciálních prognostických znaků ovlivňujících přežívání pacientů.
5. Určení supresivní aktivity Treg izolovaných z čerstvé nádorové tkáně *in vitro* kultivací s responderovými T lymfocyty.

4. Přehled využitého materiálu a metod

Pro tuto práci byly využity klinické materiály poskytnuté Klinikou otorinolaryngologie a chirurgie hlavy a krku 1. LF UK a FN Motol a Ústavem patologie a molekulární medicíny 2. LF UK a FN Motol. V rámci projektu byly využity vzorky čerstvé, nefixované nádorové tkáně pacientů s primárním karcinomem v oblasti orofaryngu a dutiny ústní (ICD-10: C01–C06, C09, C10) a periferní krev těchto pacientů. Tyto vzorky byly získávány během let 2017-2020. Dále byly použity FFPE vzorky nádorů těchto pacientů a pacientů z retrospektivní studie prováděné během let 2001-2012. Jako kontrolní materiál byly využity vzorky periferní krve dárců a FFPE vzorky tonsil.

Přehled použitých metod

- Fluorescenční imunohistochemie a multispektrální fluorescenční mikroskopie
- analýza nádorového mikroprostředí za použití programů Mantra a InForm (Akoya Biosciences) – optimalizace algoritmu pro segmentaci tkáně, segmentaci a fenotypizaci buněk
- izolace PBMC (peripheral blood mononuclear cells, mononukleární buňky periferní krve) a příprava jednobuněčné suspenze z nádorové tkáně
- hmotnostní cytometrie (CyTOF[®]), průtoková cytometrie, FACS
- práce s tkáňovými kulturami
- molekulárně biologické metody – PCR (polymerase chain reaction), kvantitativní PCR, reverzní transkripce.

Popis metod, které nejsou součástí přiložených publikací

Izolace Treg a responderových T lymfocytů z nádorové suspenze

Z buněčné suspenze, jejíž příprava z nádorové tkáně HNSCC byla popsána v publikaci Poláková a kol. 2019, bylo odebráno $1,4-4 \times 10^6$ buněk a 200 000 kontrolních buněk. Povrchové Fc receptory buněk byly blokovány $20 \times$ ředěným blokovacím roztokem TruStain Human FcX (BioLegend) v FCS pufru (PBS, 1 % FBS, 0,1 % NaN₃) v konečném objemu 100 μ l po dobu 5 minut při 4 °C, poté byly buňky promyty v 1 ml FCS pufru centrifugací (Centrifuga Hettich Universal 320R, Andreas Hettich) při 300 g a 4 °C po dobu 5 minut. Následně byly buňky značeny $5 \times$ ředěným koktejlem povrchových protilátek v FCS pufru (koktejl CD4-fluorescein isothiokyanát +

CD25-alořykocyanin, eBioscience Human Regulatory T Cell Staining kit, Thermo Fisher Scientific) v konečném objemu 100 μ l po dobu 30 minut při 4 °C a poté promyty v 1 ml FCS pufru centrifugací při 300 g a 4 °C po dobu 5 minut. Pro kontrolní buňky bylo místo primární protilátky použito 100 μ l PBS. Po centrifugaci byly buňky resuspendovány v 1 ml PBS a označeny fluorescenční barvou Hoechst 33258 (Thermo Fisher Scientific) v koncentraci 1 μ g/ml pro určení životnosti buněk. Cílové buňky byly selektovány přístrojem BD FACS Aria Fusion (BD Biosciences) do 2 ml supresivního média o teplotě 37 °C (TexMACS medium (Miltenyi Biotec) obohacené o 5% lidské AB sérum (Biosera), 0,5 % penicilin a 0,5 % streptomycin (ThermoFisher Scientific)) dle těchto kritérií: Treg byly definovány jako CD4⁺CD25⁺ buňky, přičemž selektováno bylo 5 % buněk s nejvyšší expresí znaku CD25 (Schneider and Buckner 2011), a responderové T lymfocyty byly definovány jako CD4⁺CD25⁻.

Supresivní analýza

K požadovanému množství Treg pro kokultivaci (4×10^5 buněk), kontrolních Treg (3×10^5 buněk) a kontrolních responderových T lymfocytů (3×10^5 buněk) bylo přidáno 5 objemů předehřátého supresivního média (37 °C), buňky byly stočeny centrifugací při 300 g při pokojové teplotě po dobu 10 minut. Dále byly buňky resuspendovány v supresivním médiu. Responderové T lymfocyty pro kokultivaci (10^6 buněk) byly barveny v 5 μ M roztoku CellTrace™ Far Red (Thermo Fisher Scientific), a to po dobu 20 min při pokojové teplotě. Po značení bylo k responderovým T lymfocytům přidáno 5 objemů supresivního média po dobu 5 minut, následováno centrifugací při 300 g po dobu 5 minut při pokojové teplotě. Po promytí byly buňky resuspendovány v 1 ml supresivního média, bylo odebráno 6×10^5 buněk pro kokultivační analýzu, poté bylo k buňkám přidáno 5 objemů supresivního média po dobu 5 minut, následováno centrifugací při 300 g po dobu 10 minut při pokojové teplotě. Buňky byly resuspendovány v 1 200 μ l supresivního média. Responderové T lymfocyty a Treg společně se stimulačním činidlem Treg Suppression Inspector (Miltenyi Biotec) byly pipetovány v duplikátu či triplikátu na 96jamkovou destičku v poměrech 1:0, 1:1, 2:1, 4:1, 8:1, 0:1. Dále byly na destičku pipetovány kontroly bez stimulačního činidla v poměru 1:0 a 0:1 bez roztoku Treg Suppression Inspector. Objem média v jednotlivých jamkách byl doplněn supresivním médiem do konečného objemu 210 μ l. Destička byla inkubována při 37 °C a 5 % CO₂ po dobu 24 hodin.

Po uplynutí inkubační doby byly buňky spočítány a poté barveny 500 × ředěnou fluorescenční barvou Fixable Viability Dye eFluor 455UV (Thermo Fisher Scientific) v PBS po dobu 30 minut při 4 °C pro určení životnosti a promyty v 1 ml FCS pufru centrifugací (Centrifuga Heraeus™ Megafuge™ 16R, Thermo Scientific) při 300 g a 4 °C po dobu 5 minut. Následně byly buňky značeny povrchově a intracelulárně pomocí eBioscience Human Regulatory T Cell Staining kitu (koktejl CD4-fluorescein isothiokyanát + CD25-aloxykocyanin pro povrchové značení a FoxP3-fykoerythrin pro intracelulární značení) dle protokolu výrobce. Buňky byly poté analyzovány průtokovým cytometrem BD LSRFortessa (BD Biosciences) a byly detekovány populace CD4⁺CD25⁺FOXP3⁺ Treg a CD4⁺CD25⁻ responderových T lymfocytů.

5. Výsledky

Publikace vztahující se k tématu dizertační práce

Implementation of Mass Cytometry for Immunoprofiling of Patients with Solid Tumors

Ingrid Poláková, Ondřej Pelák, Daniel Thürner, Barbora Pokrývková, Ruth Tachezy, Tomáš Kalina, Michal Šmahel*

Journal of Immunology Research, 2019, 2019, 6705949;
<https://doi.org/10.1155/2019/6705949>

IF (2019): 3,327

Tato práce se zabývá optimalizací panelu 31 protilátek pro značení vzorků krve a HNSCC metodou CyTOF[®]. V této práci (příloha 9.1.) jsem se podílela na zpracování vzorků periferní krve a vzorků nádorové tkáně metodou CyTOF[®]. Podílela jsem se na izolaci PBMC, přípravě jednobuněčné nádorové suspenze, značení buněk protilátkami a částečně se podílela na vyhodnocení cytometrických dat.

Příspěvek autora: 10 %

ARG1 mRNA Level Is a Promising Prognostic Marker in Head and Neck Squamous Cell Carcinomas

Barbora Pokrývková*, Jana Šmahelová, Natálie Dalewská, Marek Grega, Ondřej Vencálek, Michal Šmahel, Jaroslav Nunvář, Jan Klozar, Ruth Tachezy*

Diagnostics, 2021, 1(4), 628; <https://doi.org/10.3390/diagnostics11040628>

IF (2021): 3,992

V této práci (příloha 9.2.) jsme metodou multispektrální imunohistochemie detekovali a kvantifikovali TAM typu M1 a M2 v mikroprostředí HNSCC virové a neviróvé etiologie, metodou RT-qPCR určili hladinu mRNA znaků asociovaných s makrofágy a výsledná data jsme analyzovali vzhledem k prognóze pacientů. Pro tyto účely jsem optimalizovala panel protilátek pro metodu multispektrální imunohistochemie, pro detekci jednotlivých typů makrofágů. Pro tuto publikaci jsem navrhla a optimalizovala složení panelu protilátek a podílela se na kontrole provedení všech kroků metody, analýze a vizualizaci dat. Dále jsem se hlavní měrou podílela na tvorbě manuskriptu.

Příspěvek autora: 55 %

PD1+CD8+ Cells Are an Independent Prognostic Marker in Patients with Head and Neck Cancer

Barbora Pokrývková, Marek Grega, Jan Klozar, Ondřej Vencálek, Jaroslav Nunvář, Ruth Tachezy*

Biomedicines, 2022, 10(11),2794; <https://doi.org/10.3390/biomedicines10112794>

IF (2022): 4,7

V této práci (příloha 9.3.) byly vyšetřeny FFPE vzorky retrospektivní kohorty HNSCC metodou multispektrální imunohistochemie. Byla určena hladina tumor infiltruujících buněk v karcinomech virové a neviróvé etiologie a výsledná data byla analyzována vzhledem k přežívání pacientů. Pro tuto práci jsem zavedla metodu multispektrální imunohistochemie v naší laboratoři, navrhla složení čtyř panelů protilátek pro imunohistochemické značení, optimalizovala proces značení, vytvořila algoritmy pro vyhodnocení dat v programu InForm, vyšetřila FFPE vzorky pacientů a analyzovala výsledná data. Dále jsem se hlavní měrou podílela na tvorbě manuskriptu.

Příspěvek autora: 80 %

Aspartate- β -hydroxylase and Hypoxia Marker Expression in Head and Neck Carcinomas: Implications for HPV-Associated Tumors

Jana Šmahelová, Barbora Pokrývková, Eliška Šťovíčková, Marek Grega, Ondřej Vencálek, Michal Šmahel, Vladimír Koucký, Simona Maléřová, Jan Klozar, Ruth Tachezy*

Infectious Agents and Cancer, 2024; <https://doi.org/10.1186/s13027-024-00588-1>

IF (2022): 3,7

V této práci (příloha 9.4.) byla metodou RT-qPCR vyšetřena RNA pacientů s HNSCC virové a neviróvé etiologie pro určení hladiny mRNA *ASPH* a genů asociovaných s hypoxií. Dále byly vyšetřeny FFPE vzorky těchto pacientů metodou multispektrální imunohistochemie pro určení hladiny buněk produkujících ASPH a proteinů asociovaných s hypoxií. V této práci jsem navrhla a optimalizovala složení panelu protilátek pro metodu multispektrální imunohistochemie, podílela se na kontrole provedení všech kroků metody a analýze dat. Dále jsem se podílela na tvorbě manuskriptu a jeho úpravách.

Příspěvek autora: 35 %

Publikace nevztahující se k tématu dizertační práce

Detailed Characteristics of Tonsillar Tumors with Extrachromosomal or Integrated Form of Human Papillomavirus

Barbora Pokrývková, Martina Saláková*, Jana Šmahelová, Zuzana Vojtěchová, Vendula Novosadová, Ruth Tachezy

Viruses, 2020, 12(1), 42; <https://doi.org/10.3390/v12010042>

IF (2020): 5,048

Skp2 and Slug are coexpressed in aggressive prostate cancer and inhibited by neddylation blockade

Alena Mickova, Gvantsa Kharashvili*, Daniela Kurfurstova, Mariam Gachechiladze, Milan Kral, Ondrej Vacek, Barbora Pokryvkova, Martin Mistrik, Karel Soucek, Jan Bouchal*

International Journal of Molecular Sciences, 2021, 22(6), 2844;

<https://doi.org/10.3390/ijms22062844>

IF (2021): 6,208

Nepublikované výsledky vztahující se k dizertační práci

Supresivní analýza

Pro určení supresivní aktivity Treg lokalizovaných v nádorové tkáni byla zvolena *in vitro* kultivace s responderovými T lymfocyty izolovanými z téhož nádoru, kdy je sledována proliferace responderových T lymfocytů. Za tímto účelem byl zaveden protokol pro selektování Treg a responderových T lymfocytů ze vzorků čerstvé nádorové tkáně HNSCC. Buňky nádorové suspenze byly značeny povrchovými protilátkami CD25 a CD4. Poté byly pomocí FACS selektovány populace Treg (CD4⁺CD25⁺⁺) a responderových T lymfocytů (CD4⁺CD25⁻). Tyto dvě populace byly následně kokultivovány. Pro úspěšné provedení kokultivačních pokusů bylo nutné získat alespoň 4×10^5 Treg a 6×10^5 responderových T lymfocytů pro provedení pokusu v duplikátu. Z toho důvodu byly pro izolaci Treg a responderových T lymfocytů uvažovány čerstvé nádory, u kterých se podařilo izolovat aspoň 2×10^7 buněk. Ukázalo se však, že množství cílových buněk nelze nijak předpovědět s ohledem na celkový počet buněk v nádoru.

V prvním optimalizačním pokusu bylo z nádoru izolováno $3,3 \times 10^7$ buněk, z čehož 2×10^7 buněk bylo použito pro pokus. Z tohoto nádoru se podařilo izolovat přibližně $1,7 \times 10^6$ responderových T lymfocytů a $5,68 \times 10^5$ Treg. Pokračovali jsme tedy

v pilotním pokusu a provedli kokultivační analýzu, která trvala 24 hodin. Vzhledem k délce analýzy nebyla hodnocena supresivní aktivita Treg, nýbrž bylo ukázáno, že buňky přežívají. Dále byly tyto buňky značeny CD4, CD25 a FOXP3 protilátkou. Ukázalo se, že některé z $CD4^+CD25^+$ buněk nemají FOXP3 fenotyp, což mohlo být způsobenou ztrátou tohoto fenotypu v *in vitro* podmínkách.

V dalším případě bylo ze vzorku nádoru izolováno přes 7×10^7 buněk, avšak při počítání buněk bylo zjištěno, že přibližně 1/3 těchto buněk je již mrtvá. Pro pokus bylo použito 3×10^7 milionů buněk, z nichž se podařilo izolovat pouze 6×10^4 živých Treg, což nebylo dostatečné množství pro pokračování pokusu, množství responderových T lymfocytů by však bylo dostatečné.

Dále byl testován nádor, ze kterého bylo celkem izolováno pouze $1,4 \times 10^7$ buněk. Z tohoto nádoru bylo získáno pouze $1,52 \times 10^5$ Treg a překvapivě pouze $1,91 \times 10^5$ responderových T lymfocytů.

Během trvání prospektivní studie, jsme nebyli schopni z buněčných suspenzí získat dostatečné množství buněk pro provedení supresivní analýzy, tudíž jsme nebyli schopni získat žádné relevantní výsledky. Pro případné další studie je však připraven protokol pro izolaci Treg a responderových T lymfocytů z nádorové tkáně a protokol pro jejich kokultivaci.

6. Diskuze

V této dizertační práci jsem studovala nádorové mikroprostředí s důrazem na charakterizaci imunitních buněk v HNSCC virové a nevirové etiologie. Pro tyto účely jsem v Laboratoři nádorové virologie a imunoterapie zavedla a optimalizovala metodu multispektrální IHC pro detekci buněk *in situ* ve FFPE vzorcích tkáně, částečně se podílela na zavedení metody CyTOF[®] pro detekci buněk v nádorové suspenzi a PBMC a také na zavedení supresivní analýzy regulačních T lymfocytů. Optimalizace uvedených metod byla podstatnou náplní mého studia, proto se budu v první části kapitoly zabývat diskuzí metodologie a v druhé části diskuzí výsledků.

Metody studia TME prošly v posledních desetiletích značným vývojem, a to v návaznosti na zdokonalování mikroskopických přístrojů, na vývoj zcela nových technických přístupů, a v neposlední řadě v návaznosti na vývoj programů, které jsou schopny získaná data analyzovat. Metoda mIHC založená na TSA je v současné době široce využívaná pro charakterizaci TME různých typů solidních nádorů (Pokrývková et al. 2022; Pokrývková et al. 2021; Mezheyeuski et al. 2018; S.W. Hong et al. 2022; Lee et al. 2021; Parra et al. 2017; Smahelova et al. 2024). Výhodou této metody je možnost sledovat velké množství různých znaků, neboť lze využít jakékoliv specifické nekonjugované primární protilátky proti antigenu našeho zájmu. Signál se amplifikuje vazbou sekundární protilátky a kovalentní vazbou fluoroforu, což vede k získání silnějšího signálu oproti klasickému značení chromogenem, a umožňuje tak detekovat i velmi raritní antigeny (Parra et al. 2017; Toth and Mezey 2007). Náročnost této metody spočívá ve strategii optimalizace panelu. Nejdříve je nutné protilátky optimalizovat v monoplexu, zejména určit vhodné pH pufru pro odmaskování epitopů a určit délku odhalování epitopů v daném pufru. Poté se sestavuje pořadí protilátek v panelu tak, aby byly respektovány potřebné časy pro odmaskování epitopů, a následně se k jednotlivým protilátkám přiřazují vhodné fluorofory. Tato část je zcela esenciální pro získání validních výsledků. Obecně se v metodách založených na fluorescenčním značení doporučuje pro čteně exprimované znaky využít méně svítivé fluorofory, a naopak pro vzácněji exprimované znaky využít vysoce svítivé fluorofory (Lazarus et al. 2019). Pro minimalizaci vlivu spektrálních překryvů dále není vhodné pro koexprimující znaky použít fluorofory o blízké vlnové délce. Vzhledem k omezenému množství dostupných fluoroforů není vždy možné plně těmto doporučením vyhovět. V naší studii jsem detekovala imunitní buňky, pro jejichž fenotypizaci bylo nutné detekovat koexpresi více

znaků (Table 2, Pokrývková et al. 2022). V Panelu 1 jsem pro detekci Treg použila CD3-Opal620/CD4-Opal540/FOXP3-Opal520, avšak vzhledem k odlišné buněčné expresi daných znaků (jaderný signál FOXP3 a membránový signál CD4) nemůže dojít k fenotypizační chybě způsobené překryvem blízkých spekter, neboť případný překryv by byl odhalen přítomností přesahujícího fluoroforu v neočekávané buněčné lokalitě a programem InForm by tato buňka nebyla vyhodnocena jako pozitivní. Podobně v Panelu 4 jsem jadernou protilátku FOXP3 přiřadila k Opal570, abych minimalizovala vliv přesahů signálu Opal540 či Opal620.

Z principu metody mIHC vyplývá nutnost práce s FFPE řezy, neboť tato tkáň je dostatečně odolná vůči opakujícím se krokům zahřívání v kyselém či zásaditém pH. Jistým úskalím může být i příprava a skladování těchto řezů (Gaffney et al. 2018). Pilotní optimalizační pokusy jsem provedla na HNSCC vzorcích od recentních pacientů (tedy délka skladování FFPE bloků byla v řádech několika měsíců). Při pilotním přenesení optimalizovaného panelu na vzorky z retrospektivní studie se ukázalo, že rozdíly v intenzitě signálů jsou markantní a bylo nutné některé primární protilátky zcela vyměnit a znovu titrovat koncentrace všech primárních protilátek či fluoroforů. Tyto diskrepance mohou být způsobeny jednak samotným stářím tkáně a její přirozené, v čase postupující oxidaci (retrospektivní vzorky jsou staré 10–20 let) (Combs et al. 2016) a jednak možnými rozdíly v přípravě FFPE bloků (např. odlišný protokol, chemikálie či lidský faktor) (Gaffney et al. 2018).

Jednou z částí mé práce byla spolupráce na vyšetření vzorků čerstvě resektovaných nádorů pacientů s HNSCC a jejich periferní krve metodou CyTOF[®]. Pro tyto účely dr. Ingrid Poláková optimalizovala protokol pro značení buněk izolovaných z nádorů a PBMC pomocí 31 různých protilátek detekujících vybrané buněčné znaky (Polakova et al. 2019). Proces optimalizace metody CyTOF[®] pro vzorky solidních nádorů nebyl v literatuře dostatečně popsán, vzhledem k nutnosti disociace nádorů je proces optimalizace obtížnější oproti protokolům pro hematologické nádory. Dále jsme metodou CyTOF[®] vyšetřili nádory a periferní krev pacientů v rámci prospektivní studie, přičemž i v této části jsem se podílela na izolaci buněk z nádorů, izolaci PBMC, na procesu značení buněk protilátkovým koktejlem a částečně na vyhodnocení cytometrických dat. Výsledky této části prospektivní studie však zatím nejsou finálně zpracovány a publikovány, proto nejsou součástí této dizertační práce.

Další částí mé práce bylo určení supresivní aktivity Treg izolovaných z čerstvě nádorové tkáně *in vitro* kultivací s responderovými T lymfocyty. Pro tyto účely jsme

zavedli protokol pro selektování Treg a responderových T lymfocytů z nádorové suspenze pomocí FACS, kterou jsme využili i pro značení metodou CyTOF[®]. Nicméně, z některých nádorových buněčných suspenzí nebylo možné získat dostatečné množství Treg pro kokultivační pokusy s responderovými T lymfocyty a v některých případech ani dostatek responderových T lymfocytů. Vysvětlením je pravděpodobně variabilita v množství Treg a T lymfocytů v jednotlivých vzorcích a také množství resektovaného materiálu, které bylo možné získat. Dále vzhledem k potřebě živých Treg pro kokultivaci nebylo možné pro rozlišení Treg využít intracelulární znaky a tyto buňky jsme charakterizovali na základě určení povrchových znaků CD4⁺CD25⁺⁺, kdy zejména pro znak CD25 je nutné rozlišení na základě míry exprese znaku (5 % buněk s nejvyšší expresí CD25) (Schneider and Buckner 2011). Množství selektovaných Treg může proto být ovlivněno „gating“ strategií použitou pro třídění buněk.

Během posledních let se značná pozornost věnuje zastoupení TIL v TME různých nádorů v souvislosti s prognózou pacientů. Stěžejní v tomto ohledu jsou práce z roku 2014 a 2018, ve kterých skupina Jérôme Galon pro karcinom tlustého střeva představuje tzv. Imunoskóre (Galon et al. 2014; Pagès et al. 2018). Podstatou je vyhodnocení četnosti infiltrace CD3⁺ a CD8⁺ T lymfocytů v invazivním okraji nádoru pomocí IHC v FFPE řezech. Pacienti s vysokým Imunoskóre vykazují nižší míru rekurencí během 5 let sledování po operaci oproti pacientům s nízkým Imunoskóre. Vyhodnocení Imunoskóre také vykazuje vyšší přesnost predikce celkového přežití oproti zavedeným klinickým parametrům, jako je TNM (tumor, node, metastasis; stadium nádoru, zasažení uzlin, metastaze) klasifikace (Pagès et al. 2018). Recentně bylo Imunoskóre navrženo i pro hodnocení rektálních karcinomů (El Sissy et al. 2024). Ač by se mohlo zdát, že hodnocení Imunoskóre bude snadno přenositelné pro predikci přežívání pacientů s karcinomy v dalších lokalizacích, výsledky dalších studií toto zcela nepotvrzují. Například u triple negativního karcinomu prsu se Imunoskóre neukazuje jako signifikantní pro predikci přežívání těchto pacientů (X. Ren et al. 2023), u nemalobuněčného karcinomu plic se pro hodnocení přežívání navrhuje kvantifikace pouze stromálních CD8⁺ T lymfocytů (Donnem et al. 2015). U plicního adenokarcinomu (stadium III) se ukazuje, že hodnocení tzv. skóre GT, založeného na analýze nejbližší sousední buňky společně s hodnocením shlukování buněk, má silnější prediktivní vlastnosti než Imunoskóre (Z. Zeng et al. 2024). Paralelně se prognostická výhoda vysoké infiltrace TIL ukazuje u mnoha dalších nádorových onemocnění, např. melanomů,

nemalobuněčného karcinomu plic či u HNSCC (Wong et al. 2019; Donnem et al. 2015; Borsetto et al. 2021; Ruangritchankul et al. 2019). Pro nalezení prediktivního znaku přežívání pacientů s HNSCC je problematická velká heterogenita těchto karcinomů, která souvisí s rozdílnou anatomickou lokalizací a etiologií.

V našich studiích jsme detekovali vyšší procento HPV⁺ karcinomů v oblasti orofaryngu ve srovnání s nádory dutiny ústní, a rozdílnou hladinu TIL a dalších imunitních buněk v nádorech různé etiologie (Pokrývková et al. 2021; Pokrývková et al. 2022; Smahelova et al. 2024). Ukázali jsme, že HPV⁺ HNSCC jsou masivněji infiltrované TIL (CD3⁺, CD4⁺, CD8⁺ T lymfocyty), oproti nádorům HPV⁻ (Pokrývková et al. 2022), což potvrzují i výsledky dalších skupin (Qureshi et al. 2022; Tosi et al. 2022; Badoual et al. 2013). Pozitivní vliv na prognózu pacienta je nejčastěji spojován s hladinou CD8⁺ T lymfocytů, a to vzhledem k jejich cytotoxicitě vůči nádorovým buňkám (Oguejiofor et al. 2015; Nordfors et al. 2013; Mukherjee et al. 2020). U pacientů s nádory hlavy a krku je metaanalýzou potvrzena prognostická výhoda vysoké infiltrace CD8⁺ T lymfocyty. Prognostický efekt na přežívání pacientů je pozorován zejména u pacientů s HPV⁺ karcinomy, avšak popisují jej i některé studie u HPV⁻ pacientů (Borsetto et al. 2021).

V naší studii jsme u HPV⁺ karcinomů detekovali vyšší infiltraci PD-1⁺CD8⁺ T lymfocytů oproti karcinomům HPV⁻ a vyšší hladina těchto buněk byla spojena se zlepšeným přežíváním pacientů s HNSCC bez ohledu na etiologii nádoru (Pokrývková et al. 2022). Stejně výsledky jsou ukázány i dalšími studii (Tosi et al. 2022; Badoual et al. 2013). Molekula PD-1, exprimovaná aktivovanými lymfocyty, patří do skupiny imunitních kontrolních receptorů, které po vazbě ligandu inhibují aktivitu T lymfocytů (Freeman et al. 2000). Ukazuje se však, že PD-1⁺CD8⁺ T lymfocyty v TME jsou specifické vůči nádorovým antigenům a hrají klíčovou roli v regresi nádoru (Gros et al. 2014), což může vysvětlit prognostickou výhodu vysoké infiltrace těmito buňkami. Kansy a kol. ve své studii uvádí, že v HPV⁺ karcinomech se převážně vyskytují CD8⁺ T lymfocyty s nízkou expresí PD-1, kdežto v HPV⁻ karcinomech se vyskytují ve značné míře CD8⁺ lymfocyty se silnou expresí PD-1. Zdá se, že právě silná exprese PD-1 je spojena s vyčerpaným T-buněčným fenotypem a je spojena s horším přežíváním pacientů, kdežto nízká exprese PD-1 u CD8⁺ T lymfocytů se pojí s příznivou prognózou HNSCC pacientů, která může být důsledkem protinádorové aktivity aktivovaných CD8⁺ lymfocytů (Kansy et al. 2017). Také skupina Badoual popisuje, že část PD-1⁺ T lymfocytů v HNSCC nevykazuje vyčerpaný fenotyp, neboť u těchto buněk nedochází k současné expresi Tim-3 (Badoual et al. 2013). Z našich výsledků a výsledků ostatních

skupin tedy vyplývá, že PD-1⁺CD8⁺ T lymfocyty jsou stěžejní nádorově specifickou populací zodpovědnou za kontrolu nádorového růstu a nadějným prediktorem přežívání pacientů (Tosi et al. 2022; Pokrývková et al. 2022; Kansy et al. 2017; Badoual et al. 2013). Rozdíly v hladině exprese PD-1 na CD8⁺ T lymfocytech a rozdílná funkce těchto buněk v závislosti na statusu HPV mohou přispět k vysvětlení výraznější odpovědi HPV⁺ pacientů vůči imunoterapii založené na blokádě PD-1/PD-L1 oproti pacientům HPV⁻ (J. Wang et al. 2019).

Oproti CD8⁺ T lymfocytům, jejichž nespornou prognostickou úlohu diskutují výše, vliv CD4⁺ T lymfocytů na prognózu pacientů s HNSCC není jednoznačný (Simonson and Allison 2011), neboť CD4⁺ T lymfocyty zahrnují spektrum buněčných populací s odlišnými funkcemi. V naší studii jsme detekovali vyšší hladinu CD4⁺ T lymfocytů v HPV⁺ karcinomech oproti karcinomům HPV⁻, avšak nepozorovali jsme vliv této populace na prognózu pacientů (Pokrývková et al. 2022). Naše výsledky se shodují s výsledky dalších skupin studujících karcinomy dutiny ústní a orofaryngu (Oguejiofor et al. 2017; Nordfors et al. 2013; Quan et al. 2020; Badoual et al. 2013). V naší studii jsme také pozorovali zvýšenou hladinu PD-1⁺CD4⁺ T lymfocytů v nádorovém parenchymu a stroma HPV⁺ karcinomů ve srovnání s karcinomy HPV⁻, podobně jako ve studii Badoual a kol. (2013), avšak na rozdíl od zmíněné publikace jsme nepozorovali vliv této populace na přežívání pacientů (Pokrývková et al. 2022).

V naší studii jsme dále nepozorovali rozdíly v infiltraci CD4⁺FOXP3⁺ Treg mezi karcinomy HPV⁺ a HPV⁻, avšak ukázali jsme rozdílné zastoupení Treg lišící se expresí kostimulační molekuly ICOS (Pokrývková et al. 2022). Molekula ICOS podporuje transkripci FOXP3, čímž podporuje supresivní aktivitu Treg (Q. Chen et al. 2018). U karcinomů HPV⁺ jsme detekovali vyšší parenchymální hladinu Treg neexprimující ICOS (ICOS⁻ Treg), zatímco u karcinomů HPV⁻ jsme pozorovali vyšší stromální hladinu ICOS⁺ Treg (Pokrývková et al. 2022). Ukazuje se, že ICOS⁻ Treg vykazují nižší supresivní aktivitu oproti ICOS⁺ Treg (Kornete, Sgouroudis, and Piccirillo 2012). Vyšší hladina ICOS⁺ Treg tedy může napomáhat k tvorbě imunosupresivního prostředí HPV⁻ karcinomů. Hladina populací Treg či ICOS⁺/ICOS⁻ Treg však neměla v naší studii vliv na prognózu, což je popsáno i v dalších studiích (Pokrývková et al. 2022; Tosi et al. 2022; Quan et al. 2020). Na rozdíl od výsledků naší studie, v jiné studii je zvýšená infiltrace Treg pozorována u HPV⁺ karcinomů, avšak opět není pozorován vliv jejich infiltrace na prognózu pacientů (Badoual et al. 2013).

Kromě hladiny TIL naše skupina detekovala TAM, což je další prognosticky významná skupina buněk v TME nádorů hlavy a krku. Studium makrofágů v TME je komplikované vzhledem k vysoké plasticitě těchto buněk (Sica and Mantovani 2012). Spektrum možných detekovatelných subpopulací TAM je široké, s čímž souvisí nekonzistence vědeckých studií v použitých znacích pro fenotypizaci, a proto i obtížné srovnávání těchto vědeckých výstupů (Jayasingam et al. 2019). V naší studii jsme detekovali TAM dle přítomnosti pan-makrofágového znaku CD68 a dále znakem CD80 pro typ M1 a znakem CD163 a ARG1 pro typy M2 (Pokrývková et al. 2021). Ve studii Henga a kol. detekují M2 také pomocí CD163 a dále CD206 v karcinomech laryngu a také popisují populaci HLA-DR⁺⁺CD206⁺ makrofágů, která ze své podstaty stojí na pomezí mezi typy M1 a M2, neboť vykazuje znaky obou populací (Heng et al. 2023). V jiné studii jsou jako charakterizující znaky TAM použity CD68 či CD163 a jako znak M2 je použit CD206 (Qureshi et al. 2022). Použití CD163 jako pan-makrofágového znaku je překvapující, neboť v naší i mnoha dalších studiích je tento znak považován za výhradní znak M2 (Pokrývková et al. 2021; Jayasingam et al. 2019; Tosi et al. 2022; Bisheshar et al. 2022; Heng et al. 2023).

Výsledky naší studie ukázaly vyšší expresi M2-asociovaných znaků (*ARG1*, *CD163* a *PTGS2*) na úrovni mRNA a vyšší stromální infiltraci M2 produkujících ARG1 imunohistochemicky v HPV⁻ HNSCC, oproti karcinomům HPV⁺. Pomocí mIHC jsme nedetekovali rozdíl v zastoupení M1 mezi skupinami pacientů, avšak v karcinomech HPV⁺ jsme pozorovali zvýšené množství mRNA NOS2, tento znak M1 však nebyl zahrnut do našeho imunohistochemického panelu (Pokrývková et al. 2021). Podobně zvýšenou míru M2 ve stroma vykazují pacienti s HPV⁻ HNSCC, kteří jsou léčeni chemo/bioradioterapií (Ou et al. 2019). Ve studii Tosi a kol. však ukazují vyšší intratumorální i stromální infiltraci M1 i M2 u HPV⁺ karcinomů orofaryngu oproti karcinomům HPV⁻ (Tosi et al. 2022). Zvýšená četnost TAM M2 se také pojí s horší prognózou pacientů u karcinomů laryngu, dutiny ústní, či karcinomů mimo oblast hlavy a krku, např. u karcinomů prsu, ovarií, žaludku či nemalobuněčného karcinomu plic (Miyasato et al. 2017; Yin et al. 2017; Yuan et al. 2017; Soo et al. 2018; Heng et al. 2023; Hadler-Olsen and Wirsing 2019; Bisheshar et al. 2022). V naší studii jsme dále ukázali, že vyšší hladina mRNA ARG1, M2-asociovaného znaku, se pojí s horším přežíváním HNSCC pacientů, zároveň nízká hladina mRNA ARG1, kterou jsme přednostně pozorovali u HPV⁺ karcinomů nižšího patologického stádia, souvisí s lepším přežíváním těchto pacientů (Pokrývková et al. 2021). Podobný efekt na přežívání je pozorován

i u pacientů s karcinomem kolorekta (Ma et al. 2019). Mimo makrofágy M2, silnými producenty ARG1 v TME jsou také TAN či MDSC (Heuvers et al. 2013; W. Ren et al. 2020; García-Navas, Gajate, and Mollinedo 2021). V naší studii jsme detekovali vyšší parenchymální i stromální hladinu $CD68^-ARG1^+$ buněk, u kterých předpokládáme, že mohou být TAN či MDSC, tedy buňky podílející se na imunosupresivním TME (Pokrývková et al. 2021). Popisuje se, že ARG1 snižuje aktivaci cytotoxických $CD8^+$ buněk v TME, což vede ke snížení protinádorové imunity a podpoře progresu nádoru (Hurt et al. 2017). Inhibicí arginázy naopak dochází k silné indukci proliferace T lymfocytů (Vonwirth et al. 2020).

Výsledky naší skupiny poukazují na zvýšenou hladinu prozánětlivých M1 v mikroprostředí HPV⁺ karcinomů, a naopak vyšší hladinu imunosupresivních ARG1 produkujících buněk včetně M2 v mikroprostředí HPV⁻ karcinomů. Pro plné pochopení funkce TAM v mikroprostředí nádorů je nezbytná podrobná a víceznaková charakteristika TAM, která by pokryla variabilitu v populacích makrofágů.

Důležitou molekulou, která je také spojena s činností TAM, je proangiogenní faktor VEGF. Detekovali jsme vyšší hladinu VEGF v parenchymu karcinomů HPV⁻ ve srovnání s karcinomy HPV⁺ (Smahelova et al. 2024), což ukazují i výsledky další studie (Baruah et al. 2015). Vyšší hladina tohoto faktoru je spojena s výraznější agresivitou nádorů, a zároveň je rizikovější pro přežívání pacientů s HNSCC (Sauter et al. 1999; Kyzas, Cunha, and Ioannidis 2005). Hladinu VEGF ovlivňuje hypoxie nádoru, což je fenomén spojený s nepříznivou prognózou pacientů (Mohamed et al. 2004; Morand et al. 2020). V naší studii jsme sledovali hladinu dalších proteinů spojených s hypoxií a detekovali jsme vyšší hladinu proteinů Hif-1 α , GLUT1 a MMP13 u karcinomů HPV⁺ ve srovnání s karcinomy HPV⁻ (Smahelova et al. 2024). V modelech nezahrnujících status HPV se vyšší hladina proteinů Hif-1 α a GLUT1 pojila s lepším přežíváním HNSCC pacientů, což však vzhledem k jejich vyšší četnosti v HPV⁺ karcinomech může odrážet přítomnost viru, nikoliv míru hypoxie. Vyšší hladina proteinů Hif-1 α a GLUT1 se v karcinomech dutiny ústní pojí s vyšší invazivitou oproti karcinomům s nižší hladinou těchto proteinů, na druhou stranu status HPV v této studii není vyšetřován, takže výsledky této studie mohou být ovlivněny nízkou prevalencí viru v karcinomech dutiny ústní (Morand et al. 2020). Vyšší hladina proteinů Hif-1 α a GLUT1 v nádorech virové etiologie může odrážet aktivní virovou infekci, neboť je prokázán pozitivní vliv virových onkoproteinů E6 a E7 na hladinu těchto proteinů (R. Fan et al. 2016).

Vyhodnocení studií zabývajících se charakteristikou nádorového mikroprostředí HNSCC má četné limitace. Mimo biologickou variabilitu HNSCC (rozdílná lokalizace a etiologie nádorů) je pro určení prediktivního znaku přežívání pacientů překážkou odlišná metodologie studia TME, což velmi ztěžuje zobecnění výsledků těchto studií či zahrnutí do klinické praxe (Hadler-Olsen and Wirsing 2019). V řadě studií se nerozlišuje přesná anatomická lokalizace nádorů. Nádory orofaryngu jsou specifické, neboť jsou z velké části infikovány virem HPV, kdežto u nádorů dutiny ústní je virová pozitivita nižší (Partlova et al. 2015; Pokrývková et al. 2021; Pokrývková et al. 2022). Proto by oddělené studium těchto nádorů mohlo přinést signifikantnější výsledky. S tímto fenoménem souvisí také časté vynechání informace o statusu HPV při hodnocení prediktivních znaků přežívání. Mnohdy jsou provedeny pouze univariantní analýzy přežívání, avšak vzhledem k tomu, že status HPV je silným prediktorem přežívání, je zcela nezbytné provést multivariantní analýzy přežívání, ve kterých je informace o virovém statusu zahrnuta. Z hlediska metodologie studia TME také narážíme na jistá úskalí. Ukazuje se, že zastoupení imunitních buněk se liší v nádorovém parenchymu a okolním stroma, avšak v mnoha imunohistochemických studiích se nádor hodnotí jako celek. V poslední době však stále více skupin, včetně naší pracovní skupiny, provádí detailní imunohistochemickou prostorovou charakteristiku TME. Publikace se dále liší metodologií kvantifikace pozitivních buněk. V rámci IHC se setkáváme buď s přesným numerickým hodnocením (např. počty buněk vztažených na plochu tkáně), či s hodnocením míry exprese (nízká/střední/vysoká či využití mediánu). Nelze říct, že by se tyto dva přístupy vylučovaly, avšak je velmi těžké mezi sebou studie porovnat, zejména v druhém případě mohou být výstupy ovlivněny nastavením hraničních hodnot jednotlivých kategorií. Z tohoto ohledu se zdá být přístup numerické kvantifikace (s využitím počítačových algoritmů) lépe reprodukovatelný. Do budoucna je vhodné pracovat na standardizaci metodiky hodnocení TIL/imunitních znaků pro predikci přežívání pacientů s HNSCC podobně, jako je tomu v případě karcinomů kolorekta (Pagès et al. 2018). Jako velmi slibná se jeví aktivita Mezinárodní imuno-onkologické pracovní skupiny zabývající se biomarkery (International Immuno-Oncology Biomarkers Working Group), která již vydala několik doporučení pro hodnocení TIL v lidských nádorech, včetně HNSCC (Hendry et al. 2017).

7. Souhrn

V této dizertační práci jsem ukázala, že nádorové mikroprostředí HNSCC virové a neviróvé etiologie vykazuje značné rozdíly z hlediska infiltrace imunitních buněk, které svými cytokiny či vzájemnými interakcemi ovlivňují nádorový růst (tabulka 2). Karcinomy HPV⁺ jsou silněji infiltrovány TIL oproti karcinomům HPV⁻, což patrně vede k nastolení silnější protinádorové imunitní odpovědi a tím i k lepšímu přežívání pacientů s HNSCC. Infekce HPV indukuje tvorbu paměťových antivirových CD8⁺ T lymfocytů cílených proti antigenům HPV. Naopak, v karcinomech HPV⁻ se nachází více imunosupresivních makrofágů typu M2, vyšší hladina mRNA genů asociovaných s fenotypem M2 či dalšími supresivními buňkami TME, vyšší hladina VEGF, což společně s nižší infiltrací TIL naznačuje imunosupresivní mikroprostředí těchto nádorů podporující nádorovou progresi. Status HPV se zdá být stěžejním faktorem přežívání pacientů s HNSCC. Dále jsou hladiny PD-1⁺CD8⁺ T lymfocytů a mRNA ARG1 navrženy jako nezávislý faktor predikující přežívání pacientů s HNSCC. Hladina buněk produkujících HIF-1 α a GLUT1 je také spojena s přežíváním pacientů s HNSCC, avšak pouze v modelech nezahrnujících status HPV (Pokrývková et al. 2021; Pokrývková et al. 2022; Smahelova et al. 2024).

Tabulka 2. Shrnutí rozdílů mikroprostředí HNSCC virové (HPV⁺) a neviróvé (HPV⁻) etiologie:

A) rozdílné zastoupení imunitních buněk a buněk produkujících vybrané znaky, B) rozdílná hladina mRNA genů exprimovaných v TME.

A) Buněčné populace, jejichž hladina je v dané skupině nádorů signifikantně vyšší			
HPV⁺		HPV⁻	
<i>Nádorový parenchym</i>	<i>Stroma</i>	<i>Nádorový parenchym</i>	<i>Stroma</i>
CD3 ⁺ T lymfocyty ¹	CD3 ⁺ T lymfocyty ¹	ARG1 ⁺ buňky ²	ARG1 ⁺ buňky ²
CD4 ⁺ T lymfocyty ¹	CD4 ⁺ T lymfocyty ¹	VEGFA ⁺ buňky ³	CD68 ⁺ ARG1 ⁺ M2 ²
CD8 ⁺ T lymfocyty ¹	CD8 ⁺ T lymfocyty ¹		
PD-1 ⁺ CD4 ⁺ T lymfocyty ¹	PD-1 ⁺ CD4 ⁺ T lymfocyty ¹		CTLA4 ⁺ CD4 ⁺ T lymfocyty ¹
PD-1 ⁺ CD8 ⁺ T lymfocyty ¹	PD-1 ⁺ CD8 ⁺ T lymfocyty ¹		ICOS ⁺ Treg ¹
ICOS ⁻ Treg ¹			
GLUT1 ⁺ buňky ³	GLUT1 ⁺ buňky ³		
MMP13 ⁺ buňky ³	MMP13 ⁺ buňky ³		
HIF-1α ⁺ buňky ³			
ASPH ⁺ buňky ³			
B) mRNA, jejichž hladina je v dané skupině nádorů signifikantně vyšší			
HPV⁺		HPV⁻	
NOS2 ³		CD163 ²	
		ARG1 ²	
		PTGS2 (COX-2) ²	
		EPAS1 (HIF-2α) ²	

¹ Pokrývková et al. 2022 ² Pokrývková et al. 2021 ³ Smahelova et al. 2024

8. Seznam použité literatury

- Akagi, K., J. Li, T. R. Broutian, H. Padilla-Nash, W. Xiao, B. Jiang, J. W. Rocco, T. N. Teknos, B. Kumar, D. Wangsa, D. He, T. Ried, D. E. Symer, and M. L. Gillison. 2014. "Genome-wide analysis of HPV integration in human cancers reveals recurrent, focal genomic instability." *Genome Res* 24 (2): 185-99. <https://doi.org/10.1101/gr.164806.113>.
- Anantharaman, D., B. Abedi-Ardekani, D. C. Beachler, T. Gheit, A. F. Olshan, K. Wisniewski, V. Wunsch-Filho, T. N. Toporcov, E. H. Tajara, J. E. Levi, R. A. Moyses, S. Boccia, G. Cadoni, G. Rindi, W. Ahrens, F. Merletti, D. I. Conway, S. Wright, C. Carreira, H. Renard, P. Chopard, S. McKay-Chopin, G. Scelo, M. Tommasino, P. Brennan, and G. D'Souza. 2017. "Geographic heterogeneity in the prevalence of human papillomavirus in head and neck cancer." *Int J Cancer* 140 (9): 1968-1975. <https://doi.org/10.1002/ijc.30608>.
- Anayannis, N. V., N. F. Schlecht, M. Ben-Dayana, R. V. Smith, T. J. Belbin, T. J. Ow, D. M. Blakaj, R. D. Burk, S. M. Leonard, C. B. Woodman, J. L. Parish, and M. B. Prystowsky. 2018. "Association of an intact E2 gene with higher HPV viral load, higher viral oncogene expression, and improved clinical outcome in HPV16 positive head and neck squamous cell carcinoma." *PLoS One* 13 (2): e0191581. <https://doi.org/10.1371/journal.pone.0191581>.
- Andzinski, L., N. Kasnitz, S. Stahnke, C. F. Wu, M. Gereke, M. von Köckritz-Blickwede, B. Schilling, S. Brandau, S. Weiss, and J. Jablonska. 2016. "Type I IFNs induce anti-tumor polarization of tumor associated neutrophils in mice and human." *Int J Cancer* 138 (8): 1982-93. <https://doi.org/10.1002/ijc.29945>.
- Ang, K. K., J. Harris, R. Wheeler, R. Weber, D. I. Rosenthal, P. F. Nguyen-Tan, W. H. Westra, C. H. Chung, R. C. Jordan, C. Lu, H. Kim, R. Axelrod, C. C. Silverman, K. P. Redmond, and M. L. Gillison. 2010. "Human papillomavirus and survival of patients with oropharyngeal cancer." *N Engl J Med* 363 (1): 24-35. <https://doi.org/10.1056/NEJMoa0912217>.
- Antuamwine, B. B., R. Bosnjakovic, F. Hofmann-Vega, X. Wang, T. Theodosiou, I. Iliopoulos, and S. Brandau. 2023. "N1 versus N2 and PMN-MDSC: A critical appraisal of current concepts on tumor-associated neutrophils and new directions for human oncology." *Immunol Rev* 314 (1): 250-279. <https://doi.org/10.1111/imr.13176>.
- Aras, S., and M. R. Zaidi. 2017. "TAMEless traitors: macrophages in cancer progression and metastasis." *Br J Cancer*. <https://doi.org/10.1038/bjc.2017.356>.
- Arbyn, M., M. Simon, E. Peeters, L. Xu, Cjlm Meijer, J. Berkhof, K. Cuschieri, J. Bonde, A. Ostrbenk Vanlencak, F. H. Zhao, R. Rezhake, M. Gultekin, J. Dillner, S. de Sanjosé, K. Canfell, P. Hillemanns, M. Almonte, N. Wentzensen, and M. Poljak. 2021. "2020 list of human papillomavirus assays suitable for primary cervical cancer screening." *Clin Microbiol Infect* 27 (8): 1083-1095. <https://doi.org/10.1016/j.cmi.2021.04.031>.
- Badoual, C., S. Hans, N. Merillon, C. Van Ryswick, P. Ravel, N. Benhamouda, E. Levionnois, M. Nizard, A. Si-Mohamed, N. Besnier, A. Gey, R. Rotem-Yehudar, H. Pere, T. Tran, C. L. Guerin, A. Chauvat, E. Dransart, C. Alanio, S. Albert, B. Barry, F. Sandoval, F. Quintin-Colonna, P. Bruneval, W. H. Fridman, F. M. Lemoine, S. Oudard, L. Johannes, D. Olive, D. Brasnu, and E. Tartour. 2013. "PD-1-expressing tumor-infiltrating T cells are a favorable prognostic biomarker in HPV-associated head and neck cancer." *Cancer Res* 73 (1): 128-38. <https://doi.org/10.1158/0008-5472.can-12-2606>.
- Baruah, P., M. Lee, P. O. Wilson, T. Odutoye, P. Williamson, N. Hyde, J. C. Kaski, and I. E. Dumitriu. 2015. "Impact of p16 status on pro- and anti-angiogenesis factors in head and neck cancers." *Br J Cancer* 113 (4): 653-9. <https://doi.org/10.1038/bjc.2015.251>.
- Bauml, Joshua M., Charu Aggarwal, and Roger B. Cohen. 2019. "Immunotherapy for head and neck cancer: where are we now and where are we going?" *Annals of Translational Medicine*: S75. <https://atm.amegroups.org/article/view/24939>.
- Bergvall, M., T. Melendy, and J. Archambault. 2013. "The E1 proteins." *Virology* 445 (1-2): 35-56. <https://doi.org/10.1016/j.virol.2013.07.020>.

- Biffi, G., and D. A. Tuveson. 2021. "Diversity and Biology of Cancer-Associated Fibroblasts." *Physiol Rev* 101 (1): 147-176. <https://doi.org/10.1152/physrev.00048.2019>.
- Bisheshar, S. K., M. F. van der Kamp, E. J. de Ruiter, L. N. Ruiter, B. van der Vegt, G. E. Breimer, and S. M. Willems. 2022. "The prognostic role of tumor associated macrophages in squamous cell carcinoma of the head and neck: A systematic review and meta-analysis." *Oral Oncol* 135: 106227. <https://doi.org/10.1016/j.oraloncology.2022.106227>.
- Borsetto, D., M. Tomasoni, K. Payne, J. Polesel, A. Deganello, P. Bossi, J. R. Tysome, L. Masterson, G. Tirelli, M. Tofanelli, and P. Boscolo-Rizzo. 2021. "Prognostic Significance of CD4+ and CD8+ Tumor-Infiltrating Lymphocytes in Head and Neck Squamous Cell Carcinoma: A Meta-Analysis." *Cancers (Basel)* 13 (4). <https://doi.org/10.3390/cancers13040781>.
- Bray, F., M. Laversanne, H. Sung, J. Ferlay, R. L. Siegel, I. Soerjomataram, and A. Jemal. 2024. "Global cancer statistics 2022: GLOBOCAN estimates of incidence and mortality worldwide for 36 cancers in 185 countries." *CA Cancer J Clin*. <https://doi.org/10.3322/caac.21834>.
- Bronte, V., S. Brandau, S. H. Chen, M. P. Colombo, A. B. Frey, T. F. Greten, S. Mandruzzato, P. J. Murray, A. Ochoa, S. Ostrand-Rosenberg, P. C. Rodriguez, A. Sica, V. Umansky, R. H. Vonderheide, and D. I. Gabrilovich. 2016. "Recommendations for myeloid-derived suppressor cell nomenclature and characterization standards." *Nat Commun* 7: 12150. <https://doi.org/10.1038/ncomms12150>.
- Brooks, J. M., A. N. Menezes, M. Ibrahim, L. Archer, N. Lal, C. J. Bagnall, S. V. von Zeidler, H. R. Valentine, R. J. Spruce, N. Batis, J. L. Bryant, M. Hartley, B. Kaul, G. B. Ryan, R. Bao, A. Khattri, S. P. Lee, K. U. E. Ogbureke, G. Middleton, D. A. Tennant, A. D. Beggs, J. Deeks, C. M. L. West, J. B. Cazier, B. E. Willcox, T. Y. Seiwert, and H. Mehanna. 2019. "Development and Validation of a Combined Hypoxia and Immune Prognostic Classifier for Head and Neck Cancer." *Clin Cancer Res* 25 (17): 5315-5328. <https://doi.org/10.1158/1078-0432.ccr-18-3314>.
- Castellsague, X., L. Alemany, M. Quer, G. Halc, B. Quiros, S. Tous, O. Clavero, L. Alos, T. Biegner, T. Szafarowski, M. Alejo, D. Holzinger, E. Cadena, E. Claros, G. Hall, J. Laco, M. Poljak, M. Benevolo, E. Kasamatsu, H. Mehanna, C. Ndiaye, N. Guimera, B. Lloveras, X. Leon, J. C. Ruiz-Cabezas, I. Alvarado-Cabrero, C. S. Kang, J. K. Oh, M. Garcia-Rojo, E. Iljazovic, O. F. Ajayi, F. Duarte, A. Nessa, L. Tinoco, M. A. Duran-Padilla, E. C. Pirog, H. Viarheichyk, H. Morales, V. Costes, A. Felix, M. J. Germar, M. Mena, A. Ruacan, A. Jain, R. Mehrotra, M. T. Goodman, L. E. Lombardi, A. Ferrera, S. Malami, E. I. Albanesi, P. Dabed, C. Molina, R. Lopez-Revilla, V. Mandys, M. E. Gonzalez, J. Velasco, I. G. Bravo, W. Quint, M. Pawlita, N. Munoz, Sd Sanjose, and F. Xavier Bosch. 2016. "HPV Involvement in Head and Neck Cancers: Comprehensive Assessment of Biomarkers in 3680 Patients." *J Natl Cancer Inst* 108 (6): djv403. <https://doi.org/10.1093/jnci/djv403>.
- Cereceda, K., R. Jorquera, and F. Villarroel-Espíndola. 2022. "Advances in mass cytometry and its applicability to digital pathology in clinical-translational cancer research." *Adv Lab Med* 3 (1): 5-29. <https://doi.org/10.1515/almed-2021-0075>.
- Chaiwongkot, A., S. Vinokurova, C. Pientong, T. Ekalaksananan, B. Kongyingyoes, P. Kleebkaow, B. Chumworathayi, N. Patarapadungkit, M. Reuschenbach, and M. von Knebel Doeberitz. 2013. "Differential methylation of E2 binding sites in episomal and integrated HPV 16 genomes in preinvasive and invasive cervical lesions." *Int J Cancer* 132 (9): 2087-94. <https://doi.org/10.1002/ijc.27906>.
- Chang, C. I., J. C. Liao, and L. Kuo. 1998. "Arginase modulates nitric oxide production in activated macrophages." *Am J Physiol* 274 (1): H342-8. <https://doi.org/10.1152/ajpheart.1998.274.1.H342>.
- Chang, J. T., T. F. Kuo, Y. J. Chen, C. C. Chiu, Y. C. Lu, H. F. Li, C. R. Shen, and A. J. Cheng. 2010. "Highly potent and specific siRNAs against E6 or E7 genes of HPV16- or HPV18-infected cervical cancers." *Cancer Gene Ther* 17 (12): 827-36. <https://doi.org/10.1038/cgt.2010.38>.

- Che, D., S. Zhang, Z. Jing, L. Shang, S. Jin, F. Liu, J. Shen, Y. Li, J. Hu, Q. Meng, and Y. Yu. 2017. "Macrophages induce EMT to promote invasion of lung cancer cells through the IL-6-mediated COX-2/PGE(2)/ β -catenin signalling pathway." *Mol Immunol* 90: 197-210. <https://doi.org/10.1016/j.molimm.2017.06.018>.
- Chellappan, S., V. B. Kraus, B. Kroger, K. Munger, P. M. Howley, W. C. Phelps, and J. R. Nevins. 1992. "Adenovirus E1A, simian virus 40 tumor antigen, and human papillomavirus E7 protein share the capacity to disrupt the interaction between transcription factor E2F and the retinoblastoma gene product." *Proc Natl Acad Sci U S A* 89 (10): 4549-53. <https://doi.org/10.1073/pnas.89.10.4549>.
- Chen, D. S., and I. Mellman. 2017. "Elements of cancer immunity and the cancer-immune set point." *Nature* 541 (7637): 321-330. <https://doi.org/10.1038/nature21349>.
- Chen, Q., L. Mo, X. Cai, L. Wei, Z. Xie, H. Li, J. Li, and Z. Hu. 2018. "ICOS signal facilitates Foxp3 transcription to favor suppressive function of regulatory T cells." *Int J Med Sci* 15 (7): 666-673. <https://doi.org/10.7150/ijms.23940>.
- Choo, K. B., C. C. Pan, and S. H. Han. 1987. "Integration of human papillomavirus type 16 into cellular DNA of cervical carcinoma: preferential deletion of the E2 gene and invariable retention of the long control region and the E6/E7 open reading frames." *Virology* 161 (1): 259-61. [https://doi.org/10.1016/0042-6822\(87\)90195-4](https://doi.org/10.1016/0042-6822(87)90195-4).
- Collin, M., and V. Bigley. 2018. "Human dendritic cell subsets: an update." *Immunology* 154 (1): 3-20. <https://doi.org/10.1111/imm.12888>.
- Combs, S. E., G. Han, N. Mani, S. Beruti, M. Nerenberg, and D. L. Rimm. 2016. "Loss of antigenicity with tissue age in breast cancer." *Lab Invest* 96 (3): 264-9. <https://doi.org/10.1038/labinvest.2015.138>.
- Corzo, C. A., T. Condamine, L. Lu, M. J. Cotter, J. I. Youn, P. Cheng, H. I. Cho, E. Celis, D. G. Quiceno, T. Padhya, T. V. McCaffrey, J. C. McCaffrey, and D. I. Gabrilovich. 2010. "HIF-1 α regulates function and differentiation of myeloid-derived suppressor cells in the tumor microenvironment." *J Exp Med* 207 (11): 2439-53. <https://doi.org/10.1084/jem.20100587>.
- Dal Maso, L., N. Torelli, E. Biancotto, M. Di Maso, A. Gini, G. Franchin, F. Levi, C. La Vecchia, D. Serraino, and J. Polesel. 2016. "Combined effect of tobacco smoking and alcohol drinking in the risk of head and neck cancers: a re-analysis of case-control studies using bi-dimensional spline models." *Eur J Epidemiol* 31 (4): 385-93. <https://doi.org/10.1007/s10654-015-0028-3>.
- Day, P. M., D. R. Lowy, and J. T. Schiller. 2008. "Heparan sulfate-independent cell binding and infection with furin-precleaved papillomavirus capsids." *J Virol* 82 (24): 12565-8. <https://doi.org/10.1128/jvi.01631-08>.
- de Jong, S. J., A. Créquer, I. Matos, D. Hum, V. Gunasekharan, L. Lorenzo, F. Jabot-Hanin, E. Imahorn, A. A. Arias, H. Vahidnezhad, L. Youssefian, J. G. Markle, E. Patin, A. D'Amico, C. Q. F. Wang, F. Full, A. Ensser, T. M. Leisner, L. V. Parise, M. Bouaziz, N. P. Maya, X. R. Cadena, B. Saka, A. H. Saeidian, N. Aghazadeh, S. Zeinali, P. Itin, J. G. Krueger, L. Laimins, L. Abel, E. Fuchs, J. Uitto, J. L. Franco, B. Burger, G. Orth, E. Jouanguy, and J. L. Casanova. 2018. "The human CIB1-EVER1-EVER2 complex governs keratinocyte-intrinsic immunity to β -papillomaviruses." *J Exp Med* 215 (9): 2289-2310. <https://doi.org/10.1084/jem.20170308>.
- de Jong, S. J., E. Imahorn, P. Itin, J. Uitto, G. Orth, E. Jouanguy, J. L. Casanova, and B. Burger. 2018. "Epidermodysplasia Verruciformis: Inborn Errors of Immunity to Human Beta-Papillomaviruses." *Front Microbiol* 9: 1222. <https://doi.org/10.3389/fmicb.2018.01222>.
- de Martel, C., M. Plummer, J. Vignat, and S. Franceschi. 2017. "Worldwide burden of cancer attributable to HPV by site, country and HPV type." *Int J Cancer* 141 (4): 664-670. <https://doi.org/10.1002/ijc.30716>.
- de Villiers, E. M. 2013. "Cross-roads in the classification of papillomaviruses." *Virology*. <https://doi.org/10.1016/j.virol.2013.04.023>.
- Di Credico, G., J. Polesel, L. Dal Maso, F. Pauli, N. Torelli, D. Luce, L. Radoi, K. Matsuo, D. Serraino, P. Brennan, I. Holcatova, W. Ahrens, P. Lagioui, C. Canova, L. Richiardi, C. M. Healy, K. Kjaerheim, D. I. Conway, G. J. Macfarlane, P. Thomson, A. Agudo, A. Znaor,

- S. Franceschi, R. Herrero, T. N. Toporcov, R. A. Moyses, J. Muscat, E. Negri, M. Vilensky, L. Fernandez, M. P. Curado, A. Menezes, A. W. Daudt, R. Koifman, V. Wunsch-Filho, A. F. Olshan, J. P. Zevallos, E. M. Sturgis, G. Li, F. Levi, Z. F. Zhang, H. Morgenstern, E. Smith, P. Lazarus, C. La Vecchia, W. Garavello, C. Chen, S. M. Schwartz, T. Zheng, T. L. Vaughan, K. Kelsey, M. McClean, S. Benhamou, R. B. Hayes, M. P. Purdue, M. Gillison, S. Schantz, G. P. Yu, S. C. Chuang, P. Boffetta, M. Hashibe, A. L. Yuan-Chin, and V. Edefonti. 2020. "Alcohol drinking and head and neck cancer risk: the joint effect of intensity and duration." *Br J Cancer* 123 (9): 1456-1463. <https://doi.org/10.1038/s41416-020-01031-z>.
- Donnem, T., S. M. Hald, E. E. Paulsen, E. Richardsen, S. Al-Saad, T. K. Kilvaer, O. T. Brustugun, A. Helland, M. Lund-Iversen, M. Poehl, K. E. Olsen, H. J. Ditzel, O. Hansen, K. Al-Shibli, Y. Kiselev, T. M. Sandanger, S. Andersen, F. Pezzella, R. M. Bremnes, and L. T. Busund. 2015. "Stromal CD8+ T-cell Density—A Promising Supplement to TNM Staging in Non-Small Cell Lung Cancer." *Clin Cancer Res* 21 (11): 2635-43. <https://doi.org/10.1158/1078-0432.ccr-14-1905>.
- Doorbar, J., S. Ely, J. Sterling, C. McLean, and L. Crawford. 1991. "Specific interaction between HPV-16 E1-E4 and cytokeratins results in collapse of the epithelial cell intermediate filament network." *Nature* 352 (6338): 824-7. <https://doi.org/10.1038/352824a0>.
- Du, M., K. M. Roy, L. Zhong, Z. Shen, H. E. Meyers, and R. C. Nichols. 2006. "VEGF gene expression is regulated post-transcriptionally in macrophages." *Febs j* 273 (4): 732-45. <https://doi.org/10.1111/j.1742-4658.2006.05106.x>.
- Duan, Y., M. Zhou, B. Ye, K. Yue, F. Qiao, Y. Wang, Q. Lai, Y. Wu, J. Cao, X. Wang, and C. Jing. 2024. "Hypoxia-induced miR-5100 promotes exosome-mediated activation of cancer-associated fibroblasts and metastasis of head and neck squamous cell carcinoma." *Cell Death Dis* 15 (3): 215. <https://doi.org/10.1038/s41419-024-06587-9>.
- Dumitru, C. A., M. K. Fechner, T. K. Hoffmann, S. Lang, and S. Brandau. 2012. "A novel p38-MAPK signaling axis modulates neutrophil biology in head and neck cancer." *J Leukoc Biol* 91 (4): 591-8. <https://doi.org/10.1189/jlb.0411193>.
- Dušek, Ladislav, Jan Mužík, Miroslav Kubásek, Jana Koptíková, Jan Žaloudík, and Rostislav Vyzula. 2005. "Epidemiologie zhoubných nádorů v České republice [online]." Masarykova Univerzita. Accessed 6 September 2023. <http://www.svod.cz>.
- Echarti, A., M. Hecht, M. Büttner-Herold, M. Haderlein, A. Hartmann, R. Fietkau, and L. Distel. 2019. "CD8+ and Regulatory T cells Differentiate Tumor Immune Phenotypes and Predict Survival in Locally Advanced Head and Neck Cancer." *Cancers (Basel)* 11 (9). <https://doi.org/10.3390/cancers11091398>.
- Eisma, R. J., J. D. Spiro, and D. L. Kreutzer. 1997. "Vascular endothelial growth factor expression in head and neck squamous cell carcinoma." *Am J Surg* 174 (5): 513-7. [https://doi.org/10.1016/s0002-9610\(97\)00166-9](https://doi.org/10.1016/s0002-9610(97)00166-9).
- El Sissy, C., A. Kirilovsky, C. Lagorce Pagès, F. Marliot, P. A. Custers, E. Dizdarevic, M. Sroussi, M. Castillo-Martin, N. Haicheur, M. Dermani, N. Loche, B. Buttard, A. M. Musina, M. G. Anitei, J. G. van den Berg, A. Broeks, S. Iseas, M. Coraglio, F. S. Loria, A. Romero, P. Laurent-Puig, A. de Reyniès, L. M. Fernandez, M. Karoui, D. Tougeron, C. A. Vaccaro, J. P. Santino, LØ Poulsen, J. Lindebjerg, J. M. O'Connor, V. Scripcariu, M. G. Dimofte, J. P. Gérard, M. Chalabi, N. Figueiredo, R. O. Perez, A. Habr-Gama, J. Galon, T. F. Hansen, L. H. Jensen, G. Beets, G. Zeitoun, and F. Pagès. 2024. "International Validation of the Immunoscore Biopsy in Patients With Rectal Cancer Managed by a Watch-and-Wait Strategy." *J Clin Oncol* 42 (1): 70-80. <https://doi.org/10.1200/jco.23.00586>.
- El-Mofty, S. K., M. Q. Zhang, and R. M. Davila. 2008. "Histologic identification of human papillomavirus (HPV)-related squamous cell carcinoma in cervical lymph nodes: a reliable predictor of the site of an occult head and neck primary carcinoma." *Head Neck Pathol* 2 (3): 163-8. <https://doi.org/10.1007/s12105-008-0066-1>.
- Fan, C. Y. 2001. "Genetic alterations in head and neck cancer: interactions among environmental carcinogens, cell cycle control, and host DNA repair." *Curr Oncol Rep* 3 (1): 66-71. <https://doi.org/10.1007/s11912-001-0045-0>.

- Fan, R., W. J. Hou, Y. J. Zhao, S. L. Liu, X. S. Qiu, E. H. Wang, and G. P. Wu. 2016. "Overexpression of HPV16 E6/E7 mediated HIF-1 α upregulation of GLUT1 expression in lung cancer cells." *Tumour Biol* 37 (4): 4655-63. <https://doi.org/10.1007/s13277-015-4221-5>.
- Fei, J., A. Hong, T. A. Dobbins, D. Jones, C. S. Lee, C. Loo, M. Al-Ghamdi, G. B. Harnett, J. Clark, C. J. O'Brien, and B. Rose. 2009. "Prognostic significance of vascular endothelial growth factor in squamous cell carcinomas of the tonsil in relation to human papillomavirus status and epidermal growth factor receptor." *Ann Surg Oncol* 16 (10): 2908-17. <https://doi.org/10.1245/s10434-009-0579-1>.
- Fontenot, J. D., M. A. Gavin, and A. Y. Rudensky. 2003. "Foxp3 programs the development and function of CD4⁺CD25⁺ regulatory T cells." *Nat Immunol* 4 (4): 330-6. <https://doi.org/10.1038/ni904>.
- Freeman, G. J., A. J. Long, Y. Iwai, K. Bourque, T. Chernova, H. Nishimura, L. J. Fitz, N. Malenkovich, T. Okazaki, M. C. Byrne, H. F. Horton, L. Fouser, L. Carter, V. Ling, M. R. Bowman, B. M. Carreno, M. Collins, C. R. Wood, and T. Honjo. 2000. "Engagement of the PD-1 immunoinhibitory receptor by a novel B7 family member leads to negative regulation of lymphocyte activation." *J Exp Med* 192 (7): 1027-34. <https://doi.org/10.1084/jem.192.7.1027>.
- Fridlender, Z. G., J. Sun, S. Kim, V. Kapoor, G. Cheng, L. Ling, G. S. Worthen, and S. M. Albelda. 2009. "Polarization of tumor-associated neutrophil phenotype by TGF- β : "N1" versus "N2" TAN." *Cancer Cell* 16 (3): 183-94. <https://doi.org/10.1016/j.ccr.2009.06.017>.
- Gaffney, E. F., P. H. Riegman, W. E. Grizzle, and P. H. Watson. 2018. "Factors that drive the increasing use of FFPE tissue in basic and translational cancer research." *Biotech Histochem* 93 (5): 373-386. <https://doi.org/10.1080/10520295.2018.1446101>.
- Galon, J., B. Mlecnik, G. Bindea, H. K. Angell, A. Berger, C. Lagorce, A. Lugli, I. Zlobec, A. Hartmann, C. Bifulco, I. D. Nagtegaal, R. Palmqvist, G. V. Masucci, G. Botti, F. Tatangelo, P. Delrio, M. Maio, L. Laghi, F. Grizzi, M. Asslaber, C. D'Arrigo, F. Vidal-Vanaclocha, E. Zavadova, L. Chouchane, P. S. Ohashi, S. Hafezi-Bakhtiari, B. G. Wouters, M. Roehrl, L. Nguyen, Y. Kawakami, S. Hazama, K. Okuno, S. Ogino, P. Gibbs, P. Waring, N. Sato, T. Torigoe, K. Itoh, P. S. Patel, S. N. Shukla, Y. Wang, S. Kopetz, F. A. Sinicrope, V. Scripcariu, P. A. Ascierto, F. M. Marincola, B. A. Fox, and F. Pagès. 2014. "Towards the introduction of the 'Immunoscore' in the classification of malignant tumours." *J Pathol* 232 (2): 199-209. <https://doi.org/10.1002/path.4287>.
- García-Navas, R., C. Gajate, and F. Mollinedo. 2021. "Neutrophils drive endoplasmic reticulum stress-mediated apoptosis in cancer cells through arginase-1 release." *Sci Rep* 11 (1): 12574. <https://doi.org/10.1038/s41598-021-91947-0>.
- Gaykalova, D. A., E. Mambo, A. Choudhary, J. Houghton, K. Buddavarapu, T. Sanford, W. Darden, A. Adai, A. Hadd, G. Latham, L. V. Danilova, J. Bishop, R. J. Li, W. H. Westra, P. Hennessey, W. M. Koch, M. F. Ochs, J. A. Califano, and W. Sun. 2014. "Novel insight into mutational landscape of head and neck squamous cell carcinoma." *PLoS One* 9 (3): e93102. <https://doi.org/10.1371/journal.pone.0093102>.
- Ghalehbandi, S., J. Yuzugulen, M. Z. I. Pranjol, and M. H. Pourgholami. 2023. "The role of VEGF in cancer-induced angiogenesis and research progress of drugs targeting VEGF." *Eur J Pharmacol* 949: 175586. <https://doi.org/10.1016/j.ejphar.2023.175586>.
- Gillison, M. L., G. D'Souza, W. Westra, E. Sugar, W. Xiao, S. Begum, and R. Viscidi. 2008. "Distinct risk factor profiles for human papillomavirus type 16-positive and human papillomavirus type 16-negative head and neck cancers." *J Natl Cancer Inst* 100 (6): 407-20. <https://doi.org/10.1093/jnci/djn025>.
- Gillison, M. L., W. M. Koch, R. B. Capone, M. Spafford, W. H. Westra, L. Wu, M. L. Zahurak, R. W. Daniel, M. Viglione, D. E. Symer, K. V. Shah, and D. Sidransky. 2000. "Evidence for a causal association between human papillomavirus and a subset of head and neck cancers." *J Natl Cancer Inst* 92 (9): 709-20. <https://doi.org/10.1093/jnci/92.9.709>.
- Gonzalez, S. L., M. Stremelau, X. He, J. R. Basile, and K. Münger. 2001. "Degradation of the retinoblastoma tumor suppressor by the human papillomavirus type 16 E7 oncoprotein is

- important for functional inactivation and is separable from proteasomal degradation of E7." *J Virol* 75 (16): 7583-91. <https://doi.org/10.1128/jvi.75.16.7583-7591.2001>.
- Gordon, S. 2007. "The macrophage: past, present and future." *Eur J Immunol* 37 Suppl 1: S9-17. <https://doi.org/10.1002/eji.200737638>.
- Gros, A., P. F. Robbins, X. Yao, Y. F. Li, S. Turcotte, E. Tran, J. R. Wunderlich, A. Mixon, S. Farid, M. E. Dudley, K. Hanada, J. R. Almeida, S. Darko, D. C. Douek, J. C. Yang, and S. A. Rosenberg. 2014. "PD-1 identifies the patient-specific CD8⁺ tumor-reactive repertoire infiltrating human tumors." *J Clin Invest* 124 (5): 2246-59. <https://doi.org/10.1172/jci73639>.
- Guan, J., S. M. Bywaters, S. A. Brendle, R. E. Ashley, A. M. Makhov, J. F. Conway, N. D. Christensen, and S. Hafenstein. 2017. "Cryo-electron Microscopy Maps of Human Papillomavirus 16 Reveal L2 Densities and Heparin Binding Site." *Structure* 25 (2): 253-263. <https://doi.org/10.1016/j.str.2016.12.001>.
- Guess, J. C., and D. J. McCance. 2005. "Decreased migration of Langerhans precursor-like cells in response to human keratinocytes expressing human papillomavirus type 16 E6/E7 is related to reduced macrophage inflammatory protein-3 α production." *J Virol* 79 (23): 14852-62. <https://doi.org/10.1128/jvi.79.23.14852-14862.2005>.
- Hadler-Olsen, E., and A. M. Wirsing. 2019. "Tissue-infiltrating immune cells as prognostic markers in oral squamous cell carcinoma: a systematic review and meta-analysis." *Br J Cancer* 120 (7): 714-727. <https://doi.org/10.1038/s41416-019-0409-6>.
- Han, J., T. Fujisawa, S. R. Husain, and R. K. Puri. 2014. "Identification and characterization of cancer stem cells in human head and neck squamous cell carcinoma." *BMC Cancer* 14: 173. <https://doi.org/10.1186/1471-2407-14-173>.
- Hanahan, D., and R. A. Weinberg. 2011. "Hallmarks of cancer: the next generation." *Cell* 144 (5): 646-74. <https://doi.org/10.1016/j.cell.2011.02.013>.
- Hanns, E., S. Job, P. Coliat, C. Wasylyk, L. Ramolu, E. Pencreach, M. Suarez-Carmona, M. Herfs, S. Ledrappier, C. Macabre, J. Abecassis, B. Wasylyk, and A. C. Jung. 2015. "Human Papillomavirus-related tumours of the oropharynx display a lower tumour hypoxia signature." *Oral Oncol* 51 (9): 848-56. <https://doi.org/10.1016/j.oraloncology.2015.06.003>.
- Hashibe, M., P. Brennan, S. Benhamou, X. Castellsague, C. Chen, M. P. Curado, L. Dal Maso, A. W. Daudt, E. Fabianova, L. Fernandez, V. Wunsch-Filho, S. Franceschi, R. B. Hayes, R. Herrero, S. Koifman, C. La Vecchia, P. Lazarus, F. Levi, D. Mates, E. Matos, A. Menezes, J. Muscat, J. Eluf-Neto, A. F. Olshan, P. Rudnai, S. M. Schwartz, E. Smith, E. M. Sturgis, N. Szeszenia-Dabrowska, R. Talamini, Q. Wei, D. M. Winn, D. Zaridze, W. Zatonski, Z. F. Zhang, J. Berthiller, and P. Boffetta. 2007. "Alcohol drinking in never users of tobacco, cigarette smoking in never drinkers, and the risk of head and neck cancer: pooled analysis in the International Head and Neck Cancer Epidemiology Consortium." *J Natl Cancer Inst* 99 (10): 777-89. <https://doi.org/10.1093/jnci/djk179>.
- He, X., and C. Xu. 2020. "Immune checkpoint signaling and cancer immunotherapy." *Cell Res* 30 (8): 660-669. <https://doi.org/10.1038/s41422-020-0343-4>.
- Hendry, S., R. Salgado, T. Gevaert, P. A. Russell, T. John, B. Thapa, M. Christie, K. van de Vijver, M. V. Estrada, P. I. Gonzalez-Ericsson, M. Sanders, B. Solomon, C. Solinas, Gggm Van den Eynden, Y. Allory, M. Preusser, J. Hainfellner, G. Pruneri, A. Vingiani, S. Demaria, F. Symmans, P. Nuciforo, L. Comerma, E. A. Thompson, S. Lakhani, S. R. Kim, S. Schnitt, C. Colpaert, C. Sotiriou, S. J. Scherer, M. Ignatiadis, S. Badve, R. H. Pierce, G. Viale, N. Sirtaine, F. Penault-Llorca, T. Sugie, S. Fineberg, S. Paik, A. Srinivasan, A. Richardson, Y. Wang, E. Chmielik, J. Brock, D. B. Johnson, J. Balko, S. Wienert, V. Bossuyt, S. Michiels, N. Ternes, N. Burchardi, S. J. Luen, P. Savas, F. Klauschen, P. H. Watson, B. H. Nelson, C. Criscitiello, S. O'Toole, D. Larsimont, R. de Wind, G. Curigliano, F. André, M. Lacroix-Triki, M. van de Vijver, F. Rojo, G. Floris, S. Bedri, J. Sparano, D. Rimm, T. Nielsen, Z. Kos, S. Hewitt, B. Singh, G. Farshid, S. Loibl, K. H. Allison, N. Tung, S. Adams, K. Willard-Gallo, H. M. Horlings, L. Gandhi, A. Moreira, F. Hirsch, M. V. Dieci, M. Urbanowicz, I. Brcic, K. Korski, F. Gaire, H. Koeppen, A. Lo, J. Giltnane, M. C. Rebelatto, K. E. Steele, J. Zha, K. Emancipator, J. W.

- Juco, C. Denkert, J. Reis-Filho, S. Loi, and S. B. Fox. 2017. "Assessing Tumor-infiltrating Lymphocytes in Solid Tumors: A Practical Review for Pathologists and Proposal for a Standardized Method From the International Immunooncology Biomarkers Working Group: Part 1: Assessing the Host Immune Response, TILs in Invasive Breast Carcinoma and Ductal Carcinoma In Situ, Metastatic Tumor Deposits and Areas for Further Research." *Adv Anat Pathol* 24 (5): 235-251. <https://doi.org/10.1097/pap.000000000000162>.
- Heng, Y., X. Zhu, H. Lin, M. Jingyu, X. Ding, L. Tao, and L. Lu. 2023. "CD206(+) tumor-associated macrophages interact with CD4(+) tumor-infiltrating lymphocytes and predict adverse patient outcome in human laryngeal squamous cell carcinoma." *J Transl Med* 21 (1): 167. <https://doi.org/10.1186/s12967-023-03910-4>.
- Heuvers, M. E., F. Muskens, K. Bezemer, M. Lambers, A. C. Dingemans, H. J. M. Groen, E. F. Smit, H. C. Hoogsteden, J. J. Hegmans, and J. G. Aerts. 2013. "Arginase-1 mRNA expression correlates with myeloid-derived suppressor cell levels in peripheral blood of NSCLC patients." *Lung Cancer* 81 (3): 468-474. <https://doi.org/10.1016/j.lungcan.2013.06.005>.
- Hladíková, K., V. Koucký, J. Bouček, J. Laco, M. Grega, M. Hodek, M. Zábrodský, M. Vošmik, K. Rozkošová, H. Vošmiková, P. Čelakovský, V. Chrobok, A. Ryška, R. Špišek, and A. Fialová. 2019. "Tumor-infiltrating B cells affect the progression of oropharyngeal squamous cell carcinoma via cell-to-cell interactions with CD8(+) T cells." *J Immunother Cancer* 7 (1): 261. <https://doi.org/10.1186/s40425-019-0726-6>.
- Hong, A., M. Zhang, A. S. Veillard, J. Jahanbani, C. S. Lee, D. Jones, G. Harnett, J. Clark, M. Elliott, C. Milross, and B. Rose. 2013. "The prognostic significance of hypoxia inducing factor 1- α in oropharyngeal cancer in relation to human papillomavirus status." *Oral Oncol* 49 (4): 354-9. <https://doi.org/10.1016/j.oraloncology.2012.11.006>.
- Hong, D., J. Liu, Y. Hu, X. Lu, B. Li, Y. Li, D. Hu, W. Lu, X. Xie, and X. Cheng. 2017. "Viral E6 is overexpressed via high viral load in invasive cervical cancer with episomal HPV16." *BMC Cancer* 17 (1): 136. <https://doi.org/10.1186/s12885-017-3124-9>.
- Hong, S. W., S. Lee, Y. J. Kim, S. Ahn, I. J. Park, S. M. Hong, S. W. Hwang, S. H. Park, D. H. Yang, B. D. Ye, J. S. Byeon, S. K. Yang, J. Kim, S. Y. Kim, and S. J. Myung. 2022. "Immune profile by multiplexed immunohistochemistry associated with recurrence after chemoradiation in rectal cancer." *J Gastroenterol Hepatol* 37 (3): 542-550. <https://doi.org/10.1111/jgh.15773>.
- Hu, Y., Q. Hu, Y. Li, L. Lu, Z. Xiang, Z. Yin, D. Kabelitz, and Y. Wu. 2023. " $\gamma\delta$ T cells: origin and fate, subsets, diseases and immunotherapy." *Signal Transduct Target Ther* 8 (1): 434. <https://doi.org/10.1038/s41392-023-01653-8>.
- Huibregtse, J. M., M. Scheffner, and P. M. Howley. 1993. "Localization of the E6-AP regions that direct human papillomavirus E6 binding, association with p53, and ubiquitination of associated proteins." *Mol Cell Biol* 13 (8): 4918-27.
- Hurt, B., R. Schulick, B. Edil, K. C. El Kasmi, and C. Barnett, Jr. 2017. "Cancer-promoting mechanisms of tumor-associated neutrophils." *Am J Surg* 214 (5): 938-944. <https://doi.org/10.1016/j.amjsurg.2017.08.003>.
- IARC, Working Group on the Evaluation of Carcinogenic Risks to Humans. 2012. "Personal habits and indoor combustions." *IARC Monogr Eval Carcinog Risks Hum* 100 (Pt E): 1-538.
- Ijsselsteijn, M. E., R. van der Breggen, A. Farina Sarasqueta, F. Koning, and N. de Miranda. 2019. "A 40-Marker Panel for High Dimensional Characterization of Cancer Immune Microenvironments by Imaging Mass Cytometry." *Front Immunol* 10: 2534. <https://doi.org/10.3389/fimmu.2019.02534>.
- Iyer, A., A. A. J. Hamers, and A. B. Pillai. 2022. "CyTOF(®) for the Masses." *Front Immunol* 13: 815828. <https://doi.org/10.3389/fimmu.2022.815828>.
- Jaganjac, M., M. Poljak-Blazi, R. J. Schaur, K. Zarkovic, S. Borovic, A. Cipak, M. Cindric, K. Uchida, G. Waeg, and N. Zarkovic. 2012. "Elevated neutrophil elastase and acrolein-protein adducts are associated with W256 regression." *Clin Exp Immunol* 170 (2): 178-85. <https://doi.org/10.1111/j.1365-2249.2012.04639.x>.

- Jayasingam, S. D., M. Citartan, T. H. Thang, A. A. Mat Zin, K. C. Ang, and E. S. Ch'ng. 2019. "Evaluating the Polarization of Tumor-Associated Macrophages Into M1 and M2 Phenotypes in Human Cancer Tissue: Technicalities and Challenges in Routine Clinical Practice." *Front Oncol* 9: 1512. <https://doi.org/10.3389/fonc.2019.01512>.
- Jhaveri, Niyati, Bassem Ben Cheikh, Nadezhda Nikulina, Ning Ma, Dmytro Klymyshyn, James DeRosa, Ritu Mihani, Aditya Pratapa, Yasmin Kassim, Sidharth Bommakanti, Olive Shang, Shannon Berry, Nicholas Ihley, Michael McLane, Yan He, Yi Zheng, James Monkman, Caroline Cooper, Ken O'Byrne, Bhaskar Anand, Michael Prater, Subham Basu, Brett G.M. Hughes, Arutha Kulasinghe, and Oliver Braubach. 2023. "Mapping the Spatial Proteome of Head and Neck Tumors: Key Immune Mediators and Metabolic Determinants in the Tumor Microenvironment." *GEN Biotechnology* 2 (5): 418-434. <https://doi.org/10.1089/genbio.2023.0029>. <https://www.liebertpub.com/doi/abs/10.1089/genbio.2023.0029>.
- Jiang, W., K. Hu, X. Liu, J. Gao, and L. Zhu. 2023. "Single-cell transcriptome analysis reveals the clinical implications of myeloid-derived suppressor cells in head and neck squamous cell carcinoma." *Pathol Oncol Res* 29: 1611210. <https://doi.org/10.3389/pore.2023.1611210>.
- Kalb, M. L., A. Glaser, G. Stary, F. Koszik, and G. Stingl. 2012. "TRAIL(+) human plasmacytoid dendritic cells kill tumor cells in vitro: mechanisms of imiquimod- and IFN- α -mediated antitumor reactivity." *J Immunol* 188 (4): 1583-91. <https://doi.org/10.4049/jimmunol.1102437>.
- Kamal, M., S. Lameiras, M. Deloger, A. Morel, S. Vacher, C. Lecerf, C. Dupain, E. Jeannot, E. Girard, S. Baulande, C. Dubot, G. Kenter, E. S. Jordanova, Emjj Berns, G. Bataillon, M. Popovic, R. Rouzier, W. Cacheux, C. Le Tourneau, A. Nicolas, N. Servant, S. M. Scholl, and I. Bièche. 2021. "Human papilloma virus (HPV) integration signature in Cervical Cancer: identification of MACROD2 gene as HPV hot spot integration site." *Br J Cancer* 124 (4): 777-785. <https://doi.org/10.1038/s41416-020-01153-4>.
- Kansy, B. A., F. Concha-Benavente, R. M. Srivastava, H. B. Jie, G. Shayan, Y. Lei, J. Moskovitz, J. Moy, J. Li, S. Brandau, S. Lang, N. C. Schmitt, G. J. Freeman, W. E. Gooding, D. A. Clump, and R. L. Ferris. 2017. "PD-1 Status in CD8(+) T Cells Associates with Survival and Anti-PD-1 Therapeutic Outcomes in Head and Neck Cancer." *Cancer Res* 77 (22): 6353-6364. <https://doi.org/10.1158/0008-5472.can-16-3167>.
- Kanzaki, R., and K. Pietras. 2020. "Heterogeneity of cancer-associated fibroblasts: Opportunities for precision medicine." *Cancer Sci* 111 (8): 2708-2717. <https://doi.org/10.1111/cas.14537>.
- Kare, A. J., L. Nichols, R. Zermeno, M. N. Raie, S. K. Tumbale, and K. W. Ferrara. 2023. "OMIP-095: 40-Color spectral flow cytometry delineates all major leukocyte populations in murine lymphoid tissues." *Cytometry A* 103 (11): 839-850. <https://doi.org/10.1002/cyto.a.24788>.
- Khariwala, S. S., D. Hatsukami, and S. S. Hecht. 2012. "Tobacco carcinogen metabolites and DNA adducts as biomarkers in head and neck cancer: potential screening tools and prognostic indicators." *Head Neck* 34 (3): 441-7. <https://doi.org/10.1002/hed.21705>.
- Kindt, N., G. Descamps, I. Seminerio, J. Bellier, J. R. Lechien, C. Pottier, D. Larsimont, F. Journé, P. Delvenne, and S. Saussez. 2016. "Langerhans cell number is a strong and independent prognostic factor for head and neck squamous cell carcinomas." *Oral Oncol* 62: 1-10. <https://doi.org/10.1016/j.oraloncology.2016.08.016>.
- Konecny, A. J., P. L. Mage, A. J. Tyznik, M. Prlic, and F. Mair. 2024. "OMIP-102: 50-color phenotyping of the human immune system with in-depth assessment of T cells and dendritic cells." *Cytometry A*. <https://doi.org/10.1002/cyto.a.24841>.
- Kornete, M., E. Sgouroudis, and C. A. Piccirillo. 2012. "ICOS-dependent homeostasis and function of Foxp3+ regulatory T cells in islets of nonobese diabetic mice." *J Immunol* 188 (3): 1064-74. <https://doi.org/10.4049/jimmunol.1101303>.
- Koslabova, E., E. Hamsikova, M. Salakova, J. Klozar, E. Foltynova, E. Salkova, E. Rotnaglova, V. Ludvikova, and R. Tachezy. 2013. "Markers of HPV infection and survival in patients

- with head and neck tumors." *Int J Cancer* 133 (8): 1832-9. <https://doi.org/10.1002/ijc.28194>.
- Koucký, V., K. Hladíková, E. Tábořská, J. Bouček, M. Grega, R. Špišek, and A. Fialová. 2021. "The cytokine milieu compromises functional capacity of tumor-infiltrating plasmacytoid dendritic cells in HPV-negative but not in HPV-positive HNSCC." *Cancer Immunol Immunother* 70 (9): 2545-2557. <https://doi.org/10.1007/s00262-021-02874-y>.
- Kreimer, A. R., G. M. Clifford, P. Boyle, and S. Franceschi. 2005. "Human papillomavirus types in head and neck squamous cell carcinomas worldwide: a systematic review." *Cancer Epidemiol Biomarkers Prev* 14 (2): 467-75. <https://doi.org/10.1158/1055-9965.epi-04-0551>.
- Kumar, V., S. Patel, E. Tcyganov, and D. I. Gabrilovich. 2016. "The Nature of Myeloid-Derived Suppressor Cells in the Tumor Microenvironment." *Trends Immunol* 37 (3): 208-220. <https://doi.org/10.1016/j.it.2016.01.004>.
- Kwak, T., F. Wang, H. Deng, T. Condamine, V. Kumar, M. Perego, A. Kossenkov, L. J. Montaner, X. Xu, W. Xu, C. Zheng, L. M. Schuchter, R. K. Amaravadi, T. C. Mitchell, G. C. Karakousis, C. Mulligan, B. Nam, G. Masters, N. Hockstein, J. Bennett, Y. Nefedova, and D. I. Gabrilovich. 2020. "Distinct Populations of Immune-Suppressive Macrophages Differentiate from Monocytic Myeloid-Derived Suppressor Cells in Cancer." *Cell Rep* 33 (13): 108571. <https://doi.org/10.1016/j.celrep.2020.108571>.
- Kyzas, P. A., I. W. Cunha, and J. P. Ioannidis. 2005. "Prognostic significance of vascular endothelial growth factor immunohistochemical expression in head and neck squamous cell carcinoma: a meta-analysis." *Clin Cancer Res* 11 (4): 1434-40. <https://doi.org/10.1158/1078-0432.ccr-04-1870>.
- Lazarus, J., Y. Akiska, M. Perusina Lanfranca, L. Delrosario, L. Sun, D. Long, J. Shi, H. Crawford, M. P. Di Magliano, W. Zou, and T. Frankel. 2019. "Optimization, Design and Avoiding Pitfalls in Manual Multiplex Fluorescent Immunohistochemistry." *J Vis Exp* (149). <https://doi.org/10.3791/59915>.
- Lee, S. W., H. Y. Lee, S. W. Kang, M. J. Kim, Y. J. Lee, C. O. Sung, and Y. M. Kim. 2021. "Application of Immunoprofiling Using Multiplexed Immunofluorescence Staining Identifies the Prognosis of Patients with High-Grade Serous Ovarian Cancer." *Int J Mol Sci* 22 (17). <https://doi.org/10.3390/ijms22179638>.
- Li, N., S. Franceschi, R. Howell-Jones, P. J. Snijders, and G. M. Clifford. 2011. "Human papillomavirus type distribution in 30,848 invasive cervical cancers worldwide: Variation by geographical region, histological type and year of publication." *Int J Cancer* 128 (4): 927-35. <https://doi.org/10.1002/ijc.25396>.
- Liu, J., X. Geng, J. Hou, and G. Wu. 2021. "New insights into M1/M2 macrophages: key modulators in cancer progression." *Cancer Cell Int* 21 (1): 389. <https://doi.org/10.1186/s12935-021-02089-2>.
- Liu, X., P. Liu, R. D. Chernock, K. A. Lang Kuhs, J. S. Lewis, Jr., H. Li, H. A. Gay, W. L. Thorstad, and X. Wang. 2022. "Impact of human papillomavirus on the tumor microenvironment in oropharyngeal squamous cell carcinoma." *Int J Cancer* 150 (3): 521-531. <https://doi.org/10.1002/ijc.33849>.
- Lonardi, S., F. Missale, S. Calza, M. Bugatti, R. Vescovi, B. Debora, R. Uppaluri, A. M. Egloff, D. Mattavelli, D. Lombardi, L. Benerini Gatta, O. Marini, N. Tamassia, E. Gardiman, M. A. Cassatella, P. Scapini, P. Nicolai, and W. Vermi. 2021. "Tumor-associated neutrophils (TANs) in human carcinoma-draining lymph nodes: a novel TAN compartment." *Clin Transl Immunology* 10 (2): e1252. <https://doi.org/10.1002/cti2.1252>.
- Lu, H., W. Dai, J. Guo, D. Wang, S. Wen, L. Yang, D. Lin, W. Xie, L. Wen, J. Fang, and Z. Wang. 2020. "High Abundance of Intratumoral $\gamma\delta$ T Cells Favors a Better Prognosis in Head and Neck Squamous Cell Carcinoma: A Bioinformatic Analysis." *Front Immunol* 11: 573920. <https://doi.org/10.3389/fimmu.2020.573920>.
- Ma, Z., J. Lian, M. Yang, J. Wuyang, C. Zhao, W. Chen, C. Liu, Q. Zhao, C. Lou, J. Han, and Y. Zhang. 2019. "Overexpression of Arginase-1 is an indicator of poor prognosis in patients with colorectal cancer." *Pathol Res Pract* 215 (6): 152383. <https://doi.org/10.1016/j.prp.2019.03.012>.

- Mansfield, J. R. 2014. "Multispectral imaging: a review of its technical aspects and applications in anatomic pathology." *Vet Pathol* 51 (1): 185-210. <https://doi.org/10.1177/0300985813506918>.
- Mantovani, A., P. Allavena, F. Marchesi, and C. Garlanda. 2022. "Macrophages as tools and targets in cancer therapy." *Nat Rev Drug Discov* 21 (11): 799-820. <https://doi.org/10.1038/s41573-022-00520-5>.
- Mantovani, A., A. Sica, S. Sozzani, P. Allavena, A. Vecchi, and M. Locati. 2004. "The chemokine system in diverse forms of macrophage activation and polarization." *Trends Immunol* 25 (12): 677-86. <https://doi.org/10.1016/j.it.2004.09.015>.
- McMurray, H. R., and D. J. McCance. 2003. "Human papillomavirus type 16 E6 activates TERT gene transcription through induction of c-Myc and release of USF-mediated repression." *J Virol* 77 (18): 9852-61.
- Mezheyeuski, A., C. H. Bergsland, M. Backman, D. Djureinovic, T. Sjöblom, J. Bruun, and P. Micke. 2018. "Multispectral imaging for quantitative and compartment-specific immune infiltrates reveals distinct immune profiles that classify lung cancer patients." *J Pathol* 244 (4): 421-431. <https://doi.org/10.1002/path.5026>.
- Mir, B. A., A. Ahmad, N. Farooq, M. V. Priya, A. H. Siddiqui, M. Asif, R. Manzoor, H. M. Ishqi, S. Y. Alomar, and P. F. Rahaman. 2023. "Increased expression of HPV-E7 oncoprotein correlates with a reduced level of pRb proteins via high viral load in cervical cancer." *Sci Rep* 13 (1): 15075. <https://doi.org/10.1038/s41598-023-42022-3>.
- Miyasato, Y., T. Shiota, K. Ohnishi, C. Pan, H. Yano, H. Horlad, Y. Yamamoto, M. Yamamoto-Ibusuki, H. Iwase, M. Takeya, and Y. Komohara. 2017. "High density of CD204-positive macrophages predicts worse clinical prognosis in patients with breast cancer." *Cancer Sci* 108 (8): 1693-1700. <https://doi.org/10.1111/cas.13287>.
- Mohamed, K. M., A. Le, H. Duong, Y. Wu, Q. Zhang, and D. V. Messadi. 2004. "Correlation between VEGF and HIF-1alpha expression in human oral squamous cell carcinoma." *Exp Mol Pathol* 76 (2): 143-52. <https://doi.org/10.1016/j.yexmp.2003.10.005>.
- Mohan, M., and N. Jagannathan. 2014. "Oral field cancerization: an update on current concepts." *Oncol Rev* 8 (1): 244. <https://doi.org/10.4081/oncol.2014.244>.
- Moody, C. A., and L. A. Laimins. 2010. "Human papillomavirus oncoproteins: pathways to transformation." *Nat Rev Cancer* 10 (8): 550-60. <https://doi.org/10.1038/nrc2886>.
- Morand, G. B., M. A. Broglie, P. Schumann, M. W. Huellner, and N. J. Rupp. 2020. "Histometabolic Tumor Imaging of Hypoxia in Oral Cancer: Clinicopathological Correlation for Prediction of an Aggressive Phenotype." *Front Oncol* 10: 1670. <https://doi.org/10.3389/fonc.2020.01670>.
- Mukherjee, G., S. Bag, P. Chakraborty, D. Dey, S. Roy, P. Jain, P. Roy, R. Soong, P. P. Majumder, and S. Dutt. 2020. "Density of CD3+ and CD8+ cells in gingivo-buccal oral squamous cell carcinoma is associated with lymph node metastases and survival." *PLoS One* 15 (11): e0242058. <https://doi.org/10.1371/journal.pone.0242058>.
- Nordfors, C., N. Grun, N. Tertipis, A. Ahrlund-Richter, L. Haegglblom, L. Sivars, J. Du, T. Nyberg, L. Marklund, E. Munck-Wikland, A. Nasman, T. Ramqvist, and T. Dalianis. 2013. "CD8+ and CD4+ tumour infiltrating lymphocytes in relation to human papillomavirus status and clinical outcome in tonsillar and base of tongue squamous cell carcinoma." *Eur J Cancer* 49 (11): 2522-30. <https://doi.org/10.1016/j.ejca.2013.03.019>.
- Oguejiofor, K., H. Galletta-Williams, S. J. Dovedi, D. L. Roberts, P. L. Stern, and C. M. West. 2017. "Distinct patterns of infiltrating CD8+ T cells in HPV+ and CD68 macrophages in HPV- oropharyngeal squamous cell carcinomas are associated with better clinical outcome but PD-L1 expression is not prognostic." *Oncotarget* 8 (9): 14416-14427. <https://doi.org/10.18632/oncotarget.14796>.
- Oguejiofor, K., J. Hall, C. Slater, G. Betts, G. Hall, N. Slevin, S. Dovedi, P. L. Stern, and C. M. West. 2015. "Stromal infiltration of CD8 T cells is associated with improved clinical outcome in HPV-positive oropharyngeal squamous carcinoma." *Br J Cancer* 113 (6): 886-93. <https://doi.org/10.1038/bjc.2015.277>.
- Ou, D., J. Adam, I. Garberis, P. Blanchard, F. Nguyen, A. Levy, O. Casiraghi, P. Gorphe, I. Breuskin, F. Janot, S. Temam, J. Y. Scoazec, E. Deutsch, and Y. Tao. 2019. "Influence

- of tumor-associated macrophages and HLA class I expression according to HPV status in head and neck cancer patients receiving chemo/bioradiotherapy." *Radiother Oncol* 130: 89-96. <https://doi.org/10.1016/j.radonc.2018.08.013>.
- Ozaki, T., and A. Nakagawara. 2011. "Role of p53 in Cell Death and Human Cancers." *Cancers (Basel)* 3 (1): 994-1013. <https://doi.org/10.3390/cancers3010994>.
- Pagès, F., B. Mlecnik, F. Marliot, G. Bindea, F. S. Ou, C. Bifulco, A. Lugli, I. Zlobec, T. T. Rau, M. D. Berger, I. D. Nagtegaal, E. Vink-Börger, A. Hartmann, C. Geppert, J. Kolwelter, S. Merkel, R. Grützmann, M. Van den Eynde, A. Jouret-Mourin, A. Kartheuser, D. Léonard, C. Remue, J. Y. Wang, P. Bavi, M. H. A. Roehrl, P. S. Ohashi, L. T. Nguyen, S. Han, H. L. MacGregor, S. Hafezi-Bakhtiari, B. G. Wouters, G. V. Masucci, E. K. Andersson, E. Zavadova, M. Vocka, J. Spacek, L. Petruzela, B. Konopasek, P. Dundr, H. Skalova, K. Nemejcova, G. Botti, F. Tatangelo, P. Delrio, G. Ciliberto, M. Maio, L. Laghi, F. Grizzi, T. Fredriksen, B. Buttard, M. Angelova, A. Vasaturo, P. Maby, S. E. Church, H. K. Angell, L. Lafontaine, D. Bruni, C. El Sissy, N. Haicheur, A. Kirilovsky, A. Berger, C. Lagorce, J. P. Meyers, C. Paustian, Z. Feng, C. Ballesteros-Merino, J. Dijkstra, C. van de Water, S. van Lent-van Vliet, N. Knijn, A. M. Muşină, D. V. Scripcariu, B. Popivanova, M. Xu, T. Fujita, S. Hazama, N. Suzuki, H. Nagano, K. Okuno, T. Torigoe, N. Sato, T. Furuhashi, I. Takemasa, K. Itoh, P. S. Patel, H. H. Vora, B. Shah, J. B. Patel, K. N. Rajvik, S. J. Pandya, S. N. Shukla, Y. Wang, G. Zhang, Y. Kawakami, F. M. Marincola, P. A. Ascierto, D. J. Sargent, B. A. Fox, and J. Galon. 2018. "International validation of the consensus Immunoscore for the classification of colon cancer: a prognostic and accuracy study." *Lancet* 391 (10135): 2128-2139. [https://doi.org/10.1016/s0140-6736\(18\)30789-x](https://doi.org/10.1016/s0140-6736(18)30789-x).
- Pang, L., K. T. Ng, J. Liu, W. O. Yeung, J. Zhu, T. S. Chiu, H. Liu, Z. Chen, C. M. Lo, and K. Man. 2021. "Plasmacytoid dendritic cells recruited by HIF-1 α /eADO/ADORA1 signaling induce immunosuppression in hepatocellular carcinoma." *Cancer Lett* 522: 80-92. <https://doi.org/10.1016/j.canlet.2021.09.022>.
- Park, L. M., J. Lannigan, and M. C. Jaimes. 2020. "OMIP-069: Forty-Color Full Spectrum Flow Cytometry Panel for Deep Immunophenotyping of Major Cell Subsets in Human Peripheral Blood." *Cytometry A* 97 (10): 1044-1051. <https://doi.org/10.1002/cyto.a.24213>.
- Parra, E. R., N. Uraoka, M. Jiang, P. Cook, D. Gibbons, M. A. Forget, C. Bernatchez, C. Haymaker, Wistuba, II, and J. Rodriguez-Canales. 2017. "Validation of multiplex immunofluorescence panels using multispectral microscopy for immune-profiling of formalin-fixed and paraffin-embedded human tumor tissues." *Sci Rep* 7 (1): 13380. <https://doi.org/10.1038/s41598-017-13942-8>.
- Partlova, S., J. Boucek, K. Kloudova, E. Lukesova, M. Zabrodsky, M. Grega, J. Fucikova, I. Truxova, R. Tachezy, R. Spisek, and A. Fialova. 2015. "Distinct patterns of intratumoral immune cell infiltrates in patients with HPV-associated compared to non-virally induced head and neck squamous cell carcinoma." *Oncoimmunology* 4 (1): e965570. <https://doi.org/10.4161/21624011.2014.965570>.
- Paul, S., and G. Lal. 2017. "The Molecular Mechanism of Natural Killer Cells Function and Its Importance in Cancer Immunotherapy." *Front Immunol* 8: 1124. <https://doi.org/10.3389/fimmu.2017.01124>.
- Pinatti, L. M., W. Gu, Y. Wang, A. Elhossiny, A. D. Bhangale, C. V. Brummel, T. E. Carey, R. E. Mills, and J. C. Brenner. 2021. "SearchHPV: A novel approach to identify and assemble human papillomavirus-host genomic integration events in cancer." *Cancer* 127 (19): 3531-3540. <https://doi.org/10.1002/cncr.33691>.
- Pinto, B., A. C. Henriques, P. M. A. Silva, and H. Bousbaa. 2020. "Three-Dimensional Spheroids as In Vitro Preclinical Models for Cancer Research." *Pharmaceutics* 12 (12). <https://doi.org/10.3390/pharmaceutics12121186>.
- Pokřývková, B., M. Grega, J. Klozar, O. Vencálek, J. Nunvář, and R. Tachezy. 2022. "PD1(+)/CD8(+) Cells Are an Independent Prognostic Marker in Patients with Head and Neck Cancer." *Biomedicines* 10 (11). <https://doi.org/10.3390/biomedicines10112794>.

- Pokřývková, B., M. Saláková, J. Šmahelová, Z. Vojtěchová, V. Novosadová, and R. Tachezy. 2019. "Detailed Characteristics of Tonsillar Tumors with Extrachromosomal or Integrated Form of Human Papillomavirus." *Viruses* 12 (1). <https://doi.org/10.3390/v12010042>.
- Pokřývková, B., J. Šmahelová, N. Dalewská, M. Grega, O. Vencálek, M. Šmahel, J. Nunvář, J. Klozar, and R. Tachezy. 2021. "ARG1 mRNA Level Is a Promising Prognostic Marker in Head and Neck Squamous Cell Carcinomas." *Diagnostics (Basel)* 11 (4). <https://doi.org/10.3390/diagnostics11040628>.
- Polakova, I., O. Pelak, D. Thurner, B. Pokryvkova, R. Tachezy, T. Kalina, and M. Smahel. 2019. "Implementation of Mass Cytometry for Immunoprofiling of Patients with Solid Tumors." *J Immunol Res* 2019: 6705949. <https://doi.org/10.1155/2019/6705949>.
- Ponzetta, A., R. Carriero, S. Carnevale, M. Barbagallo, M. Molgora, C. Perucchini, E. Magrini, F. Gianni, P. Kunderfranco, N. Polentarutti, F. Pasqualini, S. Di Marco, D. Supino, C. Peano, F. Cananzi, P. Colombo, S. Pilotti, S. Y. Alomar, E. Bonavita, M. R. Galdiero, C. Garlanda, A. Mantovani, and S. Jaillon. 2019. "Neutrophils Driving Unconventional T Cells Mediate Resistance against Murine Sarcomas and Selected Human Tumors." *Cell* 178 (2): 346-360.e24. <https://doi.org/10.1016/j.cell.2019.05.047>.
- Poropatich, K., J. Fontanarosa, S. Swaminathan, D. Dittmann, S. Chen, S. Samant, and B. Zhang. 2017. "Comprehensive T-cell immunophenotyping and next-generation sequencing of human papillomavirus (HPV)-positive and HPV-negative head and neck squamous cell carcinomas." *J Pathol* 243 (3): 354-365. <https://doi.org/10.1002/path.4953>.
- Puntigam, L. K., S. S. Jeske, M. Götz, J. Greiner, S. Laban, M. N. Theodoraki, J. Doescher, S. E. Weissinger, C. Brunner, T. K. Hoffmann, and P. J. Schuler. 2020. "Immune Checkpoint Expression on Immune Cells of HNSCC Patients and Modulation by Chemo- and Immunotherapy." *Int J Mol Sci* 21 (15). <https://doi.org/10.3390/ijms21155181>.
- Quail, D. F., B. Amulic, M. Aziz, B. J. Barnes, E. Eruslanov, Z. G. Fridlender, H. S. Goodridge, Z. Granot, A. Hidalgo, A. Huttenlocher, M. J. Kaplan, I. Malanchi, T. Merghoub, E. Meylan, V. Mittal, M. J. Pittet, A. Rubio-Ponce, I. A. Udalova, T. K. van den Berg, D. D. Wagner, P. Wang, A. Zychlinsky, K. E. de Visser, M. Egeblad, and P. Kubes. 2022. "Neutrophil phenotypes and functions in cancer: A consensus statement." *J Exp Med* 219 (6). <https://doi.org/10.1084/jem.20220011>.
- Quan, H., Z. Shan, Z. Liu, S. Liu, L. Yang, X. Fang, K. Li, B. Wang, Z. Deng, Y. Hu, Z. Yao, J. Huang, J. Yu, K. Xia, Z. Tang, and L. Fang. 2020. "The repertoire of tumor-infiltrating lymphocytes within the microenvironment of oral squamous cell carcinoma reveals immune dysfunction." *Cancer Immunol Immunother* 69 (3): 465-476. <https://doi.org/10.1007/s00262-020-02479-x>.
- Qureshi, H. A., X. Zhu, G. H. Yang, M. Steadele, R. H. Pierce, N. D. Futran, S. M. Lee, E. Méndez, and A. M. Houghton. 2022. "Impact of HPV status on immune responses in head and neck squamous cell carcinoma." *Oral Oncol* 127: 105774. <https://doi.org/10.1016/j.oraloncology.2022.105774>.
- Ren, W., X. Zhang, W. Li, Q. Feng, H. Feng, Y. Tong, H. Rong, W. Wang, D. Zhang, Z. Zhang, and S. Tu. 2020. "Circulating and tumor-infiltrating arginase 1-expressing cells in gastric adenocarcinoma patients were mainly immature and monocytic Myeloid-derived suppressor cells." *Sci Rep* 10 (1): 8056. <https://doi.org/10.1038/s41598-020-64841-4>.
- Ren, X., Y. Song, J. Pang, L. Chen, L. Zhou, Z. Liang, and H. Wu. 2023. "Prognostic value of various immune cells and Immunoscore in triple-negative breast cancer." *Front Immunol* 14: 1137561. <https://doi.org/10.3389/fimmu.2023.1137561>.
- Rodolico, V., W. Arancio, M. C. Amato, F. Aragona, F. Cappello, O. Di Fede, G. Pannone, and G. Campisi. 2011. "Hypoxia inducible factor-1 alpha expression is increased in infected positive HPV16 DNA oral squamous cell carcinoma and positively associated with HPV16 E7 oncoprotein." *Infect Agent Cancer* 6 (1): 18. <https://doi.org/10.1186/1750-9378-6-18>.
- Rodríguez-Pinto, D. 2005. "B cells as antigen presenting cells." *Cell Immunol* 238 (2): 67-75. <https://doi.org/10.1016/j.cellimm.2006.02.005>.

- Romanczuk, H., and P. M. Howley. 1992. "Disruption of either the E1 or the E2 regulatory gene of human papillomavirus type 16 increases viral immortalization capacity." *Proc Natl Acad Sci U S A* 89 (7): 3159-63. <https://doi.org/10.1073/pnas.89.7.3159>.
- Romanczuk, H., F. Thierry, and P. M. Howley. 1990. "Mutational analysis of cis elements involved in E2 modulation of human papillomavirus type 16 P97 and type 18 P105 promoters." *J Virol* 64 (6): 2849-59. <https://doi.org/10.1128/jvi.64.6.2849-2859.1990>.
- Rosenthal, E. L., and L. M. Matrisian. 2006. "Matrix metalloproteases in head and neck cancer." *Head Neck* 28 (7): 639-48. <https://doi.org/10.1002/hed.20365>.
- Rossi, N. M., J. Dai, Y. Xie, D. Wangsa, K. Heselmeyer-Haddad, H. Lou, J. F. Boland, M. Yeager, R. Orozco, E. A. Freitas, L. Mirabello, E. Gharzouzi, and M. Dean. 2023. "Extrachromosomal Amplification of Human Papillomavirus Episomes Is a Mechanism of Cervical Carcinogenesis." *Cancer Res* 83 (11): 1768-1781. <https://doi.org/10.1158/0008-5472.can-22-3030>.
- Ruangritchankul, K., A. Sandison, F. Warburton, T. Guerrero-Urbano, M. Reis Ferreira, M. Lei, and S. Thavaraj. 2019. "Clinical evaluation of tumour-infiltrating lymphocytes as a prognostic factor in patients with human papillomavirus-associated oropharyngeal squamous cell carcinoma." *Histopathology* 75 (1): 146-150. <https://doi.org/10.1111/his.13873>.
- Sauter, E. R., M. Nesbit, J. C. Watson, A. Klein-Szanto, S. Litwin, and M. Herlyn. 1999. "Vascular endothelial growth factor is a marker of tumor invasion and metastasis in squamous cell carcinomas of the head and neck." *Clin Cancer Res* 5 (4): 775-82.
- Savina, A., and S. Amigorena. 2007. "Phagocytosis and antigen presentation in dendritic cells." *Immunol Rev* 219: 143-56. <https://doi.org/10.1111/j.1600-065X.2007.00552.x>.
- Schlecker, E., A. Stojanovic, C. Eisen, C. Quack, C. S. Falk, V. Umansky, and A. Cerwenka. 2012. "Tumor-infiltrating monocytic myeloid-derived suppressor cells mediate CCR5-dependent recruitment of regulatory T cells favoring tumor growth." *J Immunol* 189 (12): 5602-11. <https://doi.org/10.4049/jimmunol.1201018>.
- Schneider, A., and J. H. Buckner. 2011. "Assessment of suppressive capacity by human regulatory T cells using a reproducible, bi-directional CFSE-based in vitro assay." *Methods Mol Biol* 707: 233-41. https://doi.org/10.1007/978-1-61737-979-6_15.
- Sedivy, R., J. Beck-Mannagetta, C. Haverkamp, W. Battistutti, and S. Hönigschnabl. 2003. "Expression of vascular endothelial growth factor-C correlates with the lymphatic microvessel density and the nodal status in oral squamous cell cancer." *J Oral Pathol Med* 32 (8): 455-60. <https://doi.org/10.1034/j.1600-0714.2003.00168.x>.
- Shafti-Keramat, S., A. Handisurya, E. Kriehuber, G. Meneguzzi, K. Slupetzky, and R. Kirnbauer. 2003. "Different heparan sulfate proteoglycans serve as cellular receptors for human papillomaviruses." *J Virol* 77 (24): 13125-35. <https://doi.org/10.1128/jvi.77.24.13125-13135.2003>.
- Shen, M., P. Hu, F. Donskov, G. Wang, Q. Liu, and J. Du. 2014. "Tumor-associated neutrophils as a new prognostic factor in cancer: a systematic review and meta-analysis." *PLoS One* 9 (6): e98259. <https://doi.org/10.1371/journal.pone.0098259>.
- Sica, A., and A. Mantovani. 2012. "Macrophage plasticity and polarization: in vivo veritas." *J Clin Invest* 122 (3): 787-95. <https://doi.org/10.1172/jci59643>.
- Simonson, William T. N., and Kimberly H. Allison. 2011. "Tumour-infiltrating lymphocytes in cancer: implications for the diagnostic pathologist." *Diagnostic Histopathology* 17 (2): 80 - 90. <https://doi.org/10.1016/j.mpdhp.2010.10.006>.
- Singh, P., D. Augustine, R. S. Rao, S. Patil, K. H. Awan, S. V. Sowmya, V. C. Haragannavar, and K. Prasad. 2021. "Role of cancer stem cells in head-and-neck squamous cell carcinoma - A systematic review." *J Carcinog* 20: 12. https://doi.org/10.4103/jcar.JCar_14_20.
- Smahelova, J., B. Pokryvkova, E. Stovickova, M. Grega, O. Vencalek, M. Smahel, V. Koucky, S. Malerova, J. Klozar, and R. Tachezy. 2024. "Aspartate- β -hydroxylase and hypoxia marker expression in head and neck carcinomas: implications for HPV-associated tumors." *Infect Agent Cancer* 19 (1): 26. <https://doi.org/10.1186/s13027-024-00588-1>.

- Soo, R. A., Z. Chen, R. S. Yan Teng, H. L. Tan, B. Iacopetta, B. C. Tai, and R. Soong. 2018. "Prognostic significance of immune cells in non-small cell lung cancer: meta-analysis." *Oncotarget* 9 (37): 24801-24820. <https://doi.org/10.18632/oncotarget.24835>.
- South, A. P., N. Y. den Breems, T. Richa, U. Nwagu, T. Zhan, S. Poojan, U. Martinez-Outschoorn, J. M. Johnson, A. J. Luginbuhl, and J. M. Curry. 2019. "Mutation signature analysis identifies increased mutation caused by tobacco smoke associated DNA adducts in larynx squamous cell carcinoma compared with oral cavity and oropharynx." *Sci Rep* 9 (1): 19256. <https://doi.org/10.1038/s41598-019-55352-y>.
- Spanos, W. C., P. Nowicki, D. W. Lee, A. Hoover, B. Hostager, A. Gupta, M. E. Anderson, and J. H. Lee. 2009. "Immune response during therapy with cisplatin or radiation for human papillomavirus-related head and neck cancer." *Arch Otolaryngol Head Neck Surg* 135 (11): 1137-46. <https://doi.org/10.1001/archoto.2009.159>.
- Stein, A. P., S. Saha, J. L. Kraninger, A. D. Swick, M. Yu, P. F. Lambert, and R. J. Kimple. 2015. "Prevalence of Human Papillomavirus in Oropharyngeal Cancer: A Systematic Review." *Cancer J* 21 (3): 138-46. <https://doi.org/10.1097/ppo.000000000000115>.
- Stern, L., H. McGuire, S. Avdic, S. Rizzetto, B. Fazekas de St Groth, F. Luciani, B. Slobedman, and E. Blyth. 2018. "Mass Cytometry for the Assessment of Immune Reconstitution After Hematopoietic Stem Cell Transplantation." *Front Immunol* 9: 1672. <https://doi.org/10.3389/fimmu.2018.01672>.
- Stransky, N., A. M. Egloff, A. D. Tward, A. D. Kostic, K. Cibulskis, A. Sivachenko, G. V. Kryukov, M. S. Lawrence, C. Sougnez, A. McKenna, E. Shefler, A. H. Ramos, P. Stojanov, S. L. Carter, D. Voet, M. L. Cortés, D. Auclair, M. F. Berger, G. Saksena, C. Guiducci, R. C. Onofrio, M. Parkin, M. Romkes, J. L. Weissfeld, R. R. Seethala, L. Wang, C. Rangel-Escareño, J. C. Fernandez-Lopez, A. Hidalgo-Miranda, J. Melendez-Zajgla, W. Winckler, K. Ardlie, S. B. Gabriel, M. Meyerson, E. S. Lander, G. Getz, T. R. Golub, L. A. Garraway, and J. R. Grandis. 2011. "The mutational landscape of head and neck squamous cell carcinoma." *Science* 333 (6046): 1157-60. <https://doi.org/10.1126/science.1208130>.
- Struckmeier, A. K., A. Radermacher, M. Fehrenz, T. Bellin, D. Alansary, P. Wartenberg, U. Boehm, M. Wagner, A. Scheller, J. Hess, J. Moratin, C. Freudlsperger, J. Hoffmann, L. Thurner, K. Roemer, K. Freier, and D. Horn. 2023. "IDO1 is highly expressed in macrophages of patients in advanced tumour stages of oral squamous cell carcinoma." *J Cancer Res Clin Oncol* 149 (7): 3623-3635. <https://doi.org/10.1007/s00432-022-04277-7>.
- Sun, L., Y. Su, A. Jiao, X. Wang, and B. Zhang. 2023. "T cells in health and disease." *Signal Transduct Target Ther* 8 (1): 235. <https://doi.org/10.1038/s41392-023-01471-y>.
- Sun, Y., Z. Wang, S. Qiu, and R. Wang. 2021. "Therapeutic strategies of different HPV status in Head and Neck Squamous Cell Carcinoma." *Int J Biol Sci* 17 (4): 1104-1118. <https://doi.org/10.7150/ijbs.58077>.
- Swartz, J. E., I. Wegner, R. Noorlag, P. M. W. van Kempen, R. J. J. van Es, R. de Bree, and S. M. W. Willems. 2021. "HIF-1a expression and differential effects on survival in patients with oral cavity, larynx, and oropharynx squamous cell carcinomas." *Head Neck* 43 (3): 745-756. <https://doi.org/10.1002/hed.26530>.
- Symer, D. E., K. Akagi, H. M. Geiger, Y. Song, G. Li, A. K. Emde, W. Xiao, B. Jiang, A. Corvelo, N. C. Toussaint, J. Li, A. Agrawal, E. Ozer, A. K. El-Naggar, Z. Du, J. B. Shewale, B. Stache-Crain, M. Zucker, N. Robine, K. R. Coombes, and M. L. Gillison. 2022. "Diverse tumorigenic consequences of human papillomavirus integration in primary oropharyngeal cancers." *Genome Res* 32 (1): 55-70. <https://doi.org/10.1101/gr.275911.121>.
- Tachezy, R., J. Smahelova, M. Salakova, M. Arbyn, L. Rob, P. Skapa, T. Jirasek, and E. Hamsikova. 2011. "Human papillomavirus genotype distribution in Czech women and men with diseases etiologically linked to HPV." *PLoS One* 6 (7): e21913. <https://doi.org/10.1371/journal.pone.0021913>.
- Taylor, J. R., D. J. Fernandez, S. M. Thornton, J. G. Skeate, K. P. Lühen, D. M. Da Silva, R. Langen, and W. M. Kast. 2018. "Heterotetrameric annexin A2/S100A10 (A2t) is essential

- for oncogenic human papillomavirus trafficking and capsid disassembly, and protects virions from lysosomal degradation." *Sci Rep* 8 (1): 11642. <https://doi.org/10.1038/s41598-018-30051-2>.
- Tel, J., G. Schreiber, S. P. Sittig, T. S. Mathan, S. I. Buschow, L. J. Cruz, A. J. Lambeck, C. G. Figdor, and I. J. de Vries. 2013. "Human plasmacytoid dendritic cells efficiently cross-present exogenous Ags to CD8+ T cells despite lower Ag uptake than myeloid dendritic cell subsets." *Blood* 121 (3): 459-67. <https://doi.org/10.1182/blood-2012-06-435644>.
- Tosi, A., B. Parisatto, A. Menegaldo, G. Spinato, M. Guido, A. Del Mistro, R. Bussani, F. Zanconati, M. Tofanelli, G. Tirelli, P. Boscolo-Rizzo, and A. Rosato. 2022. "The immune microenvironment of HPV-positive and HPV-negative oropharyngeal squamous cell carcinoma: a multiparametric quantitative and spatial analysis unveils a rationale to target treatment-naïve tumors with immune checkpoint inhibitors." *J Exp Clin Cancer Res* 41 (1): 279. <https://doi.org/10.1186/s13046-022-02481-4>.
- Toth, Z. E., and E. Mezey. 2007. "Simultaneous visualization of multiple antigens with tyramide signal amplification using antibodies from the same species." *J Histochem Cytochem* 55 (6): 545-54. <https://doi.org/10.1369/jhc.6A7134.2007>.
- Troy, J. D., J. L. Weissfeld, A. O. Youk, S. Thomas, L. Wang, and J. R. Grandis. 2013. "Expression of EGFR, VEGF, and NOTCH1 suggest differences in tumor angiogenesis in HPV-positive and HPV-negative head and neck squamous cell carcinoma." *Head Neck Pathol* 7 (4): 344-55. <https://doi.org/10.1007/s12105-013-0447-y>.
- van Imhoff, L. C., G. G. Kranenburg, S. Macco, N. L. Nijman, E. J. van Overbeeke, I. Wegner, W. Grolman, and A. J. Pothen. 2016. "Prognostic value of continued smoking on survival and recurrence rates in patients with head and neck cancer: A systematic review." *Head Neck* 38 Suppl 1: E2214-20. <https://doi.org/10.1002/hed.24082>.
- Vonwirth, V., Y. Bülbül, A. Werner, H. Echchannaoui, J. Windschmitt, A. Habermeier, S. Ioannidis, N. Shin, R. Conradi, M. Bros, S. Tenzer, M. Theobald, E. I. Closs, and M. Munder. 2020. "Inhibition of Arginase 1 Liberates Potent T Cell Immunostimulatory Activity of Human Neutrophil Granulocytes." *Front Immunol* 11: 617699. <https://doi.org/10.3389/fimmu.2020.617699>.
- Vu, H. L., A. G. Sikora, S. Fu, and J. Kao. 2010. "HPV-induced oropharyngeal cancer, immune response and response to therapy." *Cancer Lett* 288 (2): 149-55. <https://doi.org/10.1016/j.canlet.2009.06.026>.
- Wang, B., S. Zhang, F. Tong, Y. Wang, and L. Wei. 2022. "HPV(+) HNSCC-derived exosomal miR-9-5p inhibits TGF- β signaling-mediated fibroblast phenotypic transformation through NOX4." *Cancer Sci* 113 (4): 1475-1487. <https://doi.org/10.1111/cas.15281>.
- Wang, H., and L. Zheng. 2022. "Construction of a hypoxia-derived gene model to predict the prognosis and therapeutic response of head and neck squamous cell carcinoma." *Sci Rep* 12 (1): 13538. <https://doi.org/10.1038/s41598-022-17898-2>.
- Wang, J., H. Sun, Q. Zeng, X. J. Guo, H. Wang, H. H. Liu, and Z. Y. Dong. 2019. "HPV-positive status associated with inflamed immune microenvironment and improved response to anti-PD-1 therapy in head and neck squamous cell carcinoma." *Sci Rep* 9 (1): 13404. <https://doi.org/10.1038/s41598-019-49771-0>.
- Wei, Y., C. X. Huang, X. Xiao, D. P. Chen, H. Shan, H. He, and D. M. Kuang. 2021. "B cell heterogeneity, plasticity, and functional diversity in cancer microenvironments." *Oncogene* 40 (29): 4737-4745. <https://doi.org/10.1038/s41388-021-01918-y>.
- Weigert, A., B. Weichand, D. Sekar, W. Sha, C. Hahn, J. Mora, S. Ley, S. Essler, N. Dehne, and B. Brüne. 2012. "HIF-1 α is a negative regulator of plasmacytoid DC development in vitro and in vivo." *Blood* 120 (15): 3001-6. <https://doi.org/10.1182/blood-2012-03-417022>.
- Wharton, K. A., Jr., D. Wood, M. Manesse, K. H. Maclean, F. Leiss, and A. Zuraw. 2021. "Tissue Multiplex Analyte Detection in Anatomic Pathology - Pathways to Clinical Implementation." *Front Mol Biosci* 8: 672531. <https://doi.org/10.3389/fmolb.2021.672531>.
- Wicks, E. E., and G. L. Semenza. 2022. "Hypoxia-inducible factors: cancer progression and clinical translation." *J Clin Invest* 132 (11). <https://doi.org/10.1172/jci159839>.

- Windon, M. J., G. D'Souza, E. M. Rettig, W. H. Westra, A. van Zante, S. J. Wang, W. R. Ryan, W. K. Mydlarz, P. K. Ha, B. A. Miles, W. Koch, C. Gourin, D. W. Eisele, and C. Fakhry. 2018. "Increasing prevalence of human papillomavirus-positive oropharyngeal cancers among older adults." *Cancer* 124 (14): 2993-2999. <https://doi.org/10.1002/ncr.31385>.
- Wong, P. F., W. Wei, J. W. Smithy, B. Acs, M. I. Toki, K. R. M. Blenman, D. Zelterman, H. M. Kluger, and D. L. Rimm. 2019. "Multiplex Quantitative Analysis of Tumor-Infiltrating Lymphocytes and Immunotherapy Outcome in Metastatic Melanoma." *Clin Cancer Res* 25 (8): 2442-2449. <https://doi.org/10.1158/1078-0432.ccr-18-2652>.
- Wood, O., J. Woo, G. Seumo, N. Savelyeva, K. J. McCann, D. Singh, T. Jones, L. Peel, M. S. Breen, M. Ward, E. Garrido Martin, T. Sanchez-Elsner, G. Thomas, P. Vijayanand, C. H. Woelk, E. King, and C. Ottensmeier. 2016. "Gene expression analysis of TIL rich HPV-driven head and neck tumors reveals a distinct B-cell signature when compared to HPV independent tumors." *Oncotarget* 7 (35): 56781-56797. <https://doi.org/10.18632/oncotarget.10788>.
- Woodham, A. W., D. M. Da Silva, J. G. Skeate, A. B. Raff, M. R. Ambroso, H. E. Brand, J. M. Isas, R. Langen, and W. M. Kast. 2012. "The S100A10 subunit of the annexin A2 heterotetramer facilitates L2-mediated human papillomavirus infection." *PLoS One* 7 (8): e43519. <https://doi.org/10.1371/journal.pone.0043519>.
- Xie, J., X. Qi, Y. Wang, X. Yin, W. Xu, S. Han, Y. Cai, and W. Han. 2021. "Cancer-associated fibroblasts secrete hypoxia-induced serglycin to promote head and neck squamous cell carcinoma tumor cell growth in vitro and in vivo by activating the Wnt/ β -catenin pathway." *Cell Oncol (Dordr)* 44 (3): 661-671. <https://doi.org/10.1007/s13402-021-00592-2>.
- Xu, K., Y. Fu, Y. Han, R. Xia, S. Xu, S. Duan, Z. Zhang, and J. Li. 2020. "Fewer tumour-specific PD-1(+)/CD8(+) TILs in high-risk "Infiltrating" HPV(-) HNSCC." *Br J Cancer* 123 (6): 932-941. <https://doi.org/10.1038/s41416-020-0966-8>.
- Ye, B., Y. Duan, M. Zhou, Y. Wang, Q. Lai, K. Yue, J. Cao, Y. Wu, X. Wang, and C. Jing. 2023. "Hypoxic tumor-derived exosomal miR-21 induces cancer-associated fibroblast activation to promote head and neck squamous cell carcinoma metastasis." *Cell Signal* 108: 110725. <https://doi.org/10.1016/j.cellsig.2023.110725>.
- Yin, S., J. Huang, Z. Li, J. Zhang, J. Luo, C. Lu, and H. Xu. 2017. "The Prognostic and Clinicopathological Significance of Tumor-Associated Macrophages in Patients with Gastric Cancer: A Meta-Analysis." *PLoS One* 12 (1): e0170042. <https://doi.org/10.1371/journal.pone.0170042>.
- Yuan, X., J. Zhang, D. Li, Y. Mao, F. Mo, W. Du, and X. Ma. 2017. "Prognostic significance of tumor-associated macrophages in ovarian cancer: A meta-analysis." *Gynecol Oncol* 147 (1): 181-187. <https://doi.org/10.1016/j.ygyno.2017.07.007>.
- Zandberg, D. P., A. V. Menk, M. Velez, D. Normolle, K. DePeaux, A. Liu, R. L. Ferris, and G. M. Delgoffe. 2021. "Tumor hypoxia is associated with resistance to PD-1 blockade in squamous cell carcinoma of the head and neck." *J Immunother Cancer* 9 (5). <https://doi.org/10.1136/jitc-2020-002088>.
- Zeng, P. Y. F., M. J. Cecchini, J. W. Barrett, M. Shammas-Toma, L. De Cecco, M. S. Serafini, S. Cavalieri, L. Licitra, F. Hoebbers, R. H. Brakenhoff, C. R. Leemans, K. Scheckenbach, T. Poli, X. Wang, X. Liu, F. Laxague, E. Prisman, C. Poh, P. Bose, J. C. Dort, M. H. Shaikh, S. E. B. Ryan, A. Dawson, M. I. Khan, C. J. Howlett, W. Stecho, P. Plantinga, S. Daniela da Silva, M. Hier, H. Khan, D. MacNeil, A. Mendez, J. Yoo, K. Fung, P. Lang, E. Winquist, D. A. Palma, H. Ziai, A. L. Amelio, S. S. Li, P. C. Boutros, J. S. Mymryk, and A. C. Nichols. 2022. "Immune-based classification of HPV-associated oropharyngeal cancer with implications for biomarker-driven treatment de-intensification." *EBioMedicine* 86: 104373. <https://doi.org/10.1016/j.ebiom.2022.104373>.
- Zeng, Z., W. Du, F. Yang, Z. Hui, Y. Wang, P. Zhang, X. Zhang, W. Yu, X. Ren, and F. Wei. 2024. "The spatial landscape of T cells in the microenvironment of stage III lung adenocarcinoma." *J Pathol* 262 (4): 517-528. <https://doi.org/10.1002/path.6254>.
- Zhang, Q., Y. Wang, C. Xia, L. Ding, Y. Pu, X. Hu, H. Cai, and Q. Hu. 2021. "Integrated analysis of single-cell RNA-seq and bulk RNA-seq reveals distinct cancer-associated fibroblasts

- in head and neck squamous cell carcinoma." *Ann Transl Med* 9 (12): 1017. <https://doi.org/10.21037/atm-21-2767>.
- Zhang, S., B. Wang, F. Ma, F. Tong, B. Yan, T. Liu, H. Xie, L. Song, S. Yu, and L. Wei. 2021. "Characteristics of B lymphocyte infiltration in HPV(+) head and neck squamous cell carcinoma." *Cancer Sci* 112 (4): 1402-1416. <https://doi.org/10.1111/cas.14834>.
- Zhang, Z., J. I. Helman, and L. J. Li. 2010. "Lymphangiogenesis, lymphatic endothelial cells and lymphatic metastasis in head and neck cancer--a review of mechanisms." *Int J Oral Sci* 2 (1): 5-14. <https://doi.org/10.4248/ijos10006>.
- Zheng, Z. M., and C. C. Baker. 2006. "Papillomavirus genome structure, expression, and post-transcriptional regulation." *Front Biosci* 11: 2286-302. <https://doi.org/10.2741/1971>.

9. Přílohy

9.1. Příloha č. 1

Hindawi
Journal of Immunology Research
Volume 2019, Article ID 6705949, 10 pages
<https://doi.org/10.1155/2019/6705949>



Research Article

Implementation of Mass Cytometry for Immunoprofiling of Patients with Solid Tumors

Ingrid Poláková ¹, Ondřej Pelák,² Daniel Thürner,² Barbora Pokrývková ¹,
Ruth Tachezy,¹ Tomáš Kalina,² and Michal Šmahel ¹

¹Department of Genetics and Microbiology, Faculty of Science, Charles University, BIOCEV, Průmyslová 595, 25250 Vestec, Czech Republic

²CLIP-Childhood Leukaemia Investigation Prague, Department of Paediatric Haematology and Oncology, Second Faculty of Medicine, Charles University and Motol University Hospital, V Úvalu 84, 15006 Prague 5, Czech Republic

Correspondence should be addressed to Michal Šmahel; smahelm@natur.cuni.cz

Received 31 July 2018; Revised 12 November 2018; Accepted 21 November 2018; Published 11 February 2019

Guest Editor: Jianjun Zhang

Copyright © 2019 Ingrid Poláková et al. This is an open access article distributed under the Creative Commons Attribution License, which permits unrestricted use, distribution, and reproduction in any medium, provided the original work is properly cited.

Monitoring immune responses to solid cancers may be a better prognostic tool than conventional staging criteria, and it can also serve as an important criterion for the selection of individualized therapy. Multiparametric phenotyping by mass cytometry extended possibilities for immunoprofiling. However, careful optimization of each step of such method is necessary for obtaining reliable results. Also, with respect to procedure length and costs, sample preparation, staining, and storage should be optimized. Here, we designed a panel of 31 antibodies which allows for identification of several subpopulations of lymphoid and myeloid cells in a solid tumor and peripheral blood simultaneously. For sample preparation, disaggregation of tumor tissue with two different collagenases combined with DNase I was compared, and removal of dead or tumor cells by magnetic separation was evaluated. Two possible procedures of barcoding for single-tube staining of several samples were examined. While the palladium-based barcoding affected the stability of several antigens, the staining with two differently labeled CD45 antibodies was suitable for cells isolated from a patient's blood and tumor. The storage of samples in the intercalation solution for up to two weeks did not influence results of the analysis, which allowed the measurement of samples collected within this interval on the same day. This procedure optimized on samples from patients with head and neck squamous cell carcinoma enabled identification of various immune cells including rare subpopulations.

1. Introduction

Cancer generation and progression are critically affected by the host immune system. Therefore, the systemic and local detection and characterization of immune cells can be important for the evaluation of disease prognosis and prediction of the effect of available therapeutic options, including therapy harnessing the immune system.

Cancer immunotherapy was revitalized in recent years, and its clinical use is progressively increasing, especially after the US Food and Drug Administration (FDA) approval of the monoclonal antibodies ipilimumab, in 2011, and nivolumab and pembrolizumab, in 2014, targeting the immune

checkpoints cytotoxic T lymphocyte-associated antigen 4 (CTLA-4; CD152) and programmed cell death protein 1 (PD-1; CD279), respectively. Besides these antibodies, other promising immunotherapeutic approaches against malignant diseases—adoptive transfer of modified T cells, cancer vaccines, and chimeric monoclonal antibodies called bispecific T cell engager (BiTE)—are now available [1, 2].

The development of cancer immunotherapy is associated with the detection of immune reactions, cells, and markers that enables the monitoring of the effect of therapy but is also important for prognosis and prediction of treatment success because only a minority of patients is responsive to immunotherapy. Moreover, immunomonitoring can also be beneficial

for conventional cancer chemotherapy and radiotherapy as immune reactions can contribute to the effect of these treatment modalities [3].

Tumors are usually infiltrated by various types of immune cells that interact with tumor cells and influence tumor development. The assumption that the detection of these immune cells has a prognostic value led to the concept of “immunoscore” where immune cells are quantified in tumors by immunohistochemistry and their prognostic potential is evaluated. For early-stage colorectal cancer, the immunoscore seems to be a superior prognostic factor in comparison to tumor-node-metastasis (TNM) classification [4].

The immunoscore is mostly based on the detection of subpopulations of T lymphocytes, particularly cytotoxic CD8⁺ T cells [5], which are commonly supposed to be the major effector antitumor cells. However, at least in some tumors, other immune cells might play a crucial role in direct elimination of tumor cells [6, 7], and various immune cells are involved in complex regulation of immune reactions in the tumor microenvironment. Multiparametric phenotyping of immune cells from both tumors and peripheral blood can identify new markers for prognosis and monitoring the patient's immune status. Mass cytometry, capable of detecting over 40 parameters, is particularly suitable for such deep immunoprofiling [8].

In this study, we optimized sample preparation and staining for simultaneous analysis of immune cells in tumors and blood of patients with head and neck squamous cell carcinoma (HNSCC) by mass cytometry.

2. Materials and Methods

2.1. Sample Collection. Human blood samples of healthy volunteers were provided by the Institute of Hematology and Blood Transfusion in Prague and stored at room temperature (RT) after the collection and during the transport. Tumor tissue samples from tonsillar carcinoma were obtained from the Department of Otorhinolaryngology and Head and Neck Surgery of Motol University Hospital in Prague after the approval by the Institutional Review Board of the hospital and the obtainment of signature of the informed consent by patients. The tumor tissues were stored in RPMI medium (Sigma-Aldrich, St. Louis, MO) at 4°C during the transportation. Both types of samples were processed immediately upon the delivery.

2.2. Human Blood Cell Isolation. The Ficoll-Paque PLUS cell preparation protocol (GE Healthcare, Uppsala, Sweden) was used to obtain peripheral blood mononuclear cells (PBMCs) from noncoagulable (EDTA-treated) blood samples.

2.3. Tumor Cell Isolation. The tumor tissue was rinsed with phosphate-buffered saline (PBS), cut to pieces, and treated with 1 mg/ml collagenase D (Col D; Roche Diagnostics, Mannheim, Germany) or 1 mg/ml collagenase NB8 (Col NB8; SERVA, Heidelberg, Germany) and 100 µg/ml DNase I (Roche Diagnostics) in RPMI medium. The gentleMACS Octo Dissociator with Heaters (Miltenyi Biotec, Bergisch Gladbach, Germany) and its h_tumor_01_01 and 37C_m_

TDK_2 predefined programs were used to dissociate the tumor tissue at 37°C. Then, the samples were filtered through a 70 µm strainer to get a single-cell suspension. Erythrocytes were removed by an ACK lysing buffer (0.15 M NH₄Cl, 10 mM KHCO₃, and 0.5 M EDTA (pH 7.2–7.4)).

2.4. Magnetic Separation of Cells. Cells labeled with antibodies conjugated to magnetic beads were separated by the autoMACS Pro Separator (Miltenyi Biotec). For disposal of dead cells from PBMCs or tumor cell suspensions, the Dead Cell Removal Kit (Miltenyi Biotec) was used. To concentrate tumor-infiltrating immune cells, epithelial tumor cells were removed after labeling with CD326 (EpcAM) Microbeads (Miltenyi Biotec). Before labeling, the Fc receptor of non-epithelial cells was blocked with FcR Blocking Reagent (Miltenyi Biotec). Positive and negative fractions obtained after separation of cells were fluorescently stained with monoclonal antibodies FITC anti-CD326 (clone HEA-125) and PE anti-CD45 (clone 5B1; both Miltenyi Biotec). The stained cells were measured on an LSRFortessa flow cytometer (BD Biosciences, San Diego, CA) and analyzed using the FlowJo v10.4.1 Software (BD Biosciences).

2.5. Mass Cytometry. To distinguish live and dead cells, blood and tumor samples were first stained with Cell-ID Cisplatin-¹⁹⁸Pt (Fluidigm, South San Francisco, CA). Then, samples were barcoded with the Cell-ID 20-Plex Pd Barcoding Kit (Fluidigm). For this barcoding, samples underwent fixation (Fix I Buffer) and gentle permeabilization (Barcode Perm Buffer) to be labeled with the combination of three palladium isotopes. The labeling pattern for debarcoding is indicated in the user guide of the kit. Alternatively, samples were barcoded with two differently labeled anti-CD45 antibodies, CD45-156Gd and CD45-89Y (both clone HI30, Fluidigm), according to the Maxpar Cell Surface Staining protocol (Fluidigm). Cells were resuspended in 100 µl of total staining volume of Maxpar Cell Staining Buffer with 1 µl of antibody and incubated at RT for 30 minutes. Cell barcoding was followed by the staining of surface and nuclear antigens observing the procedure recommended by the Maxpar Nuclear Antigen Staining kit (Fluidigm). In brief, cells were washed by Maxpar Cell Staining Buffer after barcoding and incubated at RT for 30 minutes with the surface antibody cocktail in 100 µl of total staining volume. The surface staining was followed by a washing step and incubation in 1 ml of Nuclear Antigen Staining Buffer for another 30 minutes. Then, two washing steps with Nuclear Antigen Staining Perm were performed, and the cells were stained with the intracellular antibody cocktail for 40 minutes. After another two washings with Maxpar Cell Staining Buffer, 1 ml of Cell-ID Intercalator-Ir solution was added to the cells. Antibodies (Table 1) obtained mostly from Fluidigm were pre-conjugated with metal isotopes. Some antibodies were purchased from other companies and required conjugation with isotope tags applying the Maxpar Antibody Labeling Kit (Fluidigm). Stained and fixed cells were stored at 4°C until ready to run on a CyTOF2 mass cytometer (Fluidigm). The data were exported as flow cytometry file (.fcs) format.

TABLE 1: Panel of antibodies for mass cytometry.

#	Antigen	Isotope	Clone	Staining	Company
1	CD1c (BDCA-1)*	166Er	AD5-8E7	Surface	Miltenyi Biotec
2	CD3	154Sm	UCHT1	Surface	Fluidigm
3	CD4	145Nd	RPA-T4	Surface	Fluidigm
4	CD8a	146Nd	RPA-T8	Surface	Fluidigm
5	CD11b (Mac-1)	209Bi	ICRF44	Surface	Fluidigm
6	CD11c*	152Sm	Bu15	Surface	BioLegend
7	CD14	151Eu	M5E2	Surface	Fluidigm
8	CD15*	173Yb	MEM-158	Surface	Exbio
9	CD16	148Nd	3G8	Surface	Fluidigm
10	CD19	142Nd	HIB19	Surface	Fluidigm
11	CD25	169Tm	2A3	Surface	Fluidigm
12	CD39	160Gd	A1	Surface	Fluidigm
13	CD45	89Y or 156Gd	HI30	Surface	Fluidigm
14	CD45RA	155Gd	HI100	Surface	Fluidigm
15	CD45RO	164Dy	UCHL1	Surface	Fluidigm
16	CD56 (NCAM)	176Yb	N901	Surface	Fluidigm
17	CD62L (L-selectin)	153Eu	DREG-56	Surface	Fluidigm
18	CD68	171Yb	Y1/82A	Intracellular	Fluidigm
19	CD69	144Nd	FN50	Surface	Fluidigm
20	CD127 (IL-7R α)	149Sm	A019D5	Surface	Fluidigm
21	CD141 (BDCA-3)*	165Ho	AD5-14H12	Surface	Miltenyi Biotec
22	CD152 (CTLA-4)	161Dy	14D3	Intracellular	Fluidigm
23	CD197 (CCR7)	159Tb	G043H7	Surface	Fluidigm
24	CD275 (ICOS-L)*	163Dy	2D3/B7-H2	Surface	BD Biosciences
25	CD278 (ICOS)	143Nd	DX29	Surface	Fluidigm
26	CD279 (PD-1)	175Lu	EH12.2H7	Surface	Fluidigm
27	CD303 (BDCA-2)	147Sm	201A	Surface	Fluidigm
28	CD366 (Tim-3)	150Nd	F38-2E2	Surface	BioLegend
29	Foxp3	162Dy	259D/C7	Intracellular	Fluidigm
30	HLA-DR	170Er	L243	Surface	Fluidigm
31	Ki-67	172Yb	B56	Intracellular	Fluidigm

* In-house conjugation with isotope tags applying the Maxpar Antibody Labeling Kit (Fluidigm).

3. Results

3.1. Designing a Panel of 31 Antibodies for Immunomonitoring of Cancer Patients. We designed a panel of antibodies for multiparametric phenotyping of blood and tumor samples of patients with malignant diseases. Using the Maxpar Panel Designer (Fluidigm), we created a panel of 31 antibodies suitable for mass cytometry (Table 1). In this panel, we focused on various subpopulations of T lymphocytes (naïve, activated, and memory cells and effector and regulatory cells) and myeloid cells (monocytes, macrophages, and dendritic cells). Additionally, B cells and NK cells can also be identified.

3.2. Collagenase D Was Suitable for Enzymatic Dissociation of the Tumor Tissue. To optimize the staining of cells for mass cytometry, we first optimized sample preparation. As we plan

to apply the established procedure for the analysis of tumors from patients with HNSCC, we used samples from tonsillar carcinomas in the optimization part of the study. For isolation of single cells from these tumors, we combined mechanical and enzymatic disaggregation techniques. Collagenase and DNase I are enzymes commonly used for the dissociation of tumor tissues, and their applicability for mass cytometry has recently been demonstrated [9]. Based on our prior experiences with the usage of Col NB8 (SERVA) for preparation of tumor-infiltrating cells from mouse tumors [10] and Col D (Roche) for HNSCC [11], we compared these two types of collagenases. Tumor samples were divided into two parts of the same weight and processed in the gentleMACS Octo Dissociator using predefined programs with the enzymatic treatment at 37°C for 40 min. Regardless of the collagenase used, the total numbers of cells and their viability were repeatedly comparable. Isolated cells

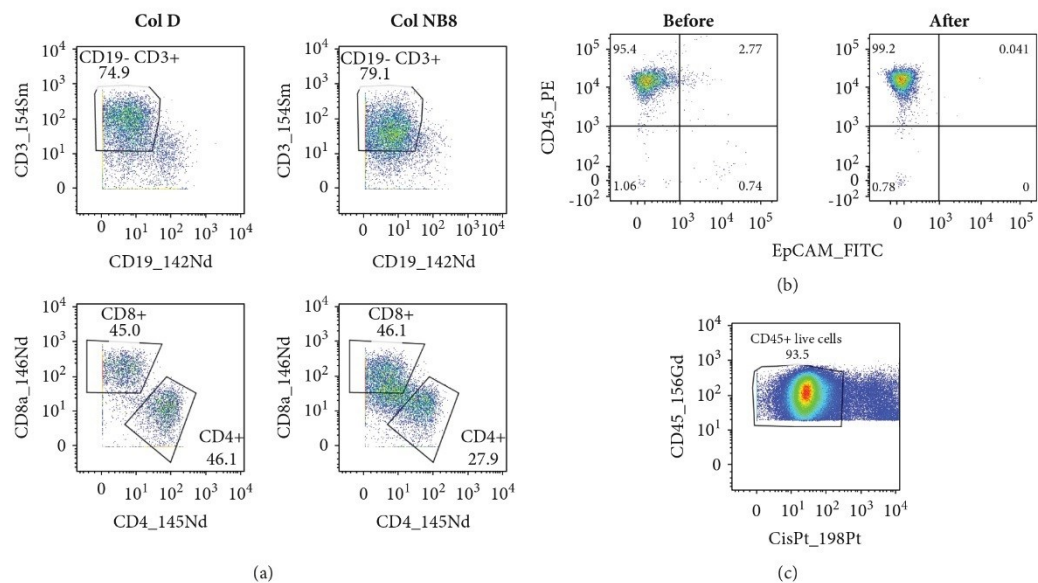


FIGURE 1: Sample preparation. (a) Tumor tissue was halved and treated with either Col D or Col NB8 together with DNase I using a gentleMACS Octo Dissociator and its predefined programs. After lysis of erythrocytes, the single-cell suspensions were stained with the designed panel of antibodies. The same gates were applied to cell populations originated from the tissues treated with Col D or Col NB8. (b) Samples of cells prepared from tumors were labeled with fluorescent anti-CD45 and anti-EpCAM antibodies before and after magnetic removal of epithelial cells. (c) Cells isolated from the tumor sample were stained with cisplatin for viability detection. The experiments were repeated with similar results.

were stained with the designed panel of antibodies and evaluated by mass cytometry. We found that the treatment with Col D better preserved the detected antigens as documented in Figure 1(a) by gating of CD3⁺, CD4⁺, and CD8⁺ cells. As the determination of these crucial cell populations was nearly impossible after the treatment of the tumor tissue with Col NB8, we decided to use Col D for further analysis.

3.3. Removal of Dead Cells and Epithelial Tumor Cells from the Dissociated Tumor Tissue Was Not Usually Necessary. In comparison with flow cytometry, measurement of samples by a mass cytometer is more time-consuming (because of a low acquisition rate) and more expensive (because of argon consumption). Therefore, a high proportion of appropriate cells in measured samples are desirable. Single-cell suspensions prepared by dissociation of tumors contain various numbers of tumor-infiltrating immune cells and epithelial tumor cells that can further differ in viability. To concentrate live tumor-infiltrating immune cells, we considered the removal of dead cells and/or epithelial tumor cells by magnetic separation on autoMACS after labeling of annexin V or EpCAM, respectively. The labeled cells were efficiently removed, but about a half of all cells were lost during this procedure. With respect to a low portion of EpCAM⁺ cells (usually less than 15%; Figure 1(b)) and dead cells (mostly about 20–35%) in single-cell suspensions prepared from tumors and high loss of cells in magnetic separations, we omitted the concentration of immune cells in the following experiments. However, to distinguish live and dead cells in

the sample, the cells were labeled with cisplatin, containing the ¹⁹⁸Pt isotope, before surface and intracellular staining (Figure 1(c)).

3.4. Pd-Based Barcoding Affected Stability of Several Antigens. To decrease high costs of cell labeling and sample measurement, we tested a single-tube staining of cells obtained from multiple samples and analyzed tumor and blood cells from several patients together. To distinguish cells isolated from blood and tumors and from different patients, a commercial barcoding kit based on palladium (Pd) isotopes was first tested. This kit is able to barcode, subsequently stain, and measure up to 20 samples as a one multiplexed sample. Samples were labeled with a combination of three Pd isotopes after fixation and gentle permeabilization steps. The barcoded samples were then combined in a single tube and stained with the designed panel of antibodies. After analysis of staining intensity, we observed a considerable population shift for some markers when comparing the barcoded samples with samples without barcoding (Figure 2). CD62L, CD16, CD56, CD11c, and CD25 were the markers with the most prominent reduction of positivity after barcoding, which disabled proper identification of cell populations (Figure 2(a)). On the contrary, the boundary between some populations (CD15⁺, CD3⁺, CD4⁺, and CD8⁺; Figure 2(b)) became more evident. As our main intent is to preserve the integrity of all cellular markers, the Pd-based barcoding technique is not applicable to our panel of antibodies.

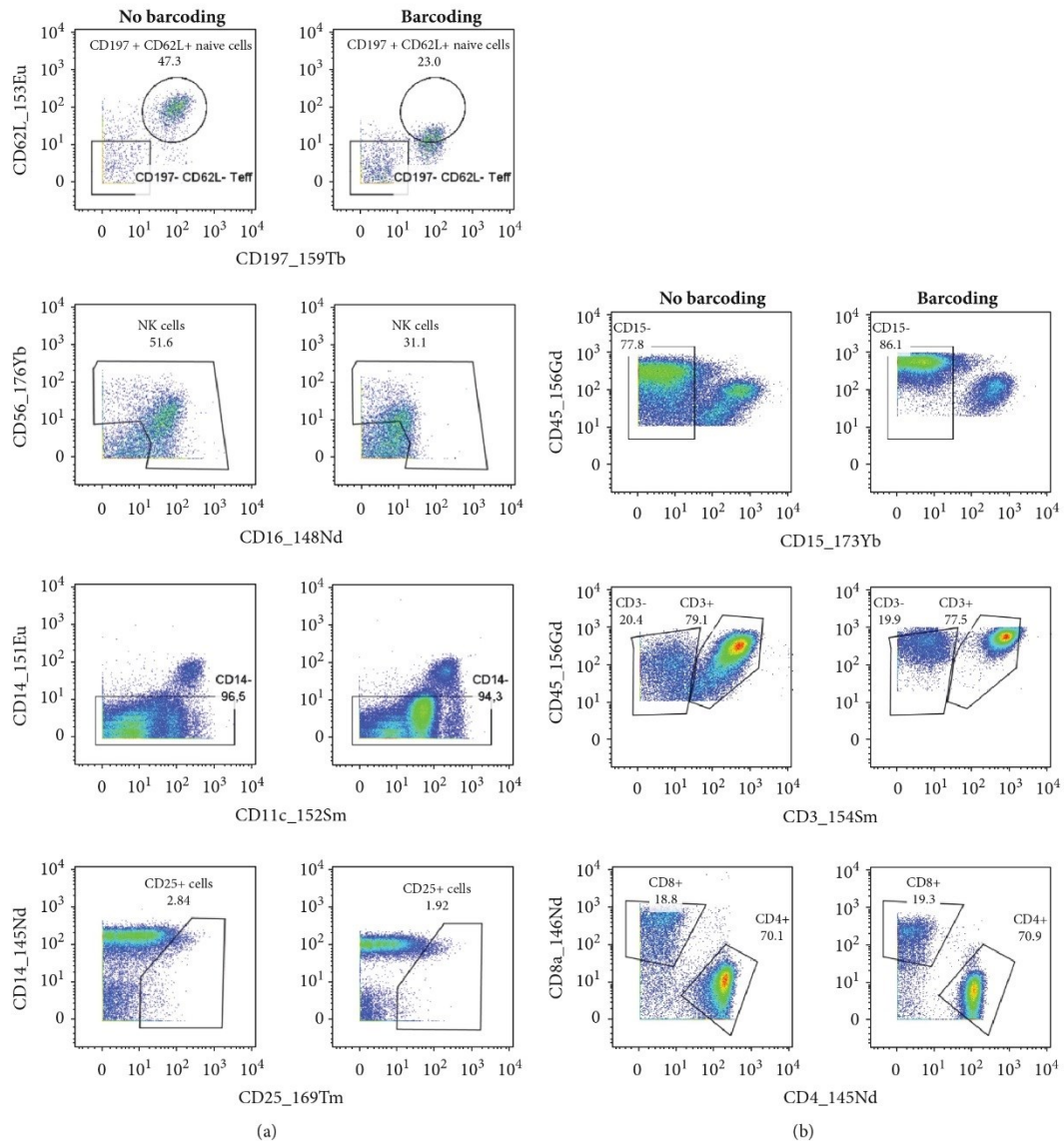


FIGURE 2: Stability of several antigens was affected by Pd-based barcoding. Ficoll-isolated PBMCs from a healthy donor were stained for live and dead cells and halved. One part of the cells was barcoded with the Cell-ID 20-Plex Pd Barcoding Kit, and the rest of the cells were used as a control without barcoding. Subsequently, the cells were stained with the designed panel of antibodies. The labeled cells were stored in the intercalator solution until measurement on CyTOF. After measurement, the barcoded cells were debarcoded according to the labeling pattern of the barcoding kit. (a) Markers with reduced intensity and (b) cell populations become more evident after Pd barcoding. The same gates (adjusted for the cells without barcoding) were applied to measured cells.

3.5. CD45-Based Barcoding Did Not Affect Detection of Cell Markers. Antibody against CD45 molecules labeled with different isotopes is another possibility of sample barcoding [12]. To distinguish between cells from blood and tumors, we tested two metal-labeled antibodies (CD45-156Gd and CD45-89Y). For comparison of their staining efficacy and their effect on the detection of other cell markers, we halved the cells from a tumor sample and barcoded them with the

CD45 antibodies. Subsequently, the barcoded cells were combined and stained together with the remaining antibodies from the CyTOF panel. Figure 3 demonstrates that antibodies against CD45 identified practically identical cell populations, and parallel samples labeled with these antibodies did not differ in cell subpopulations detected by other antibodies. In view of these results, we decided to apply CD45-based barcoding to our samples.

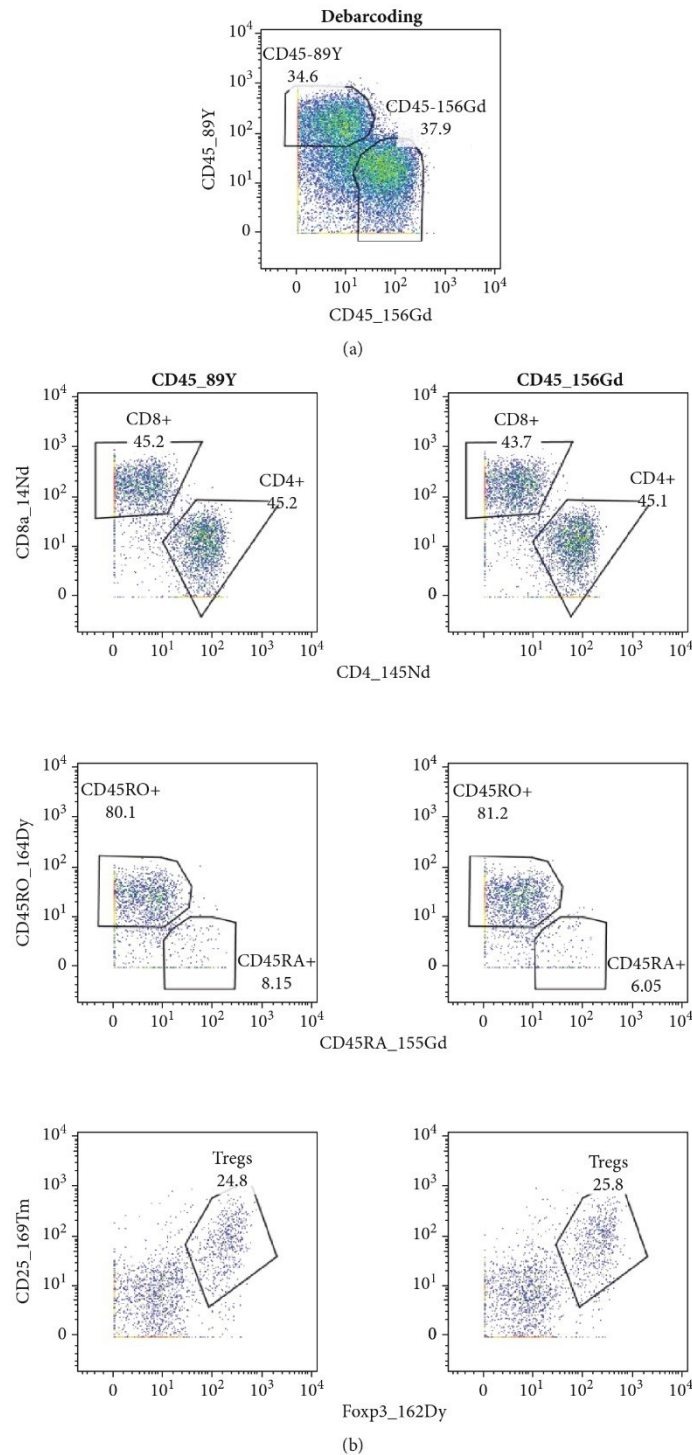


FIGURE 3: CD45-based barcoding. A single-cell suspension was prepared from tonsillar carcinoma, stained for live and dead cells, and halved for barcoding. After barcoding with CD45-89Y and CD45-156Gd antibodies, the samples were combined and stained with the rest of the antibodies. (a) Debarcoding and (b) dot plots with a selection of representative antigens. The same gates were applied to measured cells.

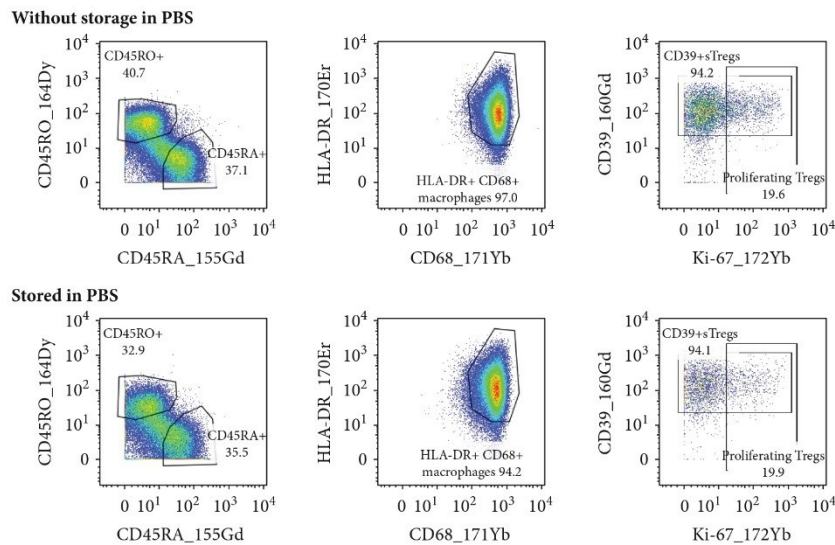


FIGURE 4: Sample storage in PBS with 1% BSA. Tumor cells and PBMCs were isolated from a patient with HNSCC and stained for viability. After CD45-based barcoding, samples were halved. One part of the cells was stained with the panel of antibodies immediately, and the other part was stored in PBS with 1% BSA at 4°C overnight and labeled the next day. Dot plots display some representative markers of the blood sample. Gates were adjusted for cell samples stained immediately after isolation.

3.6. Sample Storage Conditions. The sample preparation, barcoding, staining, and measurement are time-consuming procedures that can be further complicated by the fact that sample collection, processing, and analysis are carried out at different sites. This long procedure might be interrupted in a few points. One possibility is to stop the procedure after sample preparation. Simultaneously with testing the Pd-based barcoding, we attempted to store the prepared samples in Maxpar Fix I Buffer that is a component of the barcoding kit and is used for treatment of cells prior to the barcoding itself. After storing the samples in Fix I Buffer at 4°C overnight, changes obtained after Pd-based barcoding were intensified, and staining of several other antigens was affected (data not shown). Therefore, the Fix I Buffer turned out to be unsuitable for sample storage.

As another option, we examined storing the CD45-barcoded samples in PBS with 1% BSA at 4°C overnight. We found that this way of storage did not have any impact on the antigen stability and population gating (Figure 4).

Collecting several samples labeled on different days to measure them at a time can also reduce the measurement costs and may be useful when a limited number of samples are stained per day. Sample staining terminates with resuspending the cells in an intercalator solution, which is intended to store the samples at 4°C until the measurement. We compared samples stored in the intercalator solution for one or two weeks with a sample measured immediately (on the next day) after labeling. As we did not observe any differences among these samples (Figure 5), we considered

appropriate to store the labeled samples in the intercalator solution for at least two weeks.

4. Discussion

Mass cytometry with its capability to detect a large number of parameters is a convenient method for accurate immunoprofiling of cancer patients. Exposing the phenotype of the immune cells may contribute to disease prognosis and treatment selection. Therefore, we designed a panel of antibodies to detect a wide range of lymphoid and myeloid subpopulations in blood and tumor samples and optimized the procedure of sample preparation and labelling for simultaneous analysis of peripheral blood cells and immune cells isolated from a solid tumor of the same patient.

Whereas a standard Ficoll gradient centrifugation protocol exists for PBMC separation, the storage conditions of blood samples until processing had to be considered. The drawn blood should be stored at RT and processed within 8 hours to avoid granulocyte contamination during PBMC isolation and to preserve T cells [13]. Moreover, it has been proven that the prolonged sample storage at RT before testing may cause a contact-dependent exchange of the CD3 antigen between T and B cells [14]. Fortunately, these phenomena were not observed in our experiments due to the immediate sample processing after delivery.

The tumor tissue, transported in RPMI medium on ice, was likewise promptly processed. The tissue dissociation (mechanically and/or enzymatically), leading to a single-cell suspension, is an essential step in immunoprofiling of solid tumors. As mass cytometry was developed recently, only

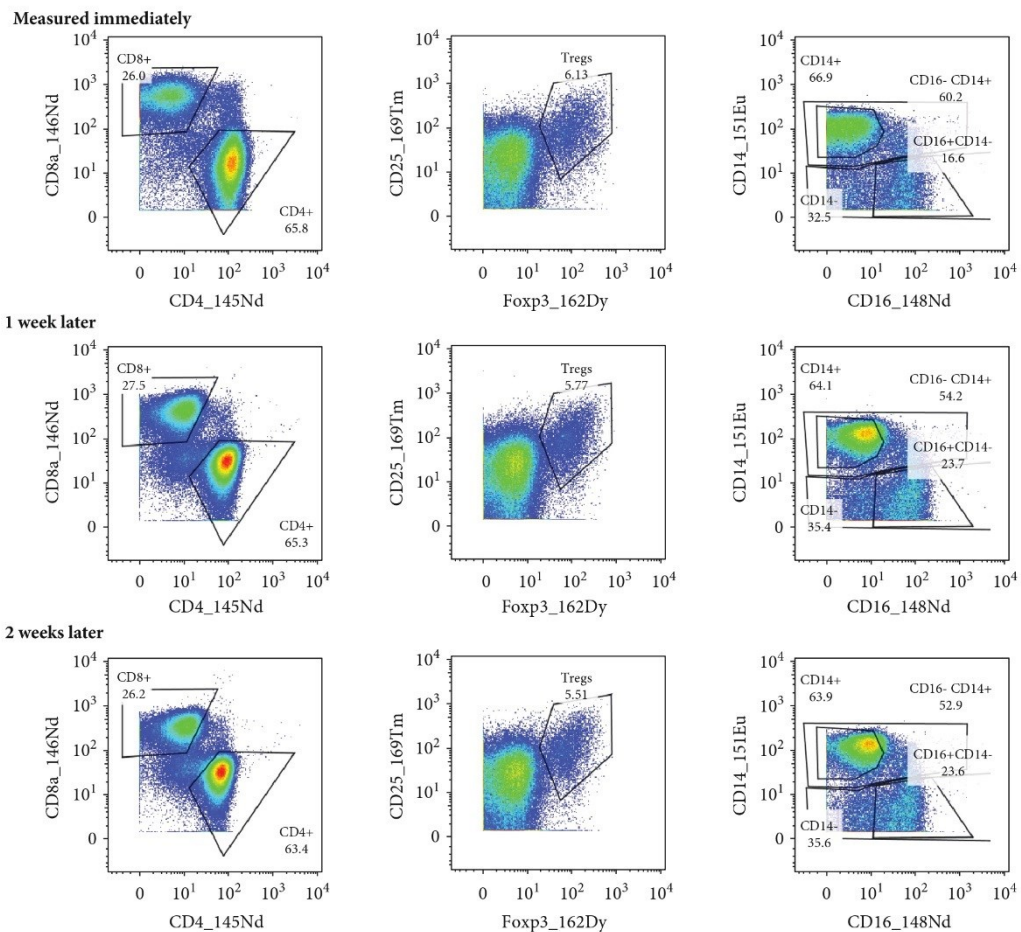


FIGURE 5: Storage of labeled samples in the intercalator solution. PBMCs were isolated from a blood sample of a patient with HNSCC, stained for live and dead cells, and divided for further labeling. The stained cells were measured the next day or stored in the intercalator solution for one or two weeks. The same gates (adjusted for the sample measured immediately) were applied to measured cells.

few articles deal with tumor dissociation methods. To preserve the viability, integrity, and functionality of cells infiltrating a tumor, it is necessary to choose a suitable enzyme and determine the timing of tumor processing. Leelatian and his group compared several collagenases and DNases and their combinations [9] and proposed a protocol for human tumor dissociation [15]. Based on our previous experience with mouse and human tumor tissues, we compared the combination of DNase I with Col D or Col NB8. Although the viability of the cells isolated from tumors was similarly preserved in both combinations and the yield was comparable, it was not possible to define the basic cell populations after treatment with Col NB8. Consequently, the combination of DNase I and Col D was applied in further experiments.

Besides its many advantages, mass cytometry has two crucial limitations. The experiments carried out and the measurements may be costly and time-consuming. Therefore, it is essential to measure primarily the cells of our

interest. To meet this requirement, we tried to remove dead and epithelial cells from the tumor samples prior to labeling. However, magnetic depletion of dead cells or EpCAM⁺ cells led to significant loss of desired population of viable immune cells. Additionally, flow cytometric analyses of several samples showed that the viability of isolated cells was high (usually >60%) and the portion of epithelial cells in samples from tonsillar carcinomas was mostly negligible. Therefore, we decided to remove only dead cells whenever their proportion was higher than 50% of all cells and the number of isolated cells was sufficient (at least 6×10^6). Cisplatin staining prior to surface labeling was chosen to gate live and dead cells.

The staining and measurement costs could be further pushed down by a single-tube analysis of tumor and blood cells from several patients. Mass-tag cellular barcoding (MCB) techniques have been developed for experiment multiplexing. These techniques are based on lanthanide isotopes loaded on the compound maleimido-mono-amide-DOTA (mDOTA) [16], isothiocyanobenzyl-EDTA-loaded

palladium isotopes [17], or osmium and ruthenium isotopes [18]. In our experiments, we tested the commercially available Pd-based barcoding kit, which is able to barcode up to 20 samples, but this kit was not usable in combination with our antibody panel as the staining procedure affected the stability of several antigens of our interest. Our following measurements revealed (data not shown) that at least 1.5×10^6 (ideally 2.5×10^6) cells isolated from both blood and tumor need to be stained to collect also the rare populations of cells. Moreover, as it was concluded that more than 4×10^6 cells cannot be stained in a single tube, our only option was a combination of blood and tumor cells from only one patient into a single tube. Since it was sufficient to apply two barcodes for this purpose, we tested a multiplexing method directed against the cell surface-expressed CD45 [12, 19] that does not require fixation and partial permeabilization unlike the Pd-based barcoding. Staining of the blood and tumor samples originated from one patient with two differently labeled anti-CD45 antibodies was satisfying—none of the antigens was affected by the barcoding.

As the time from sample collection to its processing, staining, and measurement may vary, we searched for pause points in this long procedure. Prolonged incubation in the Fix I Buffer that is applied during the Pd-based barcoding could be a suitable way of interruption. However, overnight incubation of samples in this transient fixation buffer influenced the stability of several antigens. This result suggests that the effect of the Fix I Buffer is the reason why Pd barcoding is not applicable to our antibody panel. Another option was to store the isolated, viability-stained, and barcoded cells in PBS with 1% BSA at 4°C overnight before staining with the panel of antibodies. This delay in sample processing did not affect staining results when compared to the samples labeled immediately after barcoding. Accordingly, it was possible to interrupt the sample staining, under time pressure, via storing the barcoded cells in PBS with BSA.

The very last step of sample staining is resuspension of the labeled cells in the intercalation solution, which labels the nucleated cells with iridium isotopes. This procedure requires fixation and permeabilization of the cells. Using the Maxpar Nuclear Antigen Staining kit (Fluidigm), the intercalator is diluted in Fix & Perm Buffer that contains paraformaldehyde. The manufacturer's recommendation is to store the cells in the intercalator solution at 4°C until measurement on a mass cytometer, but no longer than 48 hours. However, Zunder and his group showed that it was possible to keep the samples in an in-house-prepared intercalation solution at 4°C for up to one month [17]. Therefore, we prolonged the sample storage in the intercalation solution to one and two weeks and compared the outcome with the sample measured the next day after labeling. As no differences were found among the compared samples, we concluded that the storage of the labeled cells in this solution is acceptable for at least two weeks.

5. Conclusions

A panel of 31 antibodies was designed for mass cytometry immunoprofiling of blood and tumor samples from patients with HNSCC. The method of tumor tissue dissociation was

optimized by the combination of DNase I with the proper collagenase, and suitable barcoding of cells isolated from blood and tumor samples originated from one patient was incorporated in cell labeling. Next, a possible pause point in the long sample processing was found, and the storage of labeled samples until measurement on a mass cytometer was solved. Consequently, all surface and intracellular antigens of our interest were preserved and procedure costs were minimized.

Data Availability

The data used to support the findings of this study are available from the corresponding author upon request.

Conflicts of Interest

The authors declare no conflict of interest.

Acknowledgments

We thank K. Klečáková and P. Veselá for the technical assistance and M. Grega, V. Koucký, and S. Maléřová for the sample collection. This study was supported by the Ministry of Education, Youth and Sports of the Czech Republic (MEYS) (Grant No. LQ1604; National Sustainability Program II, Project BIOCEV-FAR), the Agency for Medical Research of the Ministry of Health of the Czech Republic (Grant No. 17-28055A), and the European Regional Development Fund (ERDF) and MEYS (Grant No. CZ.1.05/1.1.00/02.0109, CZ.2.16/3.1.00/21540, and CZ.1.05/2.1.00/19.0400).



References

- [1] M. L. Drakes and P. Stiff, "Harnessing immunosurveillance: current developments and future directions in cancer immunotherapy," *ImmunoTargets and Therapy*, vol. 2014, pp. 151–165, 2014.
- [2] S. Menon, S. Shin, and G. Dy, "Advances in cancer immunotherapy in solid tumors," *Cancers*, vol. 8, no. 12, p. 106, 2016.
- [3] W. H. Fridman, L. Zitvogel, C. Sautès-Fridman, and G. Kroemer, "The immune contexture in cancer prognosis and treatment," *Nature Reviews Clinical Oncology*, vol. 14, no. 12, pp. 717–734, 2017.
- [4] F. Pagès, A. Kirilovsky, B. Mlecnik et al., "In situ cytotoxic and memory T cells predict outcome in patients with early-stage colorectal cancer," *Journal of Clinical Oncology*, vol. 27, no. 35, pp. 5944–5951, 2009.
- [5] P. A. Ascierto, M. Capone, W. J. Urba et al., "The additional facet of immunoscore: immunoprofiling as a possible predictive tool for cancer treatment," *Journal of Translational Medicine*, vol. 11, no. 1, p. 54, 2013.
- [6] N. Bercovicí and A. Trautmann, "Revisiting the role of T cells in tumor regression," *OncoImmunology*, vol. 1, no. 3, pp. 346–350, 2012.
- [7] M. Thoreau, H. X. L. Penny, K. W. Tan et al., "Vaccine-induced tumor regression requires a dynamic cooperation between T cells and myeloid cells at the tumor site," *Oncotarget*, vol. 6, no. 29, pp. 27832–27846, 2015.
- [8] M. H. Spitzer and G. P. Nolan, "Mass cytometry: single cells, many features," *Cell*, vol. 165, no. 4, pp. 780–791, 2016.

- [9] N. Leelatian, D. B. Doxie, A. R. Greenplate et al., "Single cell analysis of human tissues and solid tumors with mass cytometry," *Cytometry Part B: Clinical Cytometry*, vol. 92, no. 1, pp. 68–78, 2017.
- [10] I. Kašťánková, I. Poláková, M. Dušková, and M. Šmahel, "Combined cancer immunotherapy against Aurora kinase A," *Journal of Immunotherapy*, vol. 39, no. 4, pp. 160–170, 2016.
- [11] S. Partlová, J. Bouček, K. Kloudová et al., "Distinct patterns of intratumoral immune cell infiltrates in patients with HPV-associated compared to non-virally induced head and neck squamous cell carcinoma," *Oncotmunology*, vol. 4, no. 1, article e965570, 2015.
- [12] L. Lai, R. Ong, J. Li, and S. Albani, "A CD45-based barcoding approach to multiplex mass-cytometry (CyTOF)," *Cytometry Part A*, vol. 87, no. 4, pp. 369–374, 2015.
- [13] R. Mallone, S. I. Mannering, B. M. Brooks-Worrell et al., "Isolation and preservation of peripheral blood mononuclear cells for analysis of islet antigen-reactive T cell responses: position statement of the T-Cell Workshop Committee of the Immunology of Diabetes Society," *Clinical & Experimental Immunology*, vol. 163, no. 1, pp. 33–49, 2011.
- [14] A. Nagel, C. Möbs, H. Raifer, H. Wiendl, M. Hertl, and R. Eming, "CD3-positive B cells: a storage-dependent phenomenon," *PLoS One*, vol. 9, no. 10, 2014.
- [15] N. Leelatian, D. B. Doxie, A. R. Greenplate, J. Sinnaeve, R. A. Ihrie, and J. M. Irish, "Preparing viable single cells from human tissue and tumors for cytomic analysis," *Current Protocols in Molecular Biology*, vol. 118, no. 1, pp. 25C.1.1–25C.1.23, 2017.
- [16] B. Bodenmiller, E. R. Zunder, R. Finck et al., "Multiplexed mass cytometry profiling of cellular states perturbed by small-molecule regulators," *Nature Biotechnology*, vol. 30, no. 9, pp. 858–867, 2012.
- [17] E. R. Zunder, R. Finck, G. K. Behbehani et al., "Palladium-based mass tag cell barcoding with a doublet-filtering scheme and single-cell deconvolution algorithm," *Nature Protocols*, vol. 10, no. 2, pp. 316–333, 2015.
- [18] R. Catena, A. Özcan, N. Zivanovic, and B. Bodenmiller, "Enhanced multiplexing in mass cytometry using osmium and ruthenium tetroxide species," *Cytometry Part A*, vol. 89, no. 5, pp. 491–497, 2016.
- [19] H. E. Mei, M. D. Leipold, A. R. Schulz, C. Chester, and H. T. Maecker, "Barcoding of live human peripheral blood mononuclear cells for multiplexed mass cytometry," *The Journal of Immunology*, vol. 194, no. 4, pp. 2022–2031, 2015.

Article

ARG1 mRNA Level Is a Promising Prognostic Marker in Head and Neck Squamous Cell Carcinomas

Barbora Pokrývková ^{1,*} , Jana Šmahelová ¹, Natálie Dalewská ¹, Marek Grega ², Ondřej Vencálek ³, Michal Šmahel ¹ , Jaroslav Nunvář ¹, Jan Klozar ⁴ and Ruth Tachezy ^{1,*}

- ¹ Department of Genetics and Microbiology, Faculty of Science, Charles University, BIOCEV, 252 50 Vestec, Czech Republic; jana.smahelova@natur.cuni.cz (J.Š.); dalewska@hotmail.cz (N.D.); michal.smahel@natur.cuni.cz (M.Š.); jaroslav.nunvar@natur.cuni.cz (J.N.)
- ² Department of Pathology and Molecular Medicine, 2nd Faculty of Medicine, Charles University, 150 06 Prague, Czech Republic; Marek.Grega@fnmotol.cz
- ³ Department of Mathematical Analysis and Applications of Mathematics, Faculty of Science of the Palacky University in Olomouc, 771 46 Olomouc, Czech Republic; ondrej.vencalek@upol.cz
- ⁴ Department of Otorhinolaryngology and Head and Neck Surgery, 1st Faculty of Medicine, Charles University, University Hospital Motol, 150 06 Prague, Czech Republic; Jan.Klozar@fnmotol.cz
- * Correspondence: barbora.pokryvkova@natur.cuni.cz (B.P.); ruth.tachezy@natur.cuni.cz (R.T.); Tel.: +420-77-6337595 (B.P.); +420-73-7355521 (R.T.)



Citation: Pokrývková, B.; Šmahelová, J.; Dalewská, N.; Grega, M.; Vencálek, O.; Šmahel, M.; Nunvář, J.; Klozar, J.; Tachezy, R. ARG1 mRNA Level Is a Promising Prognostic Marker in Head and Neck Squamous Cell Carcinomas. *Diagnostics* **2021**, *11*, 628. <https://doi.org/10.3390/diagnostics11040628>

Academic Editor:
Gustavo Baldassarre

Received: 5 March 2021
Accepted: 29 March 2021
Published: 31 March 2021

Publisher's Note: MDPI stays neutral with regard to jurisdictional claims in published maps and institutional affiliations.



Copyright: © 2021 by the authors. Licensee MDPI, Basel, Switzerland. This article is an open access article distributed under the terms and conditions of the Creative Commons Attribution (CC BY) license (<https://creativecommons.org/licenses/by/4.0/>).

Abstract: Head and neck squamous cell carcinomas (HNSCC) can be induced by smoking or alcohol consumption, but a growing part of cases relate to a persistent high-risk papillomavirus (HPV) infection. Viral etiology has a beneficial impact on the prognosis, which may be explained by a specific immune response. Tumor associated macrophages (TAMs) represent the main immune population of the tumor microenvironment with a controversial influence on the prognosis. In this study, the level, phenotype, and spatial distribution of TAMs were evaluated, and the expression of TAM-associated markers was compared in HPV positive (HPV+) and HPV negative (HPV−) tumors. Seventy-three formalin and embedded in paraffin (FFPE) tumor specimens were examined using multispectral immunohistochemistry for the detection of TAM subpopulations in the tumor parenchyma and stroma. Moreover, the mRNA expression of TAM markers was evaluated using RT-qPCR. Results were compared with respect to tumor etiology, and the prognostic significance was evaluated. In HPV− tumors, we observed more pro-tumorigenic M2 in the stroma and a non-macrophage arginase 1 (ARG1)-expressing population in both compartments. Moreover, higher mRNA expression of M2 markers—cluster of differentiation 163 (CD163), ARG1, and prostaglandin-endoperoxide synthase 2 (PTGS2)—was detected in HPV− patients, and of M1 marker nitric oxide synthase 2 (NOS2) in HPV+ group. The expression of ARG1 mRNA was revealed as a negative prognostic factor for overall survival of HNSCC patients.

Keywords: head and neck carcinoma; arginase 1; HPV; prognosis; macrophages

1. Introduction

Every year, more than 750,000 new patients are diagnosed worldwide with head and neck squamous cell carcinomas (HNSCC) [1]. Most cases relate to smoking and alcohol consumption, but a growing part of these tumors originates as a consequence of persistent infection with high-risk human papillomavirus (HR HPV) [2]. HNSCC tumors occur in a number of anatomical locations, but HPV positive (HPV+) tumors are mostly localized in the oropharynx [3]. Patients with HNSCC of viral etiology are younger and have a better prognosis, which may be explained by a specific immune response [2–5]. Currently, researchers are focusing on searching and defining new biomarkers for early disease detection and prognosis prediction as an addition to the classical tumor-node-metastasis (TNM) staging and histological grading.

The tumor microenvironment (TME) is a complex system of tumor cells and surrounding stroma, which originates from normal tissue cells, fibroblasts, endothelial cells, pericytes, immune cells, and extracellular matrix. As for the tumor cells, genetic alterations resulting in uncontrolled proliferation and phenotype changes are characteristic, the stromal cells remain genetically unchanged, but their activity is largely influenced by cytokines produced by tumor cells themselves or by other cells of the TME [6]. Tumor associated macrophages (TAMs) are the most abundant immune cells of the TME. Functionally, macrophages can be polarized into two extreme groups: classical M1 with pro-inflammatory and anti-tumorigenic functions and alternative M2, which act as anti-inflammatory and pro-tumorigenic. Additionally, M2 macrophages can be subdivided into M2a, M2b, M2c, and M2d phenotypes, linked to different inducers but sharing similar functional activities [7]. Between M1 and M2 polarizations, the phenotype plasticity was described, reflecting the complex cytokine environment in tumors. Thus, the categorization of TAMs into M1 and M2 is simplified [8,9]. During the early phase of tumorigenesis, macrophage precursors migrate into the TME in response to chemoattractants produced by tumor or stromal cells. The level of these chemoattractants, such as C-C motif chemokine ligand 2 (CCL2), colony-stimulating factor 1 (CSF1), or vascular endothelial growth factor (VEGF), is enhanced by the hypoxic environment [10,11]. After entering the TME, macrophage precursors polarize to the M1 phenotype upon the autocrine or paracrine stimulus with interferon gamma (IFN- γ) or other molecules, such as tumor necrosis factor alpha (TNF- α) and toll-like receptor (TLR) ligands. The M1 macrophages produce inflammatory cytokines, such as interleukin (IL)-1, IL-6, IL-12, TNF- α , and IFN- γ . The inflammatory environment generates reactive nitrogen and oxygen species leading to genome instability [12]. Consequently, macrophages acquire the M2 phenotype, which contributes to tumor progression [12,13]. For M2 polarization, mainly the presence of transforming growth factor beta (TGF- β) and IL-4, IL-10, and IL-13 seems crucial [7,13]. The role of M2 macrophages is mainly connected with VEGF, platelet derived growth factor (PDGF), fibroblast growth factor (FGF), and TGF- β production, as well as with matrix metalloproteinases (MMPs) secretion, all resulting in the increased migration and invasiveness of tumor cells. Moreover, by the secretion of CCL17, CCL22, and CCL24 by M2 TAMs, some other immune cells are attracted, such as Th2 lymphocytes, regulatory T cells, or basophiles, leading to the tumor tolerance [8]. As M2 TAMs were found to be connected with a worse prognosis in breast [14], gastric [15], rectal [16], and pancreatic carcinomas [17] as well as in HNSCC [18], the research is now focused on M2 TAMs detection and characterization in different tumor specimens. For TAMs detection, the pan-macrophage CD68 marker is used, but for characterization of the phenotype, additional markers are needed, e.g., CD80, CD11c, inducible nitric oxide synthase 2 (NOS2), or human leukocyte antigen-DR isotype (HLA-DR) for M1 and CD163, CD204, CD206, or arginase 1 (ARG1) for M2 [19–21]. The M1/M2 TAMs stratification also reflects the difference in the metabolism of the amino acid arginine, which has a huge impact on TAMs function in the TME. M1 TAMs predominantly metabolize L-arginine by NOS2 resulting in NO increase in the tissue and inhibition of proliferation, while M2 TAMs utilize arginine mainly via ARG1 to generate urea and ornithine. The ARG1 pathway potentiates proliferation and tissue repair and supports the tumor growth [22]. Because both metabolic pathways utilize the same substrate, the activity of one pathway is cross-inhibited by the other one [21].

The indoleamine-2,3-dioxygenase 1 (IDO1) can serve as another marker of the M2 phenotype [23]. IDO1 is an immunoregulatory enzyme degrading tryptophan to kynurenine, resulting in the local immunosuppressive environment and neovascularization. Continual expression of IDO1 is enabled by prostaglandin-endoperoxide synthase 2 (PTGS2; also known as cyclooxygenase-2, COX-2) [24], which is crucial for M2 TAMs polarization maintenance [25]. Increased IDO1 expression correlates with poor prognosis in patients with colorectal [26], breast [25], endometrial [27], and ovarian carcinomas [28]. Higher PTGS2 expression has been associated with worse prognosis in many cancers including HNSCC [29,30].

In this study, we analyzed the levels and distribution of M1 and M2 subpopulations of TAMs in different compartments of head and neck tumors of different etiology using multispectral fluorescent immunohistochemistry (fIHC). We also examined, in the corresponding samples of tumors, the mRNA levels of the selected TAMs markers IDO1, NOS2, PTGS2, CD163, and ARG1 by reverse transcription followed by quantitative polymerase chain reaction (RT-qPCR). Regardless of the tumor etiology, the stroma was always more infiltrated by macrophages of both phenotypes M1 and M2 than the tumor parenchyma. In comparison to HPV+ tumors, the stroma of HPV negative (HPV−) HNSCC was more infiltrated by the M2 TAMs. In these tumors, RNA expression of the M2 TAMs markers was also higher. An increased level of ARG1 mRNA and higher tumor stage were found as negative prognostic factors of patients with HNSCC.

2. Materials and Methods

2.1. Sample Collection, Processing, and Characterization

We analyzed 73 samples of primary HNSCC located in the oral cavity and oropharynx (ICD10: C01, C06, C09, C10). Samples were obtained within the study conducted in our laboratory in cooperation with the Department of Otorhinolaryngology and Head and Neck Surgery, First Faculty of Medicine, Charles University, and Motol University Hospital, Prague. All patients signed an informed consent and completed a questionnaire related to risk factors for HPV infection and HNSCC induction. The study was approved by the Ethical Committee of the Motol University Hospital. All samples were processed and checked by a pathologist immediately after surgery. Samples were classified using the TNM nomenclature (8th edition), and the Charlson comorbidity index was calculated (<https://www.mdcalc.com/charlson-comorbidity-index-cci>, accessed on 5 March 2021). One part of the tumor was fixed in 10% neutral formalin and embedded in paraffin (FFPE), and the other part was transported to the laboratory in RPMI medium (Sigma-Aldrich, St. Luis, MO, USA) at 4 °C. Tumor single cell suspension was isolated instantly as described previously [31] and was stored in RNAlater[®] Stabilization Solution (Life Technologies, Carlsbad, CA, USA) at −80 °C until processing. DNA and total RNA were isolated using the NucleoSpin RNA/DNA buffer set (Macherey-Nagel, Düren, Germany) according to the manufacturer's instructions. The concentration of DNA and total RNA was measured by a NanoDrop 2000 Spectrophotometer (Thermo Fisher Scientific, Waltham, MA, USA), and the quality of RNA was checked by the Experion[™] Automated Electrophoresis System (Bio-Rad, Hercules, CA, USA), both according to the manufacturer's protocols. Until analysis, DNA was stored at −20 °C and RNA at −80 °C. The presence and type of HPV in samples was evaluated by PCR with broad spectrum GP5+/6+-5' bio primers followed by reverse line blot analysis as specified before [32]. The active viral infection was determined by HPV E6 mRNA detection as described previously [33,34]. For one sample, DNA was not available, but the RNA analysis revealed the presence of HPV16 E6 mRNA.

2.2. Gene Expression Analysis

For relative quantification of the expression of selected TAMs markers (IDO1, PTGS2, NOS2, ARG1, and CD163), we performed RT-qPCR. Firstly, total RNA was treated by DNase and then reverse transcribed using M-MLV Reverse Transcriptase (both Promega, Madison, WI, USA), according to the manufacturer's instructions. The qPCR reactions were performed in 10 µL volume of the reaction mixture in duplicates using Xceed qPCR SG 2x Mix Lo-ROX (IAB, Prague, Czech Republic), 0.4 µM primers, and 2 µL of 4 × diluted cDNA on a CFX96[™] Real-Time System instrument (Bio-Rad, Hercules, CA, USA). The reaction conditions were as follows: 3 min at 95 °C followed by 40 cycles of 10 s at 95 °C and 30 s at 60 °C. All reactions were followed by a melting curve analysis. The *β-glucuronidase* (*GUS*) and *actin beta* (*ACTB*) genes were used as the reference genes for normalization. The sequences of primers are listed in Table 1. The obtained amplification plots were analyzed by Bio-Rad CFX Maestro (Bio-Rad, Hercules, CA, USA). The relative quantification was

done by the GenEx™ v.6 software (MultiD Analyses AB, Gothenburg, Sweden) using the $\Delta\Delta C_t$ method.

Table 1. Sequences of primers with expected product lengths.

Gene		Sequence 5'–3'	Length [bp]
IDO1	F	AAGAACTGGAAGTGCCTCCT	121
	R	CACGAAATGAGAACAAAACGTCC	
ARG1	F	GGCAGAAGTCAAGAAGAACGGA	127
	R	GTGAGCATCCACCCAGATGA	
CD163	F	GCAATGGGGTGGACTTACCT	120
	R	TGCTTCACTCAACACGTCC	
NOS2	F	GCTGTGCTCCATAGTTTCCAG	137
	R	GGGACCAGCCAAATCCAGTC	
PTGS2	F	GCATTCTTTGCCAGCACTT	142
	R	GGCGCAGTTTACGCTGTCT	
GUS	F	GAAAATATGTGGTTGGAGAGCTCAIT	101
	R	CCGAGTGAAGATCCCCTTTTAA	
ACTB	F	CCACGAAACTACCTTCAACTCCA	132
	R	GTGATCTCCTTCTGCATCCTGTC	

F—forward; R—reverse; bp—base pairs.

2.3. Tissue Slides Preparation and IHC Validation

From FFPE tumors, 2 μ m sections were prepared on StarFrost Advanced Adhesive microscope slides (Knittel-Glass, Braunschweig, Germany). In the first and the last sections from paraffin blocks, the pathologist confirmed the tumor presence. Sections were stored at 4 °C and processed within three weeks from preparation. Slides were deparaffinized at 60 °C for two hours, brightened in xylene three times for 10 min, hydrated by alcohols of descending grades (all from Penta, Prague, Czech Republic), and fixed in 10% neutral buffered formalin (Diapath, Martinengo, Italy) for 20 min. Antigen retrieval (AR) was performed using microwave in AR9 Tris-EDTA buffer, pH 9.0 (Zytomed Systems, Berlin, Germany) or AR6 citrate buffer, pH 6.0 (Akoya Biosciences, Menlo Park, CA, USA) depending on the antibody used. Prior to a primary antibody incubation, the tissue was demarcated with an Elite Pap pen (Diagnostic BioSystems, Pleasanton, CA, USA) and blocked using Antibody Diluent/Block (Akoya Biosciences, Menlo Park, CA, USA) for 10 min at room temperature (RT). Primary antibodies against CD68 (clone KP1; Santa Cruz Biotechnology, Dallas, TX, USA), CD80 (62N3G8; Novus Biological, Centennial, CO, USA), CD163 (10D6; Thermo Fisher Scientific, Waltham, MA, USA), arginase 1 (A-2; Santa Cruz Biotechnology, Dallas, TX, USA), and Cytokeratin Pan Type I/II (AE1/AE3; Thermo Fisher Scientific, Waltham, MA, USA) were diluted in Antibody Diluent/Block (Akoya Biosciences, Menlo Park, CA, USA) and stained separately. Primary antibody incubation was followed by 10 min of staining with Opal Polymer HRP Ms+Rb, TSA-based Opal™ fluorophores, and DAPI counterstain, all from the Opal 7-Color Manual IHC Kit (Akoya Biosciences, Menlo Park, CA, USA). The stained tissue sections were mounted with Fluoromount™ Aqueous Mounting Medium (Sigma-Aldrich, St. Louis, MO, USA). Slides were imaged with a magnification of 20 \times 10 using the Mantra Snap 2.0.0 software, and pictures were analyzed in the InForm 2.4.6 software (both Akoya Biosciences, Menlo Park, CA, USA). The reliability of the staining was confirmed by no primary and isotype controls, where the primary antibody was substituted with Antibody Diluent/Block or an appropriate isotype antibody, respectively.

2.4. Multiplex IHC Staining

After monoplex staining validation, a panel for multiplexed staining was designed. The order of the stained antibodies was determined according to the epitope stability after

multiple stripping rounds. Fluorophores have been assigned to antibodies to minimize spectral overlapping. Subsequent titration of antibodies and fluorophores was performed to obtain reliable staining with a fluorophore signal between 5 and 20 and a signal/noise ratio of >10. The order of antibody staining, reagent dilutions, and reaction conditions are listed in Table 2. For all antibodies in the panel, a stripping quality control was performed.

Table 2. Design of the panel for multiplex fluorescent immunohistochemistry (fIHC) staining.

#	AR	Antibody	Dilution	Incubation	Secondary	OPAL	Dilution
1	6	CD68	1:200	1 h/RT	Ms + Rb	540	1:200
2	6	CD163	1:100	OVN/4 °C	Opal	620	1:100
3	9	ARG1	1:200	1 h/RT	HRP	650	1:200
4	9	CD80	1:50	OVN/4 °C	polymer	520	1:50
5	6	Cytokeratin	1:800	1 h/RT		690	1:200
6	6	DAPI	1:15	5 min/RT	–	–	–

AR—antigen retrieval buffer; RT—room temperature; OVN—overnight.

2.5. Multiplex fIHC Data Analysis

From each tumor sample, five regions of interest (ROI) were randomly selected across the tumor parenchyma and stromal area, and snapped using the Mantra Snap 1.0.3 software (Akoya Biosciences, Menlo Park, CA, USA), with a magnification of 20×10 . Pictures were analyzed in batches using the InForm 2.4.6. software (Akoya Biosciences, Menlo Park, CA, USA) with the prepared algorithm. This algorithm consists of linear unmixing using the prepared spectral libraries and trainable steps of tissue segmentation, cell segmentation, and cell phenotyping. For tissue segmentation training, we marked the cytokeratin positive area as the tumor parenchyma, the cytokeratin-free area as the stroma, and the empty (DAPI-free) area as the background. Each step was optimized in different tumor pictures from the set of samples and then applied to the analyses of additional samples in the batches. We introduced six different cell phenotypes: M1 macrophages (M1; CD68+CD80+), M2 macrophages (M2; CD68+CD163+), M2 macrophages producing ARG1 (M2-ARG; CD68+ARG+), cells exclusive of macrophages producing ARG1 (ARG; ARG+), CD80+ only cells (CD80; CD80+), and the remaining cells negative for any macrophage marker (other). For the further analysis, the phenotypes “other” and “CD80” were not included as they serve only for phenotyping algorithm setting. For the final analysis, cells with the confidence of phenotyping higher than 75% were counted. According to our observation, this level was suitable for reliable phenotyping. For all the samples, the percentages of unsatisfactory cells ranged between 5% and 15%. The numbers of positive cells in the compartments were then calculated per megapixel (Mpx).

2.6. Statistical Analysis

All patients were grouped according to the HPV E6 mRNA positivity into HPV+ and HPV− groups. The levels of M1, M2, M2−ARG, and ARG phenotypes were expressed as cells per Mpx and were evaluated separately for the tumor parenchyma and stroma compartments in both sample groups. The differences in cell numbers/Mpx between groups were evaluated using the Mann–Whitney U test, and the differences between the tumor parenchyma and stroma parts in the corresponding patients were analyzed using the sign test. For RT-qPCR data analyses, the unpaired *T*-test was used to see the differences between groups, and the paired *T* test was performed for the comparison between compartments. To analyze the possible correlation between mRNA expression levels, the Pearson correlation coefficient was applied. The Cox proportional hazards model was used for the overall specific survival (OS) analysis. The Akaike information criterion (AIC) was used for model selection. The following demographic and clinical pathological factors were included: gender, age, education (≤ 12 years, > 12 years), smoking (nonsmoker, ex-smoker, smoker), alcohol use (nondrinker, ex-drinker, drinker), location (oropharyngeal, oral), tumor extension (pT1-4), nodal status (pN0-3), tumor stage (S I, II,

III, IV), metastasis (M 0, 1), extracapsular spreading (0, 1), Charlson comorbidity index, and HPV status (HPV E6 mRNA negative, HPV16 E6 mRNA positive). In addition to these factors, qPCR factors (mRNA expression of *IDO1*, *NOS2*, *PTGS2*, *CD163*, and *ARG1*) and IHC factors (M1, M2, M2-ARG, and ARG cells/Mpx in both the tumor parenchyma and stroma) were tested. Tumor extension, nodal status, tumor stage, and histological grading were numeric measures. As an addition to the Cox model, plots for Kaplan–Meier estimator were created.

A *p* value of < 0.05 was considered as a significant difference. All statistical analyses were performed using the GraphPad Prism 8.4.2 software (GraphPad Software, San Diego, CA, USA) and R version 4.0.2 (<https://www.R-project.org/>, accessed on 5 March 2021) [35].

3. Results

3.1. Patients Characterization

For this study, a total of 73 patient samples of primary HNSCC were collected and characterized. The median follow-up period was 18.5 months. HPV DNA was found in 46/72 (64%) samples. Of 46 HPV DNA positive samples, 44 (96%) were HPV16 DNA positive, one (2%) sample was positive for HPV16 and HPV53, and one (2%) sample was positive for HPV35 DNA. We divided the samples according to the presence of viral E6 mRNA, a marker of active viral infection, into HPV+ (38/73, 52%) and HPV– (35/73, 48%). In 10 cases of 35 HPV– tumors (29%), only HPV DNA and no E6 mRNA was detected pointing to non-active viral infection. All 38 HPV+ tumors were located in the oropharynx, unlike the HPV– tumors, with the majority of samples (23/35, 66%) obtained from the oral cavity and the remaining samples (12/35, 34%) from the oropharynx. The age of patients ranged from 41 to 83 years, with a median of 60 years for HPV+ patients and of 62.5 for HPV– cases. Consistently with previous observations [33,36], the tumors were mostly collected from men (57/73, 78%). Detailed patient and tumor characteristics are listed in Table 3.

Table 3. Demographic and clinical characterization of the cohort.

Characteristics		Total No. (%)	HPV+ No. (%)	HPV– No. (%)
No. of patients		73 (100%)	38 (52%)	35 (48%)
Age (years)	Mean age	61.86	61.66	62.14
	Median age	61.50	60.00	62.50
Gender	female	16 (22%)	3 (8%)	13 (37%)
	male	57 (78%)	35 (92%)	22 (63%)
Localization	oropharynx	50 (68%)	38 (100%)	12 (34%)
	oral cavity	23 (32%)	0 (0%)	23 (66%)
Education	>12 years	31 (50%)	19 (54%)	12 (44%)
	≤12 years	31 (50%)	16 (46%)	15 (56%)
Smoking	never	24 (33%)	19 (50%)	5 (14%)
	past	23 (31%)	12 (32%)	11 (32%)
	current	26 (36%)	7 (18%)	19 (54%)
Alcohol consumption	never	20 (27%)	14 (37%)	6 (17%)
	past	11 (15%)	2 (5%)	9 (26%)
	current	42 (58%)	22 (58%)	20 (57%)
Tumor extension (pT)	T1	17 (23%)	7 (18%)	10 (29%)
	T2	48 (66%)	29 (76%)	19 (54%)
	T3	4 (5.5%)	1 (3%)	3 (8.5%)
	T4	4 (5.5%)	1 (3%)	3 (8.5%)

Table 3. Cont.

Characteristics		Total No. (%)	HPV+ No. (%)	HPV– No. (%)
No. of patients		73 (100%)	38 (52%)	35 (48%)
Nodal status (pN)	N0	30 (41%)	10 (29%)	20 (57%)
	N1	32 (44%)	26 (68%)	6 (17%)
	N2	5 (7%)	1 (1.5%)	4 (12%)
	N3	6 (8%)	1 (1.5%)	5 (14%)
Metastasis presence (M)	0	69 (95%)	38 (100%)	31(89%)
	1	4 (5%)	0 (0%)	4 (11%)
Tumor stage (S)	I	40 (55%)	32 (84%)	8 (23%)
	II	12 (16%)	3 (8%)	9 (26%)
	III	6 (8%)	2 (5%)	4 (11%)
	IV	15 (21%)	1 (3%)	14 (40%)
Extracapsular spreading	0	57 (78%)	28 (74%)	29 (83%)
	1	16 (22%)	10 (26%)	6 (17%)
Charlson comorbidity index	0	2 (3%)	2 (5%)	0 (0%)
	1	19 (26%)	13 (34%)	6 (17%)
	2	16 (22%)	7 (18.5%)	9 (26%)
	3	16 (22%)	7 (18.5%)	9 (26%)
	4	10 (13%)	6 (16%)	4 (11%)
	5	5 (7%)	1 (3%)	4 (11%)
	6	2 (3%)	0 (0%)	2 (6%)
7	3 (4%)	2 (5%)	1 (3%)	

3.2. Expression of M2 TAM Markers Is Higher in HPV– Tumors

We examined the mRNA level of TAMs associated genes—*ARG1*, *CD163*, *NOS2*, *IDO1*, and *PTGS2*—in HPV+ and HPV– tumors. For this purpose, we performed RT-qPCR analysis with relative quantification by the $\Delta\Delta C_t$ approach using *GUS* and *ACTB* as the reference genes in 69 samples (38 HPV+ and 31 HPV–). Remaining four samples of the cohort were excluded due to insufficient RNA quality. We detected significantly higher levels of *CD163* ($p = 0.0035$), *ARG1* ($p = 0.0009$), and *PTGS2* ($p = 0.0402$) mRNA in HPV– tumors (Figure 1). These genes are considered as M2 associated markers. Next, *NOS2* mRNA, the M1 marker, was detected in higher level in HPV+ tumors ($p = 0.0103$). On the contrary, we did not observe any differences in the *IDO1* mRNA level between HPV+ and HPV– tumors.

These results show higher expression of the M2 markers *ARG1*, *CD163* together with *PTGS2*, which directly supports the M2 TAMs polarization and maintenance, in HPV– patients. To analyze the relationships among TAMs markers, we performed correlation analysis of mRNA levels by computing the Pearson correlation coefficient. As demonstrated in Figure 2, we observed a positive association between *CD163* and *ARG1* mRNA ($r = 0.3179$, $p = 0.0078$) and *ARG1* and *PTGS2* mRNA ($r = 0.251$, $p = 0.0375$). We also detected weak inverse correlation between *ARG1* and *NOS2* mRNA ($r = -0.2824$, $p = 0.0187$) which suggests an exclusive activity of *ARG1* and *NOS2* enzymes in M2 and M1 TAMs, respectively. Next, we observed weak association between *IDO1* and *NOS2* mRNA ($r = 0.253$, $p = 0.0359$), which points to a co-expression of these enzymes in inflammatory conditions [23].

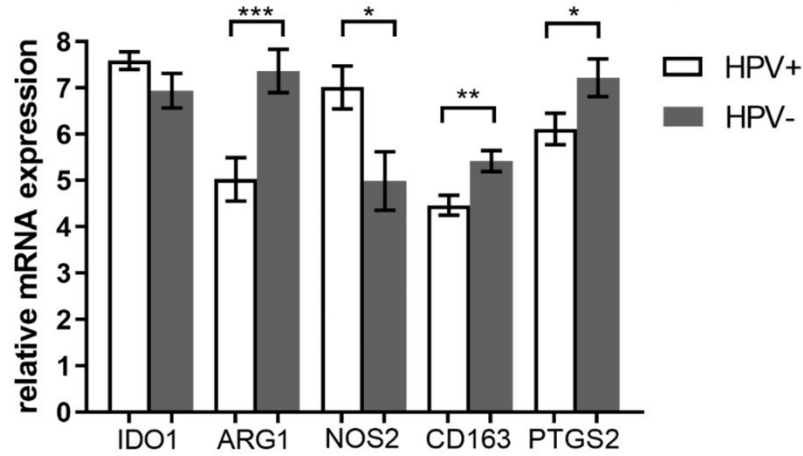


Figure 1. Comparison of gene expression in HPV+ and HPV– tumors. Relative mRNA expression of M1 and M2 tumor associated macrophage (TAM)-associated markers were compared in tumors with different etiology. Measured mRNA levels were normalized to *GUS* and *ACTB* reference genes using $\Delta\Delta C_t$ approach. Significantly higher arginase 1 (ARG1), CD163, and prostaglandin-endoperoxide synthase 2 (PTGS2) mRNA levels were detected in the HPV– cohort (** $p = 0.0009$ for ARG1, ** $p = 0.0035$ for CD163, and * $p = 0.0402$ for PTGS2 by unpaired *t*-test) and higher nitric oxide synthase 2 (NOS2) mRNA level was detected in the HPV+ cohort (* $p = 0.0103$ by unpaired *t*-test). Error bars—standard error of the mean.

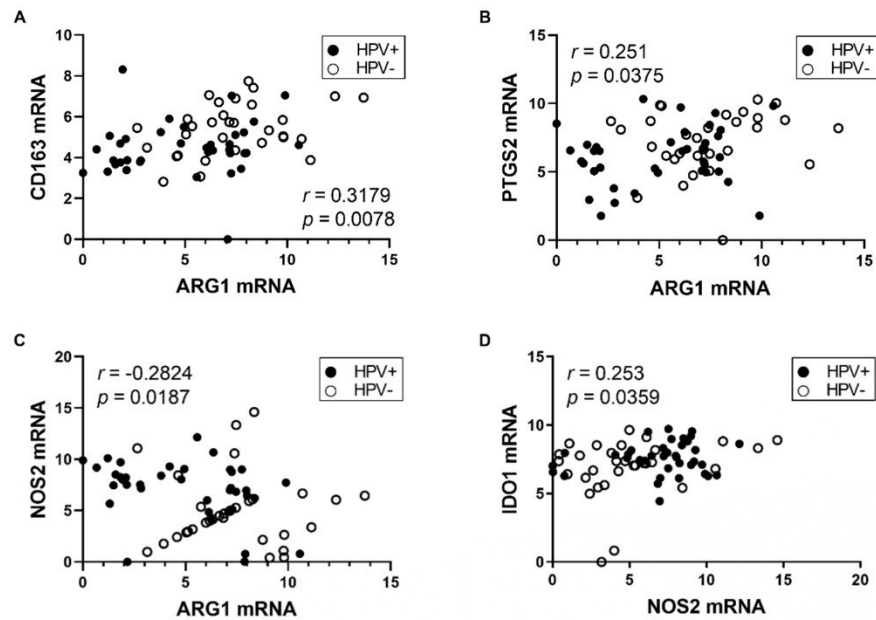


Figure 2. Correlation of relative gene expressions. Pearson correlation coefficient was measured between (A) ARG1 and CD163, (B) ARG1 and PTGS2, (C) ARG1 and NOS2, and (D) NOS2 and IDO1 relative mRNA levels.

3.3. The Stroma of HNSCC Is More Infiltrated by TAMs Than the Tumor Parenchyma

We introduced a panel of six antibodies, which can detect and quantify M1 and M2 macrophages in the tumor parenchyma and surrounding stroma (Figure S1 Supplementary Materials). A total of 73 tumor specimens were stained using multiplex fiHC and analyzed

by an algorithm for cell and tissue segmentation and cell phenotyping. This analysis revealed that the stroma was more infiltrated by TAMs of both phenotypes, M1 and M2, than the tumor parenchyma in both HPV+ and HPV− patients (Table 4).

Table 4. TAMs and arginase (ARG) phenotype infiltration in tumor parenchyma and stroma expressed by median values of cells/Mpx.

Phenotype	HPV+			HPV−			All Patients		
	Parenchyma	Stroma	<i>p</i>	Parenchyma	Stroma	<i>p</i>	Parenchyma	Stroma	<i>p</i>
M1	1.635	29.68	<0.0001	4.693	22.3	0.0001	2.361	26.9	<0.0001
M2	0.982	17.6	<0.0001	0.472	11.87	<0.0001	0.789	12.8	<0.0001
M2-ARG	0	0	0.0347	0.255	2.442	<0.0001	0.203	1.007	<0.0001
ARG	1.462	6.314	<0.0001	15.1	51.12	<0.0001	4.023	18.13	<0.0001

3.4. The Numbers of Arginase 1 Positive Cells Are Higher in Both Tumor Parenchyma and Stroma of HPV− Patients

We detected more arginase 1 producing M2 TAMs (M2-ARG) in the stroma of HPV− patients (Figure 3A; $p = 0.003$) while the level of M2-ARG in the tumor parenchyma was comparable in both groups ($p = 0.0843$). The levels of the second M2 population (CD68+CD163+) were similar in both groups ($p = 0.1869$ for tumor parenchyma and $p = 0.7626$ for stroma). Similar levels of M1 macrophages were also found ($p = 0.5309$ and $p = 0.6884$, respectively). Next, we observed significantly higher infiltration by cells expressing only ARG1 both in the tumor parenchyma and stroma of HPV− patients (Figure 3B, $p = 0.0092$ and $p = 0.0002$, respectively). According to phenotype assignment, these cells are not considered TAMs, but other ARG1 expressing cells, such as neutrophils or myeloid-derived suppressor cells (MDSCs). Representative staining of M2 and M2-ARG cells is shown in Figure S2.

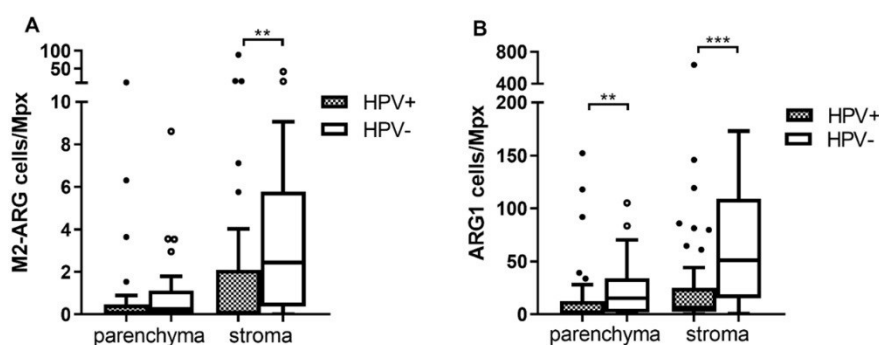


Figure 3. Multispectral fIHC analysis. Numbers of analyzed cells/Mpx in tumor parenchyma and stroma were compared between HPV+ and HPV− tumors using Mann–Whitney U test. (A) Number of M2 macrophages expressing ARG1 (M2-ARG)/Mpx was higher in stroma of HPV− patients (** $p = 0.003$), in contrast to tumor parenchyma where the difference was not significant; (B) higher number of ARG1 cells/Mpx was observed in the HPV− patients both in tumor parenchyma (** $p = 0.0092$) and stroma (** $p = 0.0002$).

3.5. ARG1 Expression Level, HPV Status, and Tumor Stage Are Factors Influencing OS

Cox proportional hazards models were used for the OS analysis. In the univariate model, HPV positivity was observed as a strong predictor of survival (HR = 0.050, $p = 0.0045$). The best model selected by the Akaike information criterion (AIC) contained three predictors, HPV status, tumor stage, and ARG1 mRNA level. According to the results, OS of patients was negatively influenced by higher ARG1 mRNA level (HR = 1.4872, $p = 0.0034$) and increasing tumor stage (HR = 1.9602, $p = 0.0246$). In this model, HPV status

was not significantly associated with the OS (HR = 0.2227, $p = 0.2116$). We observed that the majority of HPV+ patients have a lower tumor stage ($p < 0.0001$ by Fisher test) and lower ARG1 mRNA level compared to HPV− patients ($p = 0.0009$, Figure 1). Additionally, a higher ARG1 mRNA level and tumor stage (S = 4) in the HPV− cohort suggested a high risk for these patients (Figure 4). As an addition to the Cox model, Kaplan–Meier estimator plots for HPV status, tumor stage, and ARG1 mRNA level were created (Figure S3).

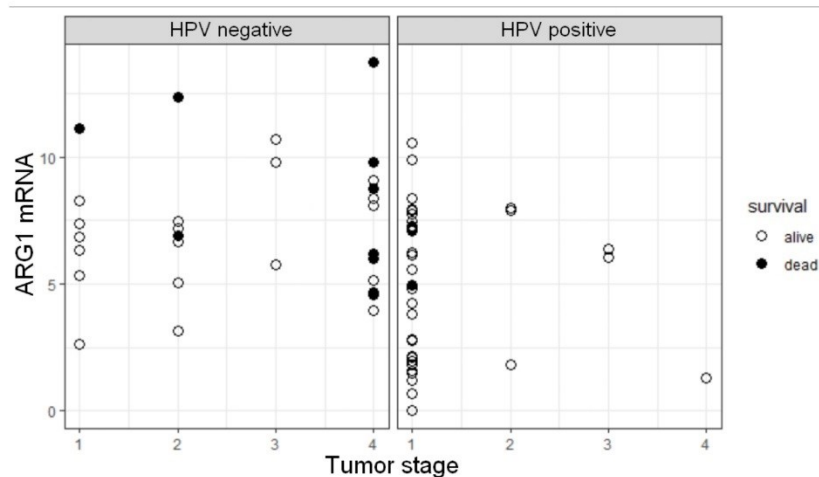


Figure 4. Relationships between ARG1 mRNA expression, tumor pathological stage, and HPV status as the predictors of overall survival. Each point reflects separate observation of a given predictor value.

These results confirm the HPV status as the predictor of survival in a univariate analysis. In the Cox model including additionally ARG1 mRNA level and tumor stage, the effect of HPV positivity to OS was not significant most likely due to the correlation of higher tumor stage and HPV negativity.

4. Discussion

In this study, we detected ARG1 expression and higher pathological stage of the tumor as a negative prognostic factor for overall survival in patients with head and neck tumors. In HPV− tumors, higher expression of markers of the pro-tumorigenic M2 macrophages ARG1, CD163, and PTGS2 was detected. These results were supported by the detection of higher levels of M2 TAMs by multispectral fIHC. Using the fIHC method, higher numbers of stromal M2 macrophages evidenced by the presence of ARG1 protein were detected in the HPV− cohort. Furthermore, in both parenchyma and stroma of tumors from the HPV− patients, we have also detected higher numbers of non-macrophage populations (ARG phenotype), represented predominantly by MDSCs or neutrophils [37–40].

The detection and detailed phenotyping of cells in the TME is enabled by the introduction of advanced multiplex immunohistochemical methods. Multispectral immunohistochemistry is a powerful tool, which allows for analyzes of immune cells in situ with respect to the localization in different tumor compartments. The stratification into the tumor parenchyma and surrounding stroma helps to understand the relationships among cells in the TME and reveals the possible influence of the type and number of immune cells in different compartments on patients' prognosis. Such approach is a basis for defining the immunoscore. This indicator, which is already routinely used for the estimation of recurrence risk in colon cancer patients, is independent of the TNM staging [41]. For HNSCC, the tumor classification using the TNM methodology is predictive of clinical outcomes. It has recently been modified for the oropharyngeal tumors by introducing an indirect marker for HPV status, overexpression of the p16 protein, which identifies active

HPV infection [3,42]. It has been shown—by us and others—that tumor etiology is an important predictor of clinical outcome in HNSCC patients [32,33,43]. In this study, we confirmed the HPV status as the strongest marker of better prognosis of these patients. However, the better prognosis of patients with HNSCC of viral etiology is still a matter of intensive research, and there is evidence that the response of the immune system varies with the etiology of tumors [44,45]. Therefore, a more accurate prediction of the prognosis and treatment response can be achieved by introducing the immunoscore into the staging system. Numerous reports analyzed types and numbers of immune cells in HNSCC tumors, but there were important differences in the methodological approaches [44–47].

In our study, we focused on the detection and characterization of TAMs as the main immune population of TME. The influence of TAMs on the prognosis or disease progression has previously been described in HNSCC with controversial conclusions [45–49]. In those studies, macrophages were only detected based on the CD68 marker, which does not allow for their detailed phenotyping and evaluation of different roles in TME. Moreover, most studies did not address the HPV status. In our study, additional markers were used for a better stratification of macrophage phenotypes and were correlated with HPV status. We showed that the stroma in HNSCC was more infiltrated by both M1 and M2 (M2 and M2-ARG) macrophages than the tumor parenchyma, regardless of HPV status. In the HPV– cohort, higher abundance of M2 macrophages producing ARG1 (M2-ARG) was detected in the stroma compared to the HPV+ patients. In contrast, the M1 and M2-CD163+ populations were equally present in HPV+ and HPV– tumors in both compartments. A similar study of Ou et al. only used the CD163 marker for the identification of M2 TAMs. Based on the CD68+ M1 to CD68+CD163+ M2 ratio, they showed higher abundance of CD68+CD163+ M2 TAMs in the stroma of HPV– HNSCC [50].

The localization of TAMs in the TME is crucial. In breast carcinoma, higher infiltration of CD163+ macrophages in the stroma correlated with worse OS [14], but higher CD163+ TAMs infiltration in tumor invasive front was correlated to an improved prognosis of colorectal carcinoma patients [51]. In a recent study using the multispectral immunohistochemistry approach, the stroma of colorectal carcinoma was predominantly infiltrated by M2 TAMs, but no effect on patients' survival was observed [52]. Similarly, using the fIHC method, higher infiltration with M2 macrophages (CD68+CD163+CD206+) in the stroma was found in gastric carcinoma, and, conversely, higher M1 populations were detected in a tumor-nest area [53]. Higher CD163+ TAMs infiltration in the stroma compared to the tumor parenchyma was also reported in esophageal carcinoma where it correlated with worse OS, but an impact of elevated CD163+ TAMs infiltration on tumor aggressiveness was observed in both compartments [54]. In HNSCC, higher infiltration with CD163+ macrophages in the stroma was related to worse survival of patients [18,55], but when the HPV status was included in the model, no prognostic effect of CD163+ cells on OS was evidenced. For progression-free survival (PFS), the presence of CD163+ cells in HPV– tumors was a negative prognostic factor [55]. The number of CD163+ TAMs increased with tumor grade in oral squamous cell carcinoma. Furthermore, in low-grade carcinomas, CD163+ TAMs were mainly located in the stroma, and the number of CD163+ TAMs in the tumor nest also increased with tumor grade [56].

Our fIHC data were further supplemented with mRNA analysis of TAM markers using RT-qPCR. In the HPV– cohort, higher expression levels of the M2 TAMs genes *ARG1*, *CD163*, and *PTGS2* were detected, while *NOS2* mRNA, the M1 marker, was more expressed in tumors of HPV+ patients. Taken together, these results suggest a higher prevalence of M2 TAMs in the TME of non-virally induced HNSCC. In the study by Ohashi et al., predominant abundance of M2 TAMs was detected in the HNSCC by qPCR measurement of CD68, CD163, and CSF1 receptor (CSF1R) mRNA, but the HPV status of tumors was not examined. They also observed higher mRNA level of TAM markers in HNSCC compared to the healthy pharyngeal tissue [57]. *PTGS2* is a well-characterized enzyme whose upregulation in HNSCC has already been described [30,44,58]. Higher expression of the *PTGS2* gene in HPV– tumors is in agreement with previously published data [44]. We further

observed the association between the expression levels of CD163 and ARG1 or ARG1 and PTGS2 markers of M2 TAMs. Moreover, we detected negative association between ARG1 and NOS2 mRNA, which points to an exclusivity of corresponding enzymes activities in M2 and M1 macrophages, respectively. It was described previously, that activities of ARG and NOS2 enzymes are cross-inhibited resulting in different arginase metabolism in M1 and M2 TAMs [21]. Furthermore, we observed weak association between IDO1 and NOS2 mRNA. Our results are in agreement with the recent study of Wang et al., who observed correlation of IDO1 and NOS2 mRNA in pancreatic carcinoma [59] and with the study of Soliman et al., who observed positive correlation of IDO1 and NOS2 on the protein level on breast cancer tissue sections [60]. It was described that IDO1 and NOS2 are co-expressed as a result of infection or inflammation in human tissues. Moreover, NOS2-mediated NO increase results in inhibition of IDO1 activity in human tissues [23], but Wang et al. proposed the opposite mechanism where increasing NO potentiates the IDO1 activity [59]. The IDO1 activity in tumorigenesis is a complex system, which needs further clarification.

Besides the TAMs analysis, we also detected the non-macrophage cells producing ARG1 in the TME using IHC. In addition to M2 TAMs, ARG1 is an accepted marker for MDSCs in gastric carcinoma [38], non-small cell lung carcinoma [39], and pancreatic adenocarcinoma [40] or a marker of neutrophils [61]. Here, we detected non-macrophage ARG1 expressing populations in higher numbers in both tumor parenchyma and stroma of HPV– tumors. ARG1 expression was described as a factor promoting tumor growth [22]. The increased amount of the ARG1 protein in TAM or non-macrophage populations of HPV– tumors was also reflected by an increase in ARG1 mRNA. In HPV– patients, higher level of ARG1 mRNA was detected by RT-qPCR. Interestingly, a higher ARG1 mRNA level was associated with worse OS of HNSCC patients in our study. To our knowledge, our results are the first to show the impact of ARG1 mRNA expression on the prognosis of HNSCC. Similar results were observed in patients with colorectal cancer, where a higher ARG1 mRNA level was associated with worse OS and disease-free survival (DFS) [62], or classic Hodgkin lymphoma, where an elevated level of ARG1 negatively influenced PFS [37]. The overexpression of ARG1 in HNSCC tissue and peripheral blood compared to healthy donors was described by Shrivastava et al. [63], but opposite results were shown by Ohashi et al. [57]. Both studies did not address tumor etiology or prognosis, which may explain the discrepancy of the results.

5. Conclusions

In this study, the levels and distribution of M1 and M2 TAMs were analyzed in the TME of HNSCC, and expression of TAM-associated markers was evaluated with respect to HPV status. Regardless of the tumor etiology, higher levels of both M1 and M2 TAMs were detected in the stroma. In HPV– tumors, the stroma was more infiltrated by M2 TAMs expressing ARG1 compared to HPV+ tumors. Moreover, expression of the M2 TAM-associated markers CD163, ARG1, and PTGS2, was higher in HPV– tumors. In HPV– patients, higher non-macrophage populations expressing ARG1 were detected in both compartments. A higher level of ARG1 mRNA was found to be a new negative prognostic factor for OS of patients with HNSCC.

Supplementary Materials: The following are available online at <https://www.mdpi.com/article/10.3390/diagnostics11040628/s1>, Figure S1: Detection of M1 and M2 macrophages, Figure S2: Cell phenotyping, Figure S3: Kaplan–Meier estimator plots, Table S1.

Author Contributions: Conceptualization, R.T. and M.Š.; methodology, B.P., J.Š.; software, N.D., B.P.; validation, B.P., J.Š.; formal analysis, N.D.; investigation, N.D.; resources, J.K., M.G.; data curation, O.V., J.N., J.Š., B.P.; writing—original draft preparation, B.P.; writing—review and editing, B.P., J.Š., M.Š., R.T.; visualization, N.D.; supervision, B.P., J.Š., R.T.; project administration, B.P., R.T.; funding acquisition, B.P., R.T. All authors have read and agreed to the published version of the manuscript.

Funding: This research was funded by the Charles University, grant numbers GAUK 1502118 and SVV 260568; the Czech Health Research Council, grant number 17-28055A; and the European Regional Development Fund and the Ministry of Education, Youth and Sports of the Czech Republic, grant numbers CZ.1.05/2.1.00/19.0400 and CZ.02.1.01/0.0/0.0/16_019/0000785.

Institutional Review Board Statement: The study was conducted according to the guidelines of the Declaration of Helsinki and approved by the Ethical Committee of the Motol University Hospital (June 22, 2016).

Informed Consent Statement: Informed consent was obtained from all subjects involved in the study.

Data Availability Statement: The data presented in this study are available in Table S1.

Acknowledgments: The authors thank Pavlína Veselá and Nela Václavíková for the excellent technical assistance and Adrianna Piataková for a critical reading of the manuscript.

Conflicts of Interest: The authors declare no conflict of interest. The funders had no role in the design of the study; in the collection, analyses, or interpretation of data; in the writing of the manuscript, or in the decision to publish the results.

References

- Bray, F.; Ferlay, J.; Soerjomataram, I.; Siegel, R.L.; Torre, L.A.; Jemal, A. Global cancer statistics 2018: GLOBOCAN estimates of incidence and mortality worldwide for 36 cancers in 185 countries. *CA Cancer J. Clin.* **2018**, *68*, 394–424. [\[CrossRef\]](#)
- Rettig, E.M.; D'Souza, G. Epidemiology of head and neck cancer. *Surg. Oncol. Clin. N. Am.* **2015**, *24*, 379–396. [\[CrossRef\]](#)
- Economopoulou, P.; Kotsantis, I.; Psyrri, A. Special Issue about Head and Neck Cancers: HPV Positive Cancers. *Int. J. Mol. Sci.* **2020**, *21*, 3388. [\[CrossRef\]](#)
- Ferris, R.L. Immunology and Immunotherapy of Head and Neck Cancer. *J. Clin. Oncol.* **2015**, *33*, 3293–3304. [\[CrossRef\]](#)
- Andersen, A.S.; Koldjaer Sølling, A.S.; Ovesen, T.; Rusan, M. The interplay between HPV and host immunity in head and neck squamous cell carcinoma. *Int. J. Cancer* **2014**, *134*, 2755–2763. [\[CrossRef\]](#) [\[PubMed\]](#)
- Balkwill, F.R.; Capasso, M.; Hagemann, T. The tumor microenvironment at a glance. *J. Cell Sci.* **2012**, *125*, 5591–5596. [\[CrossRef\]](#) [\[PubMed\]](#)
- Mantovani, A.; Sica, A.; Sozzani, S.; Allavena, P.; Vecchi, A.; Locati, M. The chemokine system in diverse forms of macrophage activation and polarization. *Trends Immunol.* **2004**, *25*, 677–686. [\[CrossRef\]](#) [\[PubMed\]](#)
- Galdiero, M.R.; Bonavita, E.; Barajon, I.; Garlanda, C.; Mantovani, A.; Jaillon, S. Tumor associated macrophages and neutrophils in cancer. *Immunobiology* **2013**, *218*, 1402–1410. [\[CrossRef\]](#) [\[PubMed\]](#)
- Mantovani, A.; Marchesi, F.; Malesci, A.; Laghi, L.; Allavena, P. Tumour-associated macrophages as treatment targets in oncology. *Nat. Rev. Clin. Oncol.* **2017**, *14*, 399–416. [\[CrossRef\]](#)
- Lewis, C.; Murdoch, C. Macrophage responses to hypoxia: Implications for tumor progression and anti-cancer therapies. *Am. J. Pathol.* **2005**, *167*, 627–635. [\[CrossRef\]](#)
- Henze, A.T.; Mazzone, M. The impact of hypoxia on tumor-associated macrophages. *J. Clin. Investig.* **2016**, *126*, 3672–3679. [\[CrossRef\]](#) [\[PubMed\]](#)
- Qian, B.Z.; Pollard, J.W. Macrophage diversity enhances tumor progression and metastasis. *Cell* **2010**, *141*, 39–51. [\[CrossRef\]](#)
- Chanmee, T.; Ontong, P.; Konno, K.; Itano, N. Tumor-associated macrophages as major players in the tumor microenvironment. *Cancers* **2014**, *6*, 1670–1690. [\[CrossRef\]](#) [\[PubMed\]](#)
- Medrek, C.; Pontén, F.; Jirström, K.; Leandersson, K. The presence of tumor associated macrophages in tumor stroma as a prognostic marker for breast cancer patients. *BMC Cancer* **2012**, *12*, 306. [\[CrossRef\]](#)
- Park, J.Y.; Sung, J.Y.; Lee, J.; Park, Y.K.; Kim, Y.W.; Kim, G.Y.; Won, K.Y.; Lim, S.J. Polarized CD163+ tumor-associated macrophages are associated with increased angiogenesis and CXCL12 expression in gastric cancer. *Clin. Res. Hepatol. Gastroenterol.* **2016**, *40*, 357–365. [\[CrossRef\]](#)
- Shabo, I.; Olsson, H.; Sun, X.F.; Svanvik, J. Expression of the macrophage antigen CD163 in rectal cancer cells is associated with early local recurrence and reduced survival time. *Int. J. Cancer* **2009**, *125*, 1826–1831. [\[CrossRef\]](#)
- Ino, Y.; Yamazaki-Itoh, R.; Shimada, K.; Iwasaki, M.; Kosuge, T.; Kanai, Y.; Hiraoka, N. Immune cell infiltration as an indicator of the immune microenvironment of pancreatic cancer. *Br. J. Cancer* **2013**, *108*, 914–923. [\[CrossRef\]](#) [\[PubMed\]](#)
- Troiano, G.; Caponio, V.C.A.; Adipietro, L.; Tepedino, M.; Santoro, R.; Laino, L.; Lo Russo, L.; Cirillo, N.; Lo Muzio, L. Prognostic significance of CD68(+) and CD163(+) tumor associated macrophages in head and neck squamous cell carcinoma: A systematic review and meta-analysis. *Oral Oncol.* **2019**, *93*, 66–75. [\[CrossRef\]](#) [\[PubMed\]](#)
- Heusinkveld, M.; van der Burg, S.H. Identification and manipulation of tumor associated macrophages in human cancers. *J. Transl. Med.* **2011**, *9*, 216. [\[CrossRef\]](#)
- Jayasingam, S.D.; Citartan, M.; Thang, T.H.; Mat Zin, A.A.; Ang, K.C.; Ch'ng, E.S. Evaluating the Polarization of Tumor-Associated Macrophages Into M1 and M2 Phenotypes in Human Cancer Tissue: Technicalities and Challenges in Routine Clinical Practice. *Front. Oncol.* **2019**, *9*, 1512. [\[CrossRef\]](#)

21. Rath, M.; Müller, I.; Kropf, P.; Closs, E.I.; Munder, M. Metabolism via Arginase or Nitric Oxide Synthase: Two Competing Arginine Pathways in Macrophages. *Front. Immunol.* **2014**, *5*, 532. [[CrossRef](#)]
22. Colegio, O.R.; Chu, N.Q.; Szabo, A.L.; Chu, T.; Rhebergen, A.M.; Jairam, V.; Cyrus, N.; Brokowski, C.E.; Eisenbarth, S.C.; Phillips, G.M.; et al. Functional polarization of tumour-associated macrophages by tumour-derived lactic acid. *Nature* **2014**, *513*, 559–563. [[CrossRef](#)]
23. Yeung, A.W.; Terentis, A.C.; King, N.J.; Thomas, S.R. Role of indoleamine 2,3-dioxygenase in health and disease. *Clin. Sci. (Lond.)* **2015**, *129*, 601–672. [[CrossRef](#)]
24. Hennequart, M.; Pilotte, L.; Cane, S.; Hoffmann, D.; Stroobant, V.; Plaen, E.; Eynde, B. Constitutive IDO1 Expression in Human Tumors Is Driven by Cyclooxygenase-2 and Mediates Intrinsic Immune Resistance. *Cancer Immunol. Res.* **2017**, *5*, 695–709. [[CrossRef](#)] [[PubMed](#)]
25. Li, H.; Yang, B.; Huang, J.; Lin, Y.; Xiang, T.; Wan, J.; Chouaib, S.; Ren, G. Cyclooxygenase-2 in tumor-associated macrophages promotes breast cancer cell survival by triggering a positive-feedback loop between macrophages and cancer cells. *Oncotarget* **2015**, *6*, 29637–29650. [[CrossRef](#)]
26. Chen, I.C.; Lee, K.H.; Hsu, Y.H.; Wang, W.R.; Chen, C.M.; Cheng, Y.W. Expression Pattern and Clinicopathological Relevance of the Indoleamine 2,3-Dioxygenase 1/Tryptophan 2,3-Dioxygenase Protein in Colorectal Cancer. *Dis. Markers* **2016**, *2016*, 8169724. [[CrossRef](#)] [[PubMed](#)]
27. Mei, J.; Li, M.Q.; Ding, D.; Li, D.J.; Jin, L.P.; Hu, W.G.; Zhu, X.Y. Indoleamine 2,3-dioxygenase-1 (IDO1) enhances survival and invasiveness of endometrial stromal cells via the activation of JNK signaling pathway. *Int. J. Clin. Exp. Pathol.* **2013**, *6*, 431–444. [[PubMed](#)]
28. Inaba, T.; Ino, K.; Kajiyama, H.; Yamamoto, E.; Shibata, K.; Nawa, A.; Nagasaka, T.; Akimoto, H.; Takikawa, O.; Kikkawa, F. Role of the immunosuppressive enzyme indoleamine 2,3-dioxygenase in the progression of ovarian carcinoma. *Gynecol. Oncol.* **2009**, *115*, 185–192. [[CrossRef](#)] [[PubMed](#)]
29. Wang, Z.M.; Liu, J.; Liu, H.B.; Ye, M.; Zhang, Y.F.; Yang, D.S. Abnormal COX2 protein expression may be correlated with poor prognosis in oral cancer: A meta-analysis. *BioMed Res. Int.* **2014**, *2014*, 364207. [[CrossRef](#)] [[PubMed](#)]
30. Frejborg, E.; Salo, T.; Salem, A. Role of Cyclooxygenase-2 in Head and Neck Tumorigenesis. *Int. J. Mol. Sci.* **2020**, *21*, 9246. [[CrossRef](#)] [[PubMed](#)]
31. Polakova, I.; Pelak, O.; Thurner, D.; Pokryvkova, B.; Tachezy, R.; Kalina, T.; Smahel, M. Implementation of Mass Cytometry for Immunoprofiling of Patients with Solid Tumors. *J. Immunol. Res.* **2019**, *2019*, 6705949. [[CrossRef](#)]
32. Koslabova, E.; Hamsikova, E.; Salakova, M.; Klozar, J.; Foltynova, E.; Salkova, E.; Rotnaglova, E.; Ludvikova, V.; Tachezy, R. Markers of HPV infection and survival in patients with head and neck tumors. *Int. J. Cancer* **2013**, *133*, 1832–1839. [[CrossRef](#)]
33. Rotnaglova, E.; Tachezy, R.; Salakova, M.; Procházka, B.; Košl'abová, E.; Veselá, E.; Ludviková, V.; Hamšíková, E.; Klozar, J. HPV involvement in tonsillar cancer: Prognostic significance and clinically relevant markers. *Int. J. Cancer* **2011**, *129*, 101–110. [[CrossRef](#)]
34. Gao, G.; Chernock, R.D.; Gay, H.A.; Thorstad, W.L.; Zhang, T.R.; Wang, H.; Ma, X.J.; Luo, Y.; Lewis, J.S., Jr.; Wang, X. A novel RT-PCR method for quantification of human papillomavirus transcripts in archived tissues and its application in oropharyngeal cancer prognosis. *Int. J. Cancer* **2013**, *132*, 882–890. [[CrossRef](#)]
35. R Core Team. *R: A Language and Environment for Statistical Computing*; R Foundation for Statistical Computing: Vienna, Austria, 2020.
36. Vojtechova, Z.; Sabol, I.; Salakova, M.; Turek, L.; Grega, M.; Smahelova, J.; Vencalek, O.; Lukesova, E.; Klozar, J.; Tachezy, R. Analysis of the integration of human papillomaviruses in head and neck tumours in relation to patients' prognosis. *Int. J. Cancer* **2016**, *138*, 386–395. [[CrossRef](#)]
37. Romano, A.; Parrinello, N.L.; Vetro, C.; Tibullo, D.; Giallongo, C.; La Cava, P.; Chiarenza, A.; Motta, G.; Caruso, A.L.; Villari, L.; et al. The prognostic value of the myeloid-mediated immunosuppression marker Arginase-1 in classic Hodgkin lymphoma. *Oncotarget* **2016**, *7*, 67333–67346. [[CrossRef](#)]
38. Ren, W.; Zhang, X.; Li, W.; Feng, Q.; Feng, H.; Tong, Y.; Rong, H.; Wang, W.; Zhang, D.; Zhang, Z.; et al. Circulating and tumor-infiltrating arginase 1-expressing cells in gastric adenocarcinoma patients were mainly immature and monocytic Myeloid-derived suppressor cells. *Sci. Rep.* **2020**, *10*, 8056. [[CrossRef](#)] [[PubMed](#)]
39. Heuvers, M.E.; Muskens, F.; Bezemer, K.; Lambers, M.; Dingemans, A.C.; Groen, H.J.M.; Smit, E.F.; Hoogsteden, H.C.; Hegmans, J.; Aerts, J. Arginase-1 mRNA expression correlates with myeloid-derived suppressor cell levels in peripheral blood of NSCLC patients. *Lung Cancer* **2013**, *81*, 468–474. [[CrossRef](#)] [[PubMed](#)]
40. Khaled, Y.S.; Ammori, B.J.; Elkord, E. Increased levels of granulocytic myeloid-derived suppressor cells in peripheral blood and tumour tissue of pancreatic cancer patients. *J. Immunol. Res.* **2014**, *2014*, 879897. [[CrossRef](#)]
41. Pagès, F.; Mlecnik, B.; Marliot, F.; Bindea, G.; Ou, F.S.; Bifulco, C.; Lugli, A.; Zlobec, I.; Rau, T.T.; Berger, M.D.; et al. International validation of the consensus Immunoscore for the classification of colon cancer: A prognostic and accuracy study. *Lancet* **2018**, *391*, 2128–2139. [[CrossRef](#)]
42. El-Naggar, A.K.; Westra, W.H. p16 expression as a surrogate marker for HPV-related oropharyngeal carcinoma: A guide for interpretative relevance and consistency. *Head Neck* **2012**, *34*, 459–461. [[CrossRef](#)] [[PubMed](#)]

43. Ang, K.K.; Harris, J.; Wheeler, R.; Weber, R.; Rosenthal, D.I.; Nguyen-Tan, P.F.; Westra, W.H.; Chung, C.H.; Jordan, R.C.; Lu, C.; et al. Human papillomavirus and survival of patients with oropharyngeal cancer. *N. Engl. J. Med.* **2010**, *363*, 24–35. [[CrossRef](#)] [[PubMed](#)]
44. Partlova, S.; Boucek, J.; Kloudova, K.; Lukesova, E.; Zabrodsky, M.; Grega, M.; Fucikova, J.; Truxova, I.; Tachezy, R.; Spisek, R.; et al. Distinct patterns of intratumoral immune cell infiltrates in patients with HPV-associated compared to non-virally induced head and neck squamous cell carcinoma. *Oncoimmunology* **2015**, *4*, e965570. [[CrossRef](#)]
45. Russell, S.; Angell, T.; Lechner, M.; Liebertz, D.; Correa, A.; Sinha, U.; Kokot, N.; Epstein, A. Immune cell infiltration patterns and survival in head and neck squamous cell carcinoma. *Head Neck Oncol.* **2013**, *5*, 24.
46. Fang, J.; Li, X.; Ma, D.; Liu, X.; Chen, Y.; Wang, Y.; Lui, V.W.Y.; Xia, J.; Cheng, B.; Wang, Z. Prognostic significance of tumor infiltrating immune cells in oral squamous cell carcinoma. *BMC Cancer* **2017**, *17*, 375. [[CrossRef](#)]
47. Oguejiofor, K.; Galletta-Williams, H.; Dovedi, S.J.; Roberts, D.L.; Stern, P.L.; West, C.M. Distinct patterns of infiltrating CD8+ T cells in HPV+ and CD68 macrophages in HPV- oropharyngeal squamous cell carcinomas are associated with better clinical outcome but PD-L1 expression is not prognostic. *Oncotarget* **2017**, *8*, 14416–14427. [[CrossRef](#)]
48. Seminerio, I.; Kindt, N.; Descamps, G.; Bellier, J.; Lechien, J.R.; Mat, Q.; Pottier, C.; Journé, F.; Saussez, S. High infiltration of CD68+ macrophages is associated with poor prognoses of head and neck squamous cell carcinoma patients and is influenced by human papillomavirus. *Oncotarget* **2018**, *9*, 11046–11059. [[CrossRef](#)]
49. Ni, Y.H.; Ding, L.; Huang, X.F.; Dong, Y.C.; Hu, Q.G.; Hou, Y.Y. Microlocalization of CD68+ tumor-associated macrophages in tumor stroma correlated with poor clinical outcomes in oral squamous cell carcinoma patients. *Tumour Biol.* **2015**, *36*, 5291–5298. [[CrossRef](#)]
50. Ou, D.; Adam, J.; Garberis, I.; Blanchard, P.; Nguyen, F.; Levy, A.; Casiraghi, O.; Gorphe, P.; Breuskin, I.; Janot, F.; et al. Influence of tumor-associated macrophages and HLA class I expression according to HPV status in head and neck cancer patients receiving chemo/bioradiotherapy. *Radiother. Oncol.* **2019**, *130*, 89–96. [[CrossRef](#)] [[PubMed](#)]
51. Edin, S.; Wikberg, M.L.; Dahlin, A.M.; Rutegård, J.; Öberg, Å.; Oldenborg, P.A.; Palmqvist, R. The distribution of macrophages with a M1 or M2 phenotype in relation to prognosis and the molecular characteristics of colorectal cancer. *PLoS ONE* **2012**, *7*, e47045. [[CrossRef](#)]
52. Krijgsman, D.; De Vries, N.L.; Andersen, M.N.; Skovbo, A.; Tollenaar, R.; Møller, H.J.; Hokland, M.; Kuppen, P.J.K. CD163 as a Biomarker in Colorectal Cancer: The Expression on Circulating Monocytes and Tumor-Associated Macrophages, and the Soluble Form in the Blood. *Int. J. Mol. Sci.* **2020**, *21*, 5925. [[CrossRef](#)]
53. Huang, Y.K.; Wang, M.; Sun, Y.; Di Costanzo, N.; Mitchell, C.; Achuthan, A.; Hamilton, J.A.; Busuttill, R.A.; Boussioutas, A. Macrophage spatial heterogeneity in gastric cancer defined by multiplex immunohistochemistry. *Nat. Commun.* **2019**, *10*, 3928. [[CrossRef](#)]
54. Hu, J.M.; Liu, K.; Liu, J.H.; Jiang, X.L.; Wang, X.L.; Chen, Y.Z.; Li, S.G.; Zou, H.; Pang, L.J.; Liu, C.X.; et al. CD163 as a marker of M2 macrophage, contribute to predict aggressiveness and prognosis of Kazakh esophageal squamous cell carcinoma. *Oncotarget* **2017**, *8*, 21526–21538. [[CrossRef](#)] [[PubMed](#)]
55. Balermipas, P.; Rödel, F.; Liberz, R.; Oppermann, J.; Wagenblast, J.; Ghanaati, S.; Harter, P.N.; Mittelbronn, M.; Weiss, C.; Rödel, C.; et al. Head and neck cancer relapse after chemoradiotherapy correlates with CD163+ macrophages in primary tumour and CD11b+ myeloid cells in recurrences. *Br. J. Cancer* **2014**, *111*, 1509–1518. [[CrossRef](#)]
56. Mori, K.; Hiroi, M.; Shimada, J.; Ohmori, Y. Infiltration of m2 tumor-associated macrophages in oral squamous cell carcinoma correlates with tumor malignancy. *Cancers* **2011**, *3*, 3726–3739. [[CrossRef](#)]
57. Ohashi, T.; Aoki, M.; Tomita, H.; Akazawa, T.; Sato, K.; Kuze, B.; Mizuta, K.; Hara, A.; Nagaoka, H.; Inoue, N.; et al. M2-like macrophage polarization in high lactic acid-producing head and neck cancer. *Cancer Sci.* **2017**, *108*, 1128–1134. [[CrossRef](#)]
58. Li, L.; Wang, X.L.; Lei, Q.; Sun, C.Z.; Xi, Y.; Chen, R.; He, Y.W. Comprehensive immunogenomic landscape analysis of prognosis-related genes in head and neck cancer. *Sci. Rep.* **2020**, *10*, 6395. [[CrossRef](#)] [[PubMed](#)]
59. Wang, L.; Tang, W.; Yang, S.; He, P.; Wang, J.; Gaedcke, J.; Ströbel, P.; Azizian, A.; Ried, T.; Gaida, M.M.; et al. NO(●)/RUNX3/kynurenine metabolic signaling enhances disease aggressiveness in pancreatic cancer. *Int. J. Cancer* **2020**, *146*, 3160–3169. [[CrossRef](#)] [[PubMed](#)]
60. Soliman, H.; Rawal, B.; Fulp, J.; Lee, J.H.; Lopez, A.; Bui, M.M.; Khalil, F.; Antonia, S.; Yfantis, H.G.; Lee, D.H.; et al. Analysis of indoleamine 2-3 dioxygenase (IDO1) expression in breast cancer tissue by immunohistochemistry. *Cancer Immunol. Immunother.* **2013**, *62*, 829–837. [[CrossRef](#)] [[PubMed](#)]
61. Hurt, B.; Schulick, R.; Edil, B.; El Kasm, K.C.; Barnett, C., Jr. Cancer-promoting mechanisms of tumor-associated neutrophils. *Am. J. Surg.* **2017**, *214*, 938–944. [[CrossRef](#)] [[PubMed](#)]
62. Ma, Z.; Lian, J.; Yang, M.; Wuyang, J.; Zhao, C.; Chen, W.; Liu, C.; Zhao, Q.; Lou, C.; Han, J.; et al. Overexpression of Arginase-1 is an indicator of poor prognosis in patients with colorectal cancer. *Pathol. Res. Pract.* **2019**, *215*, 152383. [[CrossRef](#)] [[PubMed](#)]
63. Srivastava, S.; Ghosh, S.K. Modulation of L-Arginine-Arginase Metabolic Pathway Enzymes: Immunocytochemistry and mRNA Expression in Peripheral Blood and Tissue Levels in Head and Neck Squamous Cell Carcinomas in North East India. *Asian Pac. J. Cancer Prev.* **2015**, *16*, 7031–7038. [[CrossRef](#)] [[PubMed](#)]

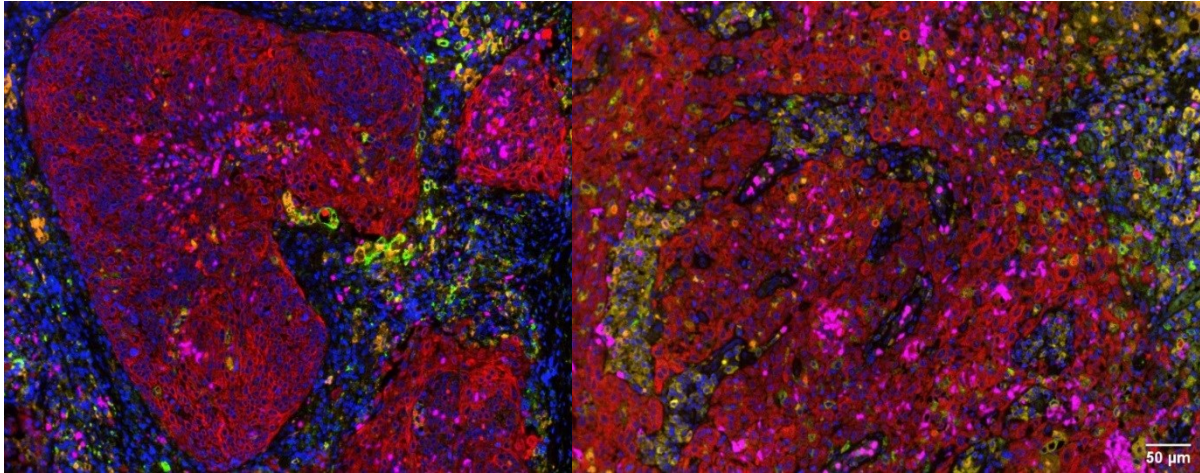


Figure S1: Detection of M1 and M2 macrophages in the tumor parenchyma and stroma using fIHC. Representative pictures of HPV+ (left) and HPV- (right) tumors stained with CD68 (orange), CD80 (yellow), CD163 (green), ARG1 (magenta), and Cytokeratin Pan Type I/II (red) antibodies and DAPI (blue). The parenchyma/stroma segmentation was performed according to a cytokeratin positivity/negativity, respectively. Pictures were snapped using the Mantra Snap 1.0.3. software (Akoya Biosciences, Menlo Park, CA, USA) with a magnification of 20×10 and analyzed with the InForm 2.4.6. software (Akoya Biosciences, Menlo Park, CA, USA) with prepared algorithm; the fluorophores intensities are normalized for exposure times. The scalebars represent $50\ \mu\text{m}$ and were added in the Fiji (ImageJ) software.

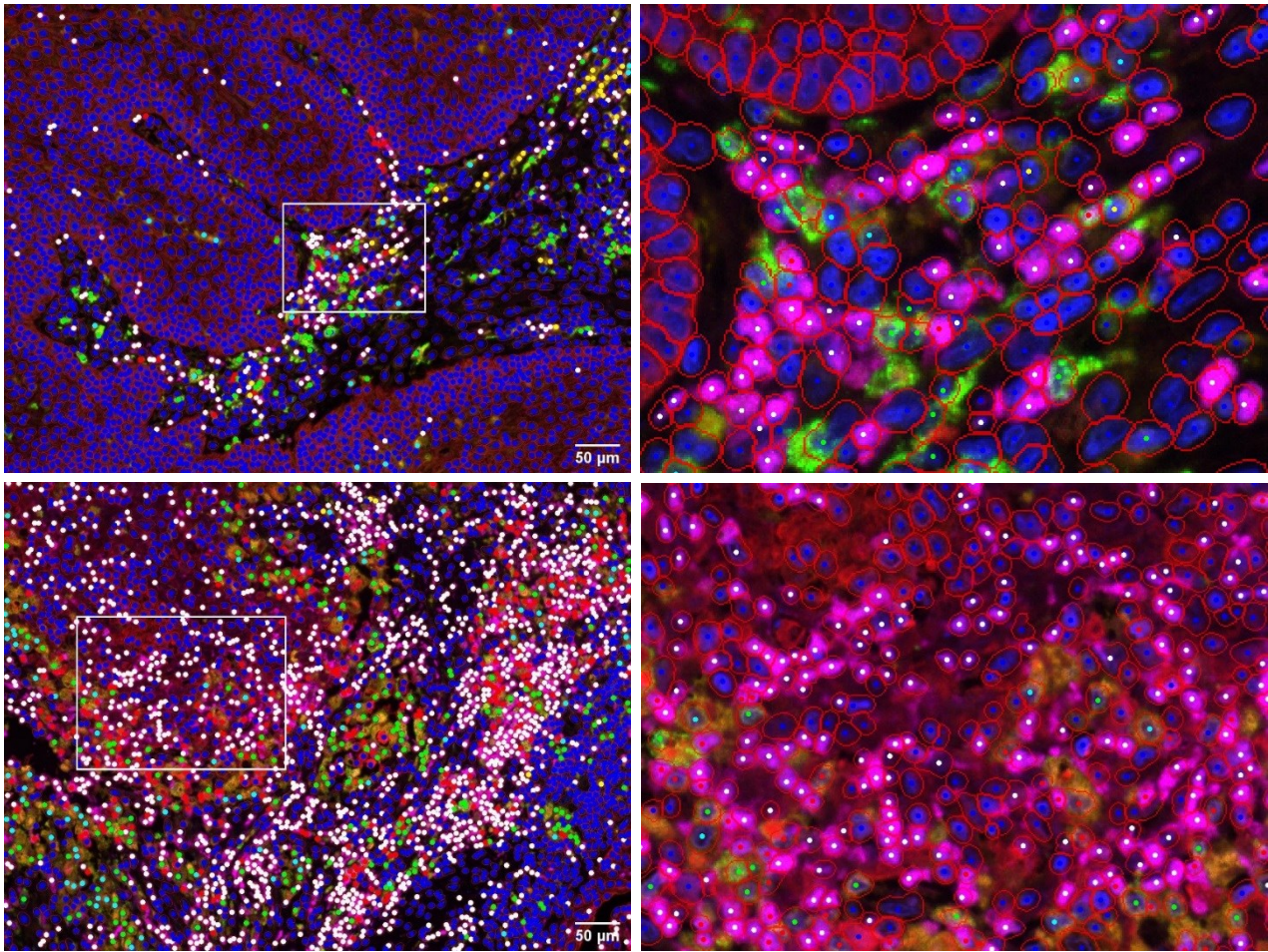


Figure S2: Cell phenotyping. Different cell populations were segmented and phenotyped using InForm 2.4.6. software (Akoya Biosciences, Menlo Park, CA, USA) with prepared algorithm. From original 20x10 pictures, representative cutouts were done in stroma (upper, cytokeratin negative area) and parenchyma (lower, cytokeratin positive area) in InForm 2.4.6. Red circles represent cell membrane. M1 (CD68+CD80+) – cyan dot, M2 (CD68+CD163+) – green dot, M2-ARG (CD68+ARG1+) – red dot, ARG1 (ARG1+) – white dot, CD80+ (CD80+) – yellow dot, other phenotypes – blue dot. The fluorophores intensities are normalized for exposure times. The scalebars represent 50 μm and were added in the Fiji (ImageJ) software.

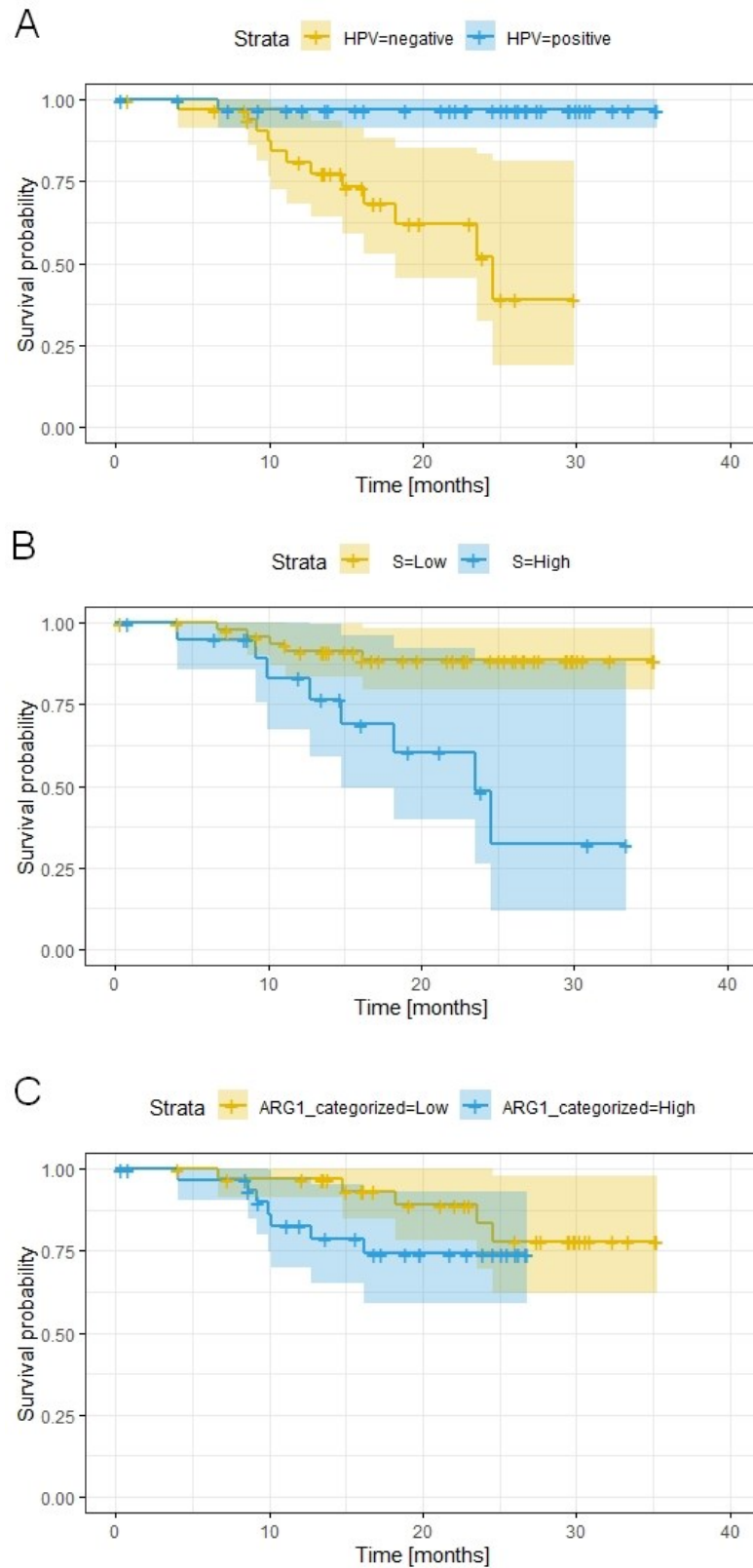


Figure S3: Kaplan-Meier estimator plots of A) HPV+ and HPV- patients, B) of tumor stage (S), where “low” represents S I + II, and “high” S III + IV, and C) of ARG1 mRNA level which was divided into two equal halves – “low” and “high” with threshold value 6.26.



Article

PD1⁺CD8⁺ Cells Are an Independent Prognostic Marker in Patients with Head and Neck Cancer

Barbora Pokrývková ¹, Marek Grega ², Jan Klozar ³, Ondřej Vencálek ⁴, Jaroslav Nunvář ¹ and Ruth Tachezy ^{1,*}¹ Department of Genetics and Microbiology, Faculty of Science, Charles University, BIOCEV, 252 50 Vestec, Czech Republic² Department of Pathology and Molecular Medicine, 2nd Faculty of Medicine, Charles University, 150 06 Prague, Czech Republic³ Department of Otorhinolaryngology and Head and Neck Surgery, 1st Faculty of Medicine, Charles University, University Hospital Motol, 150 06 Prague, Czech Republic⁴ Department of Mathematical Analysis and Applications of Mathematics, Faculty of Science, Palacky University in Olomouc, 771 46 Olomouc, Czech Republic

* Correspondence: tachezr@natur.cuni.cz; Tel.: +420-737355521



Citation: Pokrývková, B.; Grega, M.; Klozar, J.; Vencálek, O.; Nunvář, J.; Tachezy, R. PD1⁺CD8⁺ Cells Are an Independent Prognostic Marker in Patients with Head and Neck Cancer. *Biomedicines* **2022**, *10*, 2794. <https://doi.org/10.3390/biomedicines10112794>

Academic Editor: Chung-Jung Liu

Received: 7 October 2022

Accepted: 1 November 2022

Published: 3 November 2022

Publisher's Note: MDPI stays neutral with regard to jurisdictional claims in published maps and institutional affiliations.



Copyright: © 2022 by the authors. Licensee MDPI, Basel, Switzerland. This article is an open access article distributed under the terms and conditions of the Creative Commons Attribution (CC BY) license (<https://creativecommons.org/licenses/by/4.0/>).

Abstract: Head and neck squamous cell carcinomas (HNSCCs) belong to a group of diverse tumors, which can be induced by infection with human papillomavirus (HPV) or tobacco and alcohol consumption. The viral etiology of HNSCC relates to better clinical outcomes reflecting a different immune system response. Here, we retrospectively analyzed 97 tissue samples from oral and oropharyngeal carcinomas associated and non-associated with HPV infection using multispectral fluorescent immunohistochemistry. To evaluate the immune cell infiltration in tumor and stroma compartments, we designed four panels of four to five antibodies. We detected more T lymphocytes in the stroma, compared to the tumor parenchyma. In HPV positive (HPV⁺) in comparison to HPV negative (HPV⁻) tumors, higher counts of CD3⁺CD4⁺, CD3⁺CD8⁺, PD1⁺CD4⁺, PD1⁺CD8⁺ T cells, and ICOS⁻ Treg cells were detected while more ICOS⁺ Treg cells and CTLA4⁺CD4⁺ T cells were observed in HPV⁻ than in HPV⁺ tumors. The results of the univariate and multivariate analyses confirmed the predominant impact of HPV status on prognosis. More importantly, the number of CD8⁺PD-1⁺ T cells was identified as an independent factor, influencing the overall and/or disease-specific survival of patients with oral cavity or oropharyngeal carcinomas.

Keywords: head and neck cancer; PD-1; survival; HPV

1. Introduction

Head and neck squamous cell carcinomas (HNSCCs) are the world's sixth most common cancer with locations in the oropharynx, hypopharynx, nasopharynx, larynx, oral cavity, and nasal cavity [1]. Historically, most HNSCCs were associated with tobacco and alcohol consumption; however, in recent decades, a growing number of oropharyngeal (OP) and oral cavity (OC) tumors are caused by a persistent infection with high-risk human papillomavirus (HPV) [1,2]. Patients with HPV-positive (HPV⁺) tumors are younger and, compared to patients with non-virally induced tumors (HPV⁻), have better prognosis, reflecting their improved treatment response [3–5].

One of the factors that can explain the difference in clinical outcomes between patients with different tumor etiology is their immune response. The phenotypes and numbers of tumor-infiltrating lymphocytes (TIL) as one of the components of the tumor microenvironment (TME) were described as a significant prognostic factor in many tumors, including HNSCC [5–9]. Moreover, the level of CD3⁺ and CD8⁺ T lymphocytes in a tumor invasive margin in colorectal carcinoma was recently introduced as an immunoscore, which serves as a prognostic factor for colorectal carcinoma patients and is now approved as an addition

to the conventional tumor-node-metastasis (TNM) staging [6]. Multispectral fluorescence immunohistochemistry (fIHC) is a powerful tool for a detailed analysis of the TME. This method allows us to assess the phenotype and quantity of cell types in different compartments of the tumor, since, in comparison to flow cytometry, the architecture of the tissue remains preserved. The fIHC is uniquely suited for the study of the interaction between immune and cancer cells in situ.

CD4⁺ and CD8⁺ T lymphocytes are important TIL subpopulations in the TME. As CD4⁺ T lymphocytes include diverse functional subpopulations, their effect on prognosis is difficult to decipher. Many studies do not analyze T lymphocyte spatial location in the TME and HPV status of HNSCC tumors, which modify the observed correlations [10]. CD8⁺ T cells represent the main anti-tumor TIL population and are considered as a positive prognostic factor in the majority of tumors [10–12]. High CD8⁺ TILs infiltration was also shown to be associated with better survival of patients with OP, hypopharyngeal, and laryngeal SCC [9,13]. The anti-tumor function of T cells in TME may be suppressed by the FOXP3⁺ regulatory T cells (Treg) activity or by the PD-1 (programmed cell death 1)/PD-L1 (PD-1 ligand) interactions [14]. Moreover, the expression of the inducible co-stimulator (ICOS) receptor on T cells, including Treg, can regulate the checkpoint inhibitors efficacy [15]. In this retrospective study with a 10-year follow-up, we analyzed the HNSCC TME with respect to the presence of an active HPV infection and prognostic significance of the studied TILs.

2. Materials and Methods

2.1. Sample Collection, Processing, and Characterization

Samples of primary HNSCC (ICD-10: C01–C06, C09, C10) and non-malignant tonsillar tissue were provided by the Department of Otorhinolaryngology and Head and Neck Surgery, Motol University Hospital, Prague. They were collected, processed, and characterized in previous studies between 2001–2012 [4,16,17]. Briefly, they were screened for the presence and type of HPV and active viral infection and were classified by a pathologist using the TNM nomenclature as valid at the time of patients' enrollment (7th edition) [18]. For this study, 97 formalin-fixed and paraffin-embedded (FFPE) samples were selected. According to the presence of active viral infection, they were divided into HPV⁺ or HPV[−]. All patients signed an informed consent form and completed a questionnaire about risk factors for HPV infection and HNSCC induction when enrolled in the study approved by the Ethical Committee of the Motol University Hospital in 2001.

2.2. Tissue Sections Preparation and Antibodies Validation

From each FFPE tumor tissue block, 2 µm sections were prepared on Superfrost[®] Plus microscope slides (VWR, Leuven, Belgium) and confirmed by a pathologist for the presence of tumor tissue. The slides were deparaffinized at 60 °C for two hours, washed in xylene for 3 × 10 min, hydrated with descending grades of ethanol (100%, 96%, and 70%; Penta, Prague, Czech Republic), and fixed for 20 min in neutral buffered formalin, pH 7.2–7.4 (Diapath, Martinengo, Italy). Heat-induced epitope retrieval (HIER) was carried out by using microwave (96–98 °C) in buffer of pH 9.0 (AR9, Tris-EDTA; Zytomed Systems, Berlin, Germany) or pH 6.0 (AR6, citrate buffer; Akoya Biosciences, Menlo Park, CA, USA). After 10 min of blocking using Antibody Diluent/Block (Akoya Biosciences), the slides were incubated with the primary antibodies listed in Table 1 and subsequently stained with the Opal[™] 7-Color Manual IHC Kit (Akoya Biosciences), according to the manufacturers' instructions. Validation of the antibodies was carried out on samples of non-malignant tonsillar and HNSCC tissue. To verify staining specificity, the corresponding isotype controls, as well as no-primary controls, were performed using the appropriate isotype antibody or Antibody Diluent/Block, respectively.

Table 1. List of antibodies.

Name	Clone	Manufacturer
CD3e	SP7	ThermoFisher Scientific (Waltham, MA, USA)
CD4	EP204	Zeta Corporation (Arcadia, CA, USA)
CD8- α	C8/144B	Santa Cruz Biotechnology (Dallas, TX, USA)
FoxP3	206D	BioLegend (San Diego, CA, USA)
PD-1	EPR4877(2)	Abcam (Cambridge, United Kingdom)
CTLA4	F-8	Santa Cruz Biotechnology (Dallas, TX, USA)
ICOS	SP98	Abcam (Cambridge, United Kingdom)
VEGF	EP1176Y	Biocare Medical (Pacheco, CA, USA)
Ki67	sc-23900	Santa Cruz Biotechnology (Dallas, TX, USA)
CCR4	polyclonal	Novus Biological (Centennial, CO, USA)
Cytokeratin Pan Type I/II	AE1/AE3	ThermoFisher Scientific (Waltham, MA, USA)

2.3. Multispectral fIHC Panel Design and Optimization

We designed four different antibody panels. A staining order for primary antibodies was set with respect to different HIER length requirements and stability of the epitopes after multiple HIER treatments. For matching fluorophores with the primary antibodies, possible colocalization of antibodies in the panel was considered. After each round of staining, the complex of primary and secondary antibodies was removed by HIER using the antigen retrieval (AR) buffer, optimal for the following antibody in the panel. To ensure complete removal of the antibodies complex, stripping quality controls were performed. The final settings for each panel with optimized dilutions of antibodies are specified in Table S1.

2.4. Image Acquiring and Processing

All slides were snapped by using the MantraSnap 1.0.3 software included in the Mantra Quantitative Pathology Workstation (Akoya Biosciences) for DAPI, FITC, Cy3, Texas Red, and Cy5 data acquisition. From each tissue section, five different regions of interest were randomly selected with a 20X objective. Images were analyzed using the InForm 2.4.6. software (Akoya Biosciences). Four separated algorithms for trainable tissue and cell segmentation and cell phenotyping were prepared. The tissue was segmented into the tumor parenchyma, stroma, and background compartments and checked by the pathologist. The algorithms were trained to specifically phenotype the cells according to different expression of markers. The optimization workflow of algorithms is listed in Supplement Figure S1. For determining the phenotype of the cells, a phenotyping confidence cut off of 80% was set. The numbers of positive cells of different phenotypes were counted separately per megapixel (Mpx) for the tumor parenchymal and stromal compartments. We introduced several TIL phenotypes for each panel (Table 2).

Table 2. Immune cell phenotypes in Panels 1–4.

	Markers		Markers
Panel 1	Th: CD3 ⁺ CD4 ⁺	Panel 3	CD3 ⁺
	Tc: CD3 ⁺ CD8 ⁺		Ki67 ⁺
	Treg: FOXP3 ⁺ CD3 ⁺ CD4 ⁺		VEGF ⁺
Panel 2	CD4 ⁺	Panel 4	CD4 ⁺
	PD-1 ⁺ CD4 ⁺		FOXP3 ⁺ CD4 ⁺
	CTLA4 ⁺ CD4 ⁺		ICOS ⁺ CD4 ⁺
	CD8 ⁺		ICOS ⁺ FOXP3 ⁺ CD4 ⁺
	PD-1 ⁺ CD8 ⁺		CCR4 ⁺
	CTLA4 ⁺ CD8 ⁺		CD4 ⁺ FOXP3 ⁺ CCR4 ⁺

Abbreviations: Th—helper T, Tc—cytotoxic T, Treg—regulatory T, PD-1—programmed cell death 1, CTLA4—cytotoxic T lymphocyte antigen 4, VEGF—vascular endothelial growth factor, ICOS—inducible T cell co-stimulator, CCR4—C-C chemokine receptor 4.

2.5. Statistical Analysis

The numbers of cells of distinct phenotypes were evaluated separately for the parenchyma and the stroma and counted per Mpx for the five regions of interest. Differences between parenchyma and stroma infiltration were evaluated using the sign test, and the Mann–Whitney U test was used to detect differences between the HPV⁺ and HPV[−] groups. Patients were grouped based on HPV E6 mRNA detection as HPV⁺ or HPV[−].

The Cox proportional hazards model was applied for the overall survival (OS) and disease-specific survival (DSS) analyses. The following factors were included: age, gender, education (≤ 12 years, >12 years), smoking history (nonsmoker, ex-smoker, smoker), alcohol use (nondrinker, ex-drinker, drinker), tumor location (oropharyngeal, oral), pathological tumor extension (pT1–4), pathological nodal status (pN0–3), tumor stage (S I, II, III, IV), metastasis (pM1), tumor grade (1–3), and relapse (yes, no). As the samples were collected between 2001 and 2012, the tumors were classified according to the TNM 7 staging system, hence, the p16 positive tumors do not have a separate category. Furthermore, the p16 status (p16⁺, p16[−]), HPV status (HPV⁺, HPV[−]), and cell numbers of distinct phenotypes per Mpx separately in the parenchyma and the stroma or in total were evaluated. The zero values in the cell numbers were substituted by the 0.1 value as the lowest non-zero value. The models were analyzed using the Bayesian information criterion (BIC). For all the statistical tests, a *p* value of <0.05 was considered as a significant difference. The statistical analyses were performed using the GraphPad Prism 8.4.2. software (GraphPad Software, San Diego, CA, USA) and R version 4.0.2 (<https://www.R-project.org/> accessed on 02 November 2022) [19].

3. Results

3.1. Patients' Characterization

From the previously characterized cohort [4,16], 97 patients were chosen according to the HPV E6 expression status and tumor location. The selected group consisted of 78 men (78/97, 80%) and 19 women (19/97, 20%) with a median age of 58 years. The median of follow-up time was 45 months. The patients were divided based on HPV E6 mRNA detection into the HPV⁺ (45/97, 46%) and HPV[−] (52/97, 54%) groups. Of the 97 patients, 18 relapsed and 43 died. The patient demographics and clinical characteristics are listed in Table 3.

3.2. HPV⁺ Tumors Are More Infiltrated by T lymphocytes

We analyzed 97 FFPE samples with four antibody panels using multispectral fIHC (Figure 1A–D). For panel 2, three samples were excluded due to poor quality of staining. Regardless of the tumor status, the higher infiltration with CD3⁺CD4⁺ (Th), CD3⁺CD8⁺ (Tc), and Treg cells was detected in the stroma, compared to the parenchyma ($p < 0.0001$ for all cell populations, data not shown). For all measured populations, we observed a highly or moderately positive correlation of TIL counts/Mpx between the parenchyma and the stroma compartments (Table S2). Next, we analyzed the data with respect to tumor etiology. Significantly higher infiltration by all T cells (sum of Th, Tc, and Treg cells), Th cells, and Tc cells was detected both in the parenchyma and the stroma of HPV⁺ tumors (all T cells $p < 0.0001$ for parenchyma, $p = 0.0014$ for stroma; Th $p < 0.0001$ for parenchyma, $p = 0.0017$ for stroma; Tc $p = 0.0003$ for parenchyma, $p = 0.0093$ for stroma). The Treg counts did not statistically differ between the two tumor compartments neither in the HPV⁺ nor in HPV[−] groups. However, we observed statistically non-significantly higher Treg counts in HPV⁺ patients (Figure 1E,F).

Table 3. Patient demographics and clinical characteristics.

Characteristics		Total	HPV ⁺	HPV ⁻
		No. (%)	No. (%)	No. (%)
No. of patients		97 (100%)	45 (46%)	52 (54%)
Age (years)	Mean age	57.23	57.98	56.58
	Median age	58	59	56
Gender	female	19 (20%)	10 (22%)	9 (17%)
	male	78 (80%)	35 (78%)	43 (83%)
Tumor location	oropharynx	83 (86%)	45 (100%)	38 (73%)
	oral cavity	14 (14%)	0 (0%)	14 (27%)
Education ^a	>12 years	33 (34%)	18 (41%)	15 (29%)
	≤12 years	63 (66%)	26 (59%)	37 (71%)
Smoking	never	19 (20%)	15 (33%)	4 (8%)
	past	32 (33%)	19 (42%)	13 (25%)
	current	46 (47%)	11 (25%)	35 (67%)
Alcohol consumption	never	20 (21%)	12 (27%)	8 (15%)
	past	13 (13%)	7 (16%)	6 (12%)
	current	64 (66%)	26 (57%)	38 (73%)
No. of sex partners	>7	41 (46%)	15 (35%)	26 (55%)
	≤6	49 (54%)	28 (65%)	21 (45%)
Tumor size (pT)	T1	17 (18%)	7 (16%)	10 (19%)
	T2	61 (63%)	27 (60%)	34 (65%)
	T3	13 (13%)	9 (20%)	4 (8%)
	T4	6 (6%)	2 (4%)	4 (8%)
Nodal status (pN)	N0	31 (32%)	9 (20%)	22 (42%)
	N1	16 (16.5%)	5 (11%)	11 (21%)
	N2	47 (48.5%)	28 (62%)	19 (37%)
	N3	3 (3%)	3 (7%)	0 (0%)
Metastasis (M)	0	97 (100%)	45 (100%)	52 (100%)
	1	0 (0%)	0 (0%)	0 (0%)
Tumor stage (S)	I	5 (5%)	1 (2%)	4 (8%)
	II	24 (25%)	6 (13%)	18 (35%)
	III	16 (16%)	7 (16%)	9 (17%)
	IV	52 (54%)	31 (69%)	21 (40%)
Tumor grade	1	14 (14%)	3 (7%)	11 (21%)
	2	57 (59%)	25 (55%)	32 (62%)
	3	26 (27%)	17 (38%)	9 (17%)
Relapse	no	82 (85%)	41 (91%)	41 (79%)
	yes	15 (15%)	4 (9%)	11 (21%)

^a For one patient, data were not available.

3.3. PD-1⁺CD4⁺ and PD-1⁺CD8⁺ Levels Are Higher in HPV⁺ Tumors

To determine the functional status of CD4⁺ and CD8⁺ TILs, we detected the expression of PD-1 and CTLA4 proteins. As shown in Figure 2A,B, significantly higher quantities of PD-1⁺CD4⁺ and PD-1⁺CD8⁺ T cells were observed both in the parenchyma and the stroma of HPV⁺ tumors than in HPV⁻ tumors (PD-1⁺CD4⁺ $p = 0.0092$ for parenchyma, $p = 0.0125$ for stroma; PD-1⁺CD8⁺ $p = 0.0039$ for parenchyma, $p = 0.0055$ for stroma). Increased levels of CTLA4⁺CD4⁺ T cells were detected in the stroma and parenchyma of HPV⁻ tumors, but the difference was statistically significant only for the stroma ($p = 0.0021$). No difference was observed in the CTLA4⁺CD8⁺ T cell numbers between the two groups in either the parenchyma or the stroma (Figure 2C,D).

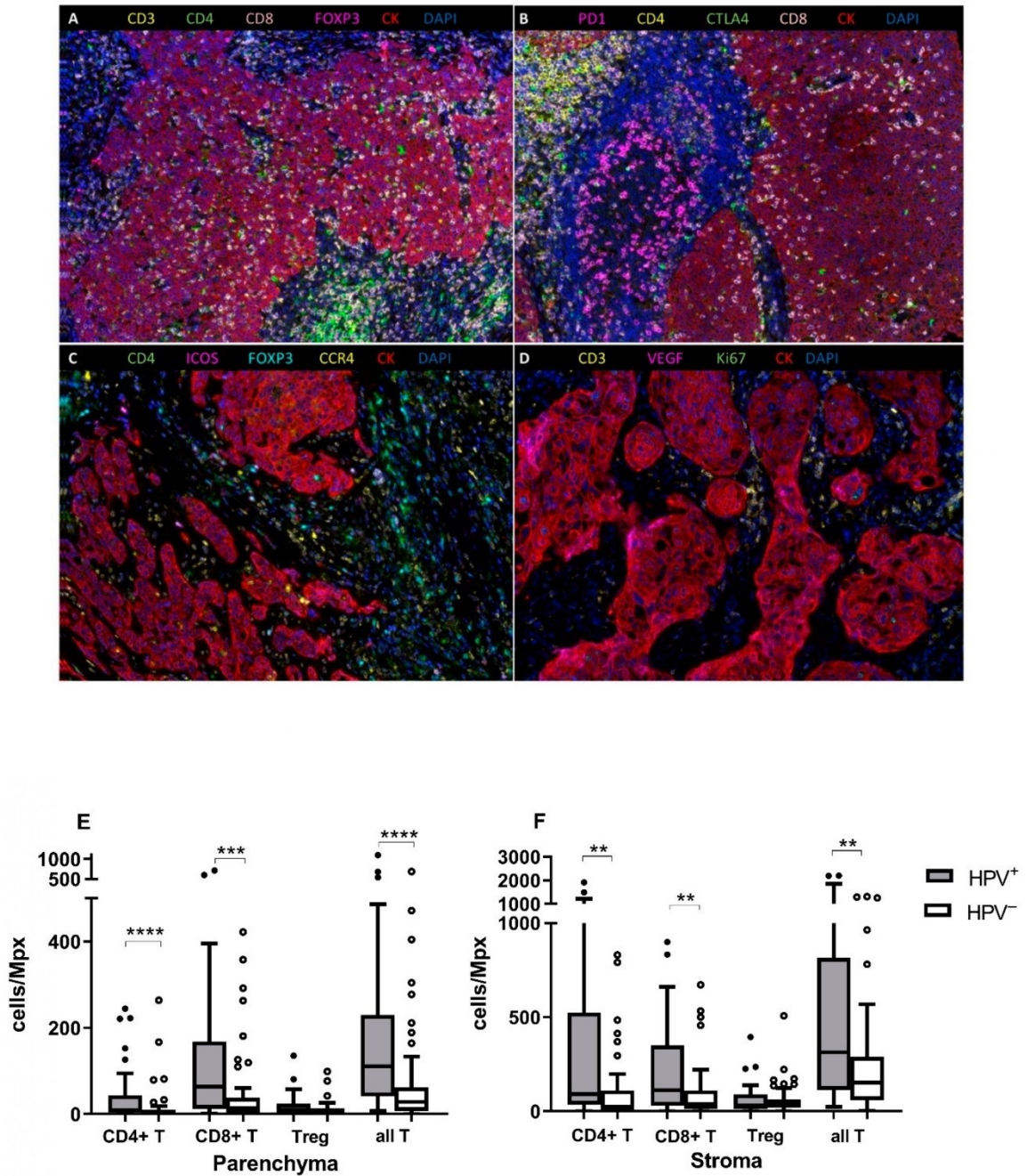


Figure 1. Representative multispectral fIHC staining of FFPE tissue samples with four antibody panels, 20X magnification. (A) CD3 (yellow), CD4 (green), CD8 (pink), FOXP3 (magenta), CK (red), and DAPI (blue) staining. (B) PD-1 (magenta), CD4 (yellow), CTLA4 (green), CD8 (pink), CK (red), and DAPI (blue) staining. (C) CD4 (green), ICOS (magenta), FOXP3 (cyan), CCR4 (yellow), CK (red), and DAPI (blue) staining. (D) CD3 (yellow), VEGF (magenta), Ki67 (green), CK (red), and DAPI (blue) staining. T lymphocytes infiltration in the parenchyma and the stroma compartments according to tumor

etiology. (E) The numbers of CD3⁺CD4⁺, CD3⁺CD8⁺, all CD3⁺ T lymphocytes, and Treg cells per Mpx were compared between the HPV⁺ and HPV⁻ groups in the parenchyma and (F) the stroma compartments. Significantly higher infiltration of CD3⁺CD4⁺, CD3⁺CD8⁺, and all CD3⁺ T lymphocytes was observed in the HPV⁺ groups in both compartments. The observed difference for Treg cells was not statistically significant. ** $p \leq 0.01$, *** $p \leq 0.001$, **** $p \leq 0.0001$, Mann-Whitney U test.

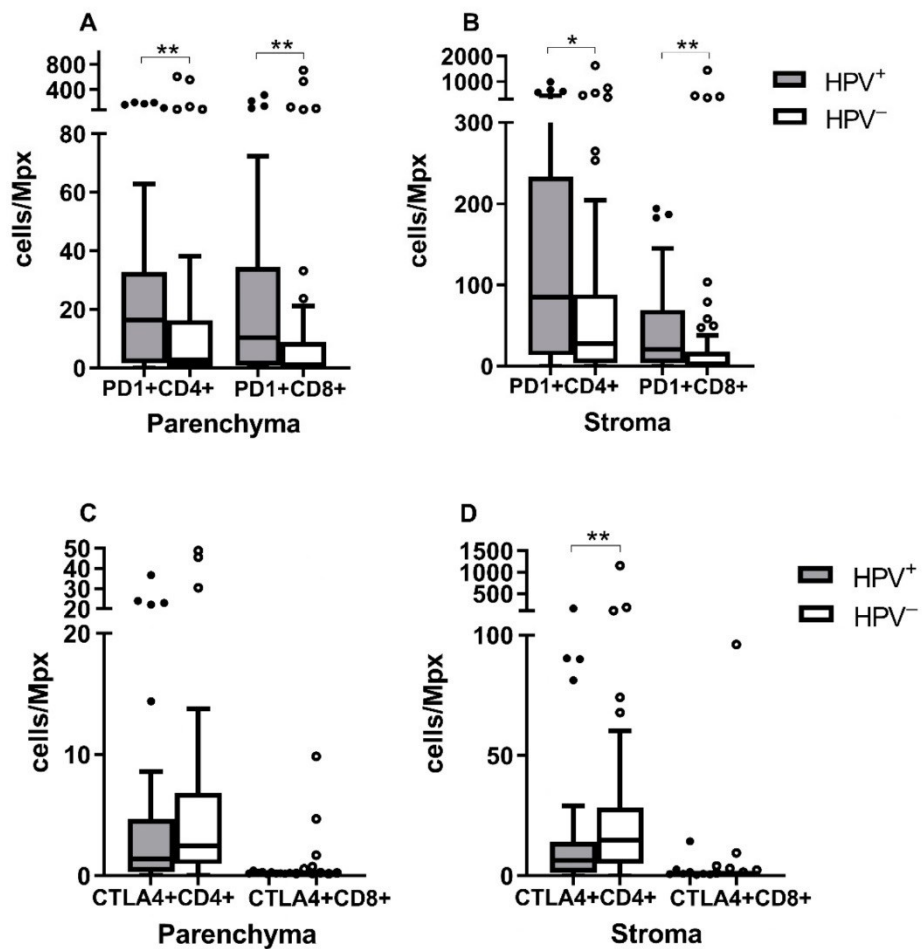


Figure 2. PD-1⁺ or CTLA4⁺ T lymphocyte infiltration in different compartments of the tumors of different etiology. The numbers of CD4⁺ and CD8⁺ T lymphocytes expressing the PD-1 molecule in (A) the parenchyma and (B) the stroma, and the numbers of CD4⁺ and CD8⁺ T lymphocytes producing the CTLA4 molecule in (C) the parenchyma and (D) the stroma were compared between groups. PD-1 expression was significantly higher in both compartments of HPV⁺ tumors, while the CTLA4 production was significantly higher only in the stroma of HPV⁻ tumors. * $p \leq 0.05$, ** $p \leq 0.01$, Mann-Whitney U test.

3.4. ICOS⁺ Treg Are More Abundant in HPV⁻ Tumors

As we did not observe differences in Treg numbers between the HPV⁺ and HPV⁻ groups, we compared the levels of the Treg subpopulation, producing the costimulatory molecule ICOS (ICOS⁺FOXP3⁺CD4⁺). The ICOS⁺ Treg subpopulation was more abundant in the HPV⁻ than in the HPV⁺ tumors ($p = 0.0034$ for the stroma, $p = 0.4334$ for the parenchyma) while the ICOS⁻ Treg (ICOS⁻FOXP3⁺CD4⁺) numbers were higher in the HPV⁺ tumors ($p = 0.2158$ for the stroma, $p = 0.0044$ for the parenchyma) (Figure 3).

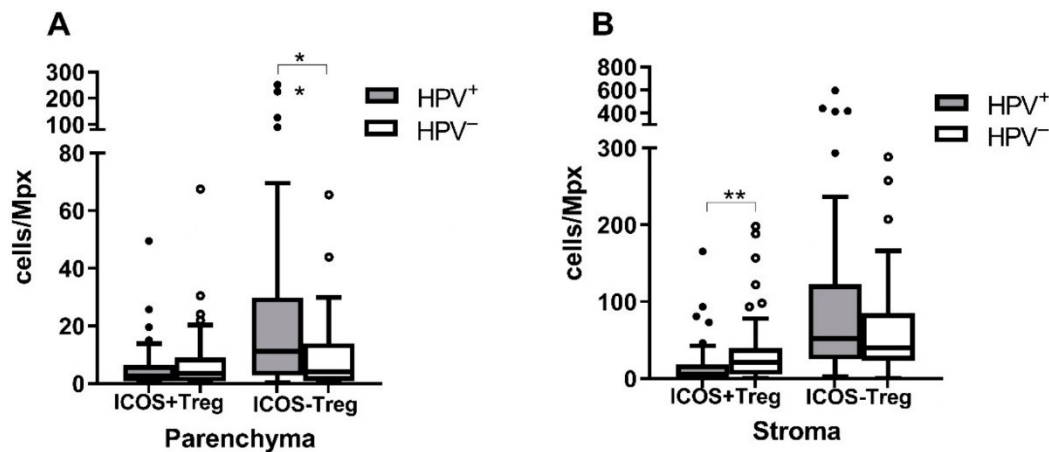


Figure 3. Comparison of the ICOS⁺ and ICOS⁻ Treg levels in the HPV⁺ and HPV⁻ tumors. The numbers of Treg cells with or without ICOS production per Mpx were compared in (A) the parenchyma and (B) the stroma of the tumors of different etiology. Higher ICOS⁺ Treg levels were observed in both the parenchyma and stroma of the HPV⁻ tumors, with the difference being significant for the stroma. Higher ICOS⁻ Treg numbers were detected again in both the parenchyma and stroma of HPV⁺ tumors, with the difference being significant for the parenchyma. * $p \leq 0.05$, ** $p \leq 0.01$, Mann–Whitney U test.

3.5. The Infiltration Level of T Cell Subpopulations Is Prognostic for OS and DSS

To evaluate the influence of TIL infiltration on prognosis, we used Cox models. We fitted 38 models for OS and DSS analyses. Models with and without HPV status and with the evaluation of the parenchyma and stroma separately or combined were tested. The models with the best BIC score are listed in Table 4, and the remaining models are shown in Table S3. In the models with HPV involvement and parenchyma/stroma distinction for OS (BIC = 308.96), the HPV RNA positivity appeared to be the strongest predictive factor for OS, and the lower tumor stage and higher number of parenchymal PD-1⁺CD8⁺ T cells related to better OS (Table 4). The best model for DSS (BIC = 169.16) includes a lower CD4⁺/Treg ratio, which was associated with better survival, along with the positive HPV RNA status and a higher number of stromal PD-1⁺CD8⁺ T cells (Table 4).

In the models where the IHC markers were evaluated without tissue segmentation but HPV status was included, HPV RNA positivity, higher number of all PD-1⁺CD8⁺ T cells, and lower tumor stage or nodal status were connected with better OS and DSS, and low number of all CTLA4⁺CD8⁺ T cells was linked to better OS (Table 4 and Supplement Table S3).

In models not including the HPV status, the main predictors of worse OS were positive smoking history, a lower number of parenchymal PD-1⁺CD8⁺ T cells, a higher number of all CTLA4⁺CD8⁺ T, and tumor size or tumor stage. Similarly, for DSS, a lower number of stromal PD-1⁺CD8⁺ T cells, together with the number of stromal CD8⁺ T cells, and higher age related to worse survival (Tables 4 and S3).

We have shown the level of stromal or parenchymal PD-1⁺CD8⁺ T cells to be a positive prognostic predictor in all models. Additionally, rising tumor stage or nodal status appeared to be a negative predictor for both OS and DSS (Table S3). Our data suggest that the level of PD-1⁺CD8⁺ TIL can serve as an independent prognostic marker for HNSCC patients and may improve the current prognosis assessment.

Table 4. Hazard ratio (HR) values for cell populations from the best models influencing overall survival (OS) and disease-specific survival (DSS).

Models Including HPV Status, IHC Markers Evaluated with Respect to the Stromal or Parenchymal Location.			
OS		DSS	
BIC = 308.96	HR (<i>p</i> value)	BIC = 169.16	HR (<i>p</i> value)
HPV RNA ⁺	0.26 (0.0003)	HPV RNA ⁺	0.15 (0.0011)
Increasing tumor stage	1.55 (0.0179)	CD3 ⁺ CD4 ⁺ /Treg ratio	3.18 (0.0016)
Parenchymal PD1 ⁺ CD8 ⁺ T	0.53 (0.0003)	Stromal PD1 ⁺ CD8 ⁺ T	0.44 (0.0007)
Models including HPV status, the IHC markers counted regardless of location.			
OS		DSS	
BIC = 307.31	HR (<i>p</i> value)	BIC = 171.50	HR (<i>p</i> value)
HPV RNA ⁺	0.26 (0.0004)	HPV RNA ⁺	0.22 (0.0057)
Increasing tumor stage	1.57 (0.0160)	CD3 ⁺ T	2.79 (0.0094)
PD1 ⁺ CD8 ⁺ T	0.52 (0.0001)	PD1 ⁺ CD8 ⁺ T	0.36 (0.0001)
Models without HPV status inclusion, the IHC markers evaluated with respect to the stromal or parenchymal location.			
OS		DSS	
BIC = 313.13	HR (<i>p</i> value)	BIC = 174.57	HR (<i>p</i> value)
Smoking (No)	0.37 (0.0055)	Increasing age	0.93 (0.0032)
Increasing tumor size	1.44 (0.0709)	Stromal CD8 ⁺ T	2.19 (0.0165)
Parenchymal PD1 ⁺ CD8 ⁺ T	0.52 (0.0003)	Stromal PD1 ⁺ CD8 ⁺ T	0.30 (0.0000)

4. Discussion

The major aim of this retrospective study was to analyze the tumor microenvironment in HNSCC of different etiology in order to explain the better prognosis of patients with HPV-positive tumors and to evaluate non-viral markers in the populations of TILs as a possible independent prognostic tool for HNSCC patients.

The prognostic significance of the TIL count was evaluated in several malignancies and recently this parameter has been approved as an additional characteristic to the TNM classification for colorectal carcinomas [5–9]. It has also been proposed that the spatial distribution of TILs in the tumor parenchyma or stroma relates to their different biological function in the process of tumorigenesis [20].

In our study, HPV-induced tumors were more infiltrated by CD3⁺CD4⁺ and CD3⁺CD8⁺ T cells. Higher infiltration by T cells of HPV⁺ tumors than HPV[−] tumors may be explained by the presence of viral antigens, which stimulate the immune response more strongly. Despite the differences in their designs, several studies have come to similar results. Badoual et al. found higher CD4⁺ T cell counts in the stroma of HNSCC tumors [21]. Other studies regardless of the method used detected a statistically significantly higher infiltration of CD3⁺, CD4⁺, and CD8⁺ T lymphocytes in both the parenchyma and the stroma of HPV⁺ tumors [22–28]. Although we observed higher Treg cell infiltration in HPV⁺ tumors, the difference from HPV[−] tumors was not statistically significant. The same was shown by IHC [25], gene expression [28], and flow cytometry analyses [27,29]. Significantly higher Treg counts in the HPV⁺ cohort, in comparison to HPV[−] tumors, were only reported by a single study for tonsillar SCC [23]. To analyze Treg cells more thoroughly, their functional status was evaluated according to the expression of the ICOS molecule. ICOS serves as a co-stimulatory receptor of immunogenic T cells, but it is also involved in the activation of Treg cells resulting in the immunosuppression [15]. ICOS⁺ Treg cells were more prevalent in the stroma and parenchyma of HPV[−] tumors, but the difference was statistically significant only for the stroma. Inversely, ICOS[−] Treg counts were higher in both compartments of HPV⁺ tumors with a statistically significant difference for parenchyma location. To our knowledge, this is the first study analyzing the spatial prevalence of ICOS on Treg cells in HNSCC of different etiology, and the results suggest that these cells can have different function in HPV⁺ and HPV[−] tumors.

Furthermore, we have detected significantly higher counts of PD-1⁺CD4⁺ and PD-1⁺CD8⁺ T cells in both the parenchyma and the stroma of HPV⁺ tumors, compared to HPV⁻ tumors. Higher levels of PD-1⁺CD4⁺ and/or PD-1⁺CD8⁺ T cells and PD-1 mRNA were also observed in HPV⁺ than in HPV⁻ HNSCC by others [27,30,31]. It was also shown that PD-1 expression was more frequent on CD4⁺ than CD8⁺ T cells in HNSCC [21,32], which agrees with our study. Oguejiofor et al. observed a higher level of PD-1⁺CD8⁺ cells in the stroma, compared to the parenchyma but with no difference in the PD-1⁺CD8⁺ counts between HPV⁺ and HPV⁻ OPSCC [22].

Thanks to the long-term follow-up, we were able to explore the impact of TILs infiltration on prognosis, which is the main benefit of this study. We fitted several models, including clinicopathological characteristics, HPV RNA status, and tissue compartment. We were also interested if any of the studied population of TILs would be an independent prognostic marker for HNSCC regardless of the HPV association. The influence of TILs on prognosis was also analyzed by others who, unfortunately, did not take account of HPV status and/or spatial distribution was not considered, which makes the comparison of results difficult. We found that a higher number of parenchymal or stromal PD-1⁺CD8⁺ T cells is associated with both better OS and DSS of OC and OPSCC patients in all of the models. When HPV status was included, the multivariate analysis confirmed HPV positivity as the strongest independent positive prognostic factor for OS and DSS [3,4].

In OC and OPSCC, a higher number of CD8⁺ T cells was associated with better OS or DFS [23,24,33–35]. However, other studies did not confirm this observation [30,36–38]. The interplay between subfamilies of TILs in different tumor compartments is as complex as the outcome of these interactions. Therefore, it is important to analyze TILs more deeply with respect to their functional status. The PD-1 molecule is expressed by activated T lymphocytes, pointing to the persistent antigen stimulation, and subsequent T cell exhaustion. However, in the TME context, the PD-1 expression may not be followed by the expression of co-inhibitory molecules and, therefore, is not a marker of T cell exhaustion [30,39]. In the HPV⁻ cohort, it has been suggested that PD1⁺CD8⁺ TIL cells act as a tumor-specific population, compared to the PD1⁻CD8⁺ TILs and play a key anti-tumor role [39]. It was also shown that high infiltration by PD-1⁺CD4⁺ T cells in HPV⁺ tumors and by PD-1⁺CD8⁺ T cells in HPV⁺ and HPV⁻ tumors related to better OS than low infiltration by these cell populations [30,39]. The increased numbers of PD-1⁺CD8⁺ T cells in tumors suggest that patients contain tumor-specific T cells that can be activated and—before silencing by inhibitory molecules, such as PD-1—exert an antitumor effect, supplementing both radiotherapy and surgery and enhancing survival. Due to the limited number of markers, which can be detected using multispectral FHC, we are not able to characterize the PD-1⁺CD8⁺ T cells in the more detailed manner, which is the limitation of this study. To describe the status of PD-1⁺CD8⁺ T cells in the TME, expression of other activation and/or exhaustion markers can be examined on a fresh tumor tissue, using other methods, such as flow cytometry. However, the results of our study and of others indicate that this marker should be included in the prognostic immunoscore for HNSCC [30,39]. The multivariate analyses did not reveal the influence of the counts of CD4⁺ T lymphocytes on prognosis, which was also observed by others [24,30]. In our study, the levels of PD-1, CTLA4, and ICOS-expressing CD4⁺ T cells were analyzed in the context of prognosis, and none of these subpopulations influenced OS or DSS.

The level of Treg cells itself did not affect OS or DSS but was positively correlated with a better locoregional control in HNSCC [21]. It was proposed that ICOS⁺ Treg cells in the TME have higher immunosuppressive capacity than the ICOS⁻ Treg population [15]. The higher ICOS⁺ Treg counts found in the HPV⁻ tumors may relate to worse outcomes of HPV⁻ patients. In our study, despite the findings of higher ICOS⁺Treg cell counts in HPV⁻ tumors, no influence of this subpopulation on OS or DSS was detected. Similar to Lukesova et al. who observed the phenomenon in the blood, in our models, we found that a low CD8⁺/FOXP3⁺ ratio related to improved OS and DSS [40]. In the study of de Ruiter et al., the CD8⁺/FOXP3⁺ ratio measured in HPV⁻ tumor tissue microarray cores

did not correlate with improved survival [41]. However, in agreement with our study, Nasman identified a high CD8⁺/FOXP3⁺ ratio, connected with better DFS in both HPV⁺ and HPV⁻ groups [23].

5. Conclusions

In this study, we evaluated the level of TILs in different compartments of the HNSCC microenvironment using multispectral IHC. We compared the TILs levels with respect to the presence of an active HPV infection and tumor compartment in a retrospective cohort of patients under long-term follow-up. The impact of different TIL infiltration levels on prognosis was studied. We revealed that higher levels of PD-1⁺CD8⁺ T lymphocytes improved the prognosis of the patients in all our models, which points out the importance of this marker and entitles it to be included in the prognostic immunoscore for patients with OC and OPSCC of different etiology.

Supplementary Materials: The following supporting information can be downloaded at: <https://www.mdpi.com/article/10.3390/biomedicines10112794/s1>, Table S1: Reaction conditions for each panel of antibodies; Table S2: Cell counts/Mpx in the parenchyma and stroma of HNSCC tumors; Table S3: Models of DSS and OS; Figure S1: Optimization of algorithms for automatic picture analysis.

Author Contributions: Conceptualization, B.P. and R.T.; methodology, B.P.; software, B.P.; validation, B.P., R.T., J.N. and O.V.; formal analysis, B.P.; investigation, B.P.; resources, J.K. and M.G.; data curation, J.N., O.V. and B.P.; writing—original draft preparation, B.P.; writing—review and editing, R.T., M.G. and J.K.; visualization, B.P.; supervision, R.T.; project administration, R.T.; funding acquisition, R.T. All authors have read and agreed to the published version of the manuscript.

Funding: This research was funded by the Czech Health Research Council, grant number 17-28055A and the European Regional Development Fund and the Ministry of Education, Youth and Sports of the Czech Republic, grant number CZ.02.1.01/0.0/0.0/16_019/0000785, by the project National Institute of Virology and Bacteriology (Programme EXCELES, ID Project No. LX22NPO5103)—Funded by the European Union—Next Generation EU, and by the Charles University, grant number SVV 260568.

Institutional Review Board Statement: The study was conducted in accordance with the Declaration of Helsinki and approved by the Institutional Review Board of the Motol University Hospital (IRB 00000947, 4/25/2001) and of the Institute of Hematology and Blood Transfusion (IRB 00001238, 4/26/2001).

Informed Consent Statement: Written informed consent was obtained from all subjects involved in the study.

Data Availability Statement: The data are publicly available on Zenodo. Barbora Pokryvkova, Marek Grega, Jan Klozar, Ondrej Vencalek, Jaroslav Nunvar, Ruth Tachezy (2022), "PD1+CD8+ cells are an independent prognostic marker in patients with head and neck cancer", doi: 10.5281/zenodo.6874821.

Conflicts of Interest: The authors declare no conflict of interest. The funders had no role in the design of the study; in the collection, analyses, or interpretation of data; in the writing of the manuscript; or in the decision to publish the results.

References

1. Tumban, E. A Current Update on Human Papillomavirus-Associated Head and Neck Cancers. *Viruses* **2019**, *11*, 922. [[CrossRef](#)] [[PubMed](#)]
2. Gillison, M.L.; Chaturvedi, A.K.; Anderson, W.F.; Fakhry, C. Epidemiology of Human Papillomavirus-Positive Head and Neck Squamous Cell Carcinoma. *J. Clin. Oncol.* **2015**, *33*, 3235–3242. [[CrossRef](#)] [[PubMed](#)]
3. Koslabova, E.; Hamsikova, E.; Salakova, M.; Klozar, J.; Foltynova, E.; Salkova, E.; Rotnaglova, E.; Ludvikova, V.; Tachezy, R. Markers of HPV infection and survival in patients with head and neck tumors. *Int. J. Cancer* **2013**, *133*, 1832–1839. [[CrossRef](#)]
4. Rotnaglova, E.; Tachezy, R.; Salakova, M.; Prochazka, B.; Koslabova, E.; Vesela, E.; Ludvikova, V.; Hamsikova, E.; Klozar, J. HPV involvement in tonsillar cancer: Prognostic significance and clinically relevant markers. *Int. J. Cancer* **2011**, *129*, 101–110. [[CrossRef](#)]

5. Ward, M.J.; Thirdborough, S.M.; Mellows, T.; Riley, C.; Harris, S.; Suchak, K.; Webb, A.; Hampton, C.; Patel, N.N.; Randall, C.J.; et al. Tumour-infiltrating lymphocytes predict for outcome in HPV-positive oropharyngeal cancer. *Br. J. Cancer* **2014**, *110*, 489–500. [[CrossRef](#)] [[PubMed](#)]
6. Pagès, F.; Mlecnik, B.; Marliot, F.; Bindea, G.; Ou, F.S.; Bifulco, C.; Lugli, A.; Zlobec, I.; Rau, T.T.; Berger, M.D.; et al. International validation of the consensus Immunoscore for the classification of colon cancer: A prognostic and accuracy study. *Lancet* **2018**, *391*, 2128–2139. [[CrossRef](#)]
7. Wong, P.F.; Wei, W.; Smithy, J.W.; Acs, B.; Toki, M.I.; Blenman, K.R.M.; Zelterman, D.; Kluger, H.M.; Rimm, D.L. Multiplex Quantitative Analysis of Tumor-Infiltrating Lymphocytes and Immunotherapy Outcome in Metastatic Melanoma. *Clin. Cancer Res.* **2019**, *25*, 2442–2449. [[CrossRef](#)] [[PubMed](#)]
8. Donnem, T.; Hald, S.M.; Paulsen, E.E.; Richardsen, E.; Al-Saad, S.; Kilvaer, T.K.; Brustugun, O.T.; Helland, A.; Lund-Iversen, M.; Poehl, M.; et al. Stromal CD8+ T-cell Density—A Promising Supplement to TNM Staging in Non-Small Cell Lung Cancer. *Clin. Cancer Res.* **2015**, *21*, 2635–2643. [[CrossRef](#)]
9. Borsetto, D.; Tomasoni, M.; Payne, K.; Polesel, J.; Deganello, A.; Bossi, P.; Tysome, J.R.; Masterson, L.; Tirelli, G.; Tofanelli, M.; et al. Prognostic Significance of CD4+ and CD8+ Tumor-Infiltrating Lymphocytes in Head and Neck Squamous Cell Carcinoma: A Meta-Analysis. *Cancers* **2021**, *13*, 781. [[CrossRef](#)]
10. Simonson, W.T.N.; Allison, K.H. Tumour-infiltrating lymphocytes in cancer: Implications for the diagnostic pathologist. *Diagn. Histopathol.* **2011**, *17*, 80–90. [[CrossRef](#)]
11. Nakano, O.; Sato, M.; Naito, Y.; Suzuki, K.; Orikasa, S.; Aizawa, M.; Suzuki, Y.; Shintaku, I.; Nagura, H.; Ohtani, H. Proliferative activity of intratumoral CD8(+) T-lymphocytes as a prognostic factor in human renal cell carcinoma: Clinicopathologic demonstration of antitumor immunity. *Cancer Res.* **2001**, *61*, 5132–5136.
12. Oudejans, J.J.; Jiwa, N.M.; Kummer, J.A.; Ossenkoppele, G.J.; van Heerde, P.; Baars, J.W.; Kluin, P.M.; Kluin-Nelemans, J.C.; van Diest, P.J.; Middeldorp, J.M.; et al. Activated cytotoxic T cells as prognostic marker in Hodgkin's disease. *Blood* **1997**, *89*, 1376–1382. [[CrossRef](#)]
13. de Ruyter, E.J.; Ooft, M.L.; Devriese, L.A.; Willems, S.M. The prognostic role of tumor infiltrating T-lymphocytes in squamous cell carcinoma of the head and neck: A systematic review and meta-analysis. *Oncoimmunology* **2017**, *6*, e1356148. [[CrossRef](#)]
14. Webb, E.S.; Liu, P.; Baleeiro, R.; Lemoine, N.R.; Yuan, M.; Wang, Y.H. Immune checkpoint inhibitors in cancer therapy. *J. Biomed. Res.* **2018**, *32*, 317–326. [[CrossRef](#)]
15. Amatore, F.; Gorvel, L.; Olive, D. Inducible Co-Stimulator (ICOS) as a potential therapeutic target for anti-cancer therapy. *Expert Opin. Ther. Targets* **2018**, *22*, 343–351. [[CrossRef](#)]
16. Vojtechova, Z.; Sabol, I.; Salakova, M.; Turek, L.; Grega, M.; Smahelova, J.; Vencalek, O.; Lukesova, E.; Klozar, J.; Tachezy, R. Analysis of the integration of human papillomaviruses in head and neck tumours in relation to patients' prognosis. *Int. J. Cancer* **2016**, *138*, 386–395. [[CrossRef](#)]
17. Tachezy, R.; Klozar, J.; Rubenstein, L.; Smith, E.; Saláková, M.; Smahelová, J.; Ludvíková, V.; Rotnáglová, E.; Kodet, R.; Hamsíková, E. Demographic and risk factors in patients with head and neck tumors. *J. Med. Virol.* **2009**, *81*, 878–887. [[CrossRef](#)]
18. Edge, S.B. *AJCC Cancer Staging Manual*; Springer: Berlin/Heidelberg, Germany, 2010; Volume 7, pp. 97–100.
19. R Core Team. *R: A Language and Environment for Statistical Computing*; R Foundation for Statistical Computing: Vienna, Austria, 2020.
20. Khoury, T.; Nagrale, V.; Opyrchal, M.; Peng, X.; Wang, D.; Yao, S. Prognostic Significance of Stromal Versus Intratumoral Infiltrating Lymphocytes in Different Subtypes of Breast Cancer Treated With Cytotoxic Neoadjuvant Chemotherapy. *Appl. Immunohistochem. Mol. Morphol.* **2018**, *26*, 523–532. [[CrossRef](#)]
21. Badoual, C.; Hans, S.; Rodriguez, J.; Peyrard, S.; Klein, C.; Agueznay Nel, H.; Mosseri, V.; Laccourreye, O.; Bruneval, P.; Fridman, W.H.; et al. Prognostic value of tumor-infiltrating CD4+ T-cell subpopulations in head and neck cancers. *Clin. Cancer Res.* **2006**, *12*, 465–472. [[CrossRef](#)]
22. Oguejiofor, K.; Galletta-Williams, H.; Dovedi, S.J.; Roberts, D.L.; Stern, P.L.; West, C.M. Distinct patterns of infiltrating CD8+ T cells in HPV+ and CD68 macrophages in HPV- oropharyngeal squamous cell carcinomas are associated with better clinical outcome but PD-L1 expression is not prognostic. *Oncotarget* **2017**, *8*, 14416–14427. [[CrossRef](#)]
23. Nasman, A.; Romanitan, M.; Nordfors, C.; Grun, N.; Johansson, H.; Hammarstedt, L.; Marklund, L.; Munck-Wikland, E.; Dalianis, T.; Ramqvist, T. Tumor infiltrating CD8+ and Foxp3+ lymphocytes correlate to clinical outcome and human papillomavirus (HPV) status in tonsillar cancer. *PLoS ONE* **2012**, *7*, e38711. [[CrossRef](#)]
24. Nordfors, C.; Grun, N.; Tertipis, N.; Ahrlund-Richter, A.; Haegglom, L.; Sivars, L.; Du, J.; Nyberg, T.; Marklund, L.; Munck-Wikland, E.; et al. CD8+ and CD4+ tumour infiltrating lymphocytes in relation to human papillomavirus status and clinical outcome in tonsillar and base of tongue squamous cell carcinoma. *Eur. J. Cancer* **2013**, *49*, 2522–2530. [[CrossRef](#)] [[PubMed](#)]
25. Oguejiofor, K.; Hall, J.; Slater, C.; Betts, G.; Hall, G.; Slevin, N.; Dovedi, S.; Stern, P.L.; West, C.M. Stromal infiltration of CD8 T cells is associated with improved clinical outcome in HPV-positive oropharyngeal squamous carcinoma. *Br. J. Cancer* **2015**, *113*, 886–893. [[CrossRef](#)] [[PubMed](#)]
26. Succaria, F.; Kvistborg, P.; Stein, J.E.; Engle, E.L.; McMiller, T.L.; Rooper, L.M.; Thompson, E.; Berger, A.E.; van den Brekel, M.; Zuur, C.L.; et al. Characterization of the tumor immune microenvironment in human papillomavirus-positive and -negative head and neck squamous cell carcinomas. *Cancer Immunol. Immunother.* **2021**, *70*, 1227–1237. [[CrossRef](#)] [[PubMed](#)]

27. Partlova, S.; Boucek, J.; Kloudova, K.; Lukesova, E.; Zabrodsky, M.; Grega, M.; Fucikova, J.; Truxova, I.; Tachezy, R.; Spisek, R.; et al. Distinct patterns of intratumoral immune cell infiltrates in patients with HPV-associated compared to non-virally induced head and neck squamous cell carcinoma. *Oncoimmunology* **2015**, *4*, e965570. [[CrossRef](#)]
28. Mito, I.; Takahashi, H.; Kawabata-Iwakawa, R.; Ida, S.; Tada, H.; Chikamatsu, K. Comprehensive analysis of immune cell enrichment in the tumor microenvironment of head and neck squamous cell carcinoma. *Sci. Rep.* **2021**, *11*, 16134. [[CrossRef](#)]
29. Poropatich, K.; Fontanarosa, J.; Swaminathan, S.; Dittmann, D.; Chen, S.; Samant, S.; Zhang, B. Comprehensive T-cell immunophenotyping and next-generation sequencing of human papillomavirus (HPV)-positive and HPV-negative head and neck squamous cell carcinomas. *J. Pathol.* **2017**, *243*, 354–365. [[CrossRef](#)]
30. Badoual, C.; Hans, S.; Merillon, N.; Van Ryswick, C.; Ravel, P.; Benhamouda, N.; Levionnois, E.; Nizard, M.; Si-Mohamed, A.; Besnier, N.; et al. PD-1-expressing tumor-infiltrating T cells are a favorable prognostic biomarker in HPV-associated head and neck cancer. *Cancer Res.* **2013**, *73*, 128–138. [[CrossRef](#)]
31. Kansy, B.A.; Concha-Benavente, F.; Srivastava, R.M.; Jie, H.B.; Shayan, G.; Lei, Y.; Moskovitz, J.; Moy, J.; Li, J.; Brandau, S.; et al. PD-1 Status in CD8(+) T Cells Associates with Survival and Anti-PD-1 Therapeutic Outcomes in Head and Neck Cancer. *Cancer Res.* **2017**, *77*, 6353–6364. [[CrossRef](#)]
32. Lechner, A.; Schlößer, H.; Rothschild, S.I.; Thelen, M.; Reuter, S.; Zentis, P.; Shimabukuro-Vornhagen, A.; Theurich, S.; Wennhold, K.; Garcia-Marquez, M.; et al. Characterization of tumor-associated T-lymphocyte subsets and immune checkpoint molecules in head and neck squamous cell carcinoma. *Oncotarget* **2017**, *8*, 44418–44433. [[CrossRef](#)]
33. Spector, M.E.; Bellile, E.; Amlani, L.; Zarins, K.; Smith, J.; Brenner, J.C.; Rozek, L.; Nguyen, A.; Thomas, D.; McHugh, J.B.; et al. Prognostic Value of Tumor-Infiltrating Lymphocytes in Head and Neck Squamous Cell Carcinoma. *JAMA Otolaryngol. Head Neck Surg.* **2019**, *145*, 1012–1019. [[CrossRef](#)] [[PubMed](#)]
34. Mukherjee, G.; Bag, S.; Chakraborty, P.; Dey, D.; Roy, S.; Jain, P.; Roy, P.; Soong, R.; Majumder, P.P.; Dutt, S. Density of CD3+ and CD8+ cells in gingivo-buccal oral squamous cell carcinoma is associated with lymph node metastases and survival. *PLoS ONE* **2020**, *15*, e0242058. [[CrossRef](#)] [[PubMed](#)]
35. Solomon, B.; Young, R.J.; Bressel, M.; Urban, D.; Hendry, S.; Thai, A.; Angel, C.; Haddad, A.; Kowanetz, M.; Fua, T.; et al. Prognostic Significance of PD-L1(+) and CD8(+) Immune Cells in HPV(+) Oropharyngeal Squamous Cell Carcinoma. *Cancer Immunol. Res.* **2018**, *6*, 295–304. [[CrossRef](#)] [[PubMed](#)]
36. Quan, H.; Shan, Z.; Liu, Z.; Liu, S.; Yang, L.; Fang, X.; Li, K.; Wang, B.; Deng, Z.; Hu, Y.; et al. The repertoire of tumor-infiltrating lymphocytes within the microenvironment of oral squamous cell carcinoma reveals immune dysfunction. *Cancer Immunol. Immunother.* **2020**, *69*, 465–476. [[CrossRef](#)] [[PubMed](#)]
37. Poropatich, K.; Hernandez, D.; Fontanarosa, J.; Brown, K.; Woloschak, G.; Paintal, A.; Raparia, K.; Samant, S. Peritumoral cuffing by T-cell tumor-infiltrating lymphocytes distinguishes HPV-related oropharyngeal squamous cell carcinoma from oral cavity squamous cell carcinoma. *J. Oral. Pathol. Med.* **2017**, *46*, 972–978. [[CrossRef](#)]
38. Wolf, G.T.; Chepeha, D.B.; Bellile, E.; Nguyen, A.; Thomas, D.; McHugh, J. Tumor infiltrating lymphocytes (TIL) and prognosis in oral cavity squamous carcinoma: A preliminary study. *Oral. Oncol.* **2015**, *51*, 90–95. [[CrossRef](#)] [[PubMed](#)]
39. Xu, K.; Fu, Y.; Han, Y.; Xia, R.; Xu, S.; Duan, S.; Zhang, Z.; Li, J. Fewer tumour-specific PD-1(+)CD8(+) TILs in high-risk "Infiltrating" HPV(-) HNSCC. *Br. J. Cancer* **2020**, *123*, 932–941. [[CrossRef](#)]
40. Lukesova, E.; Boucek, J.; Rotnaglova, E.; Salakova, M.; Koslabova, E.; Grega, M.; Eckschlager, T.; Rihova, B.; Prochazka, B.; Klozar, J.; et al. High level of Tregs is a positive prognostic marker in patients with HPV-positive oral and oropharyngeal squamous cell carcinomas. *Biomed. Res. Int.* **2014**, *2014*, 303929. [[CrossRef](#)]
41. De Ruyter, E.J.; de Roest, R.H.; Brakenhoff, R.H.; Leemans, C.R.; de Bree, R.; Terhaard, C.H.J.; Willems, S.M. Digital pathology-aided assessment of tumor-infiltrating T lymphocytes in advanced stage, HPV-negative head and neck tumors. *Cancer Immunol. Immunother.* **2020**, *69*, 581–591. [[CrossRef](#)]

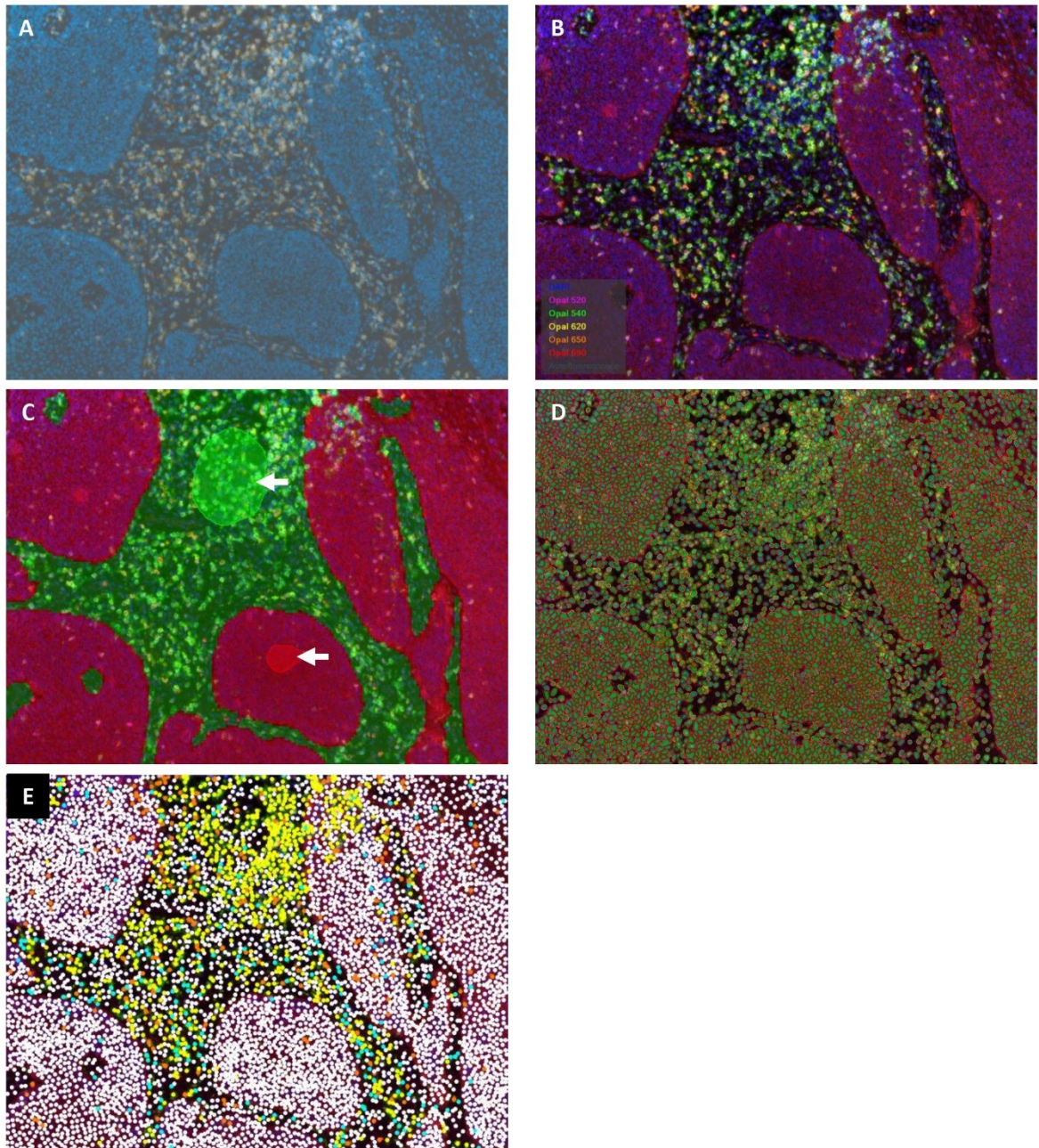


Figure S1. Optimization of algorithms for automatic picture analysis. (A) Unprocessed raw image snapped by MantraSnap software with 20x magnification in DAPI, FITC, Cy3, Texas Red, Cy5 acquiring filters. (B) Spectrally unmixed image obtained by InForm 2.4.6. software using prepared spectral libraries. The spectral libraries were prepared in InForm 2.4.6. software according to the manufacturers' instructions. (C) Tissue segmentation to tumor parenchyma (red), stroma (green). Training regions (white arrows) were selected according to the pan cytokeratin (CK) antibody staining, the components for training were DAPI and the Opal690 signal (CK antibody). The training accuracy was measured to 99,9%, the segmentation resolution was set to „medium“ with the minimum segment size to 400 px. (D) Cell segmentation to nucleus, cytoplasm, and membrane. The nuclei were recognized by the DAPI signal (relative DAPI intensity 0.21, the splitting sensitivity 0.12, minimal nucleus size 35 px). The cytoplasm was recognized by cytoplasmatic CK antibody staining and the membrane by CD4 antibody staining. The cytoplasm thickness was set to 2 px, and the membrane search distance to 3 px. (E) The phenotyping of the cells. The cells for software training were selected manually according to the expression of the markers (in this case: yellow – CD3+CD4+ cells, orange – CD3+CD8+ cells, cyan – CD3+CD4+FOXP3+ cells, white – remaining „other“ cells). Several rounds of training were performed, and re-training was done by correcting the cells' phenotype to ensure the high confidence of phenotyping.

Table S1. Reaction conditions for each panel of antibodies. The order of antibodies and buffer used for epitope retrieval (AR) are indicated as well as the reaction conditions for the primary antibody and OPAL fluorophore staining. For all slides, Opal Polymer HRP Ms+Rb as the secondary antibody and DAPI as the final nuclei counterstain were used.

Panel 1							Panel 2						
#	AR	Marker	Antibody Diln.	Incubation	OPAL λ [nm]	Diln.	#	AR	Marker	Antibody Diln.	Incubation	OPAL λ [nm]	Diln.
1	9	CD3e	1:500	1 h/RT	620	1:100	1	9	PD-1	1:50	OVN/4°C	520	1:50
2	9	CD4	1:200	OVN/4°C	540	1:100	2	9	CD4	1:200	OVN/4°C	620	1:100
3	9	CD8- α	1:500	1 h/RT	650	1:100	3	9	CTLA4	1:100	OVN/4°C	540	1:100
4	6	FoxP3	1:50	1 h/RT	520	1:100	4	9	CD8- α	1:500	1 h/RT	650	1:100
5	6	CK	1:800	1 h/RT	690	1:200	5	6	CK	1:800	1 h/RT	690	1:200

Panel 3							Panel 4						
#	AR	Marker	Antibody Diln.	Incubation	OPAL λ [nm]	Diln.	#	AR	Marker	Antibody Diln.	Incubation	OPAL λ [nm]	Diln.
1	9	CD3e	1:400	1 h/RT	620	1:100	1	9	CD4	1:200	OVN/4°C	540	1:100
2	9	VEGF	1:50	OVN/4°C	520	1:100	2	9	ICOS	1:50	OVN/4°C	520	1:50
3	6	Ki67	1:100	1 h/RT	540	1:100	3	6	FoxP3	1:50	1 h/RT	570	1:100
4	6	CK	1:800	1 h/RT	690	1:200	4	6	CCR4	1:200	1 h/RT	620	1:100
							5	6	CK	1:800	1 h/RT	690	1:200

Abbreviations: # - serial No. of antibodies, AR - antigen retrieval buffer pH, Diln. - dilution, RT - room temperature, OVN - overnight

Table S2. Cell counts/Mpx in the parenchyma and stroma of HNSCC tumors.

Panel	Cell population	Parenchyma				Stroma				Parenchyma-Stroma correlation (r)
		Zeros* (%)	Min. nonzero value	Median	Max.	Zeros* (%)	Min. nonzero value	Median	Max.	
1	CD3+CD4+ (Th)	6	0.27	5.01	264.2	1	0.46	53.85	1912.8	0.71
	CD3+CD8+ (Tc)	3	0.17	29.42	714.56	1	0.28	52.42	899.09	0.83
	CD3+CD4+FOXP3+(Treg)	9	0.21	8.24	135.58	2	0.69	35.6	507.13	0.68
	Th + Tc + Treg sum	0	0.17	53.42	1094.88	0	2.77	205.95	2205.32	0.76
2	CD4+	2	0.17	7.95	213.54	0	1.63	134.67	1563.11	0.70
	PD-1+CD4+	7	0.22	4.62	607.33	9	0.53	37.76	1630.56	0.80
	CTLA4+CD4+	11	0.17	2.09	48.85	6	0.45	9.23	1148.64	0.73
	CD8+	14	0.18	4.94	318.1	5	0.54	41.91	907.32	0.81
	PD-1+CD8+	23	0.2	2.55	709.31	21	0.25	6.41	1445	0.85
	CTLA4+CD8+	79	0.16	0	9.85	76	0.24	0	96.14	0.49
3	CD3+	2	0.48	35.46	465.77	0	0.46	192.92	1628.73	0.64
	Ki67+	27	0.18	0.82	684.08	47	0.21	0.3	656.79	0.69
	VEGF+	14	0.19	5.9	446.56	29	0.29	1.25	904.2	0.44
4	CD4+	6	0.2	4.47	599.06	0	0.33	117.77	2055.96	0.71
	FOXP3+CD4+	7	0.19	5.98	252.41	1	2.11	46.83	596.52	0.77
	ICOS+CD4+	10	0.17	2.99	125.25	8	0.25	10.64	668.6	0.76
	ICOS+FOXP3+CD4+	15	0.17	3.25	67.54	6	0.28	10.16	198.21	0.77

RESEARCH

Open Access



Aspartate- β -hydroxylase and hypoxia marker expression in head and neck carcinomas: implications for HPV-associated tumors

Jana Smahelova¹, Barbora Pokryvkova¹, Eliska Stovickova¹, Marek Grega², Ondrej Vencalek³, Michal Smahel¹, Vladimir Koucky⁴, Simona Malerova⁴, Jan Klozar⁴ and Ruth Tachezy^{1*}

Abstract

Background A proportion of head and neck carcinomas (HNSCCs) are induced by high-risk human papillomaviruses (HPVs) and are associated with better patient outcomes compared to patients with HNSCCs related to tobacco and alcohol abuse. In the microenvironment of solid tumors, including HNSCCs, oxygen levels are often reduced, and a hypoxic state is induced. This can lead to a poor treatment response and a worse patient prognosis. One of the hypoxia-responsive genes is aspartate- β -hydroxylase (ASPH), whose activity promotes the growth, invasiveness, and metastasis of many types of solid tumors.

Methods In our study, HNSCC samples were analyzed for the expression of ASPH and selected endogenous hypoxia markers by real-time PCR and/or multiplex fluorescence immunohistochemistry.

Results Except for the *EPAS1* gene, which had higher mRNA expression in the HPV-negative group of HNSCC ($p < 0.05$), we found no other differences in the expression of the tested genes that were related to HPV status. On the contrary, a statistically significantly higher number of cells producing ASPH ($p < 0.0001$), HIF1A ($p < 0.0001$), GLUT1 ($p < 0.0001$), and MMP13 ($p < 0.05$) proteins were detected in the HPV-positive tumor group than in the HPV-negative sample group. All the evaluated markers, except for MMP9/13, were more abundant in the tumor parenchyma than in the tumor stroma. The Cox proportional hazard models showed that increased numbers of cells with GLUT1 and HIF1A protein expression were positive prognostic markers for overall and disease-specific survival in patients independent of HPV tumor status.

Conclusion The study examined HNSCC samples and found that elevated ASPH and hypoxia marker proteins, typically associated with poor prognosis, may actually indicate active HPV infection, the strongest prognostic factor in HNSCC patients. In cases where HPV status is uncertain, increased expression of HIF1A and GLUT1 can serve as positive prognostic factors.

Keywords Hypoxia, Aspartate- β -hydroxylase, Human papillomavirus, Head and neck cancer, Prognosis

*Correspondence:

Ruth Tachezy
tachezr@natur.cuni.cz

¹Department of Genetics and Microbiology, Faculty of Science BIOCEV, Charles University, Prague, Czech Republic

²Department of Pathology and Molecular Medicine, Second Faculty of Medicine, Charles University and University Hospital Motol, Prague, Czech Republic

³Department of Mathematical Analysis and Applications of Mathematics, Faculty of Science, Palacky University Olomouc, Olomouc, Czech Republic

⁴Department of Otorhinolaryngology and Head and Neck Surgery, First Medical Faculty, Charles University and University Hospital Motol, Prague, Czech Republic



© The Author(s) 2024. **Open Access** This article is licensed under a Creative Commons Attribution 4.0 International License, which permits use, sharing, adaptation, distribution and reproduction in any medium or format, as long as you give appropriate credit to the original author(s) and the source, provide a link to the Creative Commons licence, and indicate if changes were made. The images or other third party material in this article are included in the article's Creative Commons licence, unless indicated otherwise in a credit line to the material. If material is not included in the article's Creative Commons licence and your intended use is not permitted by statutory regulation or exceeds the permitted use, you will need to obtain permission directly from the copyright holder. To view a copy of this licence, visit <http://creativecommons.org/licenses/by/4.0/>. The Creative Commons Public Domain Dedication waiver (<http://creativecommons.org/publicdomain/zero/1.0/>) applies to the data made available in this article, unless otherwise stated in a credit line to the data.

Background

Head and neck squamous cell carcinomas (HNSCCs) comprise a heterogeneous group of malignancies with increasing prevalence in developed countries. In addition to cigarette smoking and alcohol consumption, known risk factors include persistent infection with high-risk human papillomaviruses (HPVs), particularly the type of HPV 16. HPV-associated HNSCCs, which are predominantly located in the oropharynx (palatine tonsils, soft palate, and base of the tongue), represent a distinct group of carcinomas with different biological and clinical characteristics [1]. HPV-positive tumors are diagnosed in 5 to 10 years younger patients and have higher involvement of regional lymph nodes. These tumors are associated with greater radiosensitivity and infiltration of immune cells, and patients with these tumors have a better prognosis than HPV-negative patients do [2]. Therefore, the host immune response, the role of tumor-infiltrating lymphocytes, and relevant factors in the tumor microenvironment of HNSCCs are being investigated extensively to improve patient stratification for individualized treatment with the aim of reducing acute and late adverse consequences of treatment [3–5].

In the microenvironment of growing solid tumors, the oxygen concentration is often reduced, and a hypoxic state is induced. The central regulator of the adaptive cellular response to changes in oxygen levels is hypoxia-inducible factor 1 (HIF1), which functions as a transcription factor influencing the expression of many target genes [6]. Products of hypoxia-responsive genes include mainly proteins that influence cell metabolism (e.g., glucose transporter 1 - GLUT1, carbonic anhydrase 9 - CA9, and pyruvate dehydrogenase kinase 1 - PDK1); angiogenesis (e.g., vascular endothelial growth factor - VEGF); and the composition and function of the tumor microenvironment (e.g., matrix metalloproteinases - MMP, prolyl 4-hydroxylase subunit alpha 1 - P4HA1) [7]. The upregulation of these genes allows cells to survive under adverse conditions. Tumor hypoxia has been recognized as one of the biological indicators associated with treatment failure [8]. The clinical utility of hypoxia markers remains still unclear. Overexpression of the central hypoxia factor HIF1A in HNSCCs has been associated with worse patient outcomes [9, 10] and the utility of a hypoxia-responsive gene signature as a tool for patient stratification has been demonstrated [11]. On the other hand, the prognostic value of the 15-gene hypoxia signature was not confirmed in a cohort of patients with oropharyngeal tumors treated with accelerated chemoradiotherapy [12].

Numerous studies have shown that direct and indirect interactions of HPV 16 oncoproteins with the HIF1 factor may also affect the stability and activity of this protein [13–16]. Subsequent changes in cell signaling and metabolism can promote increased cell proliferation and

thus HPV production. In addition, other factors, such as smoking and alcohol consumption, may influence the expression of endogenous markers of hypoxia [17]. However, studies on the effects of hypoxia in HNSCC patients in relation to HPV infection and favorable treatment outcomes have been inconclusive [18].

During the malignant transformation of tumor cells, increased expression of aspartate β -hydroxylase (ASPH) has been observed [19]. ASPH belongs to the α -ketoglutarate-dependent dioxygenase family and can serve as an oxygen sensor in cells. It hydroxylates aspartyl and asparaginyl residues mainly in epidermal growth factor-like protein domains, including domains in Notch receptors and ligands, and is thus able to influence numerous cell signaling pathways. ASPH is abundantly expressed in proliferating trophoblast cells, but its activity is low or absent in adult tissues. ASPH overexpression has been shown in many types of carcinomas, including HNSCC, and has been associated with increased tumor cell migration, invasiveness and metastasis, and a significantly negative patient prognosis [20].

This study aimed to compare the expression of ASPH and selected hypoxia markers as potential therapeutic targets at the mRNA and protein levels and determine the prognostic significance of these markers in patients in relation to the viral etiology of HNSCCs.

Materials and methods

Study population

Tissue samples from HNSCCs were collected in a previous study at the Department of Otorhinolaryngology and Head and Neck Surgery, First Faculty of Medicine, Charles University, and Motol University Hospital, Prague, in 2017–2020 [21]. The study was approved by the Ethics Committee of Motol University Hospital, Prague, on 22 June 2016. All patients provided signed informed consent and completed a questionnaire on the risk factors for HPV infection and the induction of HNSCC.

Sample processing and characterization

The samples were processed as described previously [21]. Briefly, after surgical resection, histological examination and pTpn classification (UICC, 8th edition) [22], the tumor was divided by a pathologist into two parts. One part of the tissue sample was fixed in 10% neutral formalin and paraffin-embedded (FFPE) and the other part of the fresh tumor tissue was transported to the laboratory in RPMI medium (Sigma-Aldrich, St. Louis, MO, USA) at 4 °C. The tumor cells together with the tumor-infiltrating cells were immediately isolated from the tumor tissue using the gentleMACS system (Miltenyi Biotec, Auburn, CA, USA). The cell suspension was stored in RNeasy[®] stabilization solution (Life Technologies, Carlsbad, CA,

USA) at -80 °C until further processing. DNA and total RNA were isolated using NucleoSpin® RNA/DNA Buffer Set (Macherey Nagel, Germany) according to the manufacturer's protocol. The concentration of the nucleic acids was measured using a NanoDrop 2000 Spectrophotometer (Thermo Fisher Scientific, Waltham, MA, USA) and the quality and integrity of the RNA were verified by the Experion™ automated electrophoresis system (Bio-Rad, Hercules, CA, USA) according to the manufacturer's protocol.

The presence and genotype of HPV were evaluated by PCR with broad spectrum GP5+/6+-5'-bio primers followed by reverse-line blot analysis, and active viral infection was determined by type-specific HPV E6 mRNA detection, both of which were performed as described previously [23, 24].

Quantification of mRNA expression by quantitative PCR (qPCR)

Total RNA was treated with DNase I (Jena Bioscience, Jena, Germany) and reverse transcribed in a 20- μ l reaction mixture using M-MLV Reverse Transcriptase (Promega, Madison, USA) and random hexamers (IDT, Leuven, Belgium), both according to the manufacturer's instructions.

Gene-specific primers to determine the mRNA expression of ASPH and selected hypoxia markers (HIF1A - HIF1, subunit alpha; SLC2A1 - solute carrier family 2, member 1; P4HA1; VEGFA; EPAS1 - endothelial PAS domain protein 1) were designed and evaluated in our laboratory or by the Gene Core-qPCR and ddPCR Core Facility (BIOCEV, Vestec, Czech Republic) (Table 1). Quantitative PCR was performed with SYBR Green chemistry (Xceed qPCR SG 2 \times mix Lo-ROX reaction

buffer; IAB, Czech Republic) on CFX96™ Touch cycler (Bio-Rad Laboratories, Hercules, CA, USA). Briefly, the 10- μ l reaction consisted of 1 \times Xceed reaction buffer, 400 nM each of forward and reverse primers and 2 μ l of 4 \times diluted cDNA. The amplification consisted of the following steps: initiation of denaturation (3 min at 95 °C), 40 cycles of amplification (10 s at 95 °C and 30 s at 60 °C) with fluorescence reading in the SYBR Green channel and melting curve analysis at the end of the run.

The amplification plots were analyzed using Bio-Rad CFX Maestro software (Bio-Rad Laboratories, Hercules, CA, USA). The relative quantification of mRNA expression was assessed by the $\Delta\Delta$ Ct method using GenEx™ v6 software (TATAA Biocenter, Goteborg, Sweden).

Multispectral immunohistochemistry (mIHC)

From the FFPE samples, 2 μ m-thick sections were prepared on SuperFrost® Plus slides (VWR, Belgium). Prior to antibody staining, the FFPE slides were processed as described previously [21]. Heat-induced antigen retrieval (AR) was performed using a microwave in either AR6 (Akoya Biosciences, Menlo Park, CA, USA) or AR9 (Zytomed Systems, Berlin, Germany) buffer, depending on the particular antibody, and the tissue was blocked using Antibody Diluent/Block (Akoya Biosciences) at room temperature (RT) for 10 min. First, we validated the staining pattern of the primary antibodies (ASPH, polyclonal, Novus Biological [Centennial, CO, USA]; HIF1A, clone HA111, Novus Biological; GLUT1, clone EPR3915, Abcam [Cambridge, United Kingdom]; VEGFA, clone EP1176Y, Biocare Medical [Pacheco, CA, USA]; MMP9, clone 5G3, Abcam / Thermo Fisher Scientific [Waltham, MA, USA]; MMP13, clone VIII A2, Thermo Fisher Scientific; CK - cytokeratin, clone AE1/AE3, Thermo Fisher

Table 1 Primer pairs used for quantification of mRNA expression by qPCR and expected amplicon lengths

Gene	Name		Sequence 5'-3'	Product length (bp)
ASPH	Aspartate β -hydroxylase	F	TGGTGATCCCAAGGAAGGC	110
		R	CTGCCATACCTCGTGCTCAA	
HIF1A	Hypoxia inducible factor 1, subunit alpha	F	ACCCATTCCTCACCCATCAA	134
		R	GTTCCTCTGGCTCATATCCCATC	
SLC2A1	Solute carrier family 2, member 1	F	TGGCTACAACACTGGAGTCATC	128
		R	CTGAGAGGGACCAGAGCCGTG	
P4HA1	Prolyl 4-hydroxylase, subunit alpha 1	F	AGTACATGACCCCTGAGACTGGA	84
		R	GGATTTTCATAGCCAGAGAGCC	
VEGFA	Vascular endothelial growth factor A	F	GCTGTCTGGGTGCATTGG	69
		R	GCAGCCTGGGACCACTTG	
EPAS1	Endothelial PAS domain protein 1	F	TCAAAGGGCCACAGCGACAA	131
		R	CCAGCTCATAGAACACCTCCGT	
GUSB	Glucuronidase beta (reference gene)	F	GAAAATATGTGGTTGGAGAGCTCATT	101
		R	CCGAGTGAAGATCCCCTTTTTA	
ACTB	Actin beta (reference gene)	F	CCACGAAACTACCTTCAACTCCA	132
		R	GTGATCTCCTTCTGCATCTGTC	

F - forward primer, R - reverse primer

Scientific). All primary antibodies were diluted in Antibody Diluent/Block except VEGFA, for which Van Gogh Yellow Diluent (Medical Bio Care, Germany) was used. This was followed by incubation with Opal Polymer HRP Ms+Rb as a secondary antibody, then with Opal™ fluorophores, and DAPI counterstain (all from Akoya Biosciences) according to the manufacturer's instructions. The stained slides were mounted with Fluoromount™ Aqueous Mounting Medium (Sigma-Aldrich, St. Louis, MO, USA). No primary and isotype controls were performed to ensure staining specificity.

Two multiplex panels (A and B) were designed according to the pattern and labelling intensity of the selected antibodies (Table 2) (Additional file 1). Each antibody was assigned to an Opal™ fluorophore with respect to its intensity and possible spectral overlap. After staining with each antibody, the complex of primary and secondary antibodies was removed using AR buffer. Stripping controls were performed to ensure complete removal of this complex.

Five to eight representative regions of interest were randomly selected for each slide, focusing on high-quality tumor tissue, and imaged at 10×20 magnification on an Olympus BX43 microscope (Olympus Life Science, USA) using Mantra™ Snap 1.0.0 software (Akoya Biosciences). Images were analyzed using InForm 2.6.0 software (Akoya Biosciences) with pre-built algorithms unique to each panel. The algorithms consisted of linear unmixing of fluorescence spectra and trainable steps of tissue segmentation into the tumor parenchyma (CK-positive), stroma (CK-negative), and background (DAPI-free); step of cell segmentation (nuclei, cytoplasm, and membrane parts); and cell phenotyping. Each step of the algorithm was optimized on a set of different images and subsequently applied to the remaining images. The process of workflow optimization was described previously [5] and was used in this study. Finally, for each sample, three regions of the highest quality were selected from the captured images and then analyzed. For mIHC data analyses, the total number of positive cells was divided by

the analyzed area (mm²) to obtain comparable, standardized values for the whole area or for the parenchymal and stromal areas separately.

Statistical analyses

For statistical analyses, the samples were divided into two groups, HPV-positive (HPV+) and HPV-negative (HPV-), based on E6 mRNA HPV positivity, i.e., active HPV infection. The homogeneity of the two groups for various patients' characteristics was tested using the chi-square test, Fisher exact test or the Mann-Whitney U test. Subsequently, the Mann-Whitney U or Student's t-test was used to evaluate the differences in relative mRNA expression and the number of positive cells per mm² for each marker tested between tumor groups. Differences between the number of positive cells in the tumor parenchyma and stroma were compared using the paired Wilcoxon test. Pearson and Spearman correlation coefficients were used to assess the correlation between the expression of each marker at the mRNA and protein levels, respectively. The Cox proportional hazard model was used for overall survival (OS) and disease-specific survival (DSS) multivariate analyses. In addition to patient characteristics, tumor clinicopathological characteristics and HPV status, the models included the marker levels from mIHC, separately for the tumor parenchyma, stroma, and total tumor area. The best models were selected according to the Bayesian information criterion (BIC) and Akaike information criterion (AIC). The hazard ratios (HRs) presented below correspond to a difference of 1000 positive cells/mm². The level of significance was considered to be $p < 0.05$ for all the statistical tests. Statistical analyses were performed using GraphPad Prism 8.4.3 (GraphPad Software, Boston, MA, USA) and R version 4.1.2 (R Foundation for Statistical Computing, Vienna, Austria).

Table 2 Antibody panels for mIHC

Panel	#	Primary antibody (dilution, incubation)	AR buffer (incubation)	Secondary antibody	OPAL (dilution)
A	1	VEGFA (1:150, OVN/4°C)	AR9 (30 min)	Opal Polymer HRP Ms+Rb	540 (1:200)
	2	HIF1A (1:200, 1 h/RT)	AR6 (60 min)		520 (1:100)
	3	ASPH (1:1200, OVN/4°C)	AR6 (15 min)		620 (1:100)
	4	Cytokeratin (1:1000, 1 h/RT)	AR6 (15 min)		690 (1:200)
	5	DAPI (1:15, 5 min/RT)			
B	1	MMP13 (1:200, OVN/4°C)	AR9 (30 min)	Opal Polymer HRP Ms+Rb	650 (1:150)
	2	GLUT1 (1:600, 1 h/RT)	AR9 (15 min)		520 (1:150)
	3	MMP9 (1:900, OVN/4°C)	AR9 (25 min)		570 (1:150)
	4	Cytokeratin (1:1000, 1 h/RT)	AR6 (30 min)		690 (1:200)
	5	DAPI (1:15, 5 min/RT)			

AR - antigen retrieval buffer; HRP - horseradish peroxidase, OVN - overnight, RT - room temperature

Results

Study population and characterization of tumor samples

The detailed clinical and pathological characteristics of the study population are summarized in Table 3. A total of 93 HNSCC patients were enrolled. The mean age of the patients was 61.5 years (range 39–89 years), and the majority of the patients were men (70/93; 75.3%). Most of the tumors 73/93 (78.5%) were located in the oropharynx, while 20/93 (21.5%) were located in the oral cavity. For expression analyses at the mRNA level, samples of 67 patients and at the protein level, samples of 93 patients were available.

The overall prevalence of HPV DNA in the samples was 61/93 (65.6%). High-risk HPV 16 was detected in 95.1% (58/61) of HPV DNA-positive tumors. Two samples were positive for HPV 35 (2/61; 3.3%), and one was positive for HPV 33 (1/61; 1.6%). None of the oral cavity tumors were HPV DNA positive. Based on the presence of HPV E6 mRNA, we stratified the samples into HPV-associated (HPV+; 60/93 (64.5%)) and HPV-negative tumor groups (HPV-; 33/93 (35.5%)). One sample positive for HPV DNA and negative for HPV E6 mRNA was included in HPV- group.

The mRNA expression of ASPH and hypoxia markers was similar regardless of the tumor etiology

Sixty-seven samples were eligible for mRNA expression testing (46 HPV-positive and 21 HPV-negative). We examined the mRNA expression levels of the selected markers and ASPH by reverse transcription followed by qPCR using the relative quantification method. Except for the mRNA expression of *EPAS1* ($p < 0.05$) (Fig. 1), the comparison of the expression of selected markers in HPV-negative and HPV-positive HNSCC groups showed no differences. The statistically significantly positive correlations were found between the expressions of ASPH and *P4HA1* ($r = 0.63$, $p < 0.0001$), ASPH and *EPAS1* ($r = 0.57$, $p < 0.0001$), ASPH and *VEGFA* ($r = 0.55$, $p < 0.0001$), and ASPH and *SLC2A1* mRNAs ($r = 0.31$, $p < 0.01$) (data not shown).

The numbers of cells expressing ASPH and hypoxia markers were markedly different between HPV-positive and HPV-negative tumors, as well as in different tumor compartments

The expression of selected markers at the protein level was determined by the mIHC method, which allows us to reveal the complexity of the tumor microenvironment in a spatial context. In contrast to the lack of differences in the mRNA expression of most of the selected markers, we observed marked differences in the count of cells producing the majority of the evaluated markers between the HPV-positive and HPV-negative groups.

When the results were stratified by tumor etiology, cells producing ASPH ($p < 0.0001$), and HIF1A ($p < 0.0001$) were more abundant in the parenchyma of HPV-positive tumors compared to the parenchyma of HPV-negative group. In the HPV-positive tumor group, GLUT1- ($p < 0.0001$) and MMP13-positive cells ($p < 0.05$) were more abundant in both tumor compartments compared to the HPV-negative tumor group (Fig. 2A). On the contrary, the HPV-negative samples showed a higher number of VEGFA-positive cells in the tumor parenchyma than the HPV-positive group ($p < 0.05$). The number of VEGFA-positive cells in the stroma was similar in both groups of patients (Fig. 2B).

Furthermore, when stratifying the results by tumor compartment, the number of parenchymal cells expressing ASPH ($p < 0.0001$), HIF1A ($p < 0.0001$ for HPV-positive; $p < 0.001$ for HPV-negative), and GLUT1 ($p < 0.0001$) was significantly higher compared to the number of positive stromal cells in both HNSCC groups. In contrast, the number of MMP9- ($p < 0.01$) and MMP13-positive cells ($p < 0.01$ for HPV-positive; $p < 0.05$ for HPV-negative) was significantly higher in the stroma of both tumor groups (Fig. 2).

In addition to the above analysis, we compared the positive cells counts in the total tumor area (parenchyma and stroma) in both tumor groups. Significantly higher numbers of cells expressing ASPH ($p < 0.0001$) and the hypoxia markers – HIF1A ($p < 0.0001$), GLUT1 ($p < 0.0001$), and MMP13 ($p < 0.05$) – were detected in HPV-positive than in HPV-negative tumors (Additional file 2A). There were also marked differences in the positive cell counts when comparing different tumor compartments without HPV status stratification (Additional file 2B). The numbers of cells expressing ASPH ($p < 0.0001$), HIF1A ($p < 0.0001$), and GLUT1 ($p < 0.0001$) were significantly higher in the tumor parenchyma compared to the stroma, while cells expressing MMP13 ($p < 0.001$) and MMP9 ($p < 0.0001$) were more abundant in the stroma of HNSCCs (Additional file 2B). These findings are similar to the analysis involving HPV status (Fig. 2).

Several hypoxia markers were strongly correlated

We observed strong positive correlation in the parenchymal and stromal count of cells expressing MMP13 and MMP9 in both group of samples independent their HPV status (HPV-positive tumors: parenchyma $rS = 0.602$, $p < 0.001$, stroma $rS = 0.710$, $p < 0.001$; HPV-negative tumors: parenchyma $rS = 0.665$, $p < 0.001$, stroma $rS = 0.659$, $p < 0.001$). Additionally, a significantly positive correlations were observed in the abundance of parenchymal cells producing ASPH and GLUT1 ($rS = 0.428$, $p < 0.001$), ASPH and HIF1A ($rS = 0.285$, $p < 0.05$), ASPH and MMP13 ($rS = 0.499$, $p < 0.001$), and ASPH and MMP9 ($rS = 0.361$, $p < 0.01$) in the HPV-positive tumor group.

Table 3 Clinical and pathological characteristics of the study population. Samples were stratified into HPV-positive (HPV+), and HPV-negative (HPV-) groups based on the presence of an active HPV infection. Tumor classification is based on the 8th TNM Staging System [22], which includes tumor extent (T), extent of lymph node spread (N), and presence of metastasis (M)

Patients	HPV+ group	HPV- group	Total	p-value ^c
	No. (%)	No. (%)	No. (%)	
No. of patients	60 (64.5)	33 (35.5)	93 (100.0)	
Age (years) ^{##}				0.6615
Mean	61.9	60.8	61.5	
Median	60.5	62.0	61.0	
Range (years)	39–87	46–83	39–87	
Gender [§]				0.0293
Male	50 (83.3)	20 (60.6)	70 (75.3)	
Female	10 (16.7)	13 (39.4)	23 (24.7)	
Tumor location [§]				<0.0001
Oropharynx	60 (100.0)	13 (39.4)	73 (78.5)	
Oral cavity	0 (0.0)	20 (60.6)	20 (21.5)	
Smoking status [§]				0.0076
Never	27 (45.0)	5 (15.2)	32 (34.4)	
Past/current	33 (55.0)	28 (84.8)	61 (65.6)	
Alcohol consumption [§]				0.0361
Never	23 (38.3)	5 (15.2)	28 (30.1)	
Past/current	37 (61.7)	28 (84.8)	65 (69.9)	
Metastasis [§]				0.0420
Absent	60 (100.0)	30 (90.9)	90 (96.8)	
Present	0 (0.0)	3 (9.1)	3 (3.2)	
p16 status [§]				<0.0001
Positive	58 (96.7)	0 (0.0)	58 (62.4)	
Negative	2 (3.3)	33 (100.0)	35 (37.6)	
Tumor size (pT) [§]				0.1252
T1	16 (26.7)	11 (33.3)	27 (29.0)	
T2	41 (68.3)	16 (48.5)	57 (61.3)	
T3	2 (3.3)	3 (9.1)	5 (5.4)	
T4	1 (1.7)	3 (9.1)	4 (4.3)	
Nodal status (pN) [§]				0.0001
N0	16 (26.7)	19 (57.6)	35 (37.6)	
N1	37 (61.6)	5 (15.2)	42 (45.2)	
N2	6 (10.0)	4 (12.1)	10 (10.8)	
N3	1 (1.7)	5 (15.2)	6 (6.4)	
Extracapsular spread [§]				0.1413
Absent	39 (65.0)	27 (81.8)	66 (71.0)	
Present	21 (35.0)	6 (18.2)	27 (29.0)	
Tumor stage (pS) [§]				<0.0001
I	48 (80.1)	8 (24.2)	56 (60.2)	
II	8 (13.3)	8 (24.2)	16 (17.2)	
III	2 (3.3)	4 (12.1)	6 (6.5)	
IV	2 (3.3)	13 (39.4)	15 (16.1)	
Adjuvant treatment [§]				0.0198
Radiotherapy	24 (40.0)	19 ^a (57.6)	43 (46.2)	
Chemoradiotherapy	26 (43.3)	5 ^b (15.2)	31 (33.3)	
Not specified	2 (3.3)	0 (0.0)	2 (2.2)	
No	8 (13.3)	9 (27.3)	17 (18.3)	

^a Including one patient who received radiotherapy after a recurrence and one patient who died before radiotherapy^b Including one patient with resection after chemoradiotherapy^c p-value for homogeneity of the two HNSCC groups for various patient characteristics was tested using the chi-square test[§], Fisher exact test[§] or the Mann-Whitney test^{##}

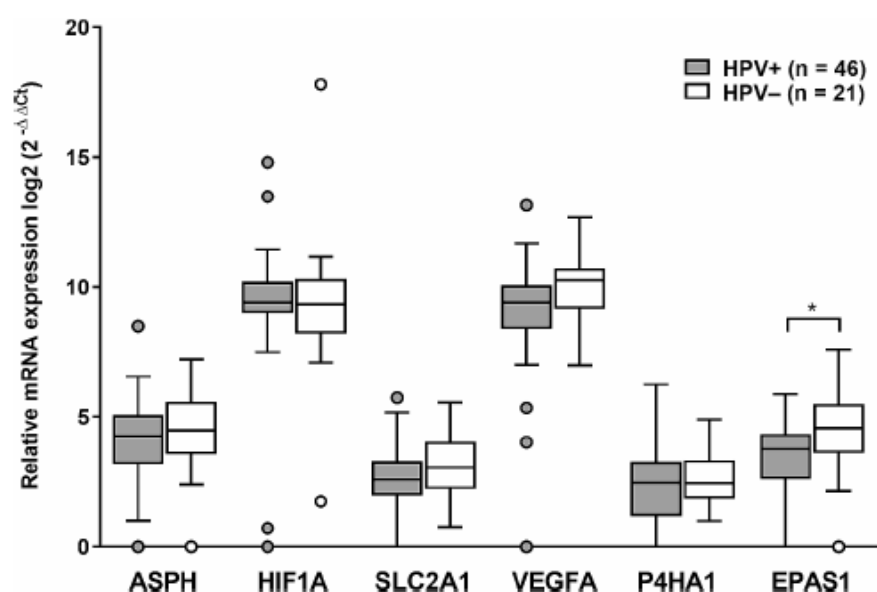


Fig. 1 mRNA expression in groups of HPV-positive (HPV+) and HPV-negative (HPV-) HNSCCs. The median values are indicated, the box borders show the upper and lower quartiles, the whiskers show the variability, and outliers are indicated. * $p < 0.05$

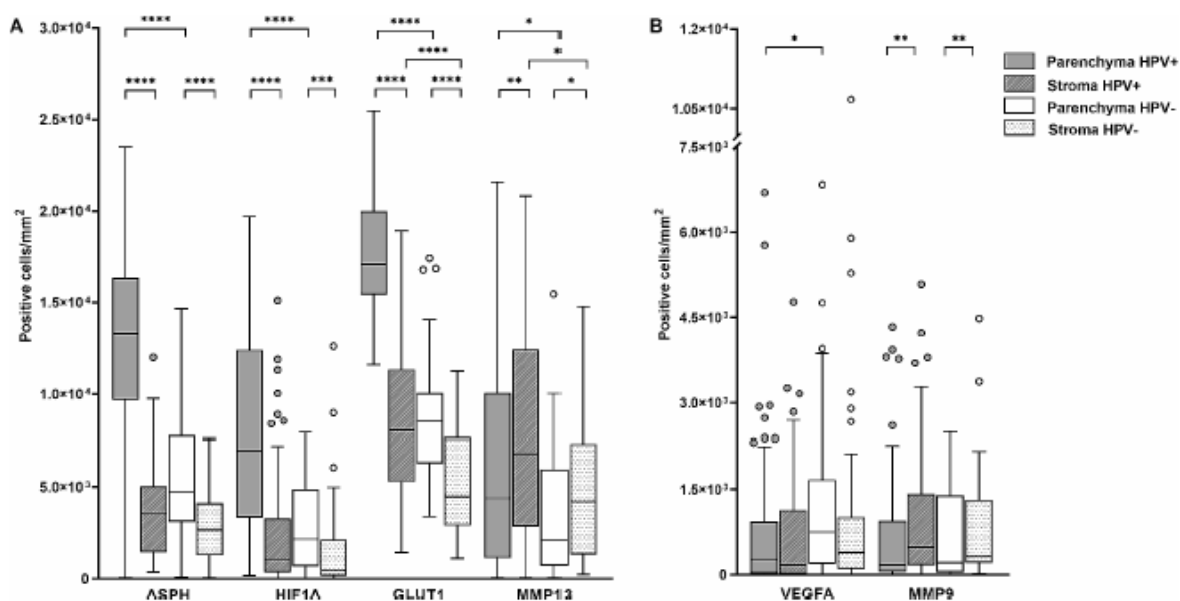


Fig. 2 Protein markers detected by mIHC in the parenchyma and stroma of HPV-positive (HPV+) and HPV-negative (HPV-) HNSCCs. Graphs show the number of cells producing (A) ASPH, HIF1A, GLUT1, and MMP13, and (B) VEGFA and MMP9. The median values are indicated; the box borders show the upper and lower quartiles; the whiskers show the variability, and outliers are indicated. * $p < 0.05$, ** $p < 0.01$, *** $p < 0.001$, **** $p < 0.0001$

In the parenchyma of HPV-negative cohort of tumors, the positive correlation was detected between ASPH and HIF1A ($rS=0.470$, $p < 0.01$), GLUT1 and MMP13 ($rS=0.456$, $p < 0.01$), and GLUT1 and MMP9 ($rS=0.481$, $p < 0.01$) numbers of cells. A significantly negative correlation was observed between VEGFA- and

GLUT1-positivity ($rS=-0.307$, $p < 0.05$) in the parenchyma of HPV-positive tumors (Fig. 3).

Associations of hypoxia markers with patient outcomes

In both etiologically distinct groups of tumors, we compared the number of parenchymal and stromal cells positive for the analyzed markers between patients who

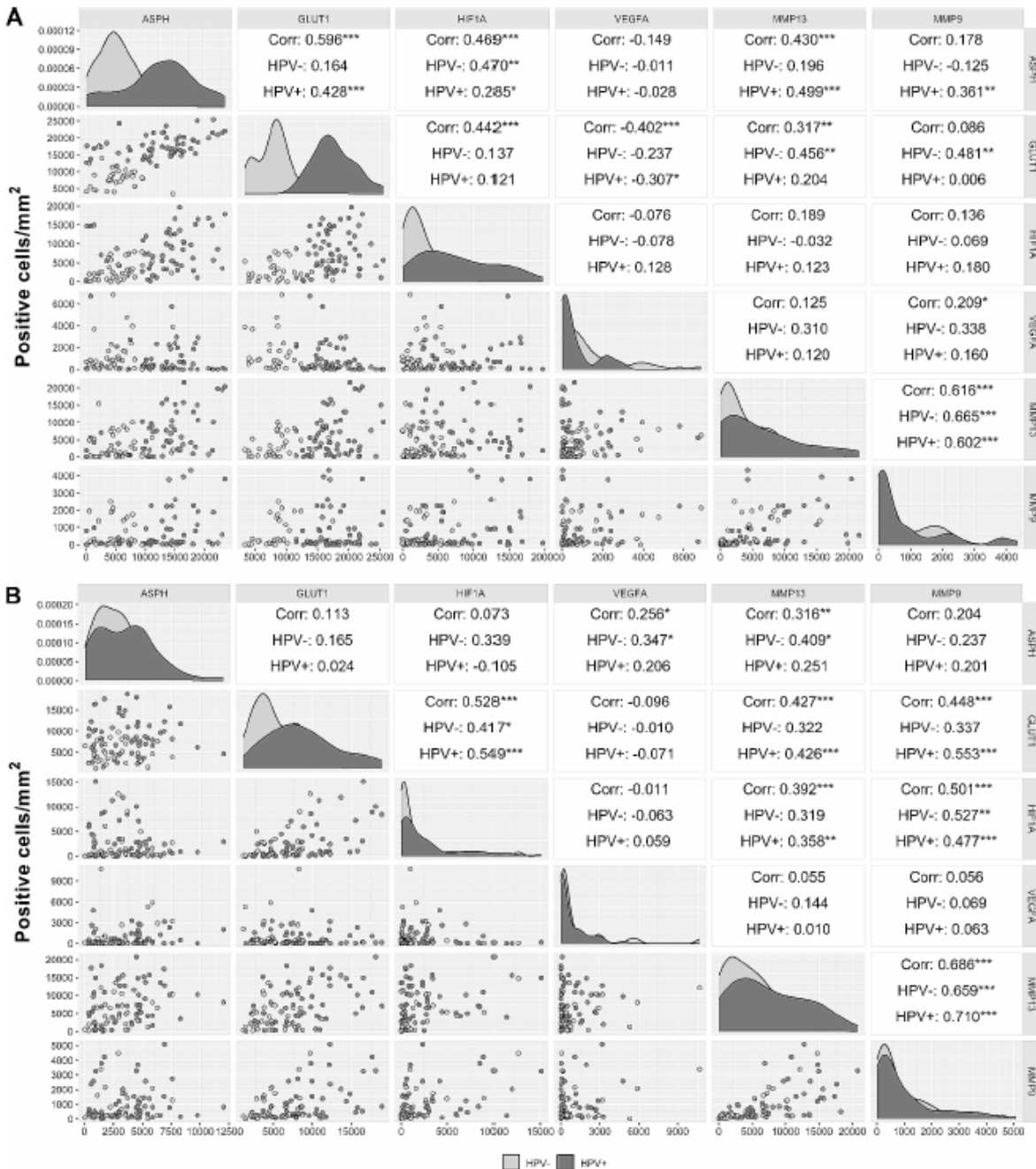


Fig. 3 Correlation of the number of cells producing ASPH and hypoxia markers in the parenchyma (A) and the stroma (B) of HNSCCs. The viral etiology of the tumors is indicated by the color. Spearman correlation coefficient is determined for the whole cohort of HNSCCs (Corr), and separately according to viral etiology of tumors (HPV+, HPV-). * $p < 0.05$, ** $p < 0.01$, *** $p < 0.001$

died and those who were alive at follow-up. The results showed that the number of parenchymal cells producing HIF1A was higher in patients who were alive, but the difference was statistically significant only in the HPV-negative group ($p < 0.05$). In addition, MMP13 and MMP9

counts of positive parenchymal cells were significantly higher in the patients who died ($p < 0.05$ and $p < 0.0001$, respectively), but these differences were observed only in the HPV-positive group of subjects (Fig. 4).

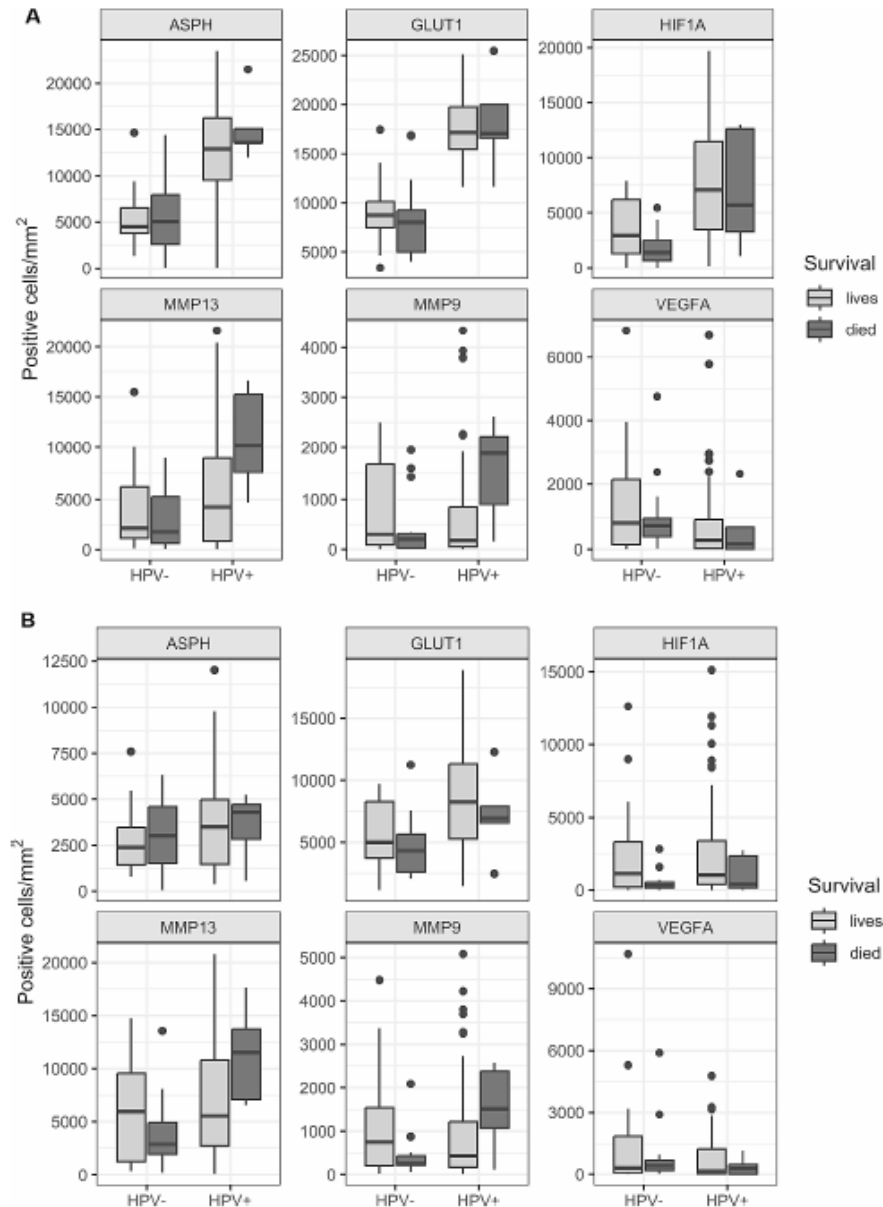


Fig. 4 Association of ASPH and hypoxia markers in the parenchyma (A) and the stroma (B) of HNSCCs according to HPV etiology of tumors and patient outcomes

Analyses of overall and disease-specific survival showed the prognostic significance of GLUT1- and HIF1A-positive cell counts

The mIHC results were used in multivariate Cox proportional hazards models to determine the impact of ASPH and hypoxia marker expression on patient prognosis. The best models selected by the BIC for initial evaluation included HPV status and age for both OS (HPV, HR=0.125, $p=0.001$; age, HR=1.061, $p=0.020$) and DSS (HPV, HR=0.141, $p=0.002$; age, HR=1.075, $p=0.019$).

Each of the IHC markers was evaluated in these models in the whole tumor area and separately in the tumor parenchyma and stroma. None of the selected IHC markers were significantly prognostic for OS or DSS. The best model for improved OS included younger age, positive HPV status, and higher numbers of cells producing HIF1A but without statistical significance ($p=0.060$) (Additional file 3). We also tested Cox models in which the HPV status, the strongest prognostic factor, was omitted. According to these models, the numbers of

GLUT1-positive cells in the whole tumor area and also separately in the tumor parenchyma and stroma were prognostic factors for both OS (HR=0.802, $p<0.0001$; HR=0.852, $p<0.0001$; HR=0.814, $p=0.007$, respectively) and DSS (HR=0.814, $p=0.005$; HR=0.862, $p=0.009$; HR=0.842, $p=0.032$, respectively). Furthermore, the numbers of cells producing HIF1A in the whole tumor area (HR=0.729, $p=0.003$), tumor parenchyma (HR=0.829, $p=0.008$), and stroma (HR=0.616, $p=0.027$) were prognostic factors for OS. The number HIF1A-positive cells in the whole tumor area (HR=0.773, $p=0.021$) was also prognostic for DSS. These results also support our observation of a close relationship between HPV status and the numbers of cells producing GLUT1 and HIF1A proteins in HNSCCs (Fig. 3).

Discussion

We investigated the expression of ASPH and selected hypoxia markers in relation to the viral etiology of HNSCC and patient survival. The abundance of cells producing ASPH and the hypoxia markers GLUT1, HIF1A, and MMP13 were statistically significantly higher in the group of HNSCC samples associated with HPV infection, while almost no differences were detected at the mRNA level. We demonstrated a strong correlation between high number of GLUT1-positive cells and HPV positivity and consequently observed an association of the higher numbers of GLUT1- and/or HIF1A-producing cells with improved OS or DSS in HNSCC patients in Cox hazard models where the HPV status was omitted.

To our knowledge, this is the first study to evaluate ASPH expression in clinical samples of HNSCC patients in relation to the viral status of tumors. High expression of the *ASPH* gene has been identified as a component of the oxygen-sensing gene signature associated with poor prognosis in patients with several types of carcinomas, including HNSCC [25]. However, the viral etiology of HNSCC was not considered in that study, and tumors of different anatomical locations of head and neck were combined into one group. In our analyses, we found a significantly increased abundance of cells producing ASPH at the protein level in HPV-positive samples. High ASPH production has been associated with more aggressive tumor behavior and metastasis in many types of solid tumors [20]. However, this marker was not recognized as an independent risk factor for patient survival in our study.

Factors that contribute to ASPH upregulation include growth factors that also activate the phosphatidylinositol-3-kinase/protein kinase B (PI3K/Akt) signaling pathway [26]. Since activation of PI3K/Akt signaling is essential for HPV-induced carcinogenesis [27], it could be responsible for the increased ASPH synthesis in HPV-positive HNSCCs found in our study. Increased ASPH

expression may also be mediated by HIF1A activity, as has been shown in neuronal cells [28].

In our group of clinical samples, where HPV-positive tumors predominated, we found no differences in the tested gene expression patterns that were associated with HPV status, except for the *EPAS1* gene. In contrast to those at the mRNA level, the numbers of cells producing ASPH and hypoxia markers at the protein level were significantly different between the non-HPV and HPV-positive tumor groups. Expression of genes at the mRNA level may differ from that at the protein synthesis level, as has been repeatedly demonstrated [29, 30]. In addition, the selective translation of mRNAs, which are essential for cell survival, may play a role in hypoxia [31].

Finally, the influence of HPV infection on cellular regulation cannot be excluded. The significant relationship between HR HPV 16 infection and HIF1A expression has been demonstrated in various cancers, including cervical, lung cancer and HNSCC [16, 32–34]. The central hypoxia factor HIF1A can also be stabilized by direct interaction with the HPV 16 E6 oncoprotein [13] and accumulated under normoxic conditions [35]. In the study by Rodolico et al. [36], an oxygen-independent positive association was observed between HIF1A and HPV 16 E7 immunoreactivity in oral squamous cell carcinoma. The significantly elevated numbers of cells producing HIF1A protein observed in HPV-associated tumors in our study may therefore be a consequence of HPV infection rather than a manifestation of actual tumor hypoxia.

Patients with HPV-positive HNSCCs have a better overall prognosis and the tumors are more radiosensitive [2]. According to the Cox proportional hazard models, a positive HPV status and younger patient age improved both OS and DSS in our study, which is in agreement with the conclusions of our study and other previous studies [5, 37, 38]. In these models, we did not observe a significant relationship between the number of cells producing ASPH or the hypoxia markers and the prognosis of HNSCC patients. On the contrary, in the models where the HPV status was omitted, we found that higher levels of cells producing HIF1A and GLUT1, which may reflect the HPV status of tumors, were associated with improved OS and DSS in HNSCC patients. As mentioned above, tumor hypoxia may be connected with treatment failure and poor patient prognosis [8]. In a systematic review, Gong et al. showed a significant association between HIF overexpression and increased mortality risk in HNSCC patients [39]. However, in detailed subgroup analyses, they observed a significantly increased mortality risk associated with HIF1A overexpression in studies from Asia, but not in European patients. In addition, the prognostic value of increased HIF1A expression varied in different HNSCC disease subgroups. Consistent with our study, two studies included in the previous meta-analysis

demonstrated significantly better OS and also disease-free survival in HNSCC patients with increased HIF1A protein levels [40, 41].

Alterations in cellular metabolism and adaptation to increased energy consumption by cancer cells have been shown in a variety of tumors [7]. This is associated with increased glucose transport and elevated activity of glycolytic enzymes. Among the glucose transporters, GLUT1, the product of the *SLC2A1* gene, has received the most attention from researchers, and its upregulation has been recognized as a negative prognostic factor in many tumor types. Two meta-analyses have reported an adverse impact of GLUT1 overexpression in solid tumors, including oral squamous cell carcinoma, on patient outcomes [42, 43]. However, these studies did not consider HPV tumor status, and oral cancers are rarely associated with HPV infection. In our study, significantly higher numbers of GLUT1-positive cells were found in the group of HPV-positive HNSCCs. An active HPV infection may again play a role, as HPV proteins stimulate cellular signaling pathways that promote glucose uptake and glycolysis [44]. In HPV-positive lung carcinomas, the studies by Fan et al. [45] and Tang et al. [33] showed that GLUT1 expression could be affected by the activities of HPV 16 E6/E7 oncoproteins.

In our study, multiplex IHC analysis allowed us to further assess the spatial distribution of ASPH and other hypoxia markers in the tumor microenvironment. While ASPH-, HIF1A-, and GLUT1-positive cells were more abundant in the tumor parenchyma, MMP9/13-expressing cells were more abundant in the tumor stroma. As MMPs are also known to be products of stromal fibroblasts, lymphocytes, granulocytes, and activated macrophages, this may reflect the higher infiltration of these cells in the stroma compared to the parenchyma of HNSCCs, which has been described by our group in the previous study [21] as well as by others [46, 47]. In addition, the E7 oncoprotein of high-risk HPV has been recognized as a factor directly contributing to the increased expression of MMPs, including MMP9 [48]. Therefore, HPV-infected keratinocytes may exhibit more aggressive behavior than those not infected with the virus. Our study showed significantly increased numbers of cells producing MMP13 but not MMP9 in patients with HPV-positive tumors, and in these patients, the increased level of MMP9/13-positive cells suggested a worse OS compared to the patients with lower abundance of MMP9/13-positive cells.

Among other hypoxia markers, the expression of VEGFA, the key proangiogenic factor in the tumor microenvironment that promotes tumor neovascularization, was evaluated. In addition to HIF1A, VEGFA expression is also supported by the HPV E6 and E7 oncoproteins, suggesting a possible difference in VEGFA

levels in tumors of different etiologies [49]. In our study, similar levels of VEGFA mRNA were observed in both groups. In contrast to our findings, higher VEGFA mRNA levels have been reported in HPV-positive samples compared to HPV-negative ones [50] and, inconsistently, the overexpression of *VEGFA* in p16-negative samples corresponding to HPV-negative tumors has been reported [51]. In our study, higher numbers of VEGFA-positive cells were detected in the parenchyma and the whole tumor area of HPV-negative samples compared to the HPV-positive samples. These data confirm the results of our retrospective study in HNSCC patients (unpublished data) and are consistent with the findings of Baruah et al. [52], who observed higher VEGFA levels in the parenchyma of p16-negative HNSCC patients. Several studies have observed the same level of the VEGFA protein in tumors regardless of HPV status [37, 50, 53]. These discrepancies may be due to the different methodologies used for VEGFA quantification – the very precise method used in our study (positive cell count/mm²) and the less precise method used in other studies (weak vs. strong expression).

We did not observe any effect of the VEGFA-positive cell amount on prognosis, which is in line with the findings of some studies [37, 51] while worse OS or DSS has been found in HNSCC patients with increased VEGF protein level by others [54, 55]. However, in these studies, HPV status was not included in the survival analyses, which may have affected the results of these studies.

This study has several limitations. As the number of intact samples usable for reverse transcription and qPCR analyses was relatively low, the evaluated differences might not be statistically significant. Additionally, investigating the expression levels of viral oncoproteins, which may influence the protein level of hypoxia markers and their activity, would be interesting. The heterogeneity of the treatment modalities may also influence the prognostic impact of the variables analyzed in our study, but our cohort was relatively homogeneous because all patients were treated with surgery, and the majority with subsequent radiotherapy or chemoradiotherapy. Lastly, the majority of patients in our study had tumor localized in the oropharynx and more tumors were HPV-positive.

Conclusions

The examination of HNSCC samples suggested that elevated ASPH and hypoxia marker protein levels, typically indicative of unfavorable prognosis, may reflect the presence of active HPV infection, the strongest prognostic factor in HNSCC patients, rather than tumor hypoxia itself. Even in cases where HPV status is uncertain, increased expression of HIF1A and GLUT1 may serve as positive prognostic factors for HNSCC patients. It should

be considered when individualizing therapy for patients with HNSCC of different etiologies.

Abbreviations

AR	Antigen retrieval
ASPH	Aspartate- β -hydroxylase
CA9	Carbonic anhydrase 9
CK	Cytokeratin
DAPI	4',6-diamidino-2-phenylindole
DSS	Disease-specific survival
EPAS1	Endothelial PAS domain protein 1 (synonym HIF2A)
FFPE	Formalin-fixed paraffin-embedded
GLUT1	Glucose transporter protein type 1
HIF1	Hypoxia inducible factor 1
HNSCC	Head and neck squamous cell carcinoma
HPV	Human papillomavirus
HR	Hazard ratio
HRP	Horseshoe peroxidase
mIHC	Multispectral immunohistochemistry
MMP9	Matrix metalloproteinase 9
MMP13	Matrix metalloproteinase 13
OS	Overall survival
OVN	Overnight
P4HA1	Prolyl 4-hydroxylase subunit alpha 1
PDK1	Pyruvate dehydrogenase kinase 1
qPCR	Quantitative polymerase chain reaction
RT	Room temperature
SLC2A1	Solute carrier family 2, member 1
VEGFA	Vascular endothelial growth factor A

Supplementary Information

The online version contains supplementary material available at <https://doi.org/10.1186/s13027-024-00588-1>.

Additional file 1. Figure S1. Representative multispectral IHC staining of FFPE HNSCC tissue, 20x magnification. (A) Panel A: Staining of GLUT1 (magenta), MMP9 (green), MMP13 (orange), pan cytokeratin AE1/AE3 (CK, red), and DAPI (blue) antibodies. (B) Panel B: Staining of HIF1A (magenta), VEGFA (green), ASPH (yellow), CK (red), and DAPI (blue) antibodies.

Additional file 2. Figure S2. ASPH and other hypoxia markers detected by the mIHC in the groups of HPV-positive (HPV+) and HPV-negative (HPV-) tumors (A), and in the parenchyma and stroma (B) of HNSCCs. The median value is indicated; the box borders show the upper and lower quartiles, the whiskers show the variability, and outliers are indicated. * $p < 0.05$, ** $p < 0.01$, *** $p < 0.001$, **** $p < 0.0001$.

Additional file 3. Table S1. Hazard ratio (HR) values for hypoxia markers influencing overall survival (OS) and disease-specific survival (DSS).

Acknowledgements

The authors thank Jaroslav Nunvar for help with the data analysis and Pavlina Vesela and Nela Vaclavikova for their technical assistance.

Author contributions

R.T. and M.S. designed the research, R.T. acquired the funding and guided the project, M.G. evaluated samples histopathologically, J.K. enrolled patients and evaluated them clinically, V.K. and S.M. managed the patients' data, R.T., B.P., J.S., and M.S. designed and validated the methods, E.S. and J.S. performed the experiments, B.P., E.S., Q.V., and J.S. analyzed and visualized the results, R.T., J.S., and O.V. interpreted the results, J.S. and B.P. wrote the original draft, R.T., M.S., and J.K. critically revised and edited the draft. All the authors read and approved the final manuscript.

Funding

This work was supported by the Ministry of Education, Youth and Sports, Czech Republic, the Inter-Excellence programme (No. LTAUSA18003) and Charles University, Prague research project SVV260679, and the Project National Institute of Virology and Bacteriology (Programme EXCELES, ID

Project No. LX22NPO5103) - Funded by the European Union - Next Generation EU.

Data availability

The dataset supporting the conclusions of this article is available in the Zenodo repository; doi: 10.5281/zenodo.10405843.

Declarations

Ethics approval and consent to participate

The study was approved by the Ethics Committee of Motol University Hospital, Prague, on 22 June 2016. All patients provided signed informed consent.

Competing interests

The authors declare no competing interests.

Received: 19 January 2024 / Accepted: 28 May 2024

Published online: 10 June 2024

References

- Wittekindt C, Wagner S, Sharma SJ, Würdemann N, Knuth J, Reder H, et al. HPV - a different view on Head and Neck Cancer. *Laryngorhinootologie*. 2018;97(Suppl 1):S48-113.
- Göttgens E-L, Osteheimer C, Span PN, Bussink J, Hammond EM. HPV, hypoxia and radiation response in head and neck cancer. *Br J Radiol*. 2019;92:20180047.
- Almangush A, Jouhi L, Atula T, Haglund C, Mäkitie AA, Hagström J, et al. Tumour-infiltrating lymphocytes in oropharyngeal cancer: a validation study according to the criteria of the International Immunology-Oncology Biomarker Working Group. *Br J Cancer*. 2022;126:1589-94.
- Bisheshar SK, van der Kamp MF, de Ruiter EJ, Ruiter LN, van der Veegt B, Breimer GE, et al. The prognostic role of tumor associated macrophages in squamous cell carcinoma of the head and neck: a systematic review and meta-analysis. *Oral Oncol*. 2022;135:106227.
- Pokřivková B, Grega M, Klozar J, Vencálek O, Nurvää J, Tachezy R. PD1 + CD8 + cells are an independent prognostic marker in patients with Head and Neck Cancer. *Biomedicines*. 2022;10:2794.
- Semenza GL. HIF-1 and mechanisms of hypoxia sensing. *Curr Opin Cell Biol*. 2001;13:167-71.
- Maxwell PH, Pugh CW, Ratcliffe PJ. Activation of the HIF pathway in cancer. *Curr Opin Genet Dev*. 2001;11:293-9.
- Multhoff G, Vaupel P. Hypoxia compromises Anti-cancer Immune responses. *Adv Exp Med Biol*. 2020;1232:131-43.
- Swartz JE, Pothen AJ, van Kempen PMW, Stegeman I, Formisma FK, Cann EMV, et al. Poor prognosis in human papillomavirus-positive oropharyngeal squamous cell carcinomas that overexpress hypoxia inducible factor-1 α . *Head Neck*. 2016;38:1338-46.
- Hong A, Zhang M, Veillard A-S, Jahanbani J, Lee CS, Jones D, et al. The prognostic significance of hypoxia inducing factor 1- α in oropharyngeal cancer in relation to human papillomavirus status. *Oral Oncol*. 2013;49:354-9.
- Toustrup K, Sørensen BS, Alsner J, Overgaard J. Hypoxia Gene Expression Signatures as prognostic and predictive markers in Head and Neck Radiotherapy. *Semin Radiat Oncol*. 2012;22:119-27.
- Deschuymer S, Sørensen BS, Dok R, Laenen A, Hauben E, Overgaard J, et al. Prognostic value of a 15-gene hypoxia classifier in oropharyngeal cancer treated with accelerated chemoradiotherapy. *Strahlenther Onkol*. 2020;196:552-60.
- Nakamura M, Bodily JM, Beglin M, Kyo S, Inoue M, Laimins LA. Hypoxia-specific stabilization of HIF-1 α by human papillomaviruses. *Virology*. 2009;387:442-8.
- Bodily JM, Mehta KPM, Laimins LA. Human papillomavirus E7 enhances hypoxia-inducible factor 1-mediated transcription by inhibiting binding of histone deacetylases. *Cancer Res*. 2011;71:1187-95.
- Guo Y, Meng X, Ma J, Zheng Y, Wang Q, Wang Y, et al. Human papillomavirus 16 E6 contributes HIF-1 α induced Warburg effect by attenuating the VHL-HIF-1 α interaction. *Int J Mol Sci*. 2014;15:7974-86.
- Knuth J, Sharma SJ, Würdemann N, Holler C, Garvalov BK, Acker T, et al. Hypoxia-inducible factor-1 α activation in HPV-positive head and neck squamous cell carcinoma cell lines. *Oncotarget*. 2017;8:89681-91.

17. Bredell MG, Ernst J, El-Kochairi I, Dahlem Y, Ikenberg K, Schumann DM. Current relevance of hypoxia in head and neck cancer. *Oncotarget*. 2016;7:50781–804.
18. Wegge M, Dok R, Nuyts S. Hypoxia and its influence on Radiotherapy response of HPV-Positive and HPV-Negative Head and Neck Cancer. *Cancers (Basel)*. 2021;13:5959.
19. Ince N, Monte SM, de la, Wands JR. Overexpression of human aspartyl (asparaginyl) β -Hydroxylase is Associated with Malignant Transformation. *Cancer Res*. 2000;60:1261–6.
20. Kanwal M, Smahel M, Olsen M, Smahelova J, Tachezy R. Aspartate β -hydroxylase as a target for cancer therapy. *J Exp Clin Cancer Res*. 2020;39:163.
21. Pokrývková B, Šmahelová J, Dalewská N, Grega M, Vencálek O, Šmahel M, et al. ARG1 mRNA level is a promising prognostic marker in Head and Neck squamous cell carcinomas. *Diagnostics (Basel)*. 2021;11:628.
22. Amin MB, Greene FL, Edge SB, Compton CC, Gershenwald JE, Brookland RK, et al. The Eighth Edition AJCC Cancer staging Manual: continuing to build a bridge from a population-based to a more personalized approach to cancer staging. *CA Cancer J Clin*. 2017;67:93–9.
23. Tachezy R, Smahelova J, Salakova M, Arbyn M, Rob L, Skapa P, et al. Human papillomavirus genotype distribution in Czech women and men with diseases etiologically linked to HPV. *PLoS ONE*. 2011;6:e21913.
24. Rotnáglóvá E, Tachezy R, Saláková M, Procházková B, Košťálová E, Veselá E, et al. HPV involvement in tonsillar cancer: prognostic significance and clinically relevant markers. *Int J Cancer*. 2011;129:101–10.
25. Chang WH, Forde D, Lai AG. Dual prognostic role of 2-oxoglutarate-dependent oxygenases in ten cancer types: implications for cell cycle regulation and cell adhesion maintenance. *Cancer Commun (Lond)*. 2019;39:23.
26. Hou G, Xu B, Bi Y, Wu C, Ru B, Sun B, et al. Recent advances in research on aspartate β -hydroxylase (ASPH) in pancreatic cancer: a brief update. *Bosn J Basic Med Sci*. 2018;18:297–304.
27. Henken FE, Banerjee NS, Snijders PJF, Meijer CJLM, De-Castro Arce J, Rösl F, et al. PI3CA-mediated PI3-kinase signalling is essential for HPV-induced transformation in vitro. *Mol Cancer*. 2011;10:71.
28. Lawton M, Tong M, Gundogan F, Wands JR, de la Monte SM. Aspartyl-(asparaginyl) β -Hydroxylase, Hypoxia-Inducible Factor-1 α and notch cross-talk in regulating neuronal motility. *Oxid Med Cell Longev*. 2010;3:347–56.
29. Vogel C, Marcotte EM. Insights into the regulation of protein abundance from proteomic and transcriptomic analyses. *Nat Rev Genet*. 2012;13:227–32.
30. Edfors F, Danielsson F, Hallström BM, Käll L, Lundberg E, Pontén F, et al. Gene-specific correlation of RNA and protein levels in human cells and tissues. *Mol Syst Biol*. 2016;12:883.
31. Chee NT, Lohse I, Brothers SP. mRNA-to-protein translation in hypoxia. *Mol Cancer*. 2019;18:49.
32. Bachtary B, Schindl M, Pötter R, Dreier B, Knocke TH, Hainfellner JA, et al. Overexpression of Hypoxia-inducible factor 1 α indicates diminished response to Radiotherapy and unfavorable prognosis in patients receiving Radical Radiotherapy for cervical Cancer 1. *Clin Cancer Res*. 2003;9:2234–40.
33. Tang J-Y, Li D-Y, He L, Qiu X-S, Wang E-H, Wu G-P. HPV 16 E6/E7 promote the glucose uptake of GLUT1 in Lung Cancer through downregulation of TXNIP due to inhibition of PTEN Phosphorylation. *Front Oncol*. 2020;10.
34. Priego-Hernández VD, Arizmendi-Izazaga A, Soto-Flores DG, Santiago-Ramón N, Feria-Valadez MD, Navarro-Tito N, et al. Expression of HIF-1 α and genes involved in glucose metabolism is increased in Cervical Cancer and HPV-16-Positive cell lines. *Pathogens*. 2023;12:33.
35. Kappler M, Pabst U, Rot S, Taubert H, Wichmann H, Schubert J, et al. Normoxic accumulation of HIF 1 α is associated with glutaminolysis. *Clin Oral Investig*. 2017;21:211–24.
36. Rodolico V, Arancio W, Amato MC, Aragona F, Cappello F, Di Fede O, et al. Hypoxia inducible factor-1 alpha expression is increased in infected positive HPV16 DNA oral squamous cell carcinoma and positively associated with HPV16 E7 oncoprotein. *Infect Agent Cancer*. 2011;6:18.
37. Fei J, Hong A, Dobbins TA, Jones D, Soon Lee C, Loo C, et al. Prognostic significance of vascular endothelial growth factor in squamous cell carcinomas of the Tonsil in relation to human papillomavirus status and epidermal growth factor receptor. *Ann Surg Oncol*. 2009;16:2908–17.
38. Ang KK, Sturgis EM. Human papillomavirus as a marker of the natural history and response to therapy of head and neck squamous cell carcinoma. *Semin Radiat Oncol*. 2012;22:128–42.
39. Gong L, Zhang W, Zhou J, Lu J, Xiong H, Shi X, et al. Prognostic value of HIFs expression in head and neck cancer: a systematic review. *PLoS ONE*. 2013;8:e75094.
40. Beasley NJP, Leek R, Alam M, Turley H, Cox GJ, Gatter K, et al. Hypoxia-inducible factors HIF-1 α and HIF-2 α in head and neck cancer: relationship to tumor biology and treatment outcome in surgically resected patients. *Cancer Res*. 2002;62:2493–7.
41. Fillies T, Werkmeister R, van Diest PJ, Brandt B, Joos U, Buerger H. HIF1- α overexpression indicates a good prognosis in early stage squamous cell carcinomas of the oral floor. *BMC Cancer*. 2005;5:84.
42. Li C-X, Sun J-L, Gong Z-C, Lin Z-Q, Liu H. Prognostic value of GLUT1 expression in oral squamous cell carcinoma. *Med (Baltim)*. 2016;95:e5324.
43. Wang J, Ye C, Chen C, Xiong H, Xie B, Zhou J, et al. Glucose transporter GLUT1 expression and clinical outcome in solid tumors: a systematic review and meta-analysis. *Oncotarget*. 2017;8:16875–86.
44. Sitarz K, Zamara K, Szostek S, Kaczor A. The impact of HPV infection on human glycogen and lipid metabolism – a review. *Biochim et Biophys Acta (BBA) - Reviews Cancer*. 2022;1877:188646.
45. Fan R, Hou W-J, Zhao Y-J, Liu S-L, Qiu X-S, Wang E-H, et al. Overexpression of HPV16 E6/E7 mediated HIF-1 α upregulation of GLUT1 expression in lung cancer cells. *Tumour Biol*. 2016;37:4655–63.
46. Fang J, Li X, Ma D, Liu X, Chen Y, Wang Y, et al. Prognostic significance of tumor infiltrating immune cells in oral squamous cell carcinoma. *BMC Cancer*. 2017;17:375.
47. Höing B, Kanaan O, Altenhoff P, Petri R, Thangavelu K, Schlüter A, et al. Stromal versus tumoral inflammation differentially contribute to metastasis and poor survival in laryngeal squamous cell carcinoma. *Oncotarget*. 2018;9:8415–26.
48. Mendonça F, Teles AM, Nascimento MDDSB, Santos APAD, Lopes FF, Paiva A, et al. Human papillomavirus modulates Matrix metalloproteinases during carcinogenesis: clinical significance and role of viral oncoproteins. *Vivo*. 2022;36:2531–41.
49. Alkharsh KR. VEGF upregulation in viral infections and its possible therapeutic implications. *Int J Mol Sci*. 2018;19:1642.
50. Jo S, Juhasz A, Zhang K, Ruel C, Loera S, Wilczynski SP, et al. Human papillomavirus infection as a prognostic factor in Oropharyngeal Squamous Cell Carcinomas Treated in a prospective phase II clinical trial. *Anticancer Res*. 2009;29:1467–74.
51. Karpathiou G, Stachowitz M-L, Dumollard JM, Gavid M, Froudarakis M, Prades JM, et al. Gene Expression Comparison between the Primary Tumor and its Lymph Node Metastasis in Head and Neck squamous cell carcinoma: a pilot study. *Cancer Genomics Proteomics*. 2019;16:155–61.
52. Baruah P, Lee M, Wilson POG, Odutoye T, Williamson P, Hyde N, et al. Impact of p16 status on pro- and anti-angiogenesis factors in head and neck cancers. *Br J Cancer*. 2015;113:653–9.
53. Troy JD, Weissfeld JL, Youk AQ, Thomas S, Wang L, Grandis JR. Expression of EGFR, VEGF, and NOTCH1 suggest differences in Tumor Angiogenesis in HPV-Positive and HPV-Negative Head and Neck squamous cell carcinoma. *Head Neck Pathol*. 2013;7:344–55.
54. Kyzas PA, Stefanou D, Batistatou A, Agnantis NJ. Prognostic significance of VEGF immunohistochemical expression and tumor angiogenesis in head and neck squamous cell carcinoma. *J Cancer Res Clin Oncol*. 2005;131:624–30.
55. Tse GM, Chan AWH, Yu K-H, King AD, Wong K-T, Chen GG, et al. Strong immunohistochemical expression of vascular endothelial growth factor predicts overall survival in Head and Neck squamous cell carcinoma. *Ann Surg Oncol*. 2007;14:3558–65.

Publisher's Note

Springer Nature remains neutral with regard to jurisdictional claims in published maps and institutional affiliations.

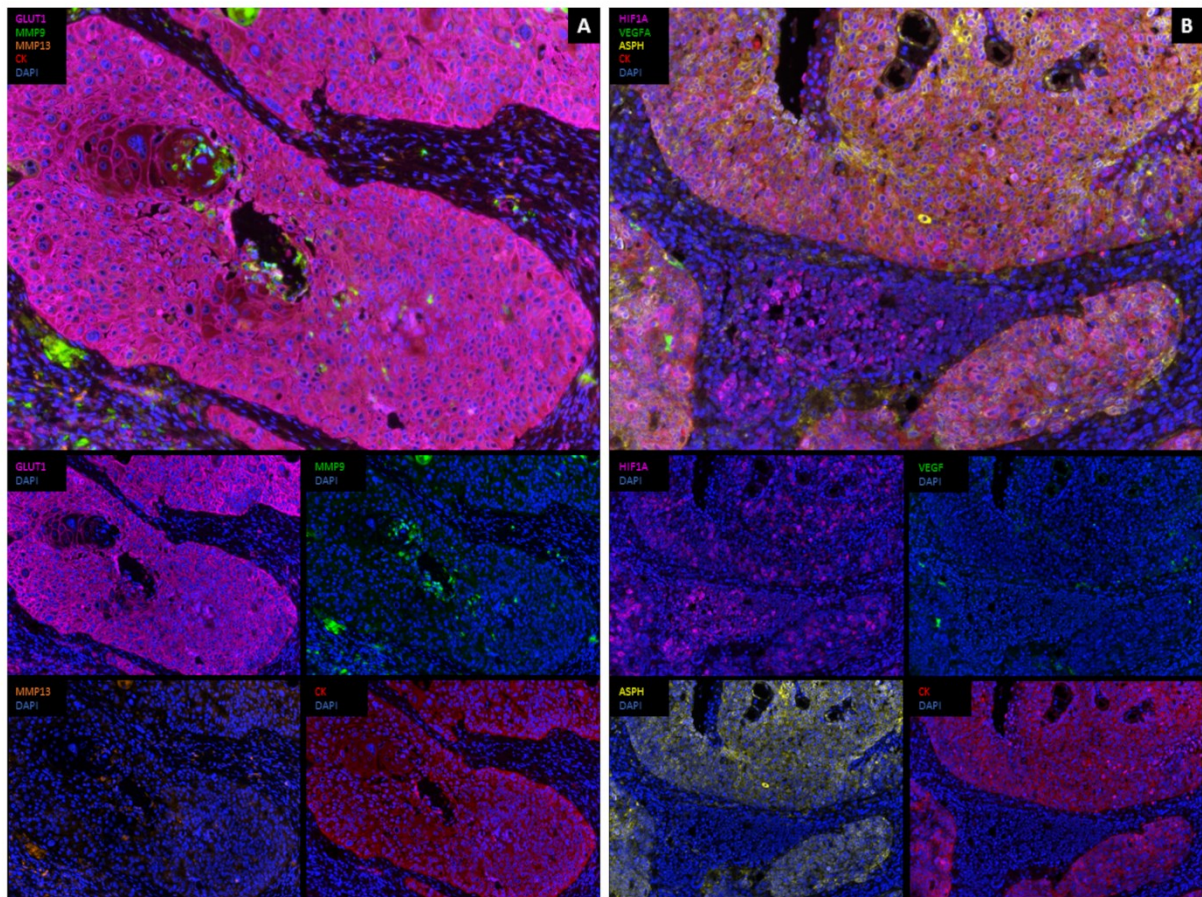
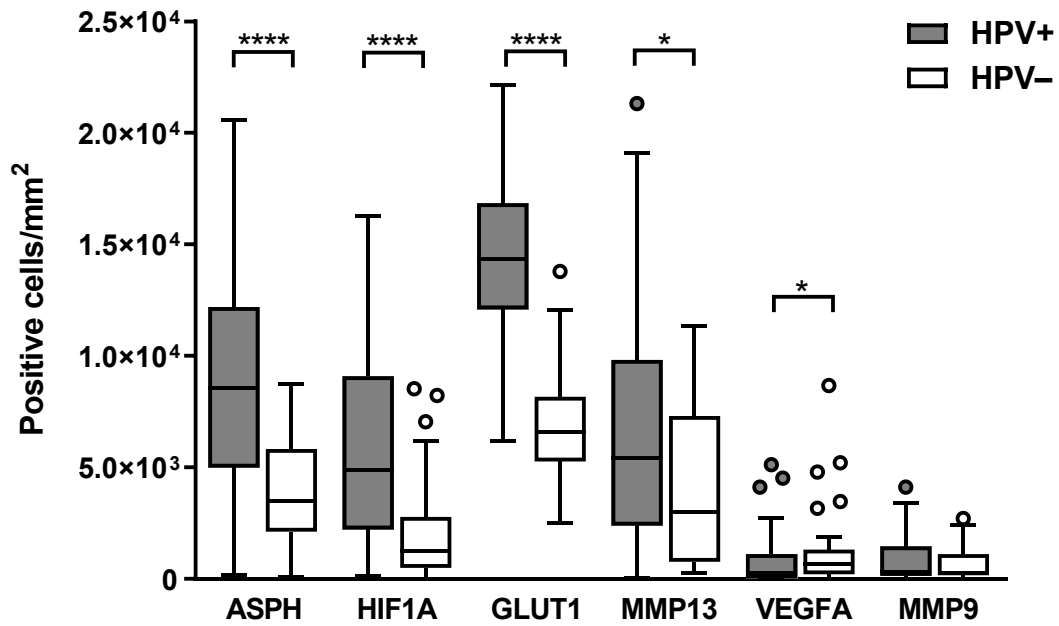


Figure S1. Representative multispectral IHC staining of FFPE HNSCC tissue, 20x magnification. Panel A) Staining of GLUT1 (magenta), MMP9 (green), MMP13 (orange), pan cytokeratin AE1/AE3 (CK, red), and DAPI (blue) antibodies. Panel B) Staining of HIF1A (magenta), VEGFA (green), ASPH (yellow), CK (red), and DAPI (blue) antibodies.

A



B

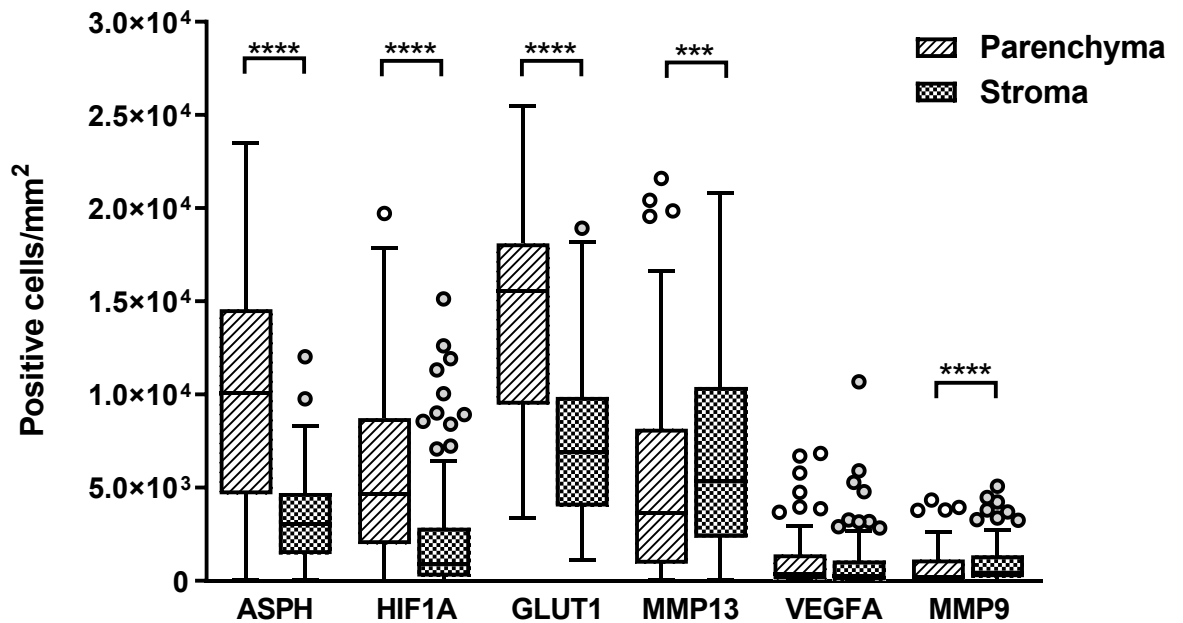


Figure S2. ASPH and other hypoxia markers detected by the mIHC in the groups of HPV-positive (HPV+) and HPV-negative (HPV-) tumours (A), and in the parenchyma and stroma (B) of HNSCCs. The median value is indicated; the box borders show the upper and lower quartiles, the whiskers show the variability, and outliers are indicated. *p < 0.05, ** p < 0.01, *** p < 0.001, **** p < 0.0001

Table S1. Hazard ratio (HR) values for hypoxia markers influencing overall survival (OS) and disease-specific survival (DSS).

Model including HPV RNA status			
OS		DSS	
	HR (p-value)		HR (p-value)
HPV RNA+	0.225 (0.008)	HPV RNA+	0.095 (0.001)
Increasing age	1.065 (0.027)	Increasing age	1.085 (0.011)
HIF1A**		MMP13**	
whole tumor	0.818 (0.060)	whole tumor	1.109 (0.074)
Models without HPV status inclusion			
OS		DSS	
	HR (p-value)		HR (p-value)
Increasing age*	1.068 (0.016)	Increasing age*	1.087 (0.015)
GLUT1**		GLUT1**	
whole tumor	0.802 (< 0.0001)	whole tumor	0.814 (0.005)
parenchyma	0.852 (< 0.0001)	parenchyma	0.862 (0.009)
stroma	0.814 (0.007)	stroma	0.842 (0.032)
OS		DSS	
	HR (p-value)		HR (p-value)
Increasing age*	1.060 (0.037)	Increasing age*	1.076 (0.026)
HIF1A**		HIF1A**	
whole tumor	0.729 (0.003)	whole tumor	0.773 (0.021)
parenchyma	0.829 (0.008)		
stroma	0.616 (0.027)		

* HR for increasing age corresponds to the model calculated for the whole tumour area

** HR corresponds to a difference of 1000 positive cells/mm²